

HEAT-INTEGRATED CRUDE OIL DISTILLATION SYSTEM DESIGN

A thesis submitted to the University of Manchester for the degree of
Doctor of Philosophy
in the Faculty of Engineering and Physical Sciences

2008

Lu Chen

**School of Chemical Engineering
and Analytical Science**

TABLE OF CONTENTS

LIST OF FIGURES	7
LIST OF TABLES.....	10
ABSTRACT	16
DECLARATION	19
COPYRIGHT STATEMENT	20
ACKNOWLEDGMENT	21
NOMENCLATURE AND ABBREVIATION	22
CHAPTER 1 INTRODUCTION	27
1.1 Features of crude oil distillation systems	28
1.2 Features of grassroots design and retrofit design of crude oil distillation processes	30
1.2.1 Grassroots design	30
1.2.2 Retrofit design	31
1.3 Motivation and objective of this work	32
1.4 Overview of the thesis	33
CHAPTER 2 LITERATURE REVIEW	35
2.1 Modelling of crude oil distillation columns.....	35
2.1.1 Short-cut models	35
2.1.2 Rigorous models	40
2.1.3 Summary of crude oil distillation column models	42
2.2 Design of heat exchanger networks	43
2.2.1 Pinch Analysis methods	43
2.2.2 Deterministic optimisation-based methods	44
2.2.3 Stochastic optimisation-based methods	47
2.3 Design and optimisation of heat-integrated crude oil distillation system	48
2.4 Conclusions	52
CHAPTER 3 SIMPLIFIED MODELLING OF CRUDE OIL DISTILLATION COLUMNS	55
3.1 Introduction.....	55
3.2 Modelling of columns with refining product specifications.....	56
3.2.1 The existing method and the limitations	58
3.2.2 True boiling curve calculations	59
3.2.3 Methodology for simple columns.....	61

3.2.4 Illustrative example 3.1: Simple distillation column	65
3.2.5 Methodology for a sequence of simple columns	67
3.3.6 Illustrative example 3.2: Atmospheric distillation column	68
3.3 Pump-around location in atmospheric distillation columns	72
3.3.1 The existing simplified model and the limitations	72
3.3.2 New simplified model to account for the effect of pump-around location on the separation performance	77
3.3.3 Illustrative example 3.3: The effect of pump-around location on separation performance in an atmospheric distillation column	79
3.3.4 Simplified modelling of atmospheric distillation units with a pump-around above the top side-stripper.....	83
3.3.5 Illustrative example 3.4: The atmospheric distillation column with pump-around located above the top side-stripper	84
3.4 Conclusions	86
CHAPTER 4 HEAT EXCHANGER NETWORK DESIGN FOR PROCESS STREAMS WITH TEMPERATURE-DEPENDENT THERMAL PROPERTIES	88
4.1 Introduction.....	88
4.2 Limitations of existing design methodologies.....	89
4.2.1 Stochastic optimisation-based design methods for grassroots and retrofit of heat exchanger networks	90
4.2.2 Network pinch design method for heat exchanger network retrofit	91
4.3 Heat exchanger network model	93
4.3.1 Process streams with temperature-dependent thermal properties.....	94
4.3.2 Heat exchanger network model	95
4.3.3 Illustrative example 4.1: Simulation of a crude oil preheat train	100
4.4 Design approaches for process streams with temperature-dependent thermal properties.....	103
4.4.1 Simulated annealing optimisation-based design method for streams with temperature-dependent thermal property.....	103
4.4.2 Illustrative example 4.2: Retrofit study of an existing crude oil preheat train using the SA algorithm.....	115
4.4.3 Methods for pinching existing networks with multi-segmented stream data and stream splitting.....	119
4.4.4 Illustrative example 4.3: Pinching an existing crude oil preheat train	125

4.4.5 Modified network pinch with combined structure searches and cost-optimisation.....	127
4.4.6 Illustrative example 4.4: Adding a new exchanger to an existing preheat train.....	131
4.5 Summary of the chapter	133
CHAPTER 5 DESIGN AND OPTIMISATION OF HEAT- INTEGRATED CRUDE OIL DISTILLATION SYSTEMS.....	135
5.1 Introduction.....	135
5.2 Simulation of heat-integrated crude oil distillation systems.....	136
5.2.1 Modelling the interactions within the crude oil distillation system.....	138
5.2.2 Generation of multi-segment stream data	141
5.3 Optimisation-based design approach	142
5.3.1 Objective function.....	143
5.3.2 Process constraints	145
5.3.3 Optimisation variables.....	146
5.3.4 Optimisation framework and algorithm.....	149
5.3.5 Implementation of the over all design approach.....	152
5.4 Studies of different column configurations	155
5.4.1 Modelling of liquid side-draw prefractionator columns.....	157
5.4.2 Illustrative example 5.1: A reboiled prefractionator column with a liquid side-draw	161
5.4.3 Installation of prefractionator column with liquid side-draw to atmospheric crude oil distillation unit.....	162
5.5 Conclusions	164
CHAPTER 6 CASE STUDIES.....	166
6.1 Case study 6.1: Energy demand reduction in an existing heat-integrated atmospheric distillation column.....	167
6.1.1 Base case problem data	168
6.1.2 Optimisation approach and results.....	171
6.1.3 Comparison of new optimisation approach with the approach without product specifications and constant thermal property stream data	178
6.2 Case study 6.2: Profit improvement by optimising product distributions in an existing heat-integrated atmospheric distillation column.....	180
6.2.1 Base case problem data	181
6.2.2 Optimisation approach and results.....	182

6.3 Case study 6.3: Energy demand reduction in existing heat-integrated crude oil distillation system	186
6.3.1 Base case problem data	187
6.3.2 Optimisation approach and results.....	190
6.4 Case study 6.4: Grassroots design for heat-integrated atmospheric crude oil distillation.....	195
6.4.1 Problem data.....	197
6.4.2 Optimisation approach and results for the configuration without a prefractionator column	202
6.4.3 Optimisation approach and results for the configuration with a prefractionator column	205
6.4.4 Optimisation approach and results for the progressive configuration.....	208
6.4.5 Optimisation approach and results for the novel configuration with a liquid-side-draw prefractionator column.....	214
6.4.6 Summary of case study	217
6.5 Summary	220
CHAPTER 7 CONCLUSIONS AND FUTURE WORK	223
7.1 Conclusions	223
7.1.1 Simplified modelling of crude oil distillation columns.....	223
7.1.2 Heat exchanger network design for process streams with temperature-dependent thermal properties	225
7.1.3 Design methodology of heat-integrated crude oil distillation system and the applications	227
7.2 Future work.....	228
REFERENCES	231
APPENDIX A: DATA FOR ILLUSTRATIVE EXAMPLE 4.1.....	238
APPENDIX B: SIMULATED ANNEALING	241
B.1 Simulated annealing.....	241
B.2 Simulated annealing parameters.....	244
APPENDIX C: DATA FOR CASE STUDY 6.1	247
C.1 Problem data.....	247
C.2 Results for optimum crude oil distillation system.....	250
C.3 Comparison of new optimisation approach with the approach without product specifications and constant thermal property stream data	252
APPENDIX D DATA FOR CASE STUDY 6.2	253

APPENDIX E DATA FOR CASE STUDY 6.3.....	254
APPENDIX F DATA FOR CASE STUDY 6.4.....	257

LIST OF FIGURES

Figure 1.1 Flowsheet of crude oil distillation system	27
Figure 2.1 Simple distillation column.....	36
Figure 2.2 Decomposition of an atmospheric tower	39
Figure 2.3 Schematic diagram of a stage at equilibrium	41
Figure 2.4 Optimisation framework for heat-integrated distillation system (Rastogi, 2006)	52
Figure 3.1 Specification of separation of crude oil distillation columns in the refining industry and simplified modelling.....	56
Figure 3.2 Decomposition of atmospheric tower (Liebmann, 1996)	57
Figure 3.3 TBP curve calculation	60
Figure 3.4 Method for identifying key components and recoveries in simple columns given product specifications	62
Figure 3.5 Levenberg-Marquardt algorithm (Gill <i>et al.</i> , 1978).....	64
Figure 3.6 Calculation history.....	67
Figure 3.7 Decomposition approach for an atmospheric distillation column.....	74
Figure 3.8 Modelling of simple column with pump-around not at the top stage	74
Figure 3.9 Decomposition approach for an atmospheric distillation column with pump-around above HN side stripper.....	76
Figure 3.10 New simplified modelling of simple columns with a pump-around not at the top stage	78
Figure 4.1 Enthalpy. temperature relationship of crude oil (industrial data)	89
Figure 4.2 Previous network pinch design strategy (Asante and Zhu, 1996)	92
Figure 4.3 Stream data	95
Figure 4.4 Node-based HEN structure representations (Rodriguez, 2005)	99
Figure 4.5 Grid diagram of the existing heat exchanger network (Gadalla, 2002) ..	101
Figure 4.6 Simulated annealing move tree for HEN design	106
Figure 4.7 Sample grid diagram for correlating node temperature and heat load of exchangers located on the stream	109
Figure 4.8 Regressed temperature (T) . enthalpy change (DH)	112
Figure 4.9 Temperature. enthalpy relation of streams that cannot be represented by the proposed polynomial correlation.....	112

Figure 4.10 Generic grid diagram for minimum temperature approach constraint and stream enthalpy balance constraint.....	114
Figure 4.11 Modified HEN for illustrative example 4.2 (with feasibility solver)	118
Figure 4.12 Optimisation approach for pinching a network	124
Figure 4.13 Pinch locations of the existing crude oil preheat train	127
Figure 4.14 Modified network pinch approach design strategy	128
Figure 4.15 The modified network pinch procedure	131
Figure 4.16 Pinch network for maximum heat recovery	131
Figure 4.17 Suggested location of adding a match by the new approach	133
Figure 5.1 Interactions between crude oil distillation columns and heat exchanger network.....	139
Figure 5.2 Sequential modular strategy in heat integration modelling.....	140
Figure 5.3 Optimisation variables in overall system design.....	147
Figure 5.4 Optimisation framework	150
Figure 5.5 Novel configuration with a liquid side-draw prefractionator column.....	157
Figure 5.6 Decomposition of crude vacuum distillation column (Rastogi, 2006)	159
Figure 5.7 Decomposition of liquid side-draw prefractionator column	159
Figure 5.8 Liquid side-draw mixing scheme in decomposed sequence	163
Figure 6.1 Case Study 6.1 : Atmospheric distillation column and thermodynamic equivalent decomposed sequence of simple columns	168
Figure 6.2 Case Study 6.1: Structure of existing heat exchanger network.....	171
Figure 6.3 Case Study 6.1: Modified heat exchanger network.....	178
Figure 6.4 Case Study 6.2: Modified heat exchanger network.....	186
Figure 6.5 Case Study 6.3: Atmospheric and vacuum distillation columns, showing the equivalent decomposed sequence of simple columns (Rastogi, 2006)	188
Figure 6.6 Case Study 6.3: Structure of existing heat exchanger network.....	190
Figure 6.7 Case Study 6.3: Modified heat exchanger network.....	195
Figure 6.8 Case Study 6.4: Conventional atmospheric distillation column without a prefractionator column, showing the equivalent decomposed sequence of simple columns (a) Atmospheric column (b) Equivalent decomposed sequence	198
Figure 6.9 Case Study 6.4: Atmospheric distillation column with a prefractionator column, showing the equivalent decomposed sequence of simple columns	199

Figure 6.10 Case Study 6.4: Progressive configuration	200
Figure 6.11 Case Study 6.5: Novel configuration with an atmospheric column and a liquid-side-draw prefractionator column.....	202
Figure 6.12 Case Study 6.4: Comparisons of the utility demand of various configurations	218
Figure 6.13 Case Study 6.4: Comparisons of the total annualised cost of various configurations	218
Figure 6.14 Case Study 6.4: Comparisons of products generated by various configurations	219

LIST OF TABLES

Table 3.1 Crude oil assay data.....	65
Table 3.2 Feed composition of crude oil mixture (derived from assay data)	66
Table 3.3 Feed data, product specifications, tolerances and initial guess of key components and recoveries	66
Table 3.4 Final solutions of key components and recoveries.....	67
Table 3.5 Specifications of atmospheric crude oil distillation column (Illustrative example 3.2)	69
Table 3.6 Product specifications	69
Table 3.7 Initial guess of key components and recoveries*	71
Table 3.8 Product properties and flow rates (Simulation results of using the initial guess of key components and recoveries)	71
Table 3.9 The key components and recoveries that meet the product specifications	71
Table 3.10 Product properties and flow rates (simulation results applying the key components and recoveries shown in Table 3.8)	71
Table 3.11 Calculated number of theoretical stages (Illustrative example 3.2)	71
Table 3.12 Atmospheric distillation column simulation results (Illustrative example 3.2)	72
Table 3.13 Key components and recoveries in each simple column (Gadalla, 2002)	80
Table 3.14 Specifications of atmospheric crude oil distillation column (illustrative example 3.3)	80
Table 3.15 Description of different scenarios	81
Table 3.16 Utility and exchanger cost (Gadalla, 2002).....	82
Table 3.17 Simulation results of atmospheric crude oil distillation column with different pump-around locations	82
Table 3.18 Specifications for pump-around 4 (PA4).....	85
Table 3.19 Atmospheric distillation column simulation results (Illustrative example 3.4)	86
Table 4.1 HEN simulation results: constant thermal properties with temperature assumed.....	101
Table 4.2 HEN simulation results: varying thermal properties.....	102

Table 4.3 Illustrative example: multi-segmented stream data of cold crude oil	111
Table 4.4 Existing heat exchangers (Illustrative example 4.2)	116
Table 4.5 Utility and exchanger modification costs	116
Table 4.6 Simulated annealing parameters (illustrative example 4.2)	117
Table 4.7 Move probabilities (illustrative example 4.2).....	117
Table 4.8 Modifications to the existing HEN (illustrative example 4.2)	118
Table 4.9 Energy and cost reduction of optimised design (illustrative example 4.2)	118
Table 4.10 Energy demand of pinched HEN	125
Table 4.11 Split fraction of branches for pinched HEN by the new two -level approach (with respect to main streams)	126
Table 4.12 Redistributed heat loads for pinched HEN by the new two -level approach	126
Table 4.13 Energy and cost reduction after adding a new match	132
Table 5.1 Prices of distillation products and crude oil feed in crude oil distillation system	145
Table 5.2 Feed conditions and column specifications	161
Table 5.3 Simulation results of reboiled liquid side-draw prefractionator column...	162
Table 6.1 Case Study 6.1: Crude oil assay data	169
Table 6.2 Case Study 6.1: Key components and recoveries in each simple column	169
Table 6.3 Case Study 6.1: Existing atmospheric crude oil distillation column (Gadalla, 2002)	170
Table 6.4 Case Study 6.1: Product information of existing atmospheric crude oil distillation column	171
Table 6.5 Case Study 6.1: Optimisation variables of atmospheric distillation column	172
Table 6.6 Case Study 6.1: Optimisation variables of preheat train.....	172
Table 6.7 Case Study 6.1: Simulated annealing parameters	173
Table 6.8 Case Study 6.1: Move probabilities.....	174
Table 6.9 Case Study 6.1: Energy consumption and operating cost of optimum system	175
Table 6.10 Case Study 6.1: Optimum operating conditions of atmospheric column	176
Table 6.11 Case Study 6.1: Product information of optimum atmospheric column	177

Table 6.12 Case Study 6.1 : Comparisons of products generated from optimum distillation unit gained by two approaches	179
Table 6.13 Case Study 6.1: Compar isons of energy saving of optimum system attained by the two approaches	180
Table 6.14 Case Study 6.2: Pri ces of distillation products and crude oil feed	182
Table 6.15 Case Study 6.2: Move p robabilities	183
Table 6.16 Case Study 6.2: Summar y of capital investment and profit improvement	184
Table 6.17 Case Study 6.2: Product information of optimum atmospheric column	184
Table 6.18 Case Study 6.2: Opt imum operating conditions of atmospheric column	185
Table 6.19 Case Study 6.3: Pr essure specifications for atmospheric and vacuum columns	188
Table 6.20 Case Study 6.3: Key components and recoveries in each simple column	189
Table 6.21 Case Study 6.3: Existing atmospheric and vacuum crude oil distillation columns (decomposition of Figure 6.5b)	189
Table 6.22 Case Study 6.3: Product information of existing atmospheric and vacuum crude oil distillation column	190
Table 6.23 Case Study 6.3 Opti misation variables for vacuum distillation column.	191
Table 6.24 Case Study 6.3: Move pr obabilities	192
Table 6.25 Case Study 6.3: Ener gy consumption and operating costs of optimum system	193
Table 6.26 Case Study 6.3: Opt imum operating conditions of atmospheric column and vacuum col umn	194
Table 6.27 Case Study 6.3: Product information of optimum columns	194
Table 6.28 Case Study 6.4: Move pr obabilities (Configuration without a prefractionator column)	203
Table 6.29 Case Study 6.4: Perfor mance summary of optimum design (Configuration without a prefractionator column)	204
Table 6.30 Case Study 6.4: Theoretical stage distribution of optimum design* (Configuration without a prefractionator column)	204
Table 6.31 Case Study 6.4: Pr oduct slate of optimum design (Configuration without a prefractionator column)	204

Table 6.32 Case Study 6.4: Move probabilities (Configuration with a prefractionator column)	206
Table 6.33 Case Study 6.4: Performance summary of optimum design (Configuration with a prefractionator column)	207
Table 6.34 Case Study 6.4: Theoretical stage distribution of optimum design* (Configuration with a prefractionator column)	207
Table 6.35 Case Study 6.4: Product slate of optimum design (Configuration with a prefractionator column)	207
Table 6.36 Case Study 6.4: Fixed product distributions (First step of the progressive configuration)	209
Table 6.37 Case Study 6.4: Limits of feed temperatures in optimisation (First step of the progressive configuration)	209
Table 6.38 Case Study 6.4: Move probabilities (First step of the progressive configuration)	210
Table 6.39 Case Study 6.4: Performance summary of optimum design (First step of the progressive configuration)	211
Table 6.40 Case Study 6.4: Theoretical stage distribution of optimum design* (First step of the progressive configuration)	211
Table 6.41 Case Study 6.4: Product slate of optimum design (First step of the progressive configuration)	212
Table 6.42 Case Study 6.4: Optimum product distributions (Second step of the progressive configuration)	213
Table 6.43 Case Study 6.4: Optimised operating pressures (Second step of the progressive configuration)	213
Table 6.44 Case Study 6.4: Performance summary of optimum design (Second step of the progressive configuration)	213
Table 6.45 Case Study 6.4: Theoretical stage distribution of optimum design* (Second step of the progressive configuration)	214
Table 6.46 Case Study 6.4: Product slate of optimum design (Second step of the progressive configuration)	214
Table 6.47 Case Study 6.4: Move probabilities (Novel configuration with a liquid side-draw prefractionator column)	215
Table 6.48 Case Study 6.4: Performance summary of optimum design (Novel configuration with a liquid side-draw prefractionator column)	216

Table 6.49 Case Study 6.4: Theoretical stage distribution of optimum design* (Novel configuration with a liquid side-draw prefractionator column)	217
Table 6.50 Case Study 6.4: Product slate of optimum design (Novel configuration with a liquid side-draw prefractionator column)	217
Table A.1 Constant stream data of illustrative example 4.1	238
Table A.2 Segmented stream data of illustrative example 4.1	239
Table A.3 Heat exchanger loads data of illustrative example 4.1	240
Table C.1.1 Case Study 6.1: Feed composition of crude oil mixture (derived from assay data, Suphanit, 1999)	247
Table C.1.2 Case Study 6.1: Process and utility stream data of existing unit	248
Table C.1.3 Case Study 6.1: Heat exchanger data	249
Table C.1.4 Case Study 6.1: Energy consumption and operating costs of existing unit	249
Table C.1.5 Case Study 6.1: Utility, stripping steam and exchanger modification costs	250
Table C.2.1 Case Study 6.1: Process and utility stream data of optimised unit	250
Table C.2.2 Case Study 6.1: Additional area and cost of optimised heat exchanger network	251
Table C.3.1 Case Study 6.1: Comparison of optimised operating conditions between two approaches	252
Table D.1 Case Study 6.2: Key components and recoveries for separation of products of optimum solution	253
Table D.2 Case Study 6.2: Additional area and cost of optimised heat exchanger network	253
Table E.1 Case Study 6.3: Heat exchanger data	254
Table E.2 Case Study 6.3: Process and utility stream data of existing unit	254
Table E.3 Case Study 6.3: Energy consumption and operating costs of existing unit	256
Table E.4 Case Study 6.3: Additional area and cost of optimised heat exchanger network	256
Table F.1 Case Study 6.4: Operating conditions of optimum design* (Configuration without a prefractionator column)	257
Table F.2 Case Study 6.4: Operating conditions of the initial design* (Configuration with a prefractionator column)	257

Table F.3 Case Study 6.4: Product slate of the initial design (Configuration with a prefractionator column)	257
Table F.4 Case Study 6.4: Operating conditions of optimum design* (Configuration with a prefractionator column)	258
Table F.5 Case Study 6.4: Operating conditions of the initial design* (Progressive configuration)	258
Table F.6 Case Study 6.4: Product slate of the initial design (Progressive configuration)	258
Table F.7 Case Study 6.4: Operating conditions of optimum design* (First step of the progressive configuration)	259
Table F.8 Case Study 6.4: Operating conditions of optimum design* (Second step of the progressive configuration)	259
Table F.9 Case Study 6.4: Operating conditions of the initial design* (Configuration with a liquid side-draw prefractionator column)	259
Table F.10 Case Study 6.4: Product slate of the initial design (Configuration with a liquid side-draw prefractionator column).....	260
Table F.11 Case Study 6.4: Operating conditions of optimum design* (Configuration with a liquid side-draw prefractionator column)	260

ABSTRACT

Heat-integrated crude oil distillation systems . the atmospheric and vacuum distillation towers and associated heat recovery system . are energy and capital intensive. The structures of the distillation columns are very complex and the distillation columns interact strongly with the preheat train. There are many degrees of freedom in this system, most of which are interlinked with each other and cannot be considered separately. A systematic design approach is necessary to exploit these design issues for increasing the efficiency with which energy and capital are employed in the overall system.

This thesis develops an optimisation-based methodology for the simultaneous design of crude oil distillation systems. Both new design and retrofit scenarios are considered. This design approach considers some significant design issues and generates design solutions that are realisable and industrially practicable. Robust and more accurate models have been developed to represent the distillation columns and heat exchanger networks (HENs) within an optimisation framework, compared with previous work.

Facilitated by the decomposition approach (Liebmann, 1996), simplified models (Suphanit, 1999; Gadalla *et al.*, 2003a; Rastogi, 2006), based on the Fenske-Underwood-Gilliland method, were developed previously to model the atmospheric distillation unit and the vacuum unit. This work extends and modifies these simplified models to account more accurately for the effect of pump-around location on the separation performance in atmospheric units. Moreover, the simplified model has been extended to consider an atmospheric distillation column with a pump-around located above the top side-stripper.

This work also proposes a new methodology to incorporate product specifications following refining conventional in the simplified models. The proposed approach enables systematic identification of key components and associated recoveries to match specified boiling temperature profiles, as these are normally used as indicators of separation performance in the refining industry. The new simplified

models are validated by comparison with rigorous simulation results of atmospheric distillation columns.

Multi-segmented stream data are implemented in the design and analysis of heat exchanger networks, in which the thermal properties of streams are temperature-dependent and cannot be assumed constant. Two existing promising HEN design approaches, the simulated annealing optimisation-based approach (Rodriguez, 2005) and the network pinch approach (Asante and Zhu, 1996), are modified and extended to apply to the HEN design with multi-segmented stream data. In the modified network pinch approach, the bottleneck of an existing HEN configuration is better overcome by varying stream split fractions and heat exchanger loads at the same time, rather than simply redistributing heat loads. The modified network pinch approach also combines structural modifications and cost optimisation in a single step to avoid missing cost-effective design solutions.

An optimisation framework, applying a stochastic optimisation method . multiple simulated annealing runs . is developed to generate grassroots and retrofit designs of the heat-integrated crude oil distillation systems. The heat integration of the system is accounted for more accurately than previously by using multi-segmented stream data. Operating conditions and pump-around locations of distillation columns are optimised, together with structural options and continuous variables of heat exchanger networks as appropriate, in a single optimisation framework.

The new degrees of freedom considered in this work include key components and associated recoveries (used in simplified models of distillation columns to express the separation of products) and operating pressures of distillation columns. The optimisation of key components and recoveries allow the systematic exploitation of product distributions and product slate in order to maximise net profit. Including operating pressures in the optimisation facilitates creation of heat recovery opportunities in configuration studies. Product specification constraints are imposed in the optimisation so that product quality is not compromised during design.

A novel distillation configuration, with a liquid side-draw prefractionator column upstream of an atmospheric distillation column, is proposed in this work. The case study shows a very promising performance with respect to energy efficiency.

Case studies illustrate the beneficial application of the proposed approach in both grassroots and retrofit design of crude oil distillation systems, with respect to energy demand and net profit improvement. Comparisons are made between different configurations, and results are given as proof of principle.

DECLARATION

No portion of the work referred to in this thesis has been submitted in support of an application for another degree or qualification of this or any other university or other institution of learning.

Lu Chen

COPYRIGHT STATEMENT

- i. The author of this thesis (including any appendices and/or schedules to this thesis) owns any copyright in it (the %Copyright+) and s/he has given The University of Manchester the right to use such Copyright for any administrative, promotional, educational and/or teaching purposes.
- ii. Copies of this thesis, either in full or in extracts, may be made only in accordance with the regulations of the John Rylands University Library of Manchester. Details of these regulations may be obtained from the Librarian. This page must form part of any such copies made.
- iii. The ownership of any patents, designs, trade marks and any and all other intellectual property rights except for the Copyright (the %Intellectual Property Rights+) and any reproductions of copyright works, for example graphs and tables (%Reproductions+), which may be described in this thesis, may not be owned by the author and may be owned by third parties. Such Intellectual Property Rights and Reproductions cannot and must not be made available for use without the prior written permission of the owner(s) of the relevant Intellectual Property Rights and/or Reproductions.
- iv. Further information on the conditions under which disclosure, publication and exploitation of this thesis, the Copyright and any Intellectual Property Rights and/or Reproductions described in it may take place is available from the Head of School of Chemical Engineering and Analytical Science and the Dean of the Faculty of Life Sciences, for Faculty of Life Sciences candidates.

ACKNOWLEDGMENT

I would like to express my sincere gratitude to my supervisors, Dr. Megan Jobson and Prof. Robin Smith, for their guidance, encouragement and support through the period of this work. I would also greatly appreciate the cooperation of Dr. Megan Jobson during the writing-up stage of this thesis.

Special thanks to Centre for Process Integration for giving me a great opportunity to study at the University of Manchester. Thanks to Process Integration Research Consortium for providing the sponsorship of this research.

I wish to thank all staffs of Centre for Process integration for their help and support whenever I need. Special thanks to Steve Doyle for his support in the programming part of my research. My sincere gratitude also goes to Dr. Nan Zhang for his valuable suggestions of this research.

I am grateful to all students of Centre for Process Integration. Thanks to them for creating a friendly and stimulating environment. I thank Yuhang, Yurong, Mian, Imran, Xuesong, Sonia, Yannis for making the research life pleasant and interesting.

I am very thankful to my parents who have always been supporting and encouraging me, to overcome the difficulties encountered these years. My deep thanks to my husband, Yongwen, for his endless support, love, patience and understanding during the past three years and being always by my side.

NOMENCLATURE AND ABBREVIATION

$A_{\cos t}$	Cost coefficient A (\$) in equation 3.10
$Area_{total}$	Total heat exchanger area (m ²)
B	Molar flow rate of bottom product (kmol/h)
B'	Specified molar flow rate of bottom product (kmol/h)
$B_{\cos t}$	Cost coefficient B (\$) in equation 3.10
$C_{\cos t}$	Cost coefficient C (dimensionless) in equation 3.10
CC	Heat exchanger capital cost (\$)
CC_{crude}	Unit price of crude oil (\$/kmol)
$CC_{prod,j}$	Unit price of product j (\$/kmol)
$CGCC$	Column grand composite curve
CP_j	Heat capacity flow rate of stream j (kW/°C)
CP_{csl}	Effective heat capacity flow rate of cold stream flowing through heat exchanger l (kW/°C)
CP_{hsl}	Effective heat capacity flow rate of hot stream flowing through heat exchanger l (kW/°C)
CP_{SP}^k	Heat capacity flow rate of a branch k after splitter SP (kW/°C)
CP_{SP}^{main}	Heat capacity flow rate of the process stream before splitter SP (kW/°C)
cu	Cold utility
D	Molar flow rate of top product (kmol/h)
D'	Specified molar flow rate of top product (kmol/h)
d_i	Molar flow rate of component i in top product (kmol/h)
DH_j	Enthalpy change of stream j (kW)
DH_i	Accumulated enthalpy change from the start of the stream to the particular node i (kW), in equations 4.11, 4.13, 4.14, defined by 4.12
$Diam$	Diameter of column (ft)
E_a	Objective function value in simulated annealing algorithm, in figure B.1
E_{exist}	Energy demand of an existing network (kW), in figures 4.2 and 4.14
$E(i, j)$	Equilibrium relationship for i^{th} component at stage j (dimensionless)
F	Molar flow rate of feed (kmol/h)
$F(i, j)$	Flow rate of i^{th} component in feed entering stage j (kmol/h)
F_c	Correction factor for shell or tray cost
F_m	Correction factor for shell or tray material
F_{mix}	Flow rate of mixture in equation 5.4 (kmol/h)
F_p	Correction factor for pressure
F_s	Correction factor for tray spacing
F_t	Correction factor for tray type
ff_{SP}^k	Split fraction of the particular branch k at splitter SP
ff_{ij}	Flow ratio of the branch to the main stream j on which the exchanger unit l is located on
GCC	Grand composite curve

H_1	Height of column (ft)
H_2	Total height from top to bottom tray (ft)
H_L	Molar enthalpy of liquid side-draw of prefractionator column in equation 5.6 (kJ/mol)
H_n	Molar enthalpy of vapour from column n in equation 5.6 (kJ/mol)
H_{mix}	Molar enthalpy of mixture in equation 5.6 (kJ/mol)
$H(j)$	Energy balance at stage j (kJ/mol)
HD	Heavy distillate
HEN	Heat exchanger network
HGO	Heavy gas oil
HK	Heavy key component
HTC_j	Heat transfer coefficient of stream j (kW/°C·m ²)
$HTCC_l$	Cold side heat transfer coefficient of exchanger l (kW/°C·m ²)
$HTCH_l$	Hot side heat transfer coefficient of exchanger l (kW/°C·m ²)
hu	Hot utility
I	Identity matrix in figure 3.5
$K(i, j)$	Equilibrium constant for i^{th} component at stage j (dimensionless)
ker	Kerosene
L	Flow rate of liquid side-draw of the prefractionator column in equations 5.4 . 5.6 (kmol/h)
L_i	Liquid stream leaving stage i in figures 3.8 and 3.10
L_{out}	Liquid stream draw in figure 3.10
L_0	Liquid reflux flow rate without a pump-around (kmol/h)
L^*	Liquid reflux flow rate with a pump-around (kmol/h) in figures 3.8 and 3.10
$L(i, j)$	Flow rate of i^{th} component in liquid stream leaving stage j (kmol/h)
LD	Light distillate
LGO	Light gas oil
LK	Light key component
LMA	Levenberg-Marquardt algorithm
$LMTD_l$	Log mean temperature difference of the heat exchanger l (°C)
LP	Linear programming
$M(i, j)$	Material balance of i^{th} component at stage j (kmol/h)
$MILP$	Mixed integer linear programming
$MINLP$	Mixed integer non-linear programming
mods	Modifications, in figures 4.2 and 4.14
N	Total number of theoretical stages
N_{BR}	Number of stream branches in a heat exchanger network
N_{COL}	Number of columns in a sequence
N_{HX}	Number of heat exchangers in a heat exchanger network
N_{min}	Minimum number of stages at total reflux
N_{PA}	Pump-around location with respect to side-draw stage
N_R	Number of theoretical stages in rectifying section
N_S	Number of theoretical stages in stripping section
N_{ST}	Number of process streams in a heat exchanger network

N_{units}	Number of heat exchangers in equation 3.10
N_{UHX}	Number of utility exchanger units in a heat exchanger network
N_{SUT}	Number of process streams on which there is a utility heat exchanger, in a heat exchanger network
NBP	Normal boiling point (°C)
NBR_{SP}	Number of branch at splitter SP
NC_{in}	Cold side inlet node of a heat exchanger
NC_{out}	Cold side outlet node of a heat exchanger
NH_{in}	Hot side inlet node of a heat exchanger
NH_{out}	Hot side outlet node of a heat exchanger
NLP	Non-linear programming
NP	Net profit
PA	Pump-around
PB	Pump-back
P_L	Pressure of liquid side-draw of prefractionator column in equation 5.7 (bar)
P_n	Pressure of vapour from column n in equation 5.7 (bar)
P_{mix}	Pressure of mixture in equation 5.7 (bar)
$PROD_j$	Flow rate of product j (kmol/h)
$PROD'_j$	Specified flow rate of product j (kmol/h)
q	Liquid fraction of feed at feed stage conditions
Q_C	Condenser duty without a pump-around (kJ/h)
Q_C^*	Hypothetical condenser duty with a pump-around (kJ/h) in figures 3.8 and 3.10
Q_l	Heat load of heat exchanger l (kW)
$Q(j)$	Energy loss from stage j (kJ/h) in equation 2.11
Q_{PA}	Pump-around duty (kJ/h)
R	Reflux ratio
R_{HK}	Recovery of heavy key component to bottom product
R_i	Recovery of i^{th} component to top product
R_{LK}	Recovery of light key component to top product
R_{max}^i	Maximum heat recovery for the network with i modifications (kW) in figures 4.2 and 4.14
R_{min}	Minimum reflux ratio
RES	Residue
SA	Simulated annealing
SQP	Successive quadratic programming
$T5$	True boiling temperature at which 5% liquid is vaporised (°C)
$T5'$	Specified true boiling temperature at which 5% liquid is vaporised (°C)
$T50$	True boiling temperature at which 50% liquid is vaporised (°C)
$T50'$	Specified true boiling temperature at which 50% liquid is vaporised (°C)
$T95$	True boiling temperature at which 95% liquid is vaporised (°C)
$T95'$	Specified true boiling temperature at which 95% liquid is vaporised (°C)

T_a	Annealing temperature in simulated annealing algorithm
TAC	Total annualised cost (MM\$/y)
TBP	True boiling point (°C)
TC_l^{in}	Inlet temperature of cold stream in heat exchanger l (°C)
TC_l^{out}	Outlet temperature of cold stream in heat exchanger l (°C)
TH_l^{in}	Inlet temperature of hot stream in heat exchanger l (°C)
TH_l^{out}	Outlet temperature of hot stream in heat exchanger l (°C)
TMX_{SP}^k	Temperature on the branch k before the remixing at splitter SP (°C)
TMX_{SP}^{out}	Temperature of stream after remixing at splitter SP (°C)
TS_j	Supply temperature of stream j (°C)
TSP_{SP}^{in}	Temperature of process stream before splitting of splitter SP (°C)
TSP_{SP}^k	Temperature of a parallel branch k after splitter SP (°C)
TT_j	Target temperature of stream j (°C)
$TT_{calc,j}$	Calculated temperature of stream j after transferring heat in a heat exchanger network, including transfer heat with utility (°C)
$TT_{ppcalc,j}$	Calculated temperature of stream j after process to process heat transfer in a heat exchanger network (°C)
TUO^{in}	Inlet temperature of a unit operation (°C)
TUO^{out}	outlet temperature of a unit operation (°C)
U_l	Overall heat transfer coefficient of a heat exchanger l (kW/°C·m ²)
$U(i, j)$	Flow rate of i^{th} component in vapour draw stream from stage j (kmol/h)
UO	Unit operation
UO_{in}	Inlet node of a unit operation
UO_{out}	Outlet node of a unit operation
V_i	Vapour stream to stage i in figures 3.8 and 3.10
V_{in}	Vapour stream feed in figure 3.10
$V(i, j)$	Flow rate of i^{th} component in vapour stream leaving stage j (kmol/h)
V_{min}	Minimum molar vapour flow rate at top pinch (kmol/h)
V'_{min}	Minimum molar vapour flow rate at bottom pinch (kmol/h)
$V_{min,top}$	Minimum molar vapour flow rate at the top of the rectifying section (kmol/h)
V_n	Flow rate of vapour stream coming from column n in equations 5.4 . 5.6 (kmol/h)
$W(i, j)$	Flow rate of i^{th} component in liquid draw stream from stage j (kmol/h) in equation 2.10
x_{bLK}	Mole fraction of light key component in bottom product
x_{dHK}	Mole fraction of heavy key component in top product
x_{fHK}	Mole fraction of heavy key component in feed
$x_{f,i}$	Mole fraction of component i in feed
x_{fLK}	Mole fraction of light key component in feed
$x_{L,i}$	Composition of i^{th} component in the liquid side-draw of the prefractionator column in equation 5.5

$x_{mix,i}$	Composition of i^{th} component in mixture of liquid and vapour , in equation 5.5
$x_{n,i}$	Composition of i^{th} component in the vapour stream coming from column n , in equation 5.5
$x(i, j)$	Composition of i^{th} component in liquid stream leaving stage j
$y(i, j)$	Composition of i^{th} component in vapour stream leaving stage j

Greek letters

α_{HK}	Volatility of heavy key component relative to a reference component
α_i	Volatility of component i relative to a reference component
α_{LK}	Volatility of light key component relative to a reference component
Δf	Difference in the objective function values of two different solutions in simulated annealing algorithm, in equation B.1
ΔT	Temperature difference (°C)
ΔT_{min}	Minimum difference temperature approach (°C)
γ	Penalty factor in equation 4.10
λ	Damping factor in figure 3.5
θ	Cooling parameter in equation B.2
ϕ	Roots of Under wood equation

Subscripts and superscripts

L	Liquid
V	Vapour
F	Feed

CHAPTER 1 INTRODUCTION

The crude oil distillation process is of great importance in the refining industry. It is a process in which a crude oil is separated into various distillation products, which will be further processed in downstream units before being blended into final products. Figure 1.1 shows a typical configuration of a crude oil distillation system. The system comprises an atmospheric column and a vacuum column, which separate the crude oil into fractions, and a preheat train, which recovers the heat rejected from hot process streams to heat up cold process streams, especially the cold crude. A flash unit or prefractionator tower upstream of the atmospheric distillation unit may also be present.

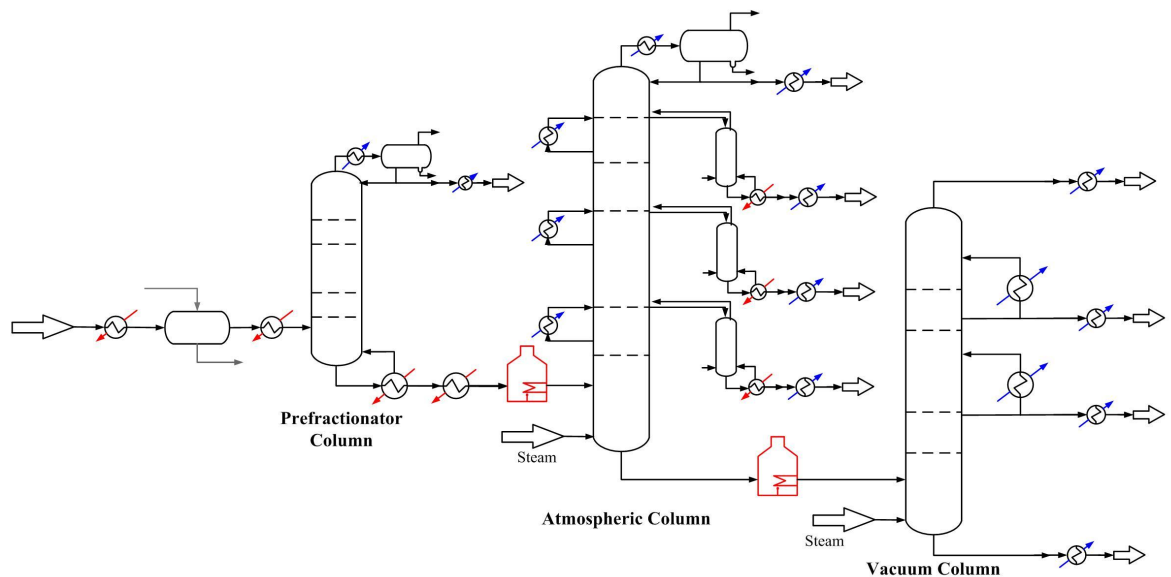


Figure 1.1 Flowsheet of crude oil distillation system

As shown in Figure 1.1, the cold crude from storage tanks is heated up in the first part of a preheat train to achieve the feed temperature of the desalter. This part of the preheat train is represented using a heater in the figure, and same for other parts of the preheat train shown in the figure. The desalter is used to remove salts in the crude feed by dissolving the salts in water. The desalted crude is further heated in the second part of the preheat train, and then fed into a prefractionator column or a preflash drum to remove light components from the crude oil feed. If a preflash drum is installed, vaporisation occurs in only one separation stage, and only the very volatile components are removed. If a prefractionator column is installed, more

separation takes place; the distillate of the prefractionator column may be a valuable product. No matter what separation facility is selected, the flow rate of the crude oil feed processed in the atmospheric and vacuum columns can be reduced. The bottom product of the prefractionator column or preflash drum is heated up in the third part of the preheat train, and then heated up in the atmospheric furnace to reach the feed temperature of the atmospheric distillation column. In the atmospheric distillation column, side-strippers are installed to remove lighter components from side-draws. Pump-arounds are present in the atmospheric distillation column, for creating internal reflux and recovering heat. The atmospheric residue, from the bottom of the atmospheric column, is heated up in a vacuum furnace and fed into the vacuum column for further separation. The reason for operating the atmospheric residue under vacuum conditions is that crude oil is heat sensitive and intensive cracking would occur if the atmospheric residue were processed at atmospheric pressure and the corresponding temperatures. Pump-arounds also exist in the vacuum column to facilitate heat recovery.

The hot distillation product and pump-around streams are cooled in heat exchangers. The heat rejected is used to heat up cold crude oil.

1.1 Features of crude oil distillation systems

Unlike chemical mixtures, crude oil and its products consist of a large number of components. The chemical structure and property of some of the components are unknown. The exact composition of the components is often difficult to measure accurately. It is extremely difficult to characterise crude oil and products using pure components (Shell, 1983). The separated refining products are normally characterised by several temperature points on boiling curves (Watkins, 1979; p.10). In the modelling of crude oil distillation columns, except light ends, pure components are not employed either. Instead, pseudo-components, which are representatives of a small range of components that have close boiling temperature, are employed (Jones, 1995; p.13). Even with pseudo-components, crude oil distillation process is still a multi-component system, which presents a significant challenge for design and analysis.

As shown in Figure 1.1, the structures of atmospheric and vacuum columns are complex. There are side-units attached to the main columns, i.e. side-strippers, pump-arounds, and pump-backs. The complex structure makes the design and analysis of these columns more difficult, compared with simple columns.

Thermal properties (e.g. heat capacity) of the crude oil and products are not constant across the temperature range of interest due to the large number of components and the wide temperature range. For example, crude oil needs to be heated up from ambient temperature to around 360 °C. Assuming a constant thermal property in such a large temperature range will bring significant inaccuracy in the design and analysis of the heat recovery system.

Crude oil distillation processes consume energy intensively, and rank second for energy consumption in the refining industry, after the catalytic reforming processes (Liebmann, 1996; p.1). A relatively small energy saving opportunity in the distillation process will have an impressive economic impact. Crude oil distillation systems have intensive heat recovery arrangements. In many existing refineries, these systems were designed years ago when energy prices were relatively low. As energy became more expensive, there appeared a great incentive to redesign the existing heat exchanger network (HEN) to identify more heat recovery opportunities.

The crude oil distillation process has a great environmental impact. The furnace and steam generation processes burn a significant amount of fuels. The combustion of fuels emits harmful gases, such as CO₂, SO₂, etc., to the environment. Improving the energy efficiency of the crude oil distillation process will bring not only economic but also environmental benefits.

There are strong interactions between distillation columns and the preheat train. Modifications to any of these sub-systems would affect others. The overall utility demand of the crude oil distillation system depends on both distillation columns and the preheat train.

1.2 Features of grassroots design and retrofit design of crude oil distillation processes

The design of crude oil distillation processes can be classified generally into two categories: grassroots design and retrofit design. Grassroots design is designing a process from scratch, and retrofit design is a revamp of an existing process. The relevant design contexts, such as degrees of freedom, design objectives, constraints, *etc.*, are different in different types of design. The design contexts of both types of design are discussed in this section.

1.2.1 Grassroots design

In the case of grassroots design, the general objective is to design a new, economic distillation process which fulfils the specified separation requirement. The design problem comprises two sub-problems: design of the separation devices and design of the preheat train.

In a distillation column, the following design issues need to be addressed: choice of feed preheat temperature; reflux ratio for the separation; locations of side-strippers; type of vaporisation (i.e. reboiler and steam stripping); number of theoretical stages required in each section of the distillation column and the diameter of each section; where pump-arounds should be located and how they should be operated (flow rate, duty and temperature drop). Many of these design issues are interlinked with each other; for example, the feed temperature affects the vapour and liquid flow rate at the feed location, which in turn changes the separation taking place and the number of theoretical stages and the diameter of each column section. The capital cost of the distillation column depends primarily on the diameter and height of the column.

The distillation columns interacts strongly with the preheat train, where pump-around streams and hot products of distillation columns heat up cold streams, especially the cold crude feed. The remaining heating and cooling requirements are fulfilled by hot and cold utilities. The grassroots design of the preheat train involves determining the configuration of the network and the required heat transfer areas. The HEN design thus determines its capital cost and utility cost. As the heating and cooling

requirements are governed by the design of the distillation system, the design of the preheat train and distillation columns are inter-dependent. Designing them both in single framework, rather than sequentially can allow these links to be exploited, which will lead to a better performance of the overall system, for example in terms of energy efficiency or total annualised cost.

1.2.2 Retrofit design

Retrofit design is a revamp of an existing process. Retrofit design is a more constrained problem than grassroots design, constrained by the existing structure of the distillation columns and the preheat train. The basis of retrofit design is to use the existing equipment as much as possible to achieve a particular retrofit objective. The objectives of retrofit design may be improving the throughput of the process, decreasing the energy demand, reducing CO₂ emissions, increasing the net profit, *etc.* Reducing energy consumption and increasing net profit are more common objectives in retrofit design than others because the dominance of profit in industry. Due to the consideration of the existing equipments, retrofit design is much more complex, compared with grassroots design.

For retrofitting a crude oil distillation system, the existing system has to be modified. Modifications might be made to the distillation process or to the heat recovery system. Modifications that can be made have different cost implications, ranging from zero cost to high capital investment (or referred to as different level of modifications). The first level of modifications in retrofitting an existing system is changing the operating conditions of the process. In distillation columns, the variations in operating conditions involve changing the feed preheat temperature, flow rates of the steam injected, pump-arounds flow rates and temperature drops, reflux ratios, *etc.* In the preheat train, the operating conditions of interest are the heat load of each heat exchanger and stream split fractions if there is stream splitting in the preheat train. The second level of modifications include modifications to the structure of the existing process; for instance, changing internals in distillation columns to attain greater throughput or more theoretical stages, installing a preflash drum or a prefractionator column, reallocating pump-arounds, re-piping or re-sequencing existing exchangers, adding new exchangers, *etc.* Capital investment is required for these structural modifications. The modifications that are beneficial to

achieve the retrofit objective are likely to be selected, and a limited number of modifications are likely to be carried out due to economical considerations.

1.3 Motivation and objective of this work

As discussed in Section 1.2, the structures of crude oil distillation columns are complex. There are many degrees of freedom in the design of the process, and many of the degrees of freedom interact with each other. A systematic design approach is necessary to explore and manipulate these variables simultaneously; such an approach needs robust modelling of distillation columns and HENs. Due to the complexity of the distillation columns and the presence of multi-component mixtures in the process, robust modelling of crude oil distillation columns is a great challenge.

Simplified distillation models were developed in the work of Suphanit (1999), Gadalla *et al.* (2003a) and Rastogi (2006) for grassroots and retrofit design of atmospheric and vacuum crude oil distillation columns. However, the existing simplified models cannot systematically support refining product specifications in terms of flow rates and true boiling temperature points. In the approach of Gadalla *et al.* (2003a), a rigorous model of a column meeting the product specifications is required to provide a component mass balance. Key components and recoveries are needed by the simplified models to characterise the separation. Based on the component mass balance, key components and recoveries are specified, so as to give good agreement between the simulation results attained by rigorous and simplified models. In the selection of key components and recoveries, trial and error is needed. In addition, although Rastogi (2006) considered different pump-around locations in simplified modelling of atmospheric crude oil columns (the pump-arounds are no longer constrained to be just below the draw stage of side-strippers), the effect on the separation taking place in the atmospheric column is ignored in the work he presented if pump-arounds are located on different trays. There is no simplified model for the design of an industrially-relevant atmospheric column with a pump-around above the top side-stripper. In this work, existing simplified models will be extended and modified to overcome these limitations.

Design of the preheat train is of great importance in minimising the energy consumption of the crude oil distillation process. The thermal properties of fluids in the process vary significantly due to the large temperature range and their multi-component nature. However, in existing studies, thermal properties, especially heat capacities, are assumed constant with temperature. The effect of this assumption on the validity of HEN models is not taken into account. In this work, variable thermal properties will be considered in the design and analysis of preheat trains. New design approaches that can deal with non-constant thermal properties will be developed. The approaches should be applicable to both grassroots and retrofit designs. New options for HEN design are needed. Firstly, the option of stream splitting should be systematically included in the proposed approaches. Secondly, utility exchangers can be located at any places in the HEN. Thirdly, the number of exchangers on a given stream or branch thereof should not be inherently limited.

The aim of this work is to develop a reliable and realistic modelling framework of the overall system, which captures the interactions between distillation columns and the preheat train. An optimisation-based approach will be developed to design distillation columns and the preheat train within the same framework. The approach should constrain product properties during the optimisation, which has not been considered in previous studies. The optimisation framework will evaluate a wide range of operating conditions and structural options to achieve a specified objective, such as minimum energy consumption or maximum profit. In a crude oil distillation process, the flow rate and property of the products, which is referred as product slate, may vary according to market demand. In some crude oil distillation configurations (e.g. progressive configuration), distributed separations take place. The distribution of the product in such configurations is an important degree of freedom. Systematic exploitation of product slate and product distributions should be carried out to achieve a particular design objective while the quality of products (e.g. true boiling point temperature) is maintained. Optimisation of column operating pressures should be considered to improve the heat recovery opportunities of the system.

1.4 Overview of the thesis

Chapter 2 reviews previous research on the modelling of crude oil distillation columns, on HEN design and on the design of the overall system.

In Chapter 3, simplified models for crude oil distillation columns are presented. The simplified models developed by Suphanit (1999), Gadalla *et al.* (2003a) and Rastogi (2006) will be extended and modified to incorporate product specifications in a systematic way and to address the effect of pump-around location on the separation performance in distillation columns. Simplified models of atmospheric columns where a pump-around is above the top side-stripper are developed. Illustrative examples are presented to validate these models against more rigorous simulation results.

Chapter 4 presents the design and analysis of heat exchanger networks (the preheat train of crude oil distillation systems) of process streams with temperature-dependent thermal properties. Two design approaches are presented in this chapter, namely a simulated annealing optimisation-based approach and a modified network pinch approach. The approaches are applied to preheat trains in illustrative examples.

In Chapter 5, the modelling of the interactions between distillation columns and the preheat train is addressed. The optimisation framework for the design of crude oil distillation systems is presented. The degrees of freedom, constraints and the objective considered in the design framework are discussed. The optimisation algorithm employed in the design framework is also addressed in this chapter. In addition, a new distillation configuration is proposed and the modelling of this configuration is presented.

Chapter 6 presents four case studies to demonstrate the capability of the proposed design framework. Results of these case studies are discussed.

Chapter 7 summarises this research work, and proposes some future work in this area.

CHAPTER 2 LITERATURE REVIEW

Crude oil distillation system is of great importance in the refining industry due to the economic and environmental significance, as discussed in Chapter 1. Significant attentions have come from academic area and industries, especially in recent years when energy price increases rapidly. In this chapter, relevant research and industrial efforts of the design of crude oil distillation systems are reviewed and discussed.

The review starts with modelling of crude oil distillation columns. Models for simple columns are discussed first; then research work on extension and application of these models to crude oil distillation columns is presented. Previous studies on the design of heat exchanger networks solely (preheat trains of crude oil distillation systems) are briefly reviewed. Previous research on the design and analysis of the overall heat-interacted crude oil distillation system is then presented.

2.1 Modelling of crude oil distillation columns

The models for design of distillation columns fall into two main categories: short-cut models and rigorous models. This section briefly presents details of these two types of models.

2.1.1 Short-cut models

The short-cut models commonly applied in the design of distillation columns are known as Fenske-Underwood-Gilliland (FUG) method, which employed the work of Fenske (1932), Underwood (1948) and Gilliland (1940). Let us use the simple distillation column (one feed, one top product and one bottom product) shown in Figure 2.1 to present this method, given the feed condition and recoveries of light and heavy key components.

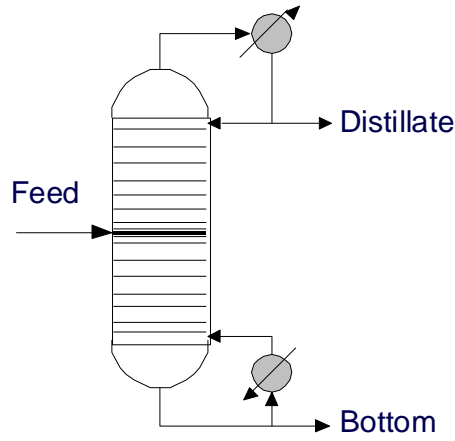


Figure 2.1 Simple distillation column

The minimum vapour flow rate (V_{\min}) and the distribution of components with volatilities between those of the key components at the top pinch location is determined by Underwood Equations 2.1 and 2.2.

$$\sum \frac{\alpha_i x_{f,i}}{\alpha_i - \phi} = 1 - q \quad (2.1)$$

$$\sum \frac{\alpha_i d_i}{\alpha_i - \phi} = V_{\min} \quad (2.2)$$

where V'_{\min} is given by:

$$V'_{\min} = V_{\min} - (1 - q)F \quad (2.3)$$

The minimum reflux ratio is calculated as follows:

$$R_{\min} = (V_{\min, \text{top}} / D) - 1 \quad (2.4)$$

Underwood equations (Equation 2.1 and 2.2) have two assumptions, constant molar flow within each column section, and constant relative volatility throughout the column.

The Fenske equation (Fenske, 1932, cited in Seader and Henley, 1998) estimates the minimum number of stages in a distillation column as shown in Equation 2.5. The condition with minimum number of stages is also referred as total reflux condition.

There is a major limiting assumption in the Fenske equation, constant relative volatilities throughout the column. Still, the Fenske equation can predict the number of stages with reasonable accuracy except where the volatilities vary considerably, or where non-linear liquids form (Seader and Henley, 1998).

$$N_{\min} = \frac{\ln \left[\frac{R_{LK} / (1 - R_{LK})}{(1 - R_{HK}) / R_{HK}} \right]}{\ln [\alpha_{LK} / \alpha_{HK}]} \quad (2.5)$$

This equation can also be rearranged in a form as in Equation 2.6 (Seader and Henley, 1998) to calculate the distribution of components between top and bottom products.

$$\frac{R_i}{(1 - R_i)} = \left(\frac{1 - R_{HK}}{R_{HK}} \right) \left(\frac{\alpha_i}{\alpha_{HK}} \right)^{N_{\min}} \quad (2.6)$$

To achieve a specified separation task, the actual reflux ratio and the number of theoretical stages should be greater than their minimum values. Generally, the actual reflux ratio is set as multiple of the minimum reflux ratio to account for the trade-offs between energy and capital costs. The corresponding number of stages is determined by proper empirical correlations or graphical methods. Among the graphical methods, the most successful and simplest one is Gilliland (1940) correlation. It relates the number of stages to actual reflux ratio, and the minimum number of stages and reflux ratio, from plant data. There are other researchers who developed analytical expressions to represent the relation (Molokanov *et al.*, 1972; Strangio and Treybal, 1974; Eduljee, 1975; Erbar and Maddox, 1961, cited in King, 1980; Rusche, 1999). The simplest one is Molokanov correlation, and it is stated as follows:

$$\frac{N - N_{\min}}{N + 1} = 1 - \exp \left[\left(\frac{1 + 54.4\xi}{11 + 117.2\xi} \right) \left(\frac{\xi - 1}{\xi^{0.5}} \right) \right] \quad (2.7)$$

where,

$$\xi = \frac{R - R_{\min}}{R + 1} \quad (2.8)$$

The number of stages is then decided by the Molokanov correlation, and the feed location can be identified by applying the Kirkbride correlation (1994) (Cited in Seader and Henley, 1998; Chapter 9):

$$\frac{N_R}{N_s} = \left[\left(\frac{B}{D} \right) \left(\frac{x_{fHK}}{x_{fLK}} \right) \left(\frac{x_{bLK}}{x_{dHK}} \right)^2 \right]^{0.206} \quad (2.9)$$

The FUG model gives good results for the separation of relatively ideal mixtures. However, for multi-component and non-ideal mixtures, the mentioned two assumptions of the Underwood method do not apply to the whole column (Seader and Henley, 1998; Suphanit, 1999). Where the underlying assumptions are not valid, the accuracy of the results will be compromised. However, even in those cases, the estimation of the minimum vapor flow rates is good in the regions where the component composition is constant (pinch zones). Some Improvements to the Underwood method have been suggested to extend its applicability.

Although the limitation of the FUG model, many researchers have proposed approaches to apply the method to different configurations of distillation columns: Petlyuk *et al.* (1965) and Stupin and Lockhart (1972) used this model to analyse the energy consumption of fully thermally coupled distillation arrangements; Cerda and Westerberg (1981) developed a short-cut method for the design of various complex distillation configurations; Glinos and Malone (1985) presented a short-cut design approach for distillation columns with side-strippers; Further developments have been carried out by Carlberg and Westerberg (1989) and Triantafyllou and Smith (1992) on applying the Underwood equations to a three-column model in fully thermally coupled distillation columns.

Considering the accuracy of minimum vapour flow rates estimation at pinch zones, Suphanit (1999) extended and modified the FUG method. Rather than assuming constant molar flow in the column, vapour flow rates calculated from Underwood equation were only applied in pinch zones. The next step was to perform an enthalpy balance around the top section to estimate the condenser duty and then the vapour

flow rate at the top of the column. The reboiler duty was calculated through an overall enthalpy balance. By performing an enthalpy balance around the reboiler, the minimum vapour flow rate at the bottom section was calculated.

In addition to simple columns with reboilers, this improved FUG method is further applied to steam-stripped simple columns by performing a stage-by-stage calculation at the stripping section. Models of complex distillation columns (e.g. columns with thermal coupling, side heat exchangers), were also developed. Because of energy balances around the column and the stage by stage calculation in steam-stripped columns, the method developed by Suphanit (1999) is referred later as simplified model (or semi-rigorous) rather than short-cut model. By following the decomposed method of Liebmann (1998), the model of Suphanit (1999) is applicable to atmospheric crude oil distillation columns. Figure 2.2 gives a visualised illustration of how to decompose a complex atmospheric tower into an indirect sequence of simple columns. The atmospheric tower is decomposed at the draw stage of each side-stripper.

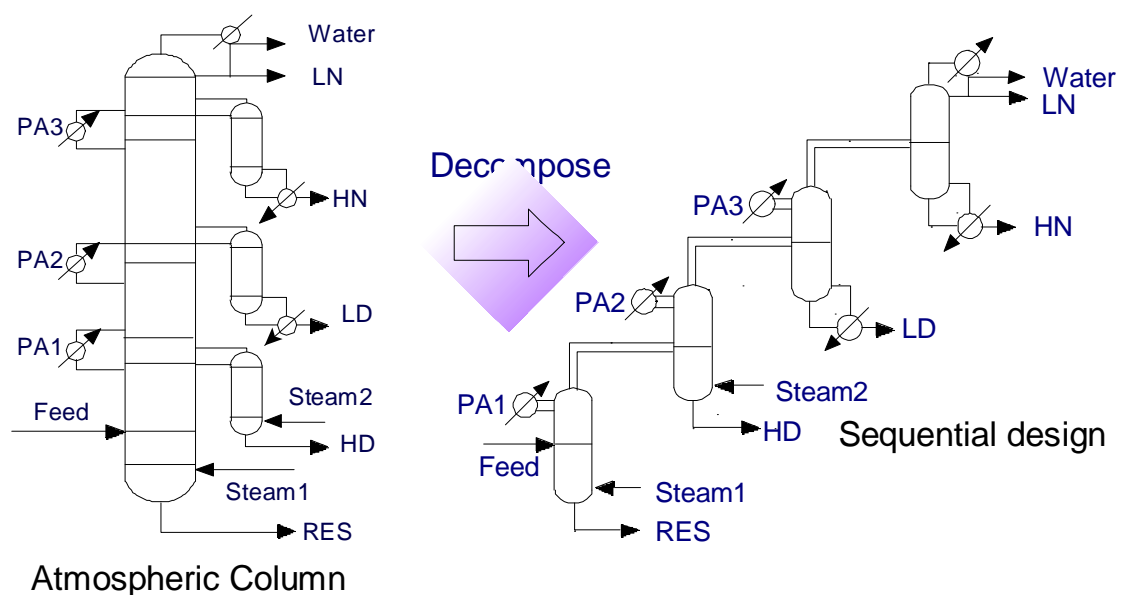


Figure 2.2 Decomposition of an atmospheric tower

Gadalla *et al.* (2003a) extended the design model of Suphanit (1999) to retrofit designs of simple distillation columns, complex distillation columns and also crude oil distillation columns. Rastogi (2006) further extended the models of Gadalla *et al.* (2003a) and Suphanit (1999) on crude oil distillation columns, taking into account pressure drop consideration and flexibility of pump-around location (a pump-around

is not required to be located on the stage just below the side-tripper draw stage, as assumed in the work of Suphanit and Gadalla.). The pump-around location is defined as where the pump-around is located in distillation columns, with respect to the side-tripper draw stage. Models of vacuum units were also developed in the work of Rastogi (2006).

Gadalla *et al.* (2002a) also developed a procedure to transform traditional product specification of crude oil distillation columns into key components and their corresponding recoveries in each column section. More details will be reviewed in Section 3.2.1.

2.1.2 Rigorous models

Rigorous models are widely used for the design and analysis of distillation columns. In the rigorous method, the columns are modelled stage-by-stage considering the mass balance, energy balance and equilibrium relationship. There are two assumptions in the rigorous method: phase equilibrium is achieved on each stage; entrainment of liquid drops in the vapour phase and vapour bubbles in the liquid phase are not considered (Seader and Henley, 1998). For a sample equilibrium stage as shown in Figure 2.3 (Seader and Henley, 1998), the mass balance equations, enthalpy balance equations and equilibrium equations (known as MESH equations if together with summation equations) for i^{th} component on stage j can be written as follows:

Mass balance equation:

$$M(i, j) = L(i, j-1) + V(i, j+1) + F(i, j) - L(i, j) - V(i, j) - W(i, j) - U(i, j) \quad (2.10)$$

Enthalpy balance equation:

$$H(j) = H_L(j-1) \times \sum_i L(i, j-1) + H_V(j+1) \times \sum_i V(i, j+1) + H_F(j) \times \sum_i F(i, j) \\ - H_L(j) \times \sum_i (L(i, j) + W(i, j)) - H_V(j) \times \sum_i (V(i, j) + U(i, j)) - Q(j) \quad (2.11)$$

Equilibrium relation:

$$E(i, j) = y(i, j) - K(i, j) \times x(i, j) \quad (2.12)$$

Where $x(i, j)$ and $y(i, j)$ are the compositions of i^{th} component in liquid and vapour phases leaving j^{th} stage, and are calculated according to:

$$x(i, j) = \frac{L(i, j)}{\sum_i L(i, j)} \quad (2.13)$$

$$y(i, j) = \frac{V(i, j)}{\sum_i V(i, j)} \quad (2.14)$$

$$K(i, j) = f(P(j), T(j), x(i, j), y(i, j)) \quad (2.15)$$

The MESH equations are applied on each stage in a column. In a column where there are C components and N stages, the total number of equations is $2 \times N \times C + N$ and the total number of unknown variables is also $2 \times N \times C + N$. For a given feed condition and column operating pressure, the unknown variables are calculated by solving all the equations simultaneously. Due to the high non-linearity of equilibrium relations and enthalpy balances, the MESH equations are difficult to solve.

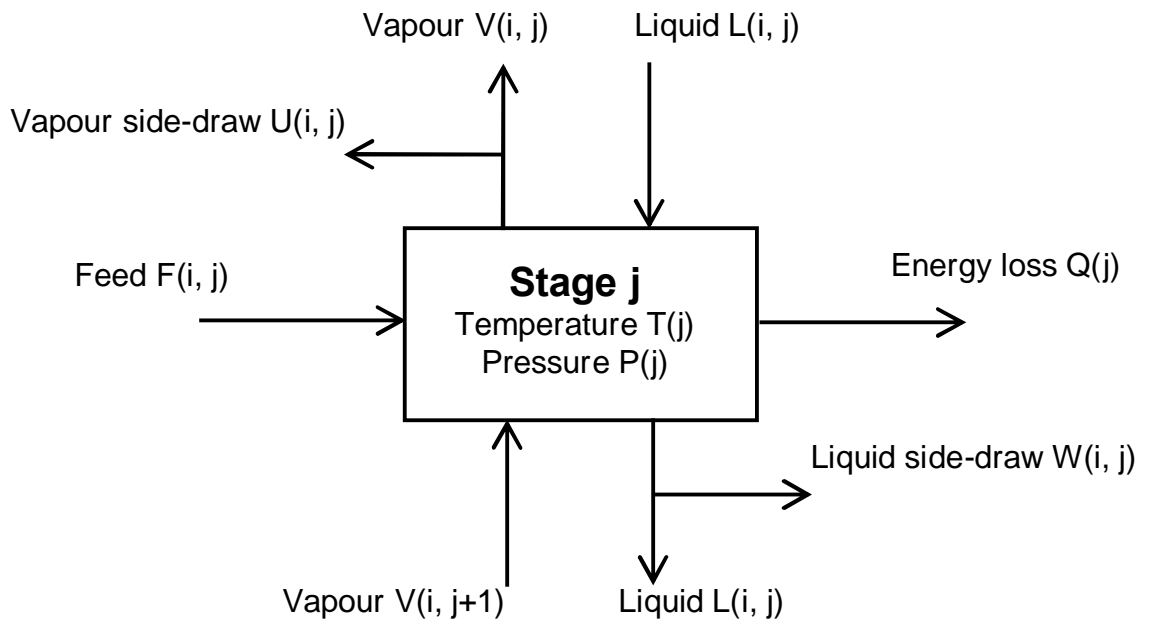


Figure 2.3 Schematic diagram of a stage at equilibrium

In Equation 2.12, the vapour and liquid streams leaving a stage are assumed in equilibrium, which is not valid in real separation. Thus, stage and component efficiencies are included to overcome this limitation. There are various iterative

methods of solving the MESH equations, such as the bubble-point (BP) method, the sum-rates (SR) method, the simultaneous correction (SC) method, and the inside-out method (Seader and Henley, 1998), *etc.* These rigorous models and the methods for solving rigorous models have been incorporated in commercial simulation packages, such as HYSYS, ASPEN Plus, PRO II, *etc.*, and used by researchers for the design and analysis of various crude oil distillation columns (Liebmann *et al.*, 1998; Bagajewicz and Ji, 2001a; Ji and Bagajewicz, 2002a; b; Al-Musilim and Dincer, 2005)

Other researchers have focused on improving rigorous models based on the basic MESH equations. Lang *et al.* (1991) developed a rigorous model for the simulation of atmospheric and vacuum distillation columns based on the MESH equations. In his work, the BP and SR methods were combined together in order to solve the model equations more efficiently. Kumar *et al.* (2001) developed a new formulation of MESH equations, which reduced the total number of model equations from $2 \times N \times C + N$ to $N \times (C + 3)$. Due to the reduction of the total number of equations, the computational time is reduced significantly. Moreover, analytical expressions for the equilibrium constant and enthalpy of liquid and vapour streams were developed in the work of Kumar *et al.* (2001). Because of the analytical expressions, the non-linearity of equilibrium relations and energy balances was reduced significantly. However, the accuracy of the solution is compromised.

2.1.3 Summary of crude oil distillation column models

Rigorous models consider mass and energy balances and the equilibrium relationship at every stage and solve these non-linear equations simultaneously. The accuracy of the results predicted by these models is relatively high, compared with those of short-cut models. As a compromise of the accuracy, this method needs good initialisation in order to converge to the final solution. Moreover, longer time is also required to run the calculation, compared with short-cut models. Although Lung (1991) and Kumar (2001) proposed rigorous models of crude distillation column to reduce computation time, the models they developed are not suitable to serve in the optimisation in which both the distillation columns and the preheat train will be studied. As in that situation, thousands of simulations are needed and initial

estimates of variables are not easy to perform. Therefore, short-cut models are more appropriate in optimisation problems due to their calculation speed and robustness in convergence.

In particular, the simplified models developed by Suphanit (1999), Gadalla *et al.* (2003a) and Rastogi (2006) are significantly useful, because of their following advantages: the underlying limitations of short-cut models are overcome; the models can be applied to both grassroots design and retrofit design of crude oil distillation columns; the relative industrial issues such as pressure drop and pump-around locations are included. Therefore, the simplified models are selected to implement in the present work for the modeling of crude oil distillation columns.

2.2 Design of heat exchanger networks

As discussed in Chapter 1, the preheat train is an important part of the crude oil distillation system. The utility consumption of the system is determined by the design of the preheat train, when the crude oil distillation columns are fixed.

Numerous investigations have been carried out to improve the performance of HEN, without considering the interactions between HEN and the background process (i.e. distillation system, reaction system, *etc.*). The HEN design approaches can be grouped into three major categories: pinch analysis methods, which are based on thermodynamic concepts; mathematical programming methods, with deterministic optimisation algorithms; stochastic optimisation methods, such as Genetic Algorithm, Tabu Search, Simulated Annealing Algorithm, *etc.*

This section summarises these three types of approaches briefly. More reviews can be found in Furman and Sahinidis (2002).

2.2.1 Pinch Analysis methods

Linnhoff and Hindmarsh (1983) developed a method called Pinch Analysis to estimate the minimum hot and cold utility demand prior to HEN design, for a set of

hot and cold streams and a selected minimum temperature approach (ΔT_{\min}). The pinch temperature, which is defined as the temperature where the driving force of heat transfer is zero, is used to divide the HEN design problem into two sub problems, below and above the pinch. Based on the pinch temperature, several heuristic rules are then used to design a network that approaches the target energy consumption. These rules are: no heat should be transferred across the pinch; no cold utility should be supplied above the pinch and no hot utility should be supplied below the pinch.

The appropriate minimum area and number of exchanger units required were developed (Ahmad *et al.*, 1990). Since the minimum utility consumption and area required depend on ΔT_{\min} , the optimum value should be determined by minimising the annualised total cost (sum of annualised capital cost of exchanger units and utility cost). Makwana and Shenoy (1993) solved the problem of determining a proper ΔT_{\min} by carrying out a sensitivity analysis.

The pinch analysis method has advantages and disadvantages. Due to the usage of heuristic rules, this method is only suitable for the design of small-scale problems (Shenoy, 1995). The advantages of this method include simplicity, capability of estimating maximum heat recovery potential without designing heat exchanger network structure, strong thermodynamic foundations and high level of designer interactions. Since it is easy to use and quick to give heat recovery target, it is used as part of other methods for HEN design (Nilsson and Sunden, 1994; Asante and Zhu, 1996; Ravagnani *et al.*, 2003) and in distillation sequencing problems where detailed HEN designs are not necessary in screening various distillation configurations (Fraga and Matias, 1996; Sobocan and Glavic, 2002).

2.2.2 Deterministic optimisation-based methods

Because pinch analysis is difficult to apply to large scale problems, mathematic modeling methods are developed. Principles are left aside and mathematical models are formulated in the forms of optimisation problems: linear programming (LP), mixed integer linear programming (MILP), non-linear programming (NLP) or mixed

integer non-linear programming (MINLP), based on the complexities of the problems considered.

Papoulias and Grossman (1983) developed a linear transshipment model to calculate the minimum utility cost for a specified ΔT_{\min} . This LP model is extended to MILP model to determine the minimum number of heat exchanger units. Cerda *et al.* (1983) and Cerda and Westerberg (1983) presented alternative LP and MILP formulations to determine the minimum utility cost and minimum number of units. Floudas *et al.* (1986) extended the transshipment model of Papoulias and Grossmann (1983), which provides how the hot streams and cold streams are matched and the amount of heat exchanged in the particular match. Then the optimised superstructure from transshipment model is fixed and used within a NLP model to obtain the network with minimum total annualised cost. Yee *et al.* (1990) proposed an NLP formulation for simultaneous optimisation of energy cost and capital cost of the HEN. This mathematical model is applicable in the design problem where the heat transfer coefficients are not the same for all streams, which is assumed in the pinch analysis method. Yee and Grossman (1991) extended the transshipment model of Papoulias and Grossman (1983) to the retrofit design of HENs.

For NLP, it is difficult to guarantee convergence to global optimal. When a poor initial guess is provided, the problem may converge to an inferior solution or even fail to converge. Even for LP where global optimal is attainable, estimation of first order (or higher) derivatives may sometimes be difficult and cause computational problems. Attempts have been made to reduce the size of problem.

Zhu *et al.* (1995) presented a block decomposition model to reduce the size of optimisation problem. Based on the physical insights obtained from the composite curves in pinch analysis method, the design problem is decomposed into blocks. The blocks are defined as enthalpy intervals on composite curves. Superstructures are generated within each block and the sub-networks are synthesised in each block individually. The optimisation problem in each block is either formulated as a MILP or MINLP problem, depending on whether the heat transfer area or capital cost is to be minimised (Zhu *et al.* 1995a, b, c). All sub-networks in each block are then merged together and optimised by NLP optimisation.

Asante and Zhu (1996) proposed a network pinch approach, which combines the pinch technology and mathematical methods. There are two stages, diagnosis stage and optimisation stage, in the approach. In the diagnosis stage, the potential modifications to the existing configuration of HEN are suggested according to pinch technology; then each candidate modification is optimised for maximum heat recovery by varying heat loads of each exchanger unit. In the optimisation stage, designers interact with the approach and select the modification they prefer, and then further cost optimisation is carried out to the selected HEN with a modified topology. Although the network pinch approach is a sequential approach, it exploits possible topology modifications in a systematic way and at the same time provides access to the design procedure. These characteristics feature the network pinch approach to be a promising retrofit approach, especially in industry area. However, stream heat capacities are assumed constant, which will introduce significant inaccuracies in designing crude oil preheat trains where the heat capacity of streams vary greatly. The network pinch approach of Asante and Z hu (1996) is selected to be modified and extended to be applicable to preheat train design, which will be presented in Chapter 4.

More investigations have been carried out to generate more realistic designs by removing assumptions such as isothermal mixing (Björk and Westerlund, 2002), or considering multi-stream mixers (Dong *et al.*, 2008), *etc.* Other researchers focus on developing more robust solvers for NLP problem which require no particular initialisation procedure (Morton, 2002; Isafiade and Fraser, 2008).

The advantage of mathematical models is that they are able to solve the HEN design of large scale industrial problems. However, mathematical programming approaches do not always have a guarantee of optimality in their solutions due to the non-convexities in the objective function and constraints of NLP and MINLP models (Shenoy, 1995). In order to increase the robustness of mathematical programming methods, simplifications are made to the modelling of HENs and complexity of HENs studied is reduced (i.e. stream splitting is not considered, fixed number of matches between a hot stream and a cold stream, only one exchanger unit allowed on a particular stream branch, *etc.*). Other drawbacks of these methods include significant computational time consumed and large memory storage required.

2.2.3 Stochastic optimisation-based methods

Compared to deterministic methods, stochastic methods have more chance to find global optimum for non-linear problems with mixed integer and continuous variables, due to the random nature of the optimisation methods. Commonly used algorithms in the synthesis of HENs are Genetic Algorithms (Wang *et al.*, 1998; Lewin *et al.*, 1998a, b; Ravagnani *et al.*, 2003, 2005), Simulated Annealing (SA) (Dolan *et al.*, 1989, 1990; Nielsen *et al.*, 1994; Athier *et al.*, 1997; Rodriguez, 2005), Tabu search (Lin and Miller, 2004) and other hybrid ones (Björk and Nordman, 2005). The SA algorithm, developed from the analogy with the process of physical annealing, combining with Monte Carlo principle, is one of the stochastic optimisation methods which have received many attentions.

Dolan *et al.* (1989, 1990) used the SA optimisation algorithm to solve HEN synthesis problems. The approach starts with an initial feasible HEN design, and various modifications have been carried out to this HEN design. The considered HEN modifications include shifting loads among exchangers, varying a stream split ratio, inserting a new heat exchanger, deleting an existing heat exchanger. The selections of modifications are determined by a random number generator. The work of Dolan *et al.* (1989, 1990) was not applicable to retrofit designs, and re-allocating of exchangers was not considered.

Nielsen *et al.* (1994) presented an approach which combines pinch analysis, mathematical programming and the SA algorithm. The minimum utility assumption of a set of process streams is determined by pinch analysis. Then, structural information of the HEN is extracted and stream matches are proposed by mathematical programming. In the end, the proposed configuration is optimised by the SA algorithm.

Other researchers also combined mathematical programming method with stochastic method, in different ways. In the work of Athier *et al.* (1996), the SA algorithm is used to select heat exchanger network configuration in the outer loop, and an NLP formulation is used to optimise the continuous variables (heat loads and split ratios) for a fixed HEN structure in the inner loop. This approach was applied to several

literature examples successfully; however, the computational time required is considerably high, compared with other approaches.

Rodriguez (2005) presented an optimisation-based approach for mitigation of fouling in heat exchanger network. Although the main aim of this work was to minimise fouling aspects when designing the HENs, the approach can also be applied to steady state design. In the approach, the SA algorithm was employed as the optimisation algorithm. Both structural options, such as re-piping, re-sequencing of existing exchangers, and continuous options, such as stream split fractions and exchanger duties, were considered without simplification of cost models and objective functions. This approach is applicable to both grassroots design and retrofit design.

There are several advantages of this stochastic optimisation-based approach: relevant level of details in HEN design is considered (i.e. stream splitting, multiple exchangers on a particular stream branch, utility exchangers located on anywhere of streams, re-allocation of exchangers are traced and constrained in retrofit design); the approach is computationally efficient. This approach is suitable to be combined in the design of crude oil distillation columns, which was successfully carried out by Rastogi (2006). This approach is chosen to be implemented in both study of the preheat train only (Chapter 4) and the design of the overall crude oil distillation system, together with distillation columns (Chapter 5).

No work above considered the varying thermal property (e.g. heat capacities) issue of process streams. Non-constant thermal property arises when multi-component streams are cooled down or heated up, which is observed in preheat trains.

2.3 Design and optimisation of heat-integrated crude oil distillation system

Until Liebmann (1998), there was not so much research on atmospheric distillation unit since 1938 when Nelson (1958) summarised the design procedure for a crude oil prefractionator and Watkins (1979) outlined the steps to design a crude oil distillation unit in one chapter of his book. They are very similar to each other in

terms of relying on experiences, guidelines, empirical correlations for determining the amount of stripping steam and number of stages. Trial and error is required in the design procedure. The structure of a crude oil distillation column is complex with many sections connected to each other, which is not taken into account in the established design procedures. Moreover, the interactions between the crude oil distillation units and the heat recovery system are not considered.

Liebmann (1998) proposed an integrated design procedure for crude oil distillation columns. The procedure starts with an initial sequence of simple columns, which is decomposed from the complex atmospheric distillation unit, and simulates each column rigorously in the commercial simulator Aspen Plus with the use of pseudo-components. Using pinch analysis, the grand composite curve (GCC) is generated for process streams. Based on GCC, possible modifications that may improve the heat integration of the distillation column are suggested and the new operating condition is re-simulated and new GCC is generated accordingly. The modified simple sequence is then merged to generate the final design of the complex column. Iterations are needed to achieve final design, and trial and error is required. The approach of Liebmann (1998) is based on heuristic rules, which are not easy to apply, and it is time consuming. (Rastogi, 2006)

Sharma *et al.* (1999) developed an alternative approach for achieving better heat integration of a crude oil distillation column. The method combines the Packie approach for crude column rating/design and the pinch analysis principle to generate column grand composite curve (CGCC). Since the generated CGCC is invariant to pump-around refluxes and only depends on the feed condition and product specifications, it can be used to set %reflux-energy-recovery+target for an unaffected separation. The developed CGCC is applicable to various types of atmospheric towers (e.g. type U, type A and type R, cited from Watkins 1979). The method is simple, and the employed Packie approach is familiar to refinery engineers. However, only the effect of pump-around streams on heat recovery is studied; and other design issues (i.e. amount of steam injected, feed temperature, etc.) are not addressed.

Suphanit (1999) developed modified short-cut models for crude oil distillation columns. The potential heat recovery and heat exchanger area needed are

estimated based on pinch analysis, accounting for the interactions between the crude oil distillation columns and the preheat train. An optimisation framework was proposed to systematically exploit the degrees of freedom (i.e. feed preheating temperature, side exchanger temperature change, flow rate of stripping steam, reflux ratio) to minimise the total annualised cost of the system. The analysis of six different crude oil distillation sequences was performed, the results show that rather than the conventional crude oil distillation scheme with a main tower and side-strippers, the progressive distillation scheme has more opportunity of energy saving and can be operated with the lowest total annualised cost.

Bagajewicz (2001a, b) and his co-worker Ji (2002a, b, c) extended the methodology of Liebmann (1998) to vacuum units, preflash units, prefractionators and process different types of crude. Rather than grand composite curve, *heat demand. supply diagram* was developed. The main advantage of this diagram is that each process stream is presented explicitly in the same diagram. It is easy to figure out the contribution of each hot and cold stream to the heat recovery. At the beginning of the design, no pump-around circuits are used. Based on the generated heat demand. supply diagram, heat is shifted from condenser to top pump-around. The modified column is re-simulated and the heat demand. supply diagram is re-generated. The performance of separation task is controlled by the flow rate of stripping steam. The separation performance is represented by the boiling temperature gap between 95% of the lighter product vaporised and 5% of the adjacent heavier product vaporised. The flow rate of stripping steam is increased if the gap becomes smaller than the desired value. The shifting of heat loads continues as long as the cost of increasing steam flow rate is less than the energy saved. The procedure stops when there is no scope of transferring more energy. Then, using the same procedure, energy is shifted from top pump-around to the next lower pump-around. The main drawback of this method is that the trade-off between capital and energy is not considered and the structure of HEN is not taken into account.

The work of Gadalla *et al.* (2003c) imposed the hydraulic constraints of distillation columns. It extended the optimised design approach of Suphanit (1999) from grassroots design to retrofit design of atmospheric columns. An Area. Energy curve was presented for the retrofit design of heat exchanger networks. The curve was generated from the analysis of the existing HEN (Asante and Zhu, 1996) and used to

estimate approximately the heat transfer area required for a given energy demand in optimising the operating conditions of the atmospheric column. After optimising the operating conditions of the atmospheric column, the new information of process streams (supply and target temperature, flow rate, heat capacity) is updated in the existing HEN. Then, based on pinch analysis, several modifications are implemented to the existing HEN (i.e. changing the heat load of an exchanger unit, re-sequencing an exiting exchanger, *etc.*). Except the minimisation of total annualised cost, other retrofit design objectives, such as minimising CO₂, increasing throughput, are considered. The operating conditions of distillation columns are optimised by a nonlinear programming (NLP) optimizer (Sequential quadratic programming, SQP). The overall drawback of the work of Gadalla *et al.* (2003b) is that it neglected the cost for structural modification.

Inamdar *et al.* (2004) presented a steady state model to simulate an industrial crude oil unit based on (C+3) iteration variables. The design is formulated as a multi-objective problem rather than a general single objective problem. The elitist non-dominated sorting genetic algorithm (NSGA- II) is applied as the optimisation algorithm to solve the problem. The interactions between the crude oil distillation columns and the preheat train are not addressed.

Heat exchanger network structure is included in the research of Rastogi (2006). The existing simplified models (Suphanit, 1999; Gadalla *et al.*, 2003a) were modified in the work of Rastogi (2006) to allow pressure drop consideration, side exchanger location flexibility with respect to location of side-draws and vacuum units. In order to analyse the structure and operating conditions of the distillation columns and the HEN simultaneously, the SA algorithm is used as the optimizer in the optimisation framework, as illustrated in Figure 2.4. The design methodology of Rastogi (2006) considers distillation columns and details of the heat exchanger network together. It is superior to other approaches in terms of better capture of the interactions between the crude oil distillation columns and the preheat train. The SA optimisation-based design approach has more chances of finding the global optimum solution, compared with deterministic methods.

However, in the work of Rastogi (2006), the separation in the distillation columns was not exploited and column operating pressures were fixed. The exploration of the

separation is important when product slate is allowed to vary in maximising the profit of the overall system. Operating pressures are also important degrees of freedom due to their effects on boiling temperature of streams, in turn heat recovery potential. The heat integration between the preheat train and the crude oil distillation columns was accounted for with process streams assuming constant heat capacities, which may lead to a exploration of the important interactions with less accuracy.

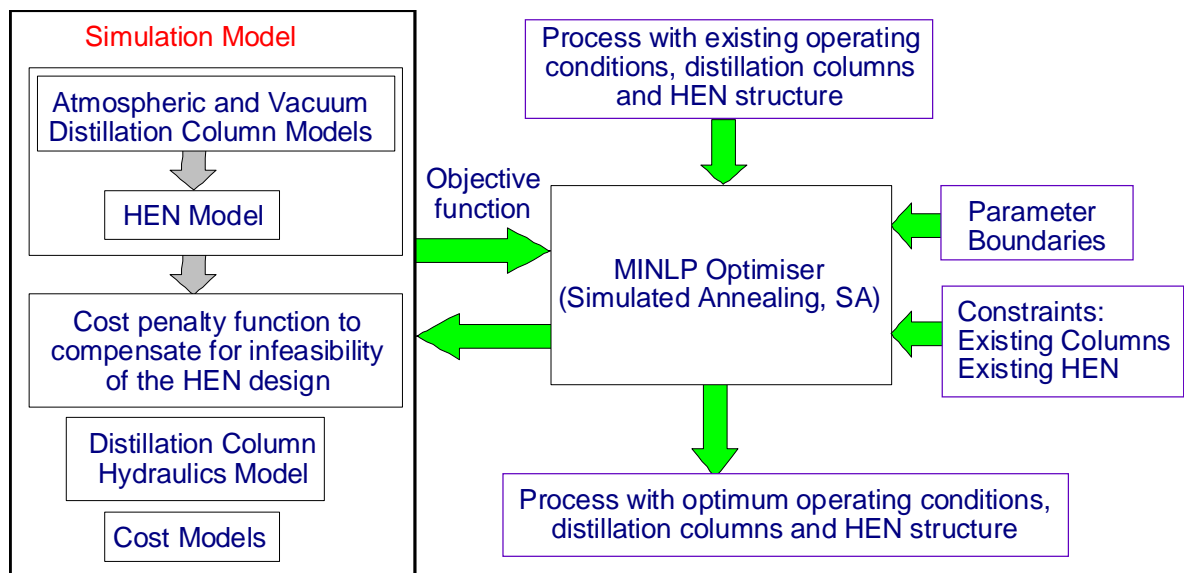


Figure 2.4 Optimisation framework for heat-integrated distillation system (Rastogi, 2006)

2.4 Conclusions

It can be seen that although various approaches and design methodologies have been proposed for the design of crude oil distillation columns and the associated preheat train, there are still limitations. The main features and limitations of the reviewed design approaches and models are summarised as following:

1. Simplified models and rigorous models of distillation columns have advantages and disadvantages. Simplified models are less accurate, but are more robustness in terms of convergence. Rigorous models may be efficient when used for simulating complex crude oil distillation columns; however, they require longer computational time and more sensible initial guess of variables. Hence, Simplified models are more appropriate to serve in the optimisation of crude oil distillation columns.

2. Simplified models are available for grassroots design and retrofit design of atmospheric distillation columns and vacuum columns (Suphanit, 1999; Gadalla, *et al.* 2003a; Rastogi, 2006). Refining products are normally specified in boiling point temperatures, which is different from general chemical mixtures. The existing approach of selecting key components and recoveries (Gadalla *et al.*, 2002a) is based on a rigorously simulated pseudo-components mass balance. Trial and error is required in the selection procedure and user judgements are needed. Moreover, effect of pump-around location (with respect to side-draw stage) on the separation performance of atmospheric column is neglected. No models have been developed for the industrially-relevant atmospheric column with a pump-around located above the top side-stripper.
3. Although there are intense research in the synthesis of heat exchanger networks, most of them are based on the constant thermal properties assumption, which is not valid in the design of preheat trains. The network pinch approach (Asante and Zhu, 1996) is a very promising retrofit design methodology, which combines the pinch analysis method and mathematical programming method. However, the underlying constant thermal property assumption limits its usage. Another drawback is that stream split fractions are kept fixed during the heat recovery maximisation in the diagnosis stage. The sequential mode of the diagnosis stage and the cost-optimisation stage may miss cost-effective designs. The approach of Rodriguez (2005) considers relative level of details in the design of HENs and it is computational efficient. However, variation of thermal properties of process streams is also neglected.
4. Although Rastogi (2006) developed an approach which can consider effectively the interactions between the distillation columns and the heat exchanger network in the same design framework, the heat integration is accounted for assuming constant thermal properties with temperature. The accuracy of the heat integration is compromised.
5. The design approach of heat-integrated crude oil distillation systems presented by Rastogi (2006) is able to optimise both operating conditions and structural options of distillation columns and preheat trains at the same time. In retrofit

design, the capacities of existing equipments are considered and various practical constraints are taken into account. However, product properties are not constrained in both grassroots design and retrofit design.

6. There is no approach available to exploit systematically the product distributions and product slate of crude oil distillation columns. The effect of operating pressure on both the separation and heat recovery potential in grassroots design is not addressed in existing research.

The above limitations of existing design methods and the importance of crude oil distillation process in the refining industry motivate the present work. The main aim is to develop a systematic approach for the design of crude oil distillation columns and the associated heat exchanger network. The design approach should exploit various degrees of freedom in distillation columns and heat exchanger networks, and account for the heat integration accurately. The generated design should meet product specifications, and other practical constraints. In order to achieve this target, accurate and robust models for distillation columns and heat exchanger network will be developed and the over all design framework will be created.

CHAPTER 3 SIMPLIFIED MODELLING OF CRUDE OIL DISTILLATION COLUMNS

3.1 Introduction

The crude oil distillation process is of great importance in the refining industry as a first step to separate the crude into fractions. The crude oil is heated in a set of exchanger units prior to enter the preflash drum or prefractionator to separate the light components to the column. These units exchange heat with the hot streams from the products and pump-around streams. Then the crude oil is further heated in a furnace before feeding into the atmospheric column.

The atmospheric column has a very complex structure, including side strippers, which strip the lighter components from the products and pump-arounds or pump-backs, which provide intermediate reflux and heat recovery opportunity for the whole system by exchanging heat between the pump-around or pump-back streams with cold crude in preheat train. The products are either stored for use or further processed in the stabiliser and vacuum column.

The vacuum column processes atmospheric residue and produces different grades of gas oil and vacuum residue.

There are many issues to consider in designing these complex columns, such as: choice of the stripping steam flow rates, feed preheating temperatures and reflux ratios for the specified separation; appropriate places of locating pump-arounds or pump-backs and how to operate them (flow rate and temperature-drop), *etc.* Besides the columns, there is a preheat train, which is strongly interlinked to the columns. The cooling and heating duties of the preheat train are determined by the distillation columns. How to operate the distillation columns is of prime importance, which not only affects the separation performance itself but also decides the energy consumption of the system. Optimisation is necessary to exploit these design issues for performance enhancement. To optimise operating conditions of the distillation columns, robust and computationally efficient models are necessary. This chapter

proposes simplified models of distillation columns for the design and analysis of crude oil distillation system. The new models include refining product specifications and consider the effect of different pump-around locations on separation in atmospheric units. Moreover, simplified model for the industrially-relevant atmospheric distillation unit with a pump-around located above the top side-stripper is developed.

3.2 Modelling of columns with refining product specifications

Due to the large number of components of crude oil, it is impossible to treat crude and its fractions as mixtures of distinct chemical components. Different characterisation methods are applied in industry. In refinery distillation design and analysis, two terms are used to define the product composition and the degree of the separation between each pair of adjacent fractions. These terms are the cut point temperature and temperature gap, and they are calculated from the boiling curves of the petroleum fractions. The cut point temperature and temperature gap are defined as follows (Watkins, 1979) and illustrated in Figure 3.1a.

- *Cut point* = $\frac{1}{2}$ [(boiling curve final temperature of light fraction) + (boiling curve initial temperature of heavy fraction)]
- *Temperature gap* = (boiling temperature of 95% of light fraction) - (boiling temperature of 5% of heavy fraction)

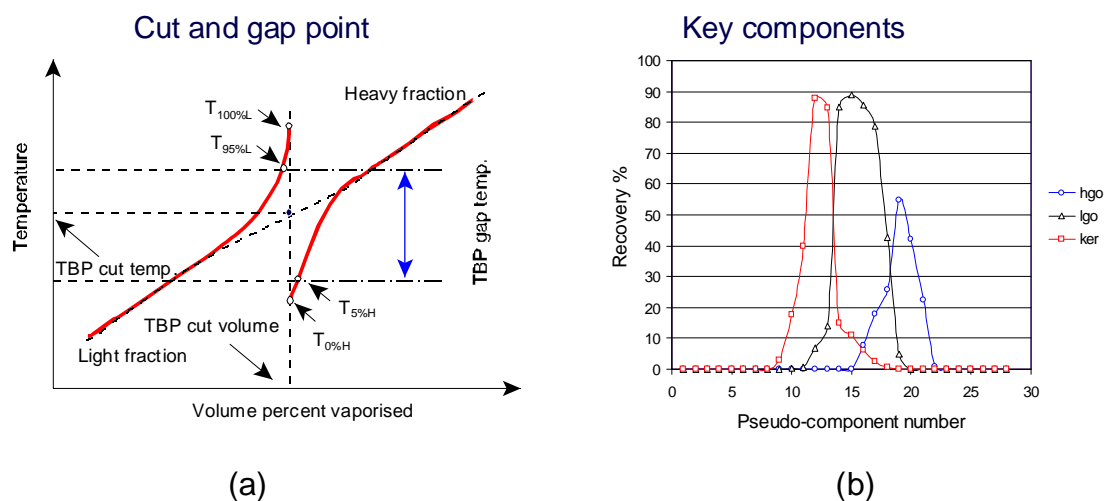


Figure 3.1 Specification of separation of crude oil distillation columns in the refining industry and simplified modelling

(a) Specification of separation in the refining industry

(b) Specification of separation in simplified models.

hgo: Heavy gas oil ; lgo: Light gas oil; ker: Kerosene

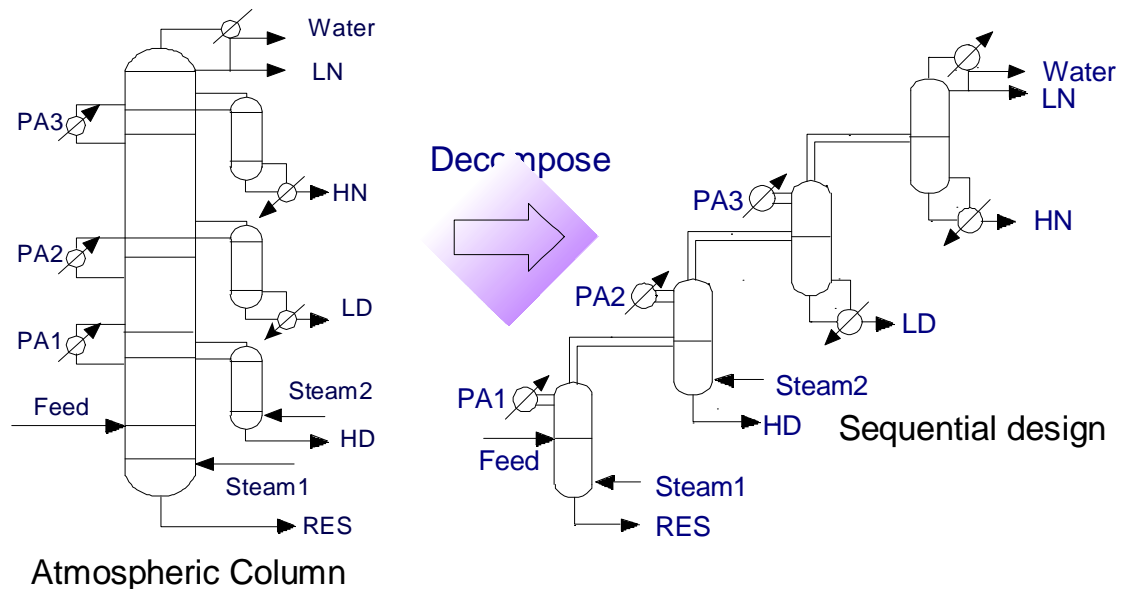


Figure 3.2 Decomposition of atmospheric tower (Liebmann, 1996)

As discussed in the literature review (Section 2.3), a column decomposition approach was developed by Liebmann (1996) for the design and analysis of atmospheric columns. Figure 3.2 shows that a complex atmospheric tower is decomposed into an indirect sequence of thermally coupled simple columns at the draw stage of each side-stripper. The decomposition approach reduces the complexity of atmospheric distillation unit and allows simplified modelling of this unit since simplified models can only be applied to simple columns.

As discussed in the literature review (Section 2.1.1), simplified models are well established for the design of crude oil distillation columns. However, as shown in Figure 3.1b, the simplified modelling of distillation columns requires key components and associated recoveries to specify the separation. In the refining industry, product specifications of the distillation process are conventionally expressed by product flow rates and boiling curve properties. Considering the different separation specification schemes used in the refining industry and simplified models, these models cannot be applied to refining processes directly.

In this section, a new methodology is developed to include conventional product specifications in simplified models, which require the specification of key components and recoveries for the design and optimisation of crude oil distillation columns. The methodology for simple columns is discussed first. Then the method of including product specifications in simplified modelling of a sequence of simple columns is presented.

3.2.1 The existing method and the limitations

Gadalla *et al.* (2002a) developed a method to transform the traditional product specifications of crude oil columns (cut point and 5-95 temperature gap) to key components and their corresponding recoveries in each column section. The steps of identifying the proper key components and recoveries are as follows:

- Specify the separation of crude oil in terms of cut and gap points according to the True Boiling Point (TBP) curve of the crude oil
- Rigorously simulate the existing crude oil distillation column to meet the given specification for each product
- Obtain data that represent the composition of each product from the rigorous simulation results
- For each product, calculate the recovery of each pseudo-component with respect to the feed to the column
- Identify potential light and heavy key components for each product
- Decompose the column into the equivalent simple sequence
- For each simple column in this sequence, calculate the recovery of the light and heavy components for the top and bottom products based on mass balance
- The key components are selected to give good agreement between the rigorous and short-cut models by trial and error

As illustrated above, this approach is based on a rigorously computed component mass balance. The limitation is that rigorous simulation of the existing distillation column is required. The problem with this requirement is that the crude oil distillation must be designed first, which is only suitable for retrofit design, and the rigorous calculation will require more calculation effort than simplified modelling only.

Moreover, the identification of key components and recoveries is not carried out in an automatic way, in which complex procedures and user judgement are required. This work presents a new methodology to overcome these limitations so that product specifications are allowed in simplified models in a straightforward and automatic way. In this work, products are specified in terms of their flow rates and three true boiling points. The reasons of selecting these specifications will be discussed in next section.

3.2.2 True boiling curve calculations

There are several types of boiling point curves, such as true boiling point curve (TBP), ASTM D86, D86 Crack Reduced, ASTM D1160, ASTM_D2887, *etc.* The differences between these types of curves are that they are measured using different equipment and under different conditions. Among them, TBP is the easiest one to calculate (Nelson, 1958), and the correlations for converting it into other boiling curves are well developed and successfully incorporated in commercial software packages such as HYSYS. Nelson (1958) suggested a method for the calculation of TBP curve as the plot of individual boiling point of hydrocarbon compounds in an ascending order against the cumulative volume percentage. In the design and simulation of crude oil distillation processes, pseudo-components are used, which are groups of hydrocarbon compounds. Similar, the TBP curve of a particular crude oil and its products can also be calculated according to this method by plotting the normal boiling temperatures of the pseudo-components against their corresponding cumulative volume percentage in an ascending order. For simplicity, molar percentage is used in current work. If volume percentage or mass percentage is required in the TBP curve, they can be easily obtained from the molar composition given density and molecular weight of the mixture. The detailed calculation procedure is as follows:

- Arrange the pseudo-components in an ascending order according to their normal boiling temperatures.
- Calculate the cumulative molar percentage of each component (sum of the composition from the lightest component to the current component).

- According to the definition of pseudo-component, additional points (cumulative molar percentage and boiling temperature) are made by using cumulative percentage of the adjacent lighter pseudo-component and boiling temperature of the heavier component. The midpoints between two adjacent points are calculated and taken as basis points for generation of TBP curve, marked as cross in Figure 3.3.
- Interpolate or extrapolate the above data as necessary to generate the full range of curve. Then the temperature point where a particular percentage of liquid is vaporised can be read.

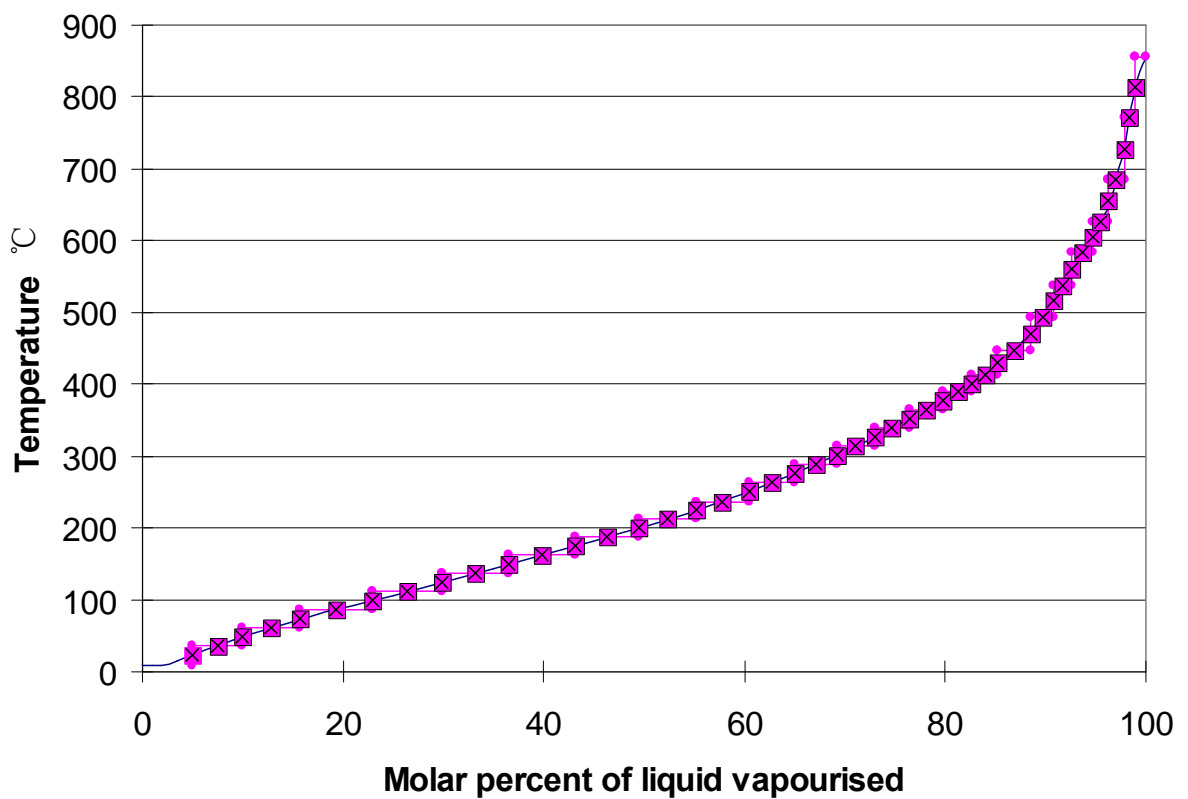


Figure 3.3 TBP curve calculation

In this work, three TBP points and the flow rate are used to specify a product. These three points are the temperature at which 5%, 50% and 95% of liquid is vaporised. They will be referred as T_5 , T_{50} and T_{95} in following discussion. These three TBP points are used to control the property of a particular product and flow rate is employed to control the quantity of the product. The reasons of selecting these three TBP points are that T_5 and T_{95} are linked to temperature gap, which is the indication of crude oil separation quality in the refining industry and T_{50} is to control the middle

point of a boiling point curve and then the shape of the curve. Other boiling temperature points or even bulk properties can be selected as specifications if needed, without affecting the application of the proposed methodology for allowing product specifications in simplified models. As long as a total number of four specifications are selected for a product, the proposed methodology can be applied.

3.2.3 Methodology for simple columns

In the case of simple columns, there are one feed and two products: distillate and bottom product. Let us use the simple distillation column shown in Figure 2.2 to present this method, given feed condition, reflux ratio and distillate specification, in terms of flow rate of the distillate (D) or bottom (B) and three TBP points at which 5%, 50% and 95% of the liquid distillate or bottom is vaporised ($T5'_{top(bottom)}$, $T50'_{top(bottom)}$, $T95'_{top(bottom)}$). Note that given the feed, only one of the top or bottom product needs to specify since the property and flow rate of the rest one can be determined by mass balance.

According to the feature of the simplified model, recoveries of key components are used to specify the separation in a distillation column (see Section 2.1.1 for more detailed review of simplified models). The independent variables concerning about separation in simplified models are: light key component (LK), heavy key component (HK), light key recovery (R_{LK}) and heavy key recovery (R_{HK}). Once a set of LK , HK , R_{LK} and R_{HK} is chosen, the flow rate and pseudo-component composition of the distillate can be calculated by applying the simplified models. Known the compositions, $T5$, $T50$ and $T95$ of the distillate can be calculated based on the method presented in last section (Section 3.2.2). Then the problem becomes solving the following design specification problem, given by:

$$\mathbf{F}(\mathbf{x}) = [f_1(\mathbf{x}), f_2(\mathbf{x}), f_3(\mathbf{x}), f_4(\mathbf{x})]^T = \mathbf{0} \quad (3.1)$$

$$\begin{aligned} f_1(\mathbf{x}) &= T5_{top(bottom)} - T5'_{top(bottom)} \\ f_2(\mathbf{x}) &= T50_{top(bottom)} - T50'_{top(bottom)} \\ f_3(\mathbf{x}) &= T95_{top(bottom)} - T95'_{top(bottom)} \\ f_4(\mathbf{x}) &= (D - D') \text{ or } (B - B') \end{aligned}$$

Where

and $\mathbf{x} = [x_1, x_2, x_3, x_4]^T$, x_1 and x_2 denotes LK and HK , x_3 and x_4 denotes R_{LK} and R_{HK} .

Note that as simplified models and the method presented in Section 3.2.2 are used to calculate the flow rate, $T5$, $T50$ and $T95$ of a product for a set of LK , HK , R_{LK} and R_{HK} , complex and iterative calculations are needed in obtaining $\mathbf{F}(\mathbf{x})$. The formulation of $\mathbf{F}(\mathbf{x})$ is not easy to write, and it is more suitable to treat it as a black-box problem. In Equation 3.1, x_1 , x_2 , are treated as continuous variables, although the selection of key components in simplified models are integer variables. They are rounded up to integers when used simplified models. Treating LK and HK as continuous variables, the design specification problem is formulated as a non-linear problem. The approach for identification of key components and recoveries in simple columns is summarised in Figure 3.4.

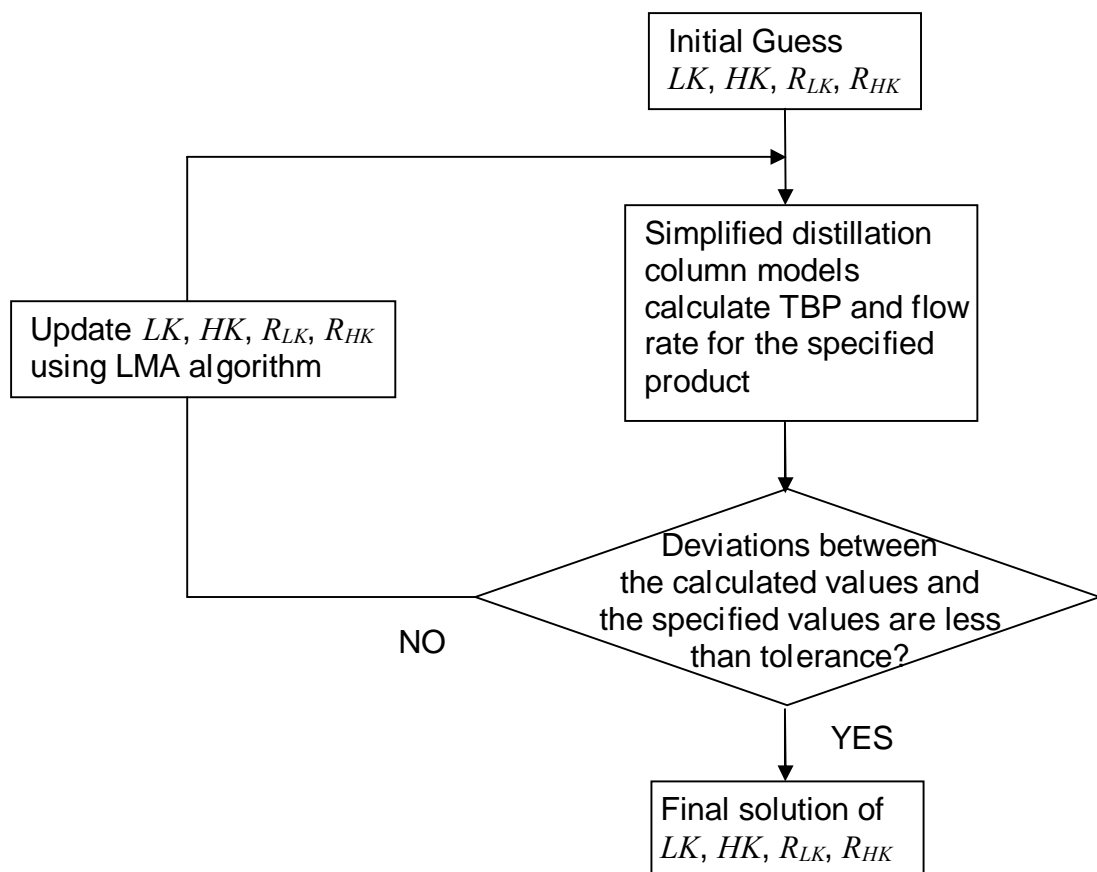


Figure 3.4 Method for identifying key components and recoveries in simple columns given product specifications

As shown in Figure 3.4, the non-linear problem is solved numerically by Levenberg-Marquardt Algorithm (LMA). The LMA algorithm is selected because of the following reasons:

- The LMA algorithm is a Quasi-Newton method, which has a fast local convergence.
- Second derivatives of the problem is not required, calculation effort can be reduced, compared with standard Newton method.
- The usage of a damping factor λ helps to adjust the increment ($\Delta \mathbf{x}$) in the searching process of the solution. The searching process can then be speed up, especially in the space that close to the final solution.

The LMA algorithm is visualised in Figure 3.5. The searching process starts with an initial guess of \mathbf{x}^0 , then $\mathbf{F}(\mathbf{x}^0)$ is calculated by simplified distillation column models and the TBP calculation method. The Jacobian matrix $\mathbf{J}(\mathbf{x}^0)$ is then calculated numerically since $\mathbf{F}(\mathbf{x})$ is treated as a black-box problem. The searching direction and length of the step $\Delta \mathbf{x}$ is determined by solving $(\mathbf{J}^T \mathbf{J} + \lambda \mathbf{I}) \Delta \mathbf{x} = -\mathbf{J}^T \mathbf{F}$. The searching process stops until the final solution is found. The setting of initial damping factor λ^0 and μ are more or less experimental and problem specific (Marquardt, 1963). In this work, these values are taken as 0.001 and 10.0 respectively based on trial and error.

Note that due to the non-linear characteristic of this design specification problem, a sensible initialisation of the key components and recoveries is necessary. Given a poor initial guess, the searching process may fail to find the solution. If this happens, another initial guess is required.

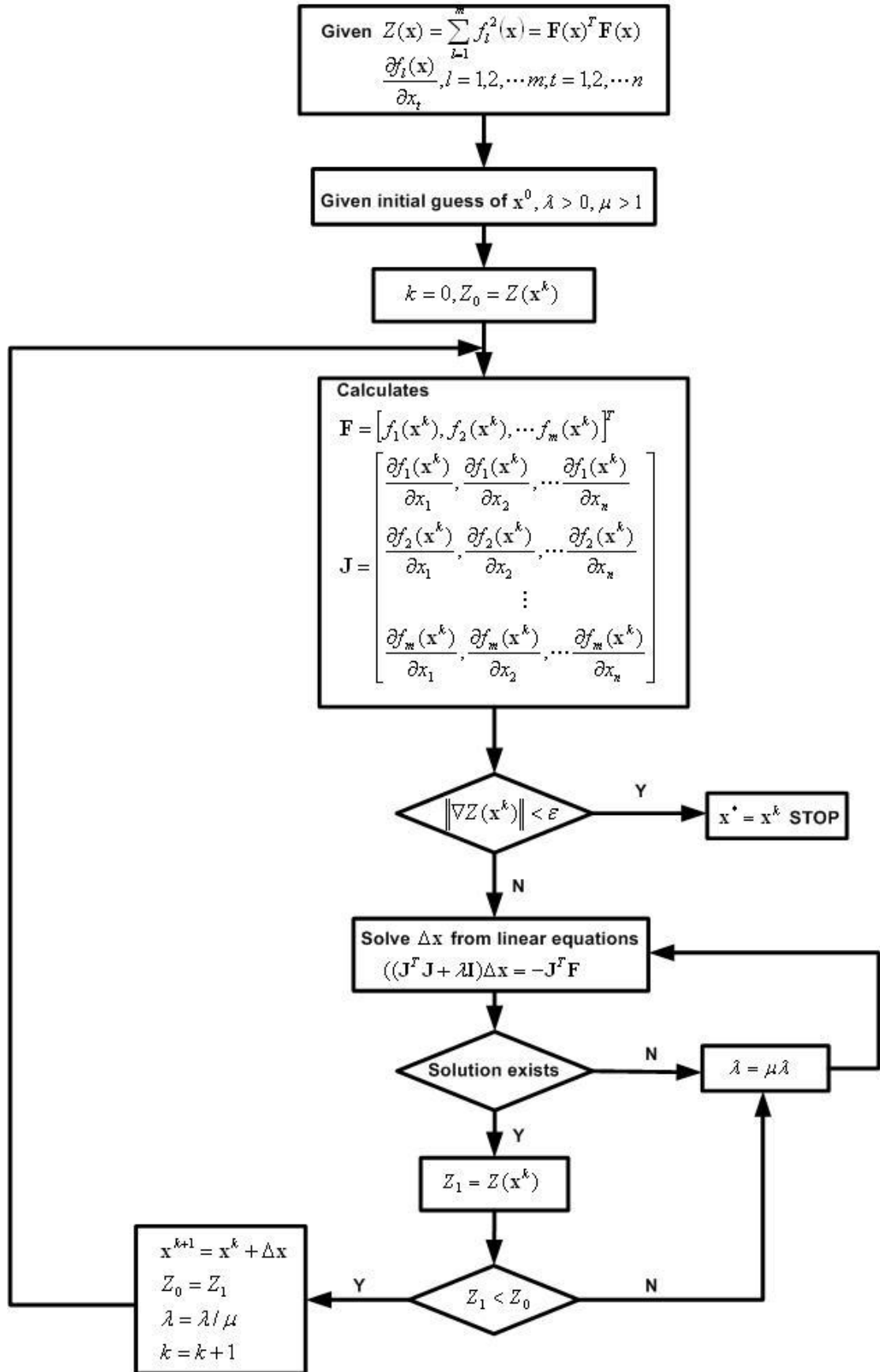


Figure 3.5 Levenberg-Marquardt algorithm (Gill *et al.*, 1978)

3.2.4 Illustrative example 3.1: Simple distillation column

The simple column studied in this example is the first column in an indirect sequence of columns obtained from applying the decomposition approach of Liebmann (1996) to an atmospheric distillation column. The distillation column configuration is shown in Figure 3.2, which also shows the equivalent sequence of four thermally coupled columns. The crude oil is fed to the atmospheric column, also fed to the first column in the decomposed sequence. The crude oil is the same as that in the work of Suphanit (1999), following one example in the textbook of Watkins (1979). The TBP data of the crude oil are given in Table 3.1. This assay is cut into 25 pseudo-components using the oil characterisation technique embedded in HYSYS process simulator (version 2004.2). The physical and thermodynamic properties (i.e. molecular weight, vapour pressure, boiling temperature, critical properties, etc.) of each pseudo-component are also calculated by the simulator.

The compositions and normal boiling temperatures of these components are listed in Table 3.2. The feed conditions, product specifications and tolerances are shown in Table 3.3. The initial guess of key components and recoveries for this column are taken from that suggested in the work of Suphanit (1999); the values are given in Table 3.3.

Table 3.1 Crude oil assay data

% Distilled (by volume)	TBP (°C)
0	-3.0
5	63.5
10	101.7
30	221.8
50	336.9
70	462.9
90	680.4
95	787.2
100	894.0

Density: 865.4 kg/m³

The key components and recoveries that meet the product specifications are shown in Table 3.4 after four iterations of calculation. It is clear that these key components and recoveries are much different from the suggested values.

Table 3.2 Feed composition of crude oil mixture (derived from assay data)

Component Number	NBP (°C)	Composition (mole fraction)
1	9	0.0503
2	36	0.0489
3	61	0.0583
4	87	0.0711
5	111	0.0701
6	136	0.0668
7	162	0.0655
8	187	0.0631
9	212	0.0585
10	237	0.0517
11	263	0.0464
12	288	0.0414
13	313	0.0375
14	339	0.0354
15	364	0.0328
16	389	0.0294
17	414	0.0257
18	447	0.0329
19	493	0.0220
20	538	0.0184
21	584	0.0209
22	625	0.0156
23	684	0.0159
24	772	0.0113
25	855	0.0103

Table 3.3 Feed data, product specifications, tolerances and initial guess of key components and recoveries

Feed conditions	
Preheated temperature (°C)	372.3
Pressure (bar)	2.25
Flow rate (kmol/h)	2610
Product specifications (Bottom)	
Flow rate (kmol/h)	571.0
T5 (°C, TBP)	319.8
T50 (°C, TBP)	483.3
T95 (°C, TBP)	809.8
Tolerance	
Temperature (°C)	3
Flow rate, with respect to the specified product	1%
Initial guess of key components and recoveries	
Light key	13
Heavy key	16
Light key component recovery	0.98
Heavy key component recovery	0.98

Table 3.4 Final solutions of key components and r ecoveries

Light key	11
Heavy key	18
Light key component r ecovery	0.964
Heavy key component r ecovery	0.984

The history of searching for the key components and recoveries and the deviation between the current solution and the specifications are shown in Figure 3.6. It can be seen from Figure 3.6 that the method converges in very few iterations. Note that if tighter tolerance is used, more iterations may be needed.

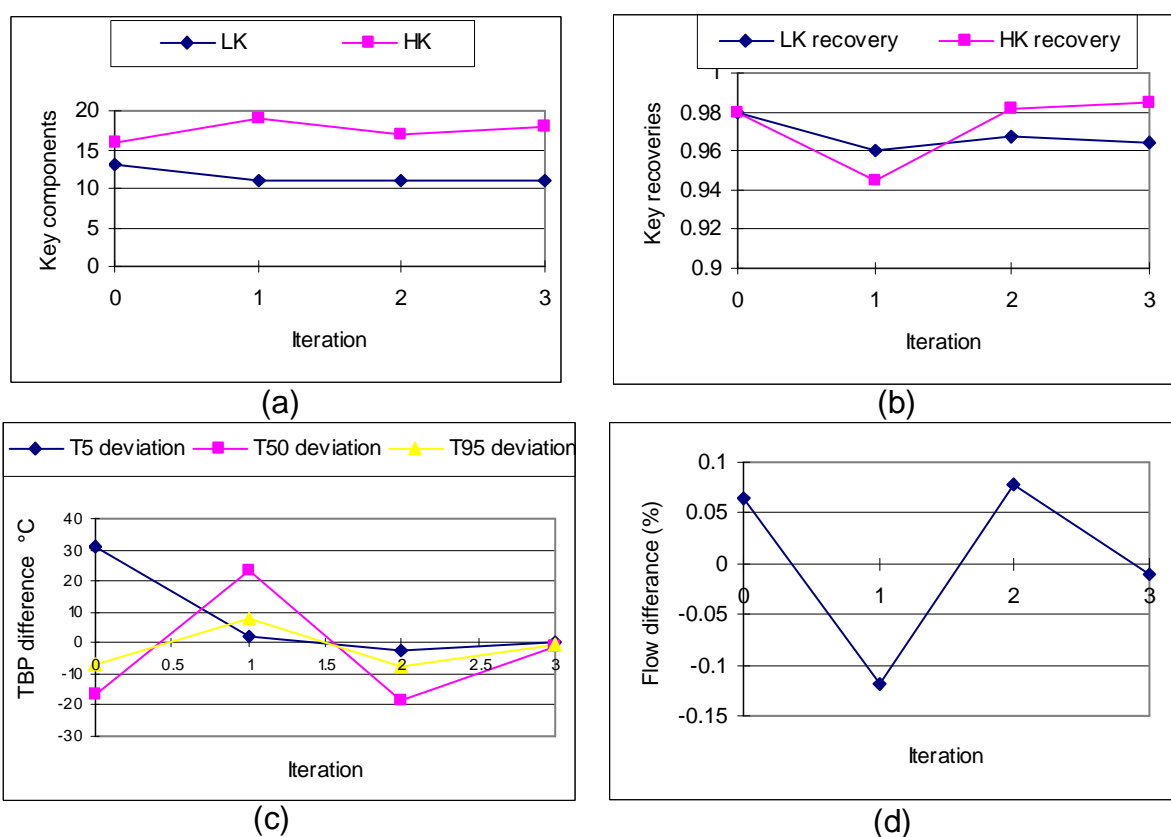


Figure 3.6 Calculation history

(a) Light key (LK) and heavy key (HK) component searching history; (b) Key component recoveries searching history; (c) TBP deviation between the current solution and the specifications; (d) Flow rate deviation between the current solution and the specified value, in percentage.

3.2.5 Methodology for a sequence of simple columns

For a sequence of simple columns, the methodology is analogous to that of simple columns. The procedure is explained as following:

- Assuming there are N_{COL} simple columns in a sequence, specify N_{COL} products by using three points on TBP curve, $T5'_j$, $T50'_j$, $T95'_j$ and flow rate $PROD'_j$ for each product j , $j = 1, 2, \dots, N_{COL}$. Note that in a sequence of N_{COL} simple columns, the number of products is equal to $(N_{COL} + 1)$. Given the feed, only N_{COL} products need to specify, the remaining one is fixed according to mass balance.
- Give an initial guess of LK , HK , R_{LK} and R_{HK} for each column to start the calculation
- Let $\mathbf{x} = [x_{4i+1}, x_{4i+2}, x_{4i+3}, x_{4i+4}]^T$, x_{4i+1} and x_{4i+2} denote LK and HK of column i , x_{4i+3} and x_{4i+4} denote R_{LK} and R_{HK} of the column i , $i = 1, 2, \dots, N_{COL}$

$$\mathbf{F}(\mathbf{x}) = [f_{4j+1}, f_{4j+2}, f_{4j+3}, f_{4j+4}]^T \quad (3.2)$$

$$\begin{aligned} f_{4j+1} &= T5'_j - T5'_j \\ f_{4j+2} &= T50'_j - T95'_j \\ f_{4j+3} &= T95'_j - T95'_j \\ f_{4j+4} &= PROD'_j - PROD'_j \end{aligned}$$

Where

- Solving specification problem $\mathbf{F}(\mathbf{x}) = \mathbf{0}$ using the LMA algorithm

The following illustrative example demonstrates this new methodology of identifying key components and recoveries systematically in simplified models of distillation columns given product specifications in terms of TBP properties and flow rates.

3.3.6 Illustrative example 3.2: Atmospheric distillation column

Given product specifications, the new methodology of systematically selecting key components and associated recoveries is applied to the same atmospheric distillation column as presented in Example 3.1. Example 3.1 presents only the first column of the equivalent indirect sequence of simple columns decomposed from the atmospheric distillation column. The assay data of the crude oil are shown in Table 3.1. Table 3.2 shows the molar composition of the crude in terms of pseudo-components. Table 3.2 also shows the boiling temperature of the pseudo-

components. For simplicity, constant pressure of 2.25 bar in the column is assumed in this example. Superheated steam at 260 °C and 4.5 bar is used as the stripping agent. Other operating conditions, such as the reflux ratio, steam flow rates and the pump-around duties and temperature drops, are shown in Table 3.5.

The four products, residue (RES), heavy distillate (HD), light distillate (LD) and heavy naphtha (HN), are specified in terms of their three TBP points (T5, T50 and T95) and flow rates. The specifications are shown in Table 3.6.

Table 3.5 Specifications of atmospheric crude oil distillation column (Illustrative example 3.2)

Column specifications	Column 1	Column 2	Column 3	Column 4
Feed preheat temp (°C)	372.3	-	-	-
Operating pressure (bar)	2.5	2.5	2.5	2.5
Vaporisation mechanism	Steam	Steam	Reboiler	Reboiler
R / R_{min}	1.85	1.48	1.21	1.08
Steam flow (kmol/h)	95.8	42.2	-	-
Pump-around duty (MW)	12.60	18.95	13.35	-
Pump-around T (°C)	45.2	35.6	45.3	-
Pump-around location (with respect to the side-draw)	1	1	1	-

Table 3.6 Product specifications

Specifications	Products			
	RES	HD	LD	HN
T5 (°C, TBP)	320.2	240.8	176.1	111.0
T50 (°C, TBP)	483.3	334.6	238.0	162.7
T95 (°C, TBP)	809.8	405.5	307.1	207.9
Flow rate (kmol/h)	571.0	291.6	512.3	396.7

The atmospheric distillation unit is simulated as a sequence of simple columns using simplified models with the initial guess of key components and recoveries shown in Table 3.7. The products generated from this initial setting (taken from Suphanit, 1999) are listed in Table 3.8. It can be seen that the products are very different from the specifications. Starting with this guess, and given that no more than 7 °C deviation of TBP is allowed and no more than 4% of flow rate deviation is allowed, the atmospheric distillation unit is simulated again using simplified models with the product specifications of Table 3.6. In the calculation, the design variables, such as the ratio of finite reflux ratio to the minimum reflux ratio (R/R_{min}), steam flow rates and the pump-around duties and temperature drop, are specified. The simplified model

systematically defines the key components and recoveries that meet the product specifications and calculates the required theoretical stages of the columns, the product flow rates and temperatures, pump-around flow rates, reboiler duties of LD stripper and HN stripper and condenser duty. The key components and recoveries that meet the product specifications are listed in Table 3.9, and the corresponding products generated are shown in Table 3.10. The simulation results of the simplified models are summarised in Table 3.12. Table 3.11 presents the calculated number of theoretical stages of columns. Using the number of stages in Table 3.11 as specification, the atmospheric unit is simulated in a rigorous simulation package (HYSYS v2004.2, Aspen Technology Inc.) with the same feed conditions, product specifications and pump-around specifications in terms of flow and temperature drop. The same properties package (Peng Robinson equation of state) is used to calculate physical properties. The rigorous simulation results are listed in Table 3.12, where they are compared with the results of simplified models.

It is clear from Table 3.10 that the new methodology is able to select key components and recoveries systematically and the deviation of products TBP and flow rates are within acceptable range. The results of the simplified models and rigorous models in Table 3.12 are in good agreement: the maximum temperature difference is 4 °C; the product flow differences are within 3%; no significant deviations are observed in duty predications (all within 3%); the difference of pump-around flow rates are less than 7%.

These results validate the approach to systematically identify key components and recoveries in short-cut models from specified product properties and properties. The new methodology allows simplified models to be applied to the simulation of analysis of crude oil distillation columns in the refining industry, where conventional product specifications (cut and gap points) are employed, rather than key components and recoveries. Moreover, the predications of product properties in terms of TBP curve facilitate constraining product properties in the optimisation of the crude oil distillation columns. The operating conditions of the distillation units are exploited without compromising product properties.

Table 3.7 Initial guess of key components and recoveries*

Parameters	Columns			
	1	2	3	4
Light key component	13	11	7	3
Heavy key component	16	14	9	6
Light key recovery	0.98	0.98	0.98	0.98
Heavy key recovery	0.98	0.98	0.98	0.98

*: Key components and recoveries suggested for the modelling of atmospheric unit in the work of Suphanit (1999)

Table 3.8 Product properties and flow rates (Simulation results of using the initial guess of key components and recoveries)

Parameters	Products			
	RES	HD	LD	HN
T5 (°C, TBP)	350.5	292.4	197.3	123.5
T50 (°C, TBP)	467.0	351.0	238.4	154.4
T95 (°C, TBP)	793.5	413.6	298.5	194.1
Flow rate (kmol/h)	607.6	208.2	462.5	361.0

Table 3.9 The key components and recoveries that meet the product specifications

Parameters	Columns			
	1	2	3	4
Light key component	11	10	7	3
Heavy key component	18	13	9	7
Light key recovery	0.974	0.852	0.900	0.980
Heavy key recovery	0.965	0.504	0.770	0.980

Table 3.10 Product properties and flow rates (simulation results applying the key components and recoveries shown in Table 3.8)

Parameters	Products			
	RES	HD	LD	HN
T5 (°C, TBP)	322.7	237.8	178.2	103.8
T50 (°C, TBP)	483.1	336.5	239.9	166.1
T95 (°C, TBP)	809.5	410.5	311.9	210.7
Flow rate (kmol/h)	563.4	284.5	508.6	393.2

Table 3.11 Calculated number of theoretical stages (Illustrative example 3.2)

Column stage distribution	Column 1	Column 2	Column 3	Column 4
Number of stage in rectifying section	5.5	4.8	3.8	6.2
Number of stage in stripping section	5.0	2.0	3.3	3.3

Table 3.12 Atmospheric distillation column simulation results (Illustrative example 3.2)

Parameter	Simplified models	Rigorous models
Product flow (kmol/h)		
Light Naphtha	861.0	834.7
Heavy Naphtha	393.2	396.7
Light Distillate	508.6	512.3
Heavy Distillate	284.5	291.6
Residue	563.4	571.0
Product temperature (°C)		
Light Naphtha	79.7	79.3
Heavy Naphtha	192.6	192.6
Light Distillate	272.7	272.7
Heavy Distillate	294.2	299.0
Residue	365.7	365.4
Pump-around flow (kmol/h)		
Pump-around 1	1142	1161
Pump-around 2	3305	3536
Pump-around 3	2480	2615
Duty (MW)		
LD stripper reboiler	1.66	1.68
HN stripper reboiler	6.79	6.79
Condenser	24.04	23.42

3.3 Pump-around location in atmospheric distillation columns

The locations of pump-around in the atmospheric distillation column impact on the temperatures of the pump-around streams; and it may be beneficial to change the pump-around locations for reducing energy demand, instead of only locating pump-arounds on the side-stripper draw stages. In addition, varying pump-around locations also change the internal reflux, and deteriorate the separation performance if other operating conditions are not changed and stages are fixed. Hence, the locations of pump-around are important degrees of freedom in grassroots and retrofit designs. Modelling of flexible pump-around locations (pump-arounds are not required to be always located on the side-tripper draw stage) in atmospheric distillation column is of great importance.

3.3.1 The existing simplified model and the limitations

Liebmann (1998) developed the decomposition approach for the design and analysis of atmospheric distillation column. In his work, the complex unit is decomposed into

an indirect sequence of simple columns at the side-draw stage of strippers (shown in Figure 3.2). Suphanit (1999) presented simplified models for simple columns and also for the more complex columns with pump-arounds or pump-backs. He introduced one concept of degree of thermal coupling between two simple columns, to facilitate the modelling of pump-arounds and pump-backs. The degree of thermal coupling is defined as the ratio of liquid flow at the top of column with pump-around to that without the pump-around. However, in the work of Suphanit (1999), the assumption that the pump-around must at the top stage of column (in atmospheric unit, the pump-around must be located just below the side-draw stage) was made. Rastogi (2006) extended the approach of Suphanit (1999) to model the atmospheric unit with pump-arounds several stages below the side-draw stage.

In the approach of Rastogi (2006), the atmospheric distillation column is decomposed at the side-stripper draw stages, no matter the location of pump-arounds. As seen in Figure 3.7, for example, pump-around 2 is not at the stage just below the LD side-draw stage; therefore, in decomposed sequence, column 2 does not have the pump-around at the top stage. Then the procedure of modelling the simple column 2 in grassroots design is as following (shown in Figure 3.8):

1. Given feed condition, key components and recoveries LK , HK , R_{LK} , R_{HK} and R/R_{\min} , the simple column is simulated by simplified models without pump-around and the total cooling duty (Q_C) and liquid reflux (L_0) are calculated.
2. The degree of thermal coupling, which is the ratio of liquid reflux flow rate when there is a pump-around (L^*) to that without a pump-around (L_0). Given this degree of freedom, L^* is calculated.
3. The enthalpy balance is applied over envelope 1 (as shown in Figure 3.8) to calculate the hypothetical condenser duty (Q_c^*). Then the pump-around duty (Q_{PA}) is calculated by:

$$Q_{PA} = Q_C - Q_c^* \quad (3.3)$$

4. The composition of liquid L_I , which is in equilibrium with V_I , is calculated.
5. Mass balance and enthalpy balance are performed over envelope 2 (shown in Figure 3.8) to predict the flow rate of L_I , and flow rate and composition of V_2 .
6. Steps 4 and 5 are repeated until the pump-around stage (N_{PA}) is reached.
7. Enthalpy balance is performed over envelope 4 to calculate the pump-around flow rate for the specified temperature drop and Q_{PA} as determined in step 3.

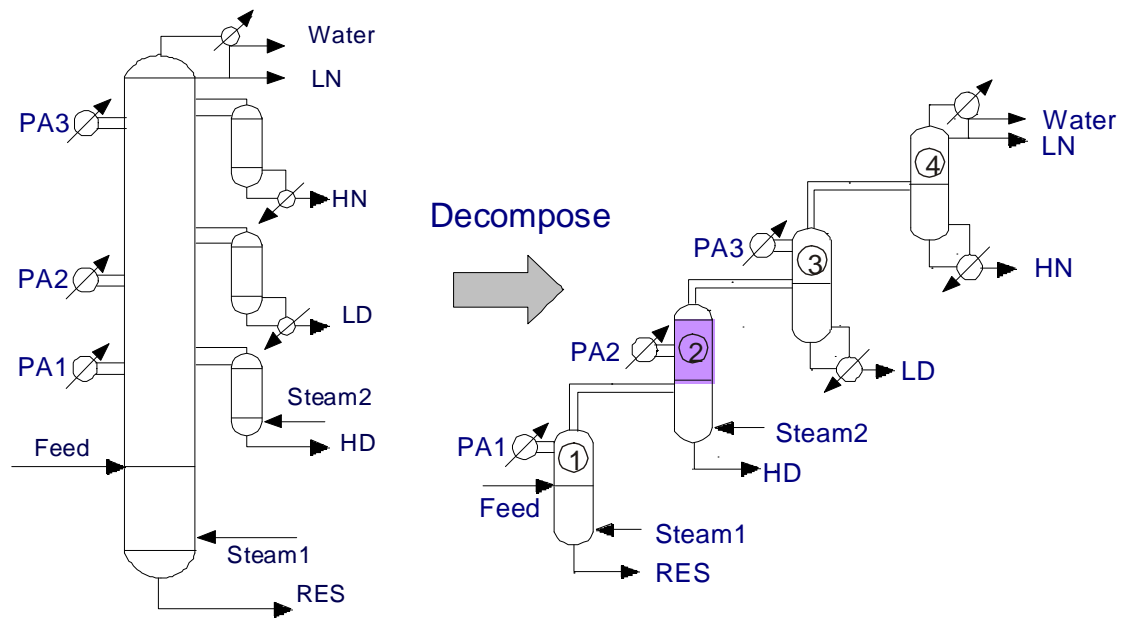


Figure 3.7 Decomposition approach for an atmospheric distillation column

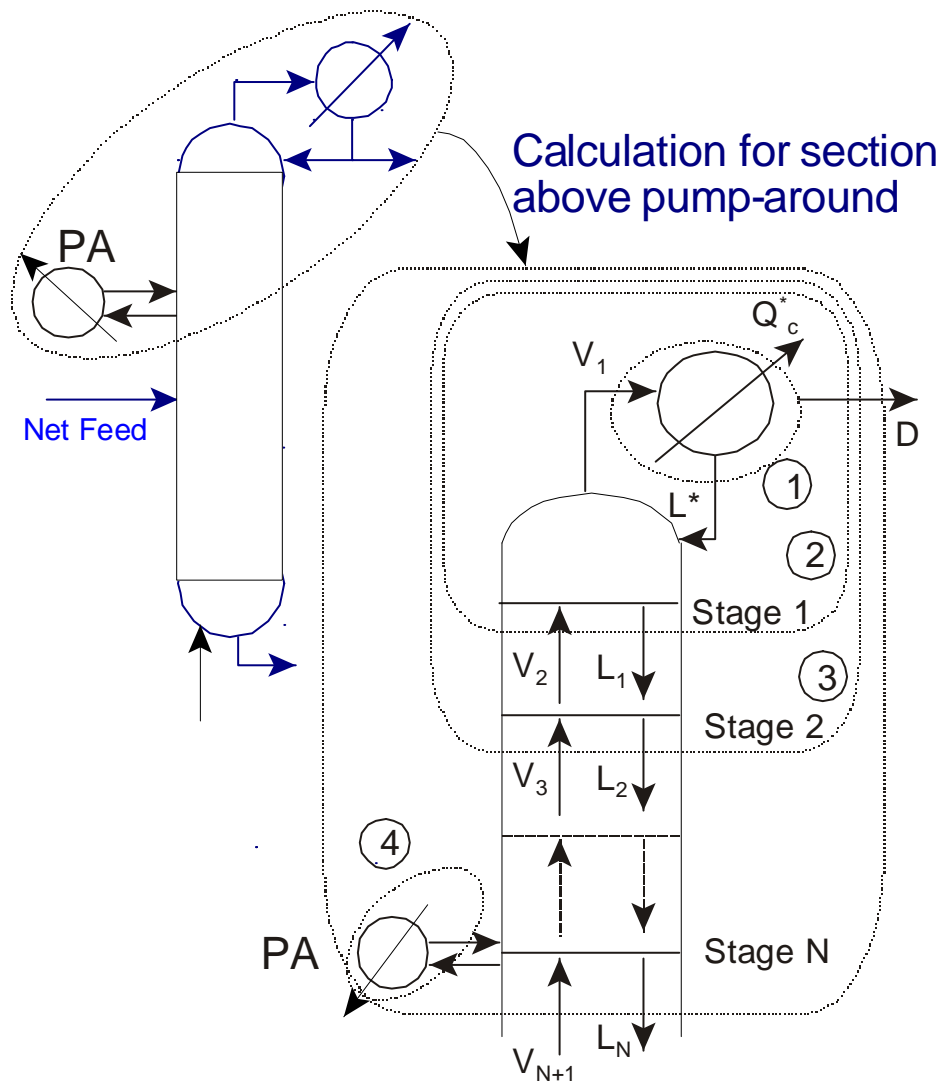


Figure 3.8 Modelling of simple column with pump-around not at the top stage

At this point, the flow rate, duty and temperature of pump-around are calculated. Then, the Fenske equation (Fenske, 1932, cited in Seader and Henley, 1998) is employed to estimate the minimum number of stages in a distillation column as shown in Equation 3.4. In Equation 3.4, the geometric mean relative volatility ($\alpha_{LK(HK)}$) of the top, feed and bottom stage, is used. Given the actual reflux ratio, the corresponding number of stages in a column is determined by Molokanov *et al.* (1972) correlation stated as Equation 3.6.

$$N_{\min} = \frac{\ln \left[\frac{R_{LK} / (1 - R_{LK})}{(1 - R_{HK}) / R_{HK}} \right]}{\ln [\alpha_{LK} / \alpha_{HK}]} \quad (3.4)$$

$$\alpha_{LK(HK)} = \sqrt[3]{\alpha_{LK(HK),Top} \cdot \alpha_{LK(HK),Feed} \cdot \alpha_{LK(HK),bottom}} \quad (3.5)$$

$$\frac{N - N_{\min}}{N + 1} = 1 - \exp \left[\left(\frac{1 + 54.4\xi}{11 + 117.2\xi} \right) \left(\frac{\xi - 1}{\xi^{0.5}} \right) \right] \quad (3.6)$$

where,

$$\xi = \frac{R - R_{\min}}{R + 1} \quad (3.7)$$

Now the number of stages in the column required for a given R is decided, and the number of stages in rectifying section (N_R) and stripping section (N_S) can be identified by applying the Kirkbride correlation (Kirkbride, 1944):

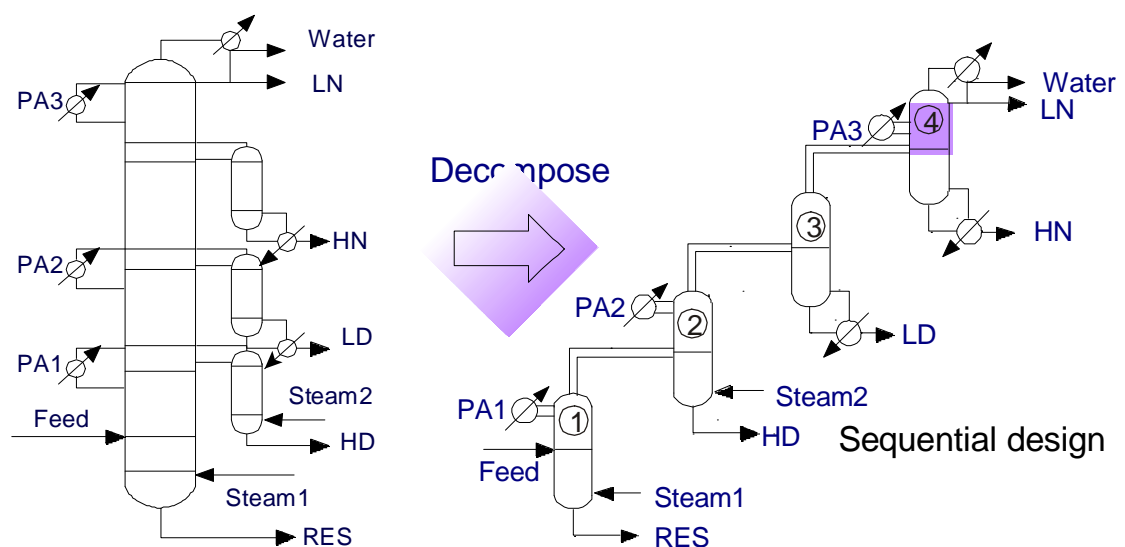
$$\frac{N_R}{N_S} = \left[\left(\frac{B}{D} \right) \left(\frac{x_{fHK}}{x_{fLK}} \right) \left(\frac{x_{bLK}}{x_{dHK}} \right)^2 \right]^{0.206} \quad (3.8)$$

Note that Equation 3.8 is only applied to reboiled columns. In the case of steam stripping columns, N_S is determined by carrying out consecutive flash calculations on each stage from the bottom stage to the feed stage (Suphanit, 1999).

However, because of the existence of pump-around, the internal reflux rate in the section above the pump-around is different from that with no pump-around. Therefore, the Fenske (Fenske, 1932, cited in Seader and Henley, 1998), Gilliland (1940), Kirkbride (1944) equations are not applicable in the rectifying section to

calculate of the number of stages when there is a pump-around. In reality, if the pump-around location is moved down and other operating conditions are fixed in a column, the separation will be deteriorated. More stages will be required if reflux ratio is not increased, compared to that with a pump-around located just below the top stage in a column. This effect on the separation performance while moving down a pump-around is ignored in the existing simplified model. To avoid these inaccuracies in determining the number of stages in the rectifying section, the existing simplified model will be modified.

The existing model of a simple column with a pump-around is based on the concept of the degree of thermal coupling, which is the ratio of liquid reflux flow rate (L_0) when there is a pump-around to that (L^*) without a pump-around. However there is some case that a pump-around is located on a column without thermal coupling with the downstream column. For example (as shown in Figure 3.9), in the atmospheric distillation unit, pump-around 3 (PA3) is above the side-draw stage of HN stripper. If we decompose this configuration using the approach of Liebmann (1996), column 4 of the decomposed sequence has a pump-around and a total condenser, and is not thermally coupled with any downstream columns; therefore, the degree of thermal coupling cannot be specified. In this work, new simplified models are developed for the design and analysis of atmospheric distillation units with a pump-around located above the top side-stripper.



Atmospheric Column
Figure 3.9 Decomposition approach for an atmospheric distillation column with pump-around above HN side stripper

3.3.2 New simplified model to account for the effect of pump-around location on the separation performance

In this section, the existing simplified model is modified to account for the effect of different pump-around location on the separation performance. In the new simplified model, the method of modelling the section above the pump-around is the same as that developed by Rastogi (2006). Then, instead of applying Fenske (Fenske, 1932, cited in Seader and Henley, 1998) equation, Gilliland (1940) and Kirkbride (1944) correlations (Equations 3.4 . 3.8) to determine the number of stages of the rectifying section (N_R) given reflux ratio, a rigorous stage-by-stage calculation is carried out in the rectifying section to determine N_R . The full calculation procedure is described as follows:

1. Given feed condition, key components and recoveries LK , HK , R_{LK} , R_{HK} and R/R_{min} , the simple column is simulated by simplified models without pump-arounds and the total cooling duty (Q_C) and the flow rate of liquid reflux (L_0) are calculated.
2. The degree of thermal coupling, which is the ratio of liquid reflux flow rate when there is a pump-around (L^*) to that without a pump-around (L_0), is specified. Given this degree of freedom, L^* is calculated.
3. The enthalpy balance is applied over envelope 1 (as shown in Figure 3.10) to calculate hypothetical condenser duty (Q_c^*). Then the pump-around duty (Q_{PA}) is calculated by:

$$Q_{PA} = Q_C - Q_c^* \quad (3.9)$$

4. The composition of liquid L_1 , which is in equilibrium with V_1 , is calculated.
5. A mass balance and an enthalpy balance are performed over envelope 2 (shown in Figure 3.10) to determine the flow rate of L_1 , and the flow rate and composition of V_2 .
6. Steps 4 and 5 are repeated until the pump-around stage (N_{PA}) is reached.
7. An enthalpy balance is performed over the pump-around to calculate the pump-around flow rate for a specified temperature drop and Q_{PA} as determined in step 3.
8. Steps 4 and 5 are repeated several stages (for example, 20 or 30 stages) down from the pump-around location. The vapour and liquid phase composition profiles on each stage are compared with the composition of vapour flow fed into the column V_{in} and liquid flow withdrawn from the column L_{out} . The stage (stage M in Figure 3.10)

that matches best is the feed stage (the difference between the composition profiles on stage M and those of the feed is the minimum). The number of stages in the rectifying section is then counted from the top stage to this feed stage.

9. For the number of stage in stripping section, in the case of reboiled column, Equations 3.4 . 3.8 are applied to the stripping section to determine N_S ; and in the case of steam stripping column, a stage-by-stage calculation is performed in the stripping section (Suphanit, 1999).

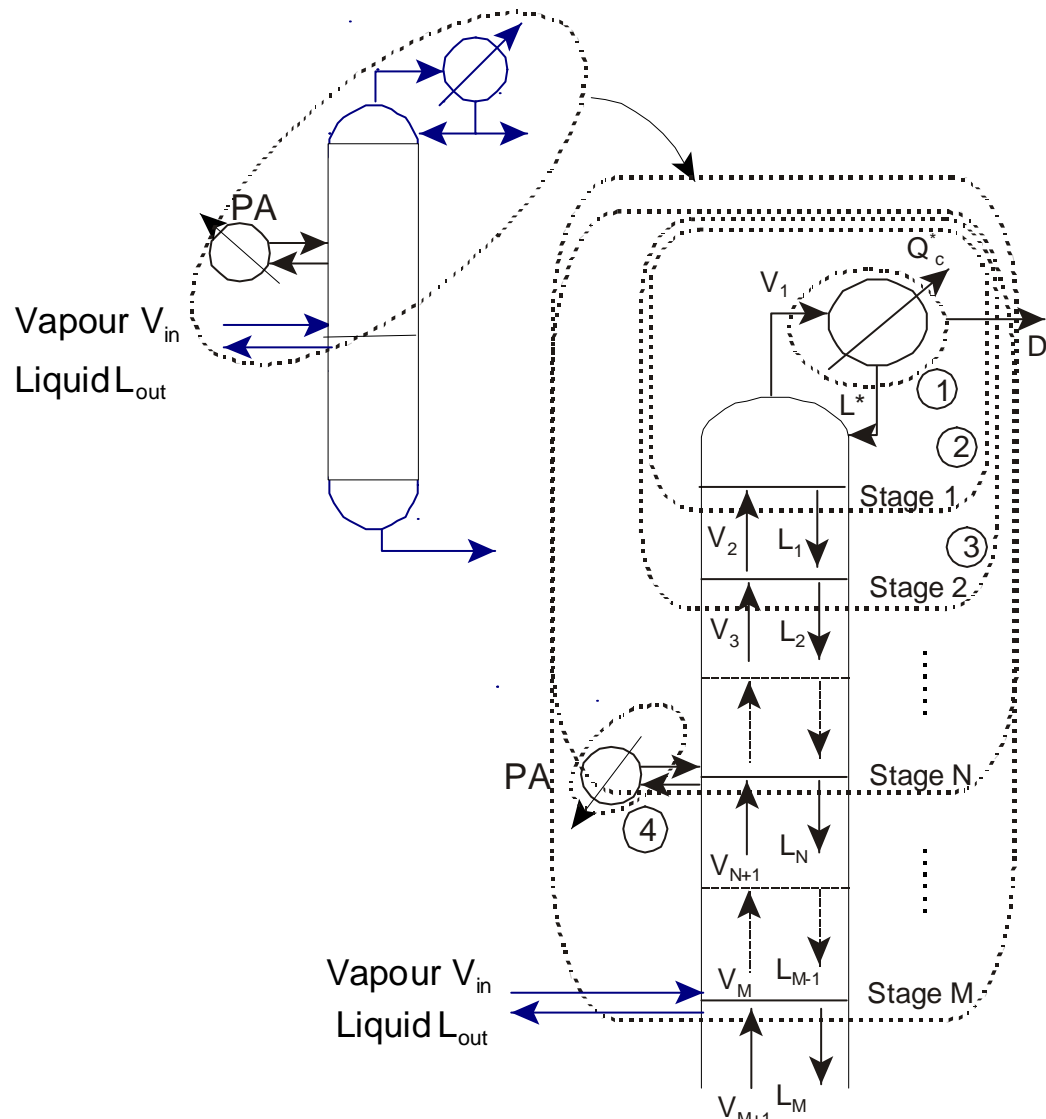


Figure 3.10 New simplified modelling of simple columns with a pump-around not at the top stage

In the case that the simple column is not thermally coupled with the upstream column in a sequence (column 1 of the decomposed sequence in Figure 3.7), no liquid flow is withdrawn from the column, and only a stream is fed to the column, the comparisons in step 8 are made between the liquid compositions profile from the

stage M to the liquid leaving the feed stage calculated from Underwood equation. If pump-around is at the top stage of column, the calculation procedure is that proposed in the work of Suphanit (1999): in the case of reboiled columns, Equations 3.4 . 3.8 are applied in the whole column to calculate N_R and N_S ; in the case of stripping steam columns, Equations 3.4 . 3.8 are applied in the rectifying section to calculate N_R , N_S is calculated by a stage-by-stage calculation in the stripping section.

In this new simplified model of distillation columns, the number of stages in rectifying section will be influenced by the location of pump-around when other design parameters (LK , HK , R_{HK} , R_{LK} , R/R_{min} , Q_{PA} , and temperature drop around the pump-around) are kept the same. This feature allows the effect on the separation to be modelled if pump-around location is moved down while other design parameters are not changed. The exploitation of pump-around location in an atmospheric distillation column is more accurate and reliable due to the rigorous stage-by-stage calculation in the rectifying section. This important degree of freedom can be optimised without compromising the separation in crude oil distillation columns.

Note that the simplified calculation explained above is for grassroots design of a simple column. In the case of retrofit design, the existing number of stages of the simple column is fixed; the key components, the degree of thermal coupling and the temperature drop around the pump-around are specified. The retrofit calculations are carried out as iterative grassroots calculations. R/R_{min} is varied if the recoveries are specified (or recoveries are varied if R/R_{min} is specified) and grassroots simplified model calculates the required number of theoretical stages in the column. The calculations terminate when the calculated and existing number of theoretical stages in the column are equal.

The illustrative example in Section 3.3.3 demonstrates the new simple model.

3.3.3 Illustrative example 3.3: The effect of pump-around location on separation performance in an atmospheric distillation column

The example in the work of Gadalla (2002) is used to demonstrate the effect of pump-around location on the separation performance in atmospheric distillation columns. The atmospheric distillation unit processes 100,000 bbl/day of Tia Juana Light crude (the same as in Illustrative examples 3.1 and 3.2; the crude assay and composition in terms of pseudo-components are listed in Tables 3.1 and 3.2) to produce five products. The configuration of the atmospheric distillation unit is shown as in Figure 3.7, where the corresponding decomposed sequence of simple columns is also shown. The operating conditions in each section of the columns, such as the steam flow rates and the pump-around duties and temperature drop, are specified in Table 3.14.

Different from the work of Gadalla (2002), the study of the crude oil unit is treated as a grassroots design rather than a retrofit design, in order to highlight the effect of pump-around location on the required number of theoretical stages given the separation requirement and reflux ratio. Therefore, the key components and recoveries specified by Gadalla (2002), are kept the same throughout the simulation. Table 3.13 presents the specified key components and recoveries for the decomposed sequence of the atmospheric distillation unit.

Table 3.13 Key components and recoveries in each simple column (Gadalla, 2002)

Parameters	Column			
	1	2	3	4
Light key component	13	11	7	4
Heavy key component	16	14	9	6
Light key recovery	0.995	0.974	0.975	0.992
Heavy key recovery	0.987	0.936	0.947	0.990

Table 3.14 Specifications of atmospheric crude oil distillation column (illustrative example 3.3)

Column specifications	Column 1	Column 2	Column 3	Column 4
Feed preheat temp (°C)	365	-	-	-
Operating pressure (bar)	2.5	2.5	2.5	2.5
Vaporisation mechanism	Steam	Steam	Reboiler	Reboiler
R/R_{min}	1.60	1.17	1.20	1.23
Steam flow (kmol/h)	1200	250	-	-
Pump-around duty (MW)	12.84	17.89	11.20	-
Pump-around T (°C)	30	50	20	-

The atmospheric unit is simulated as the sequence of columns by the simplified model under several scenarios. In each scenario, the location of pump-around 2 (PA2) is changed. Eight scenarios are studied, descriptions of which are given in Table 3.15. In the first scenario, PA2 is located on the stage below the side-draw of LD stripper (configuration as in the work of Gadalla, 2002). In the following scenarios, PA2 location is 1 stage to 7 stages below the side-draw of LD stripper. The corresponding number of stages in the section from the side-draw of LD stripper to the side-draw stage of HD stripper (N_R of column 2 in the sequence of simple columns) is calculated by the new approach and also the approach of Rastogi (2006). The calculated N_R of column 2 in each scenario is shown in Table 3.17.

Table 3.15 Description of different scenarios

Scenario ID	1	2	3	4
PA2 location	Just below side-draw of LD stripper	1 stage below side-draw of LD stripper	2 stages below side-draw of LD stripper	3 stages below side-draw of LD stripper
Scenario ID	5	6	7	8
PA2 location	4 stages below side-draw of LD stripper	5 stages below side-draw of LD stripper	6 stages below side-draw of LD stripper	7 stages below side-draw of LD stripper

It can be seen from Table 3.17 that in column 2, the number of stages required in the rectifying section when PA2 is located one stage below the top stage is the same as that when it is located just below the top stage, which is 10 stages. However, in Scenario 3, 4 and 5, when PA2 is more stages below, N_R increases to 11, and when PA2 is 5 or 6 stages below, 2 more stages are needed to compensate for the decrease in internal reflux rate. This trend continuous when PA2 is moved 7 stages down, where 13 stages are required to achieve the specified separation. The approach of Rastogi (2006) calculates that 10 stages are needed regardless the location of PA2, which means the effect of pump-around location on the separation performance is not account for in that approach.

Moreover, if Pinch Analysis method (Linnhoff and Hindmarsh, 1983) is used to estimate the energy consumption and the corresponding needed heat transfer areas, the energy target (minimum hot and cold utility demand) and area target for the atmospheric distillation unit and the required heat exchanger areas for the associated preheat train can be estimated without design of the heat recovery system. Table 3.16 presents the costs of utility and exchangers. Assuming operating

time is 8600 hours per year and the payback criteria is 2 years, the energy cost and annualised capital cost can be calculated, what are listed in Table 3.17 for all scenarios. Table 3.17 also shows the annualised total cost, which is the sum of utility costs, steam stripping cost and annualised capital cost.

Table 3.16 Utility and exchanger cost (Gadalla, 2002)
(Illustrative example 3.3)

Parameter	Unit cost
Flue gas (1500 . 800°C, \$/kW ^h)	150.0
Cooling water (10 . 40°C, \$/kW ^h)	5.25
A _{cost} (Equation 3.10, \$)	13000
B _{cost} (Equation 3.10, \$)	1530
C _{cost} (Equation 3.10)	0.63

$$\text{Note: } CC = N_{units} \times \left(A_{cost} + B_{cost} \times \left(\frac{Area_{total}}{N_{units}} \right)^{C_{cost}} \right) \quad (3.10)$$

Table 3.17 Simulation results of atmospheric crude oil distillation column with different pump-around locations

Scenario ID	N _R ¹ of column 2	N _R of column 2	Annualised total cost (MM\$)	Utility cost (MM\$)	Annualised column capital cost [*] (MM\$)
1	10	10	18.236	15.362	0.981
2	10	10	18.178	15.311	0.974
3	10	11	18.177	15.301	0.983
4	10	11	18.172	15.297	0.983
5	10	11	18.170	15.294	0.983
6	10	12	18.177	15.292	0.992
7	10	12	18.175	15.290	0.992
8	10	13	18.183	15.289	1.002

1: Simulation results calculated by approach of Rastogi (2006)

2: Simulation results calculated by new approach

*: Column cost = shell cost + tray cost (Guthrie, 1969)

$$\text{Shell cost} = \left(\frac{\text{M \& S Index}}{280} \right) 101.9 (Diam)^{1.066} (H_1)^{0.802} (2.18 + F_c) \quad (3.11)$$

Where

$$F_c = F_m F_p \quad (3.12)$$

$$\text{Tray cost} = \left(\frac{\text{M \& S Index}}{280} \right) 4.7 (Diam)^{1.55} H_2 F_c \quad (3.13)$$

where

$$F_c = F_s + F_t + F_m \quad (3.14)$$

M & S Index: 1333.4 (Chemical Engineering, 2006)

It is clear from the Table 3.17 that as the pump-around is moved down, the capital cost increases as the number of stages required in the rectifying section of column 2 increases. At the same time, the utility costs are reduced due to higher draw temperature of the pump-around flow. The trend of the capital investment and the heat recovery opportunities is opposite. Due to this opposite trend, a peak of the total annualised cost (18.170 MM\$) is observed in Scenario 5, when PA2 is 4 stages below the side-draw of HN stripper. Therefore, in the design problem of atmospheric distillation column, the pump-around locations should be optimised taking into account relevant trade-offs between the capital investment and heat recovery opportunities.

Note that in retrofit study, the structure (number of stages and diameters) of the existing atmospheric distillation unit is fixed. When the existing number of stages cannot achieve the required separation, the reflux rate must be increased. Then the stripping steam or reboiler duty will also be increased correspondingly, increasing the operating cost in turn. Therefore, the locations of pump-arounds are also important degrees of freedom in retrofit design.

3.3.4 Simplified modelling of atmospheric distillation units with a pump-around above the top side-stripper

In some industrial cases, pump-arounds are not at the stage just below or several stages below the draw stage of side-strippers in atmospheric distillation columns. For example (as shown in Figure 3.9), in the atmospheric distillation unit, pump-around 3 (PA3) is above the side-draw stage of the HN stripper. In the approach of Rastogi (2006), only pump-arounds below the draw stage of the HN side-stripper in atmospheric units are accounted for. This section presents models to consider this kind of configuration.

First of all, this configuration is decomposed at the draw stage of each side-stripper. Column 3 does not have a pump-around, while column 4 of the decomposed

sequence has a pump-around and a total condenser, and column 4 is not thermally coupled with any downstream columns. The concept of a degree of thermal coupling does not apply, so pump-around duty is specified in the simplified simulation.

In the simple column with pump-around and no thermal coupling, pump-around duty is specified directly, instead of the degree of thermal coupling. Then the procedure of modelling the simple column 4 is as follows.

1. The simple column is simulated by simplified models without pump-arounds and the total cooling duty (Q_C) and liquid reflux (L_0) are calculated.
2. The pump-around duty (Q_{PA}) is specified, then the hypothetical condenser duty (Q_c^*) is calculated by:

$$Q_c^* = Q_C - Q_{PA} \quad (3.15)$$

3. The internal reflux ratio (R^*) with a pump-around is initialised, and the liquid reflux with a pump-around is calculated according to:

$$L^* = R^* \cdot D \quad (3.16)$$

4. The enthalpy balance is applied over envelope 1 (as shown in Figure 3.9) to calculate the current hypothetical condenser duty under the assumed R^* .
5. The problem then becomes searching for the internal reflux ratio (R^*), which meets the specified hypothetical condenser duty (Q_c^*) calculated in step 2. The problem can be written as:

$$f(R^*) - Q_c^* = 0 \quad (3.17)$$

This is solved by repeating step 3 and 4 with bisection method.

6. Steps 4 . 9 in last section (Section 3.3.2) are carried out.

In step 5, the bisection method is selected because of its robustness in solving non-linear problems with only one variable, though the bisection method has only linear convergence.

The application of the new model is demonstrated in Section 3.3.5 through illustrative example 3.4.

3.3.5 Illustrative example 3.4: The atmospheric distillation column with pump-around located above the top side-stripper

The modelling of pump-around located above the top side-stripper is examined in this example. The atmospheric distillation unit presented in illustrative example 3.2 is studied. The feed conditions are shown in Table 3.3. Table 3.5 lists the product specifications and Table 3.6 summarises the operating conditions of the distillation unit. The configuration of the column is not changed except that one more pump-around is added above the side-draw of heavy naphtha (HN) stripper. The specifications for the new pump-around (PA4) are presented in Table 3.18.

Table 3.18 Specifications for pump-around 4 (PA4)

Location (stage counted from top of atmospheric unit)	3
Duty (MW)	10
Temperature drop (°C)	50

The atmospheric distillation column is simulated as the sequence of simple columns by the short-cut models. The simulation results are listed in Table 3.19. The column is also modelled using rigorous methods in HYSYS v2004.2. The results are compared with the results of simplified models in Table 3.19.

Table 3.19 shows that there are no significant differences between the rigorous results and the short-cut results. The deviations in product flows and pump-around flows are within 3% and 6% respectively. The maximum temperature difference of products and pump-arounds is 6 °C, and the deviations in duties are all less than 5%. These results validate the proposed models, which consider pump-arounds above the top side-tripper in atmospheric distillation unit. For the complex atmospheric distillation unit with three side-strippers and four pump-arounds, and also with a relatively large number of components, the good match as shown here between the simplified model and rigorous model is important.

Comparing this example with the illustrative example 3.2 without PA4, 10 MW is shifted from the condenser to the top pump-around, the draw temperature of which is 25.2 °C higher (126.1 °C compared with 151.3 °C). The potential of heat recovery in the preheat train is increased since the heat extracted from PA4 is at relatively higher temperature than that from the condenser. Although one pump-around is added and the capital cost is increased (for installing the new pump-around, and for adding more number of stages in retrofit design if needed), the resulted design in this example is better than that in illustrative example 3.2 in terms of energy recovery

potential. It may be concluded that the location and number of pump-arounds should be optimised for a better performance of the overall system. The proposed models in this work facilitate the optimisation.

Table 3.19 Atmospheric distillation column simulation results (Illustrative example 3.4)

Parameter	Simplified model	Rigorous model
Product flow (kmol/h)		
Light Naphtha	861.0	834.7
Heavy Naphtha	393.2	396.7
Light Distillate	508.6	512.3
Heavy Distillate	284.5	291.6
Residue	563.4	571.0
Product temperature (°C)		
Light Naphtha	79.7	79.3
Heavy Naphtha	192.6	191.3
Light Distillate	272.7	272.7
Heavy Distillate	294.2	299.0
Residue	365.7	365.4
Pump-around flow (kmol/h)		
Pump-around 1	1142	1161
Pump-around 2	3305	3443
Pump-around 3	2480	2625
Pump-around 4	2617	2518
Pump-around draw temperature (°C)		
Pump-around 1	321.1	323.3
Pump-around 2	246.3	240.0
Pump-around 3	186.0	180.4
Pump-around 4	151.3	148.7
Duty (MW)		
LD stripper reboiler	1.66	1.68
HN stripper reboiler	6.79	6.79
Condenser	14.04	13.48
Top vapour temperature (°C)	126.1	124.2

3.4 Conclusions

This chapter presents the new simplified models of atmospheric distillation columns.

In the new simplified models, given conventional refining product specifications, the key components and associated recoveries are identified systematically without carrying out rigorous simulation. Compared with the existing approach developed by Gadalla *et al.* (2002a), the new method is simple and straightforward; no complex

steps are carried out and no extra user judgments are required. These features of the new approach allow simplified models to be applied to the design and analysis of crude oil distillation columns. The approach is examined in a simple column specifying one product and also in the atmospheric distillation column where more products are specified. By comparison to the simulation results calculated from a rigorous simulation package (HYSYS v2004.2, Aspen Technology Inc.), the accuracy of the simplified models are validated.

The effect of changing pump-around locations on the separation is not accounted for in the existing short-cut models of Rastogi (2006). In this chapter, the simplified models are modified to determine the number of stages in the rectifying section of a simple column more accurately, considering the location of the pump-around. The new model is examined in an illustrative example in which one of the pump-around is moved down by several stages. The results justify the new approach and also show that the locations of pump-arounds are important degrees of freedom, considering the trade-offs between heat recovery potential and the separation performance.

The developed simplified model is further extended to consider the pump-around above the top side-stripper in an atmospheric distillation unit. The new models enhance the flexibility of the number of pump-arounds and their locations. They also facilitate the exploitation of atmospheric distillation unit for lower energy demand in a grassroots problem or to achieve specific target in a retrofit design. The new simplified models are validated by comparison with HYSYS simulation results.

The new models developed in this chapter will be incorporated in the optimisation algorithm to exploit the effect of pump-around location on separation performance. In the optimisation procedure, product properties will be constrained through the boiling points curve calculation presented in this chapter.

CHAPTER 4 HEAT EXCHANGER NETWORK DESIGN FOR PROCESS STREAMS WITH TEMPERATURE- DEPENDENT THERMAL PROPERTIES

4.1 Introduction

Distillation processes in petroleum refineries consume a significant portion of the energy demand of the site, in spite of extensive heat recovery. The crude oil is fractionated into various products in the atmospheric and vacuum columns. Before being fed into these columns, the crude oil or the residue from the atmospheric column needs to be heated up to a specific temperature, while hot product streams and pump-around or pump-back streams of the distillation columns require cooling. Opportunities for heat recovery are intensively exploited in the heat exchanger network. The design of the preheat train determines the matches between hot and cold streams from distillation columns, the number of heat exchanger units and heat transfer areas required for the heat exchanged, and in turn the hot utility and cold utility requirements of the distillation process. Hence, the HEN design is of great importance in crude oil distillation processes and has been received significant attention from academic research and the refining industry, as discussed in the literature review (Section 2.2).

However, in most of the published work (Section 2.2), thermal properties (e.g. heat capacity) of streams were assumed constant with temperature to maintain a linear problem formulation. Figure 4.1 shows the enthalpy. temperature relationship of one particular crude oil. The dashed line assumes average constant heat capacity and the continuous line stands for the varying heat capacity. Heat capacities of crude oil vary because of the large number of components in the crude oil and vaporisations occurring during the heating or cooling process. It can be seen from Figure 4.1 that the largest temperature difference between the two lines is around 30 °C. Clearly, assuming constant thermal property will introduce large inaccuracies when applying the developed HEN design methods to streams with a large temperature range, when the thermal properties are not constant, such as in crude oil refining.

In this chapter, the assumption of constant thermal properties with temperature in HEN design is overcome. Suitable simulation and design methodologies are presented for heat exchanger networks of process streams with temperature-dependent thermal properties. These design methods can be used for both HEN design alone and integrated systems of distillation columns and HEN, as will be seen in Chapter 5.

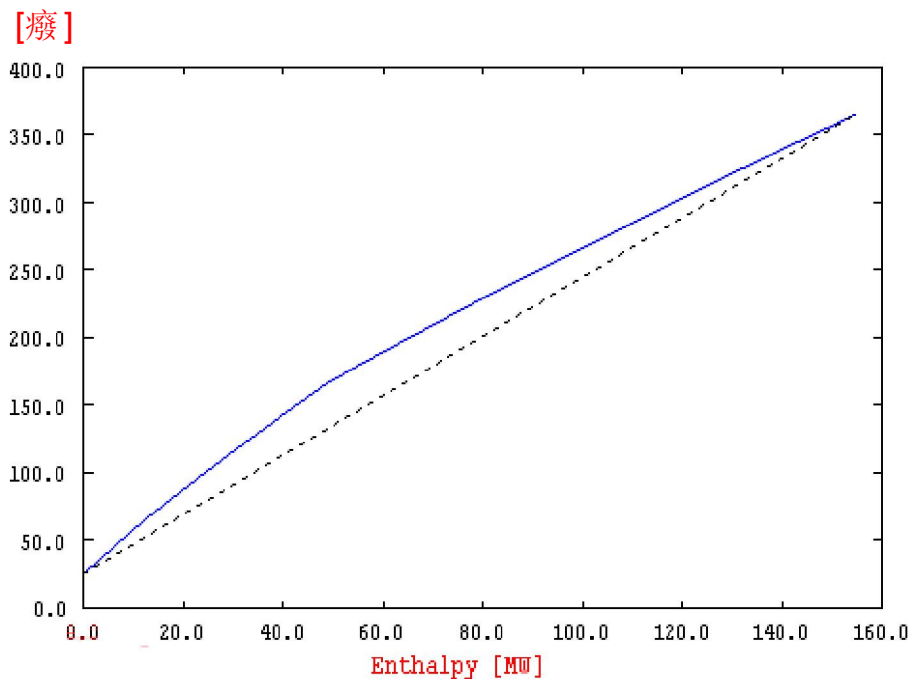


Figure 4.1 Enthalpy. temperature relationship of crude oil (industrial data)

4.2 Limitations of existing design methodologies

The synthesis of heat exchange networks involves simultaneous optimisation of energy consumption, heat transfer areas and matches between hot streams and cold streams. It requires solving non-convex mixed integer nonlinear programming problems, which are among the most difficult problems to optimise (Biegler and Grossmann, 2004). The difficulties in dealing with these problems arise mainly from the non-convex nature of non-linearity and from the combinatorial nature introduced by discrete variables. Section 2.2 presents comprehensive reviews of various design methodologies of heat exchanger networks only, without considering the interactions between HEN and the background processes (i.e. distillation system, reaction

system). As discussed in the literature review (Section 2.2.3), stochastic optimisation-based design methodologies are a promising type of methods, which have more chances of finding global optimum, compared with mathematical programming methods. Moreover, no simplification of cost calculation is necessary in stochastic methods. The network pinch design method (Asante and Zhu, 1996), which combines physical insights into the HEN synthesis problem, is another promising retrofit methodology, especially to industrial problems, in which consideration of existing networks is required and the number of modifications to existing networks is highly constrained. This section presents details of these two synthesis methods and their limitations.

4.2.1 Stochastic optimisation-based design methods for grassroots and retrofit of heat exchanger networks

Rodriguez (2005) developed an optimisation-based approach for designing heat exchanger networks such that fouling aspects will be minimised, assuming constant heat capacities. Although this approach is originally developed for dynamic state, it is applicable to steady state design of complex HENs. In the approach of Rodriguez (2005), Simulated Annealing (SA) was employed as the optimisation algorithm. Both structural options, such as re-piping, re-sequencing of existing exchangers, and continuous options, such as stream split fractions and exchanger duties, were considered without simplification of cost models and objective functions. As discussed in the literature review (Section 2.2.4), there is a trade-off between the complexity of HEN models and convergence of the optimisation problem to global optimum. HEN designs and optimisation problems are usually formulated as mixed-integer non-linear programming (MINLP) problems. Compared with deterministic methods, stochastic methods have a better chance of finding the global optimum for these complex problems. Employing a stochastic optimisation method, the design approach of Rodriguez (2005) considers various complex design issues (i.e. stream splitting and remixing, maximum number of modifications to existing networks in retrofit designs, *etc.*), without causing convergence problems. Considering the advantages of the approach of Rodriguez (2005), it is extended in the current work for the complex steady state grassroots and retrofit design of HENs.

However, some simplifications are made in the work of Rodriguez (2005). Among the main simplifications are:

- The dependence of thermal properties (e.g. heat capacity) on temperature is neglected in the models. Constant properties are assumed for the whole temperature range. As demonstrated in Section 4.1, for such streams containing large number of components and experiencing phase changes, these assumptions may introduce significant inaccuracies in the modelling of HEN and lead to worse designs (with respect to a particular design objective) when carrying out the HEN grassroots design and retrofit study.
- Stream heat transfer coefficients are assumed constant for the whole temperature range. Heat transfer areas cannot be predicted accurately, which will in turn cause inaccuracy in the estimation of the capital costs in grassroots design and also enhancements of existing HEN.

These above simplifications and limitations are overcome in the present work. Modifications to the models and optimisation of HEN are made to extend the work of Rodriguez (2005) to HEN designs of process streams with temperature-dependent thermal properties, considering relatively complex design issues.

4.2.2 Network pinch design method for heat exchanger network retrofit

As discussed in the review of literature (Section 2.2.2), the network pinch approach (Asante and Zhu, 1996) is a retrofit HEN design method which combines physical insights into the retrofit problems and mathematical programming techniques. It is composed of two stages: diagnosis stage and optimisation stage. In the diagnosis stage, there are 3 steps:

1. The HEN configuration bottleneck (referred to as the network pinch) is identified by finding the pinching matches, at which the temperature approach between hot and cold streams inevitably tends toward a pre-specified limiting value (defined as T_{min}). In this step, linear programming is employed to redistribute the transferred heat between existing matches in such a way that the heat recovery is maximised, for a given HEN topology. The redistribution of heat load of each exchanger unit makes sure that the network pinch is not caused by the existing heat transfer area

limits but the topology of the HEN. This step is referred as pinching an existing network in following discussions.

2. Topology changes are suggested to overcome the network pinch. The four possible changes are: re-piping existing matches, re-sequencing existing matches, inserting a new match and introducing additional stream splitting to the existing network.

3. Each candidate modification is tried at a time and the network is optimised for maximum heat recovery, which is used as the topology selection criteria. A list is generated after all suggested modifications are optimised, showing the corresponding maximum heat recovery for a given modified HEN topology. Then, designers are allowed to choose several particular modified HEN topologies to enter next design stage. This access to structure changes helps to avoid generating designs that are numerically optimal, but are questionable in practical applicability.

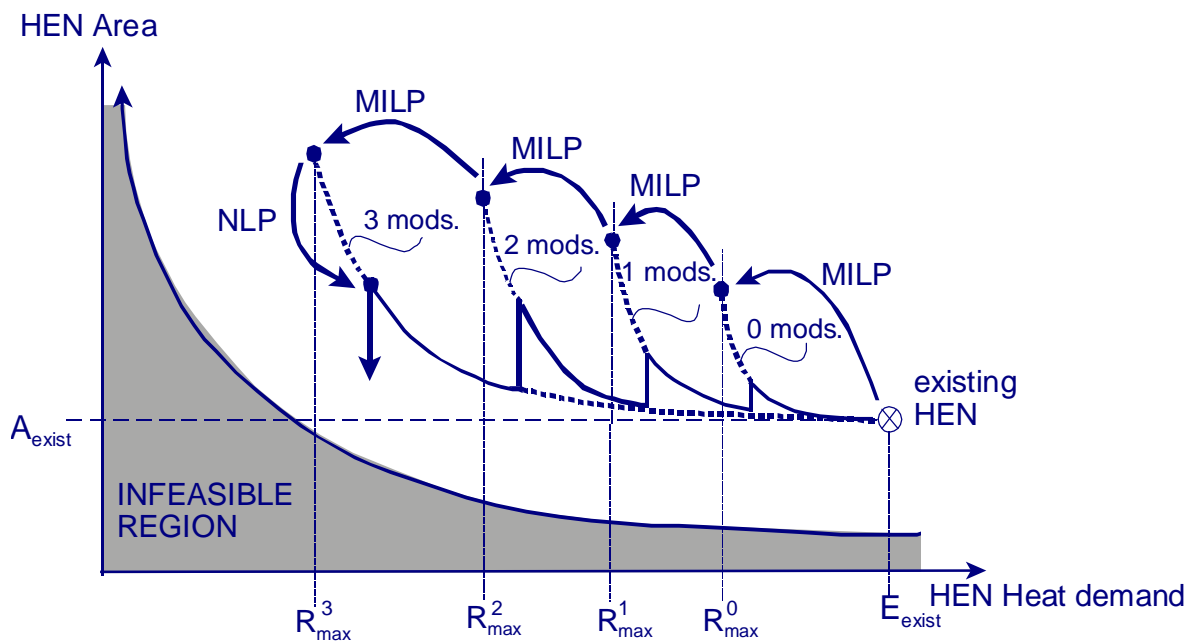


Figure 4.2 Previous network pinch design strategy (Asante and Zhu, 1996)

(mods: modifications; R_{\max}^i : maximum heat recovery with i modifications, kW; E_{exist} : energy demand of the existing network, kW)

The diagnosis stage is followed by the optimisation stage, where the selected structural modifications are further cost-optimised, varying heat loads of exchanger units. The above procedure is repeated until the maximum number of allowed modifications is reached. The design procedure is visualised in Figure 4.2. It can be seen from the figure that the difficult mixed-integer non-linear programming (MINLP)

problem is decomposed into mixed integer linear programming (MILP) problem and non-linear programming (NLP) problem. The design task then becomes a search for structural changes followed by a capital-energy optimisation.

The network pinch approach (Asante and Zhu, 1996) combines pinch technology and mathematical methods. Although it is a sequential approach, it explores possible topology modifications in a systematic way and at the same time allows user interactions in the design procedure. This characteristic makes the network pinch approach to be a promising retrofit design methodology in industrial practice.

However, there are limitations in the network pinch approach developed by Asante and Zhu (1996). First, as in the approach of Rodriguez (2005), the thermal properties of streams are assumed constant with temperature, which introduce inaccuracies in the HEN designs of systems where the thermal properties of process streams are temperature-dependent. Secondly, in step 1 and step 3 of the diagnosis stage which finds the maximum heat recovery for a fixed configuration, only heat loads between existing matches are optimised. Stream split fractions for existing splitters are kept fixed. Note that the case study shown in the work of Asante and Zhu (1996) does not have any stream splitting. Stream splitting is only introduced as a retrofit option. This limitation may lead to a false network pinch and a different ranking of potential modifications. Moreover, the existing approach only carries out cost-optimisation in the optimisation stage after the diagnosis stage. The design with minimum cost cannot be guaranteed since the selection of the potential modifications is not based on costs but energy demands. In this work, the network pinch approach is modified and extended for retrofit design of non-constant thermal property streams. Moreover, stream split fractions are considered as degrees of freedom in the optimisation for maximum heat recovery. The structural searches and cost-optimisation are combined into one stage for identifying better cost-effective designs.

4.3 Heat exchanger network model

Heat exchange networks are not just collections of heat transfer equipments. They are complex systems with intricate interactions between their components, including process exchanger units, utility exchanger units, stream splitters and mixers, and

unit operations (Unit operations are devices designed to alter either the temperature or heat content of a stream). A change in the operation of one of the components may affect the operation of the whole network. The way in which an operational change affects the performance of the network is not always easy to predict, due to complex connections of the constituent equipments. The complexity of these interactions depends on the structure of the network and the particular configuration of the individual component.

An effective model for HENs is necessary, to represent the operation of individual components and the interactions between the components in a HEN. This section presents the models for heat exchange networks. Firstly, the formulation of process streams with temperature-dependent thermal properties is discussed. Secondly, heat exchanger network structure representations and the models of the heat exchanger network are presented. The modelling of heat exchanger networks is implemented in SPRINT (v2.2), and the design approaches presented in Section 4.4 are also implemented in SPRINT.

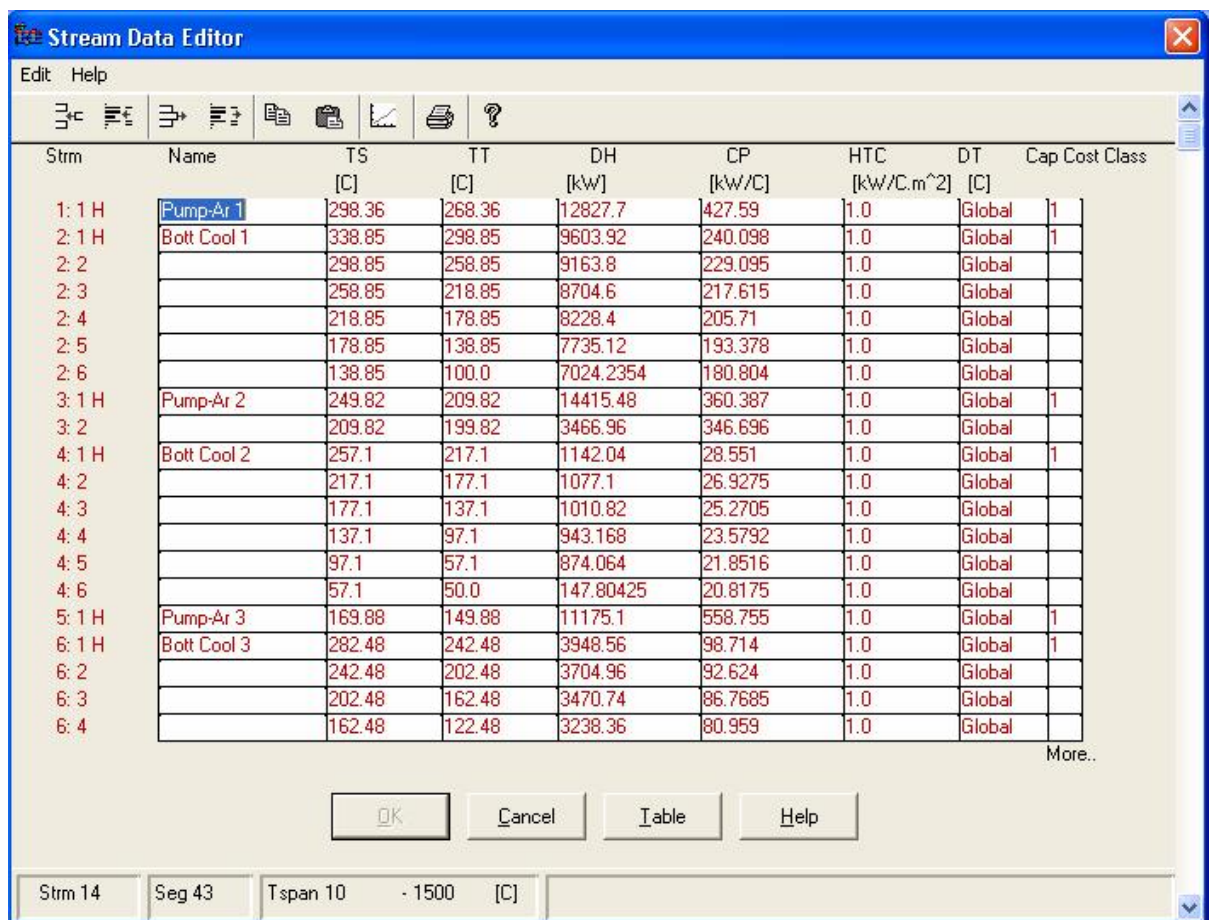
4.3.1 Process streams with temperature-dependent thermal properties

If physical properties of a stream do not change significantly throughout the relevant temperature range, it is treated as a single segment stream, for example, the stream %Rump-Ar 1+ in Figure 4.3. If the stream properties are nearly constant; only one segment is implemented for the stream. However, there are some streams for which the thermal properties (e.g. heat capacity) are highly dependent on temperature. For those streams, multi-segment formulations are employed, for example, the stream %Bott Cool 1+ in Figure 4.3. The whole temperature range is broken into several intervals (the stream in each interval is referred to as a segment) as shown in Figure 4.3. That is, non-linear behaviour is modelled as a set of piecewise linear segments, each representing the stream over a range of temperatures.

For each segment, the information relating to heating and cooling includes the segment supply temperature (TS), segment target temperature (TT), heat capacity flow rate (CP) or enthalpy change (DH) and film heat transfer coefficient (HTC). Note that only one parameter of CP and DH is independently specified, as

$$CP = \frac{DH}{(TT - TS)} \quad (4.1)$$

The multi-segmented stream data can be regressed from each exchanger unit in the existing heat exchanger network when carrying out a retrofit design or from property measurements or calculations when carrying out a grassroots design. No correlations between thermal properties and temperature are needed. It can be concluded that the formulation of streams with temperature-dependent thermal properties using multi-segments stream data is simple and easy to implement.



Strm	Name	TS [C]	TT [C]	DH [kW]	CP [kW/C]	HTC [kW/C.m ²]	DT [C]	Cap Cost Class
1: 1 H	Pump-Ar 1	298.36	268.36	12827.7	427.59	1.0	Global	1
2: 1 H	Bott Cool 1	338.85	298.85	9603.92	240.098	1.0	Global	1
2: 2		298.85	258.85	9163.8	229.095	1.0	Global	
2: 3		258.85	218.85	8704.6	217.615	1.0	Global	
2: 4		218.85	178.85	8228.4	205.71	1.0	Global	
2: 5		178.85	138.85	7735.12	193.378	1.0	Global	
2: 6		138.85	100.0	7024.2354	180.804	1.0	Global	
3: 1 H	Pump-Ar 2	249.82	209.82	14415.48	360.387	1.0	Global	1
3: 2		209.82	199.82	3466.96	346.696	1.0	Global	
4: 1 H	Bott Cool 2	257.1	217.1	1142.04	28.551	1.0	Global	1
4: 2		217.1	177.1	1077.1	26.9275	1.0	Global	
4: 3		177.1	137.1	1010.82	25.2705	1.0	Global	
4: 4		137.1	97.1	943.168	23.5792	1.0	Global	
4: 5		97.1	57.1	874.064	21.8516	1.0	Global	
4: 6		57.1	50.0	147.80425	20.8175	1.0	Global	
5: 1 H	Pump-Ar 3	169.88	149.88	11175.1	558.755	1.0	Global	1
6: 1 H	Bott Cool 3	282.48	242.48	3948.56	98.714	1.0	Global	1
6: 2		242.48	202.48	3704.96	92.624	1.0	Global	
6: 3		202.48	162.48	3470.74	86.7685	1.0	Global	
6: 4		162.48	122.48	3238.36	80.959	1.0	Global	

More..

Strm 14 Seg 43 Tspan 10 - 1500 [C]

Figure 4.3 Stream data

4.3.2 Heat exchanger network model

In the present work, the models are developed for networks containing shell-and-tube heat exchangers, which is by far the most common type of heat exchanger in

industry. The models for other more common configurations, such as 1-2 shell-and-tube heat exchangers (one shell pass and two tube passes) and groups of 1-2 shell-and-tube heat exchangers connected in series, with the model of shell-and-tube heat exchanger, are also developed.

The HEN is modelled as an interconnected set of network elements, namely process heat exchangers, utility heat exchangers, stream splitters and mixers and unit operations. The models for each component and the interconnections between the components are presented.

4.3.2.1 Modelling of heat exchangers (applied to process heat exchangers and utility heat exchangers)

In a heat exchanger l , heat is transferred from a hot stream to a cold stream. In the heat exchanger, the temperature of the hot stream decreases from TH_l^{in} to TH_l^{out} , while the cold stream is heated from TC_l^{in} to TC_l^{out} . Given the rate of heat transfer between the two streams (Q_l) and inlet conditions of the streams, the outlet conditions are calculated by

$$TH_l^{out} = TH_l^{in} - \frac{Q_l}{CP_{hsl}} \quad (4.2)$$

$$TC_l^{out} = TC_l^{in} + \frac{Q_l}{CP_{csl}} \quad (4.3)$$

where CP_{hsl} and CP_{csl} are the effective heat capacity flow rates of the hot and cold stream flowing through heat exchanger l . As multi-segments stream data are implemented in the present work to formulate the varying thermal properties of process streams, the value of CP_{hsl} and CP_{csl} is determined according to the relative temperatures.

The required exchanger area can be calculated from the well-know design equation:

$$A_l = \frac{Q_l}{U_l \cdot F_{T_l} \cdot LMTD_l} \quad (4.4)$$

where $LMTD_l$ is the log mean temperature difference of the heat exchanger l , and is calculated as follows

$$LMTD_l = \frac{(TH_l^{in} - TC_l^{out}) - (TH_l^{out} - TC_l^{in})}{\ln\left(\frac{TH_l^{in} - TC_l^{out}}{TH_l^{out} - TC_l^{in}}\right)} \quad (4.5)$$

The correlation factor F_T depends on the type of heat exchanger used. The F_T can be calculated by correlations presented in Smith (2005, p. 325).

4.3.2.2 Modelling of stream splitters and mixers

Stream splitting is employed in many HENs. Streams are split into two or more branches, and in most cases, are remixed later in the network. Stream splitters allow better use of available temperature driving forces in heat exchangers; and hence reduce the required heat transfer area. The stream split ratios are important degrees of freedom in the design of HENs. In the present work, the model of a stream splitter assumes that all the branches of a stream splitter are remixed before leaving the network. This is mathematically guaranteed by associating a mixer with each stream splitter. The splitter-mixer is considered as one unit in the model. Any number of heat exchangers can be located on each branch between the splitter and the mixer.

For a stream splitter SP , given the temperature of process stream before splitting (TSP_{SP}^{in}) in NBR_{SP} parallel branches, and the split fraction (\dot{f}_{SP}^k) of the particular branch k , the temperature of a parallel branch after splitter (TSP_{SP}^k) and the heat capacity flow rate of a parallel branch (CP_{SP}^k) is calculated by carrying out a mass balance at the splitting point:

$$TSP_{SP}^k = TSP_{SP}^{in} \quad (4.6)$$

$$CP_{SP}^k = \dot{f}_{SP}^k \cdot CP_{SP}^{main}, \quad 0 \leq \dot{f}_{SP}^k \leq 1 \quad (4.7)$$

where $k = 1, 2, \dots, NBR_{SP}$ and CP_{SP}^{main} is the heat capacity flow rate of the process stream before the splitter.

The isothermal remixing is assumed when the stream branches are remixed to the main process stream. The stream temperature after remixing (TMX_{SP}^{out}) is calculated by carrying out energy balances at the mixing points:

$$TMX_{SP}^{out} = \sum_{k=1}^{NBR_{SP}} \dot{m}_{SP}^k TMX_{SP}^k \quad (4.8)$$

where TMX_{SP}^k is the temperature on the branch k before the remixing.

4.3.2.3 Modelling of unit operations

Unit operations are devices designed to alter either the temperature or heat content of a stream. They represent the background process of the HEN without considering the actual details of the behaviour of the unit operation. For example, in preheat trains, the temperature of crude oil decreases after passing through a desalter. The desalter can be modelled as a unit operation. For a unit operation, temperature change (ΔT_{UO}) of the stream passing through is specified, given the inlet temperature (TUO^{in}), the outlet temperature (TUO^{out}) is calculated as

$$TUO^{out} = TUO^{in} + \Delta T_{UO} \quad (4.9)$$

4.3.2.4 Modelling of interconnections between components of HENs

The representation of HEN structure in this work follows the node-based representation in the work of Rodriguez (2005). As shown in Figure 4.4, the links between every component in the heat exchanger network are represented by nodes. There are four nodes assigned to a heat exchanger unit (for example, process exchanger and utility exchanger): hot side inlet node (NH_{in}), hot side outlet node (NH_{out}), cold side inlet node (NC_{in}) and cold side outlet node (NC_{out}). For unit operations, as they are only relative to one stream, two nodes associate with them, namely inlet node (UO_{in}) and outlet node (UO_{out}). Each node is associated with a unique temperature, which means that a new node is defined only if the temperature varies (e.g. the temperature of a stream branch after a splitting is the same as that before splitting). Therefore there is one node associated with supply temperature of

each stream and also one node is associated with each stream splitter. For example, there are 20 nodes defined for the network in Figure 4.4. For instance, nodes $NC_{in} = 16$, $NC_{out} = 17$, $NH_{in} = 5$, $NC_{out} = 18$ are associated with heat exchanger E5 and $UO_{in} = 7$, $UO_{out} = 20$ are for unit operation UO1. The first node of each stream is always associated with the stream supply temperature; and the last node of each stream is always associated with the stream target temperature.

The unique one-node-one-temperature data structure removes redundant data, and is able to represent very complex networks using moderate memory. Note that there are still certain limitations: Different streams cannot mix; No recycling of streams are supported, branches must be feed forward.

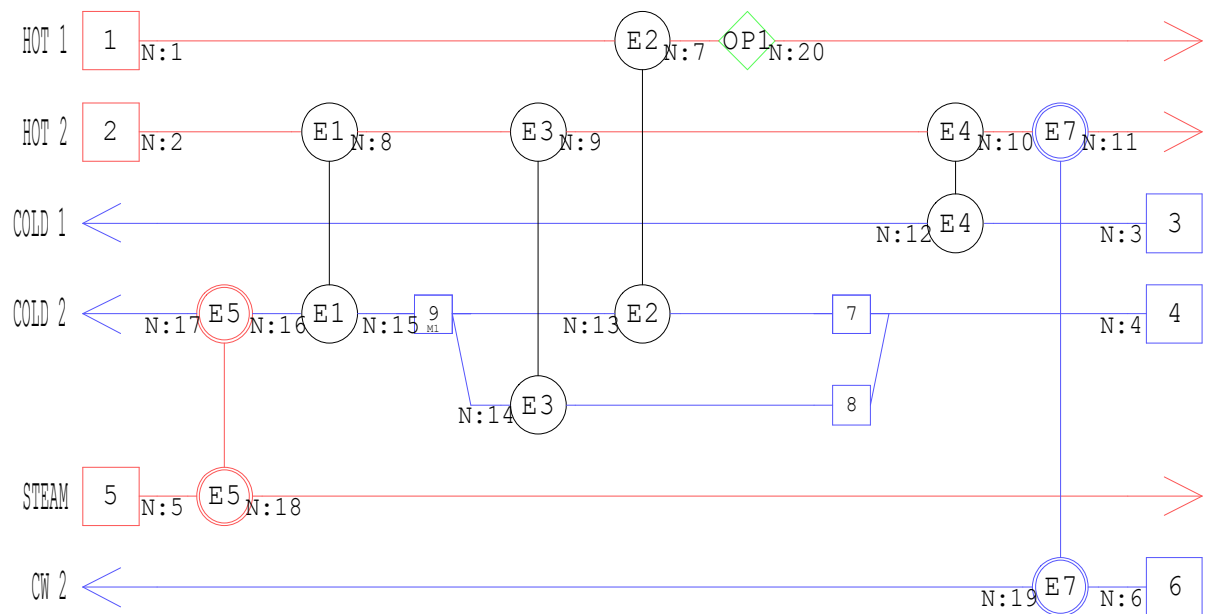


Figure 4.4 Node-based HEN structure representations (Rodriguez, 2005)

(icons start with \square are heat exchangers; exchangers in red are heaters; exchangers in blue are coolers; icons start with \diamond are unit operations)

Because multi-segmented stream data are employed, the set of equations are not linear any more with respect to temperature. Therefore, if all the exchangers are specified in terms of heat load, the temperatures for all of the streams are calculated sequentially. The calculation order is from the start of each stream to the end of that stream. After all the temperature nodes are calculated, Equations 4.4 and 4.5 are repeated for calculating required heat transfer area for each exchanger.

Section 4.3.3 presents the application of the developed HEN models through a crude oil preheat train, in which thermal property of the process streams are temperature-dependent.

4.3.3 Illustrative example 4.1: Simulation of a crude oil pre heat train

This example shows the simulation of a crude oil preheat train. The crude oil preheat train is the heat exchanger network that is associated with an existing atmospheric crude unit (Gadalla, 2002). This example was also employed in the work of Rastogi (2006) as an example to demonstrate the application of the HEN models of Rodriguez (2005). The stream data (target temperature, supply temperature, enthalpy change) are obtained from simplified modelling of the atmospheric distillation column (Chapter 3). Two sets of stream data are calculated and simulated with the same heat exchanger network: single segment stream data assuming constant heat capacity throughout the relative temperature ranges (the heat capacity in the single segment stream data are the average heat capacity in the relative temperature range) and multi-segmented stream data considering varying heat capacities. The segments of each stream are generated for each interval of 40 °C. The stream data for the case that temperature-dependence is not considered are given in Table A.1 (Appendix A), while the multi-segmented stream data are shown in Table A.2 (Appendix A). Note that in the work of Gadalla (2002), two steam streams were treated as process streams; in this work, steam streams are treated as utilities, and are cost as such. Accordingly, the heat exchangers on these two steams are treated as utility exchangers, rather than process exchangers. The resulting heat exchanger network, shown in Figure 4.5, includes 13 process exchangers and 11 utility exchangers.

Heat loads of exchangers are specified in the heat exchanger network; the heat loads specifications are listed in Table A.3 (Appendix A). The existing heat exchanger network is simulated for two sets of stream data. The calculated inlet and outlet temperatures for each heat exchanger unit under the assumption of constant thermal properties are summarised in Table 4.1. The simulation results for multi-segmented stream data are listed in Table 4.2. Minimum temperature approaches for each exchanger unit are also shown.

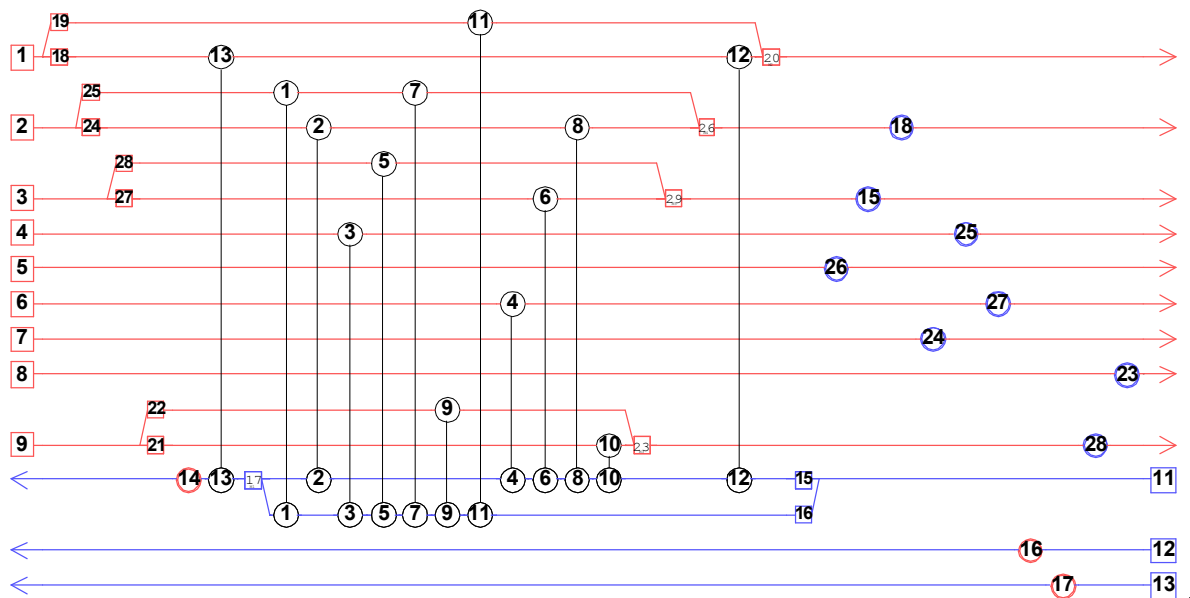


Figure 4.5 Grid diagram of the existing heat exchanger network (Gadalla, 2002)

Table 4.1 HEN simulation results: constant thermal properties with temperature assumed

Hx no.	Minimum temperature approach	Hot inlet temperature	Hot outlet temperature	Cold inlet temperature	Cold outlet temperature
	°C	°C	°C	°C	°C
1	85.5	338.9	211.6	126.1	184.3
2	90.5	338.9	215.8	125.3	183.5
3	100.5	257.1	222.8	122.3	126.1
4	156.4	282.5	281.2	124.8	125.3
5	120.3	249.8	209.7	89.5	122.3
6	114.6	249.8	207.1	92.5	124.8
7	62.5	211.6	101.9	39.3	89.5
8	66.6	215.8	108.4	41.7	92.5
9	88.0	189.2	123.4	35.4	39.3
10	83.1	189.2	115.7	32.7	41.7
11	236.2	298.4	261.2	25.0	35.4
12	241.7	274.3	269.5	25.0	32.7
13	90.4	298.4	274.3	183.9	203.2
14hu*	596.9	1510.0	800.0	203.2	365.0
15cu*	168.4	208.5	199.8	10.0	40.1
16hu	528.7	1510.0	800.0	271.3	282.5
17hu	617.8	1510.0	800.0	182.3	189.2
18cu	65.2	105.2	100.0	10.0	40.0
23cu	30.0	76.9	40.0	10.0	40.0
24cu	60.4	100.4	76.9	10.0	40.0
25cu	40.0	222.8	50.0	10.0	40.0
26cu	129.8	169.9	149.9	10.0	40.0
27cu	30.0	281.2	40.0	10.0	40.0
28cu	30.0	118.2	40.0	10.0	40.0

*: hu, cu: hot utility, cold utility exchangers, respectively

The results in the fourth and sixth column of Tables 4.1 and 4.2 show that the calculated outlet temperatures for each exchanger unit are very different with same transferred heat load. Minimum temperature approaches are also different when using single-segment data and multi-segment data. These differences in temperatures may lead to different estimation of the heat exchanger network performance and less accurate estimation when carrying out a retrofit study or a grassroots design. Applying single segment stream data is not as accurate as multi-segmented data. With implementations of the multi-segmented HEN simulations in the study of heat-integrated crude oil distillation columns, it will be more accurate to account for the interactions between distillation columns and HEN.

Table 4.2 HEN simulation results: varying thermal properties

Hx no.	Minimum temperature approach	Hot inlet temperature	Hot outlet temperature	Cold inlet temperature	Cold outlet temperature
	°C	°C	°C	°C	°C
1	63.0	338.9	221.5	158.5	213.7
2	68.1	338.9	225.7	157.6	213.0
3	72.8	257.1	226.9	154.1	158.5
4	124.4	282.5	281.4	157.1	157.6
5	95.4	249.8	210.0	113.9	154.1
6	89.6	249.8	207.3	117.7	157.1
7	56.3	221.5	102.2	45.9	113.9
8	60.4	225.7	109.8	49.4	117.7
9	88.5	189.2	128.7	40.2	45.9
10	85.0	189.2	121.2	36.2	49.4
11	236.2	298.4	261.2	25.0	40.2
12	238.1	274.3	269.5	25.0	36.2
13	60.9	298.4	274.3	213.4	230.5
14hu*	569.5	1500.0	800.0	230.5	365.0
15cu*	168.7	208.7	199.8	10.0	40.0
16hu	528.7	1500.0	800.0	271.3	282.5
17hu	617.8	1500.0	800.0	182.3	189.2
18cu	66.0	106.0	100.0	10.0	40.0
23cu	30.0	76.9	40.0	10.0	40.0
24cu	60.4	100.4	76.9	10.0	40.0
25cu	40.0	226.9	50.0	10.0	40.0
26cu	129.9	169.9	149.9	10.0	40.0
27cu	30.0	281.4	40.0	10.0	40.0
28cu	30.0	123.7	40.0	10.0	40.0

*: hu, cu: hot utility, cold utility exchangers, respectively

4.4 Design approaches for process streams with temperature-dependent thermal properties

In this section, two new approaches are presented for both the grassroots and retrofit design of heat exchanger network in which thermal properties of the streams are temperature-dependent. They are a simulated annealing optimisation-based approach (Rodriguez, 2005) and a network pinch-based approach (Asante and Zhu, 1996). The limitations (discussed in Section 4.2.2) in the existing methods are overcome in the new approaches to allow the applications of both methods to systems with multi-segmented streams.

4.4.1 Simulated annealing optimisation-based design method for streams with temperature-dependent thermal property

Simulated annealing (SA) is a widely applied stochastic optimisation algorithms. It was first proposed to solve combinatorial problems by Kirkpatrick *et al.* (1983), who observed the analogies between the physical annealing process and an optimisation problem. Then, it has been applied in the synthesis and optimisation of heat exchanger networks (Dolan *et al.*, 1989, 1990; Nielsen *et al.*, 1994; Athier *et al.*, 1997; Rodriguez, 2005). The detailed annealing algorithm proposed by Kirkpatrick and the co-workers is presented in Appendix B.1. Only the main features of the algorithm are summarise as follows:

- As a stochastic optimisation method, the SA algorithm does not require detailed information about the problem being optimised. The problem is treated as a black box in the algorithm; the only information needed by the optimiser is the objective function value of the points searched. Thus the simulation of the problem and the optimisation algorithm are completely decoupled, which is a beneficial feature for mathematically complex problems.
- The search for the optimum is based exclusively on the objective function value. Derivatives of the objective function and constraints of the problem are not required. Discontinuous or non-differentiable problems can be optimised easily. Consequently, continuous and discrete variables can be optimised simultaneously.

- Because of the random characteristics, the performance of the optimisation search is independent of the starting point. More importantly, the SA algorithm has more chances of escaping from a local optima in non-convex problems compared with deterministic methods.

In the present design problem, varying thermal properties are considered in HEN simulation; structural options and continuous variables of the HEN are needed to consider at the same time; less simplifications are required to objective function and constraints of the problems, compared with deterministic methods. All these features render the design problem non-differentiable, highly non-linear and non-convex. Therefore, SA is proposed as the optimisation algorithm in the present work, for both grassroots and retrofit design. For retrofit design, the optimisation starts with the existing HEN, while for grassroots design, the SA algorithm still needs an initial feasible design, which can be a HEN that uses utilities to fulfill process stream cooling and heating requirements.

The basic aspects and parameters of the simulated annealing algorithm applied in general optimisation, such as acceptance criteria, initial annealing temperature, cooling schedule, Markov chain length, termination criteria, *etc.*, are presented in Appendix B.2. Aspects relating to the implementation of the SA algorithm in the current particular application are discussed in this chapter.

4.4.1.1 Objective function

Normally, the objective in HEN design is to design a practical cost-effective network. Therefore, total annualised costs, comprising utility costs and annualised capital costs, is taken as the objective function in current work. As discussed in Section 4.4.1, one of the strengths of the SA algorithm is the decoupling of simulation models and the optimisation algorithm. This means that any modifications to the objective function do not require developments of a new optimisation algorithm or a new simulation model. The only change needs is on the formulation of objective function. Therefore, more complex objective functions, than those discussed in this work can also be supported.

The objective function considered in this work differentiates between grassroots design and retrofit study. In grassroots design, the capital costs of all units in the HEN are included while in a retrofit study, the costs of adding new units or installing additional area to existing heat exchanger units, and the costs of structural modifications (i.e. costs for re-piping modifications, re-sequencing modifications, etc.), are accounted for.

4.4.1.2 Simulated annealing moves

Simulated annealing moves define the search space where the optimisation algorithm searches for the optimal solution. The moves are very important issues since they account for the optimisation variables of the problem under study. The moves implemented in the heat exchanger network design problem are shown in Figure 4.6. Two types of moves are considered: continuous moves and structural moves. Continuous moves include variations of transferred heat loads for each match between hot streams and cold streams and split fractions for each splitter. Structural moves define heat exchanger network structural modifications, such as re-piping or re-sequencing an existing heat exchanger, adding a new heat exchanger, removing an existing match, adding a new stream splitter (or referred as a bypass) or removing the splitting on a particular stream. Each move generates a new design in the neighborhood of the current design.

In the optimisation procedure, a move is made depending on the random number generated and the probability assigned to the particular move. The move probabilities bias the optimisation algorithm to explore the variables which have a dominant influence on the performance of the system by assigning higher probabilities to the variables. However, the assignment of move probabilities is highly problem specific. No guidelines are available for different problems. By carrying out experiments, move probabilities that suit the HEN design problem with multi-segmented stream data were set in this work (shown in illustrative example 4.2). The set of move probabilities suggested in this work can be used as default values; however, adjustments may be needed according to the nature of the problem. Although simulating annealing moves are very important, the formulation of the move tree is not unique. Other move trees are also applicable as long as they capture all optimisation variables in the design problem.

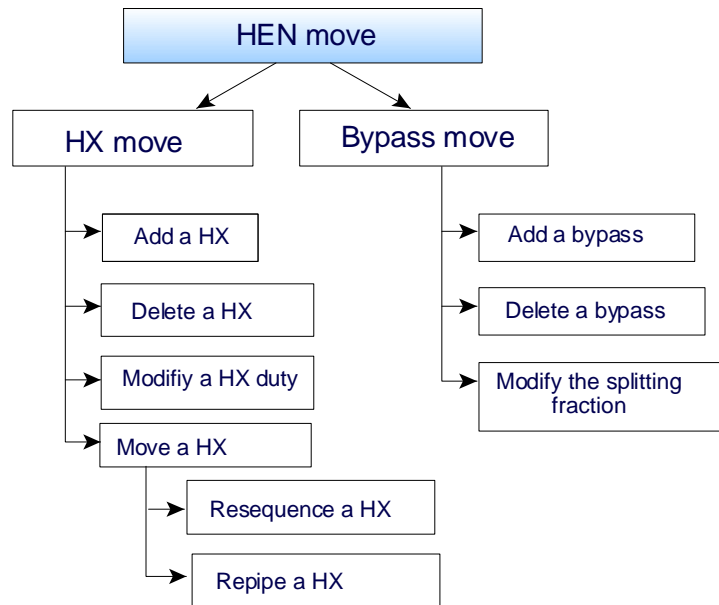


Figure 4.6 Simulated annealing move tree for HEN design

4.4.1.3 Constraints: minimum temperature approach and stream enthalpy balance

In the HEN design, the main constraint which needs to be taken into account is that the temperatures of hot streams and cold streams cannot crossover. It means that temperature approaches between hot and cold streams must be greater than or equal to zero. In practice, in order to consider the energy-capital trade-off, the minimum temperature approach must be greater than zero. Any design that violates a specified minimum temperature approach is identified as infeasible.

In addition, the stream enthalpy balances must be met in the design. The stream enthalpy balance is the second constraint. In SA, the algorithm makes random moves around the current solution. After each move, it is very likely that the HEN becomes infeasible due to the violations of those two constraints. As the purpose of the problem is to design a feasible cost-effective heat exchanger network, the way of dealing with constraints is of great importance and it will significantly influence the performance of the optimisation algorithm.

Several approaches have been proposed to deal with constraints in stochastic optimisation methods (Michalewicz, 1994). Among them, the approach most commonly employed is to transform the constrained problem to unconstrained one

by associating penalty functions in the objective with constraint violations in the form of:

$$\text{Minimise } F(x) = f(x) + \sum_{il=1}^m \gamma_{il} |h_{il}(x)|^r + \sum_{ij=1}^n \gamma_{m+ij} \max(0, g_{ij}(x))^r \quad (4.10)$$

where $F(x)$ is the unconstrained objective function, $f(x)$ is the original constrained objective function, $h_{il}(x)$ are the equality constraints, $g_{ij}(x)$ are the inequality constraints, γ_{il} and γ_{m+ij} are the penalty factors and r is a parameter normally taken as a value of one or two.

The setting of penalty factors γ is a real problem. Too small penalty factors cannot guarantee that the final solution reported by the algorithm will satisfy the constraints and too large penalty factors will cause the optimisation algorithm stops at the early stage of the optimisation, failing to escape from a particular feasible region when the feasible regions of the problem are not continuous. Dynamic penalty factors are suggested (Wang, 2001), with small penalty factors at the initial stages of optimisation and increased later so that the search is biased toward feasible region space. However, the schedule is not easily predefined; many experiments are required to make it working properly.

Another approach to deal with constraints is based on the applications of repair algorithms to restore the feasibility of any trial solution. The repair algorithms overcome the shortcomings of the approach that uses penalty function, and smoothes the exploration of search space. The drawback of this approach is that the repairing process may be time consuming and it is problem specific (Michalewicz, 1994). In this work, a repair algorithm is adopted to deal with constraints, which was also employed in the work of Rodriguez (2005). The two main sets of constraints, minimum temperature approach constraints and stream enthalpy balance constraints, are associated with temperature of nodes (Section 4.3.2) in the network. Temperature at each node is a function of the supply temperature, stream split fraction and cumulative enthalpy change from the supply temperature of a stream. As the cumulative enthalpy change is a function of heat loads of exchangers in the network, with fixed stream split fractions and stream target temperatures, the

infeasibilities may be removed by adjusting the heat loads of exchanger units in the network.

In the work of Rodriguez (2005), the minimum temperature approaches and stream energy balances are linear functions of the heat loads of the exchangers since heat capacities of streams are assumed constant. Finding a feasible point for these sets of linear constraints is relatively simple. However, it is a different scenario when the heat capacities are not constant. The approach cannot be simply extended to the system in which the heat capacities vary significantly throughout the relevant temperature ranges. The major challenges of extending the approach of Rodriguez (2005) are solving the following two problems: temperature correlation development in terms of enthalpy change for multi-segmented streams and a non-linear solver for recovering the network feasibility (convert infeasible HEN designs to feasible designs).

4.4.1.4 Temperature correlation in terms of enthalpy change for multi-segmented streams

As in this work, the limitation of assuming constant thermal properties with temperature is overcome and multi-segmented stream data are implemented in formulating the varying heat capacities of stream, the CP in Equation 4.2 and 4.3 depends on the inlet conditions of the element, in turn depend on the outlet conditions of upstream elements in the network. In order to recover the network feasibility, first of all, a correlation needs to develop to associate the node temperature (T_i) with heat loads of exchangers (Q) and the supply temperature (TS_j) of the stream on which the node i is located.

If heat capacity flow rates (CP) are constant with temperature, the relation between the node temperatures and heat loads of exchangers is given by:

$$T_i = TS_j + \frac{DH_i}{CP_j} \quad (4.11)$$

where:

i is the node associated with the temperature;

j is the stream on which the node is located;

DH_i is the accumulated enthalpy change from the start of the stream (TS_j) to the particular node i . DH_i is equal to the sum of heat loads of exchangers located on stream j from the start to the particular node i :

$$DH_i = \sum_{l=1}^{N_{HX}} \frac{y_{il} Q_l}{ff_{lj}} \quad (4.12)$$

where:

$y_{il} = 0$ or 1 , denotes the existence of exchanger unit l on the section of the stream from node i to the start of stream j

Q_l represents the heat load of exchanger unit l

ff_{lj} represents the flow ratio of the branch to the main stream j on which the exchanger unit l is located on

For example, as shown in Figure 4.7, the temperature for node 3 (T_3) is calculated by

$$T_3 = TS + \frac{(Q_1 + Q_2)}{CP}$$

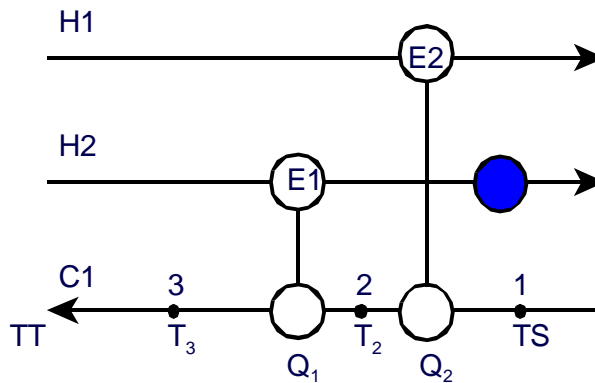


Figure 4.7 Sample grid diagram for correlating node temperature and heat load of exchangers located on the stream

Equation 4.11 can also be re-written as follows:

$$T_i = A_j + B_j \times DH_i \quad (4.13)$$

where,

$$A_j = TS_j, B_j = \frac{1}{CP_j}$$

Equation 4.13 gives a hint of the way how the temperature can be correlated as a function of the enthalpy change for multi-segmented streams. In this work, a polynomial correlation is proposed to associate the temperature and the accumulated enthalpy change from the supply temperature, as shown in Equation 4.12

$$T_i = A_j \times DH_i^4 + B_j \times DH_i^3 + C_j \times DH_i^2 + D_j \times DH_i + E_j \quad (4.14)$$

where DH_i is the accumulated enthalpy change from the start of the stream (TS_j) to the particular node i , as shown in Equation 4.12

Although there are other types of correlations that are commonly used (e.g. exponential, moving average), the polynomial correlation is proposed based on the following considerations:

- The formulation of polynomial correlation is flexible. The order of the formation can be adjusted to best suit the set of data. In this work, fourth order is proposed based on experiments, which gives the best fitting (The multi-segmented data input is treated as the original data).
- The formulation of the polynomial correlation is simple. The analytical form of the first and second order derivatives can be attained easily. This allows employment of deterministic methods, which require detailed formulation and derivatives of the problem, in recovering the network feasibility (the repair algorithm in dealing with network constraints). As mentioned above, the drawback of the repair algorithm is that it may consume more time. A simple formulation is helpful to reduce the calculation time in recovering feasibility.
- In the simulation of HEN, no formulation between the temperature and thermal properties are required since the stream data with varying thermal properties are input as multiple linear segments. It is simple to attain the coefficients in Equation 4.14 from the multi-segmented stream data due to the popularity of the polynomial correlation and availability of the regression in many commercial tools. In this work, the Least Squares method (Wolberg, 2005) is incorporated to do the regression.

One example is presented to illustrate how the multi-segmented stream data are used to attain the coefficients of the polynomial correlation and how well the regression is. The example involves a cold crude oil in an existing crude heat train taken from industry. The data are attained by recording the relative temperature range of an existing exchanger unit and the heat load for the exchanger. The data (segment supply temperature TS, segment target temperature TT and enthalpy change DH in the segment) are listed in Table 4.3. The cumulative enthalpy changes are calculated from the first segment to the particular segments. This set of cumulative enthalpy changes, together with TS of each segment plus the TT of the last segment, comprise the basic data which are used in regression to give the coefficients of the polynomial correlation for the stream. Following this process, the cumulative enthalpy changes and temperature points for the example are calculated and shown in Table 4.3 (used as original data to do comparison in Figure 4.8). Based on the set of temperature and cumulative enthalpy data, the regressed formulation is shown in Equation 4.15.

$$T = (-1.0551E - 18) \times DH^4 + (2.3672E - 13) \times DH^3 + (-2.6711E - 8) \times DH^2 + (4.72121E - 3) \times DH + 10.435 \quad (4.15)$$

Table 4.3 Illustrative example: multi-segmented stream data of cold crude oil

Name	TS °C	TT °C	DH kW	T °C	Cumulative DH kW
Cold Crude	10.4	36.3	5663.1	10.4	0.0
	36.3	47.3	2493.8	36.3	5663.1
	47.3	62.1	3505.4	47.3	8156.9
	62.1	77.3	3682.7	62.1	11662.3
	77.3	92.5	3783.0	77.3	15345.0
	92.5	107.3	3894.9	92.5	19128.0
	107.3	128.2	5602.1	107.3	23022.9
	128.2	133.9	1586.4	128.2	28625.0
	133.9	176.5	12079.6	133.9	30211.4
	176.5	183.8	2163.4	176.5	42291.0
	183.8	216.5	9858.1	183.8	44454.4
	216.5	234.3	5637.1	216.5	54312.5
	234.3	258.8	7922.8	234.3	59949.6
	258.8	267.8	2998.2	258.8	67872.4
	267.8	301.2	11470.7	267.8	70870.6
	301.2	312.8	4376.8	301.2	82341.3
	312.8	324.4	4480.1	312.8	86718.1
	324.4	336.1	4593.4	324.4	91198.2
				336.1	95791.6

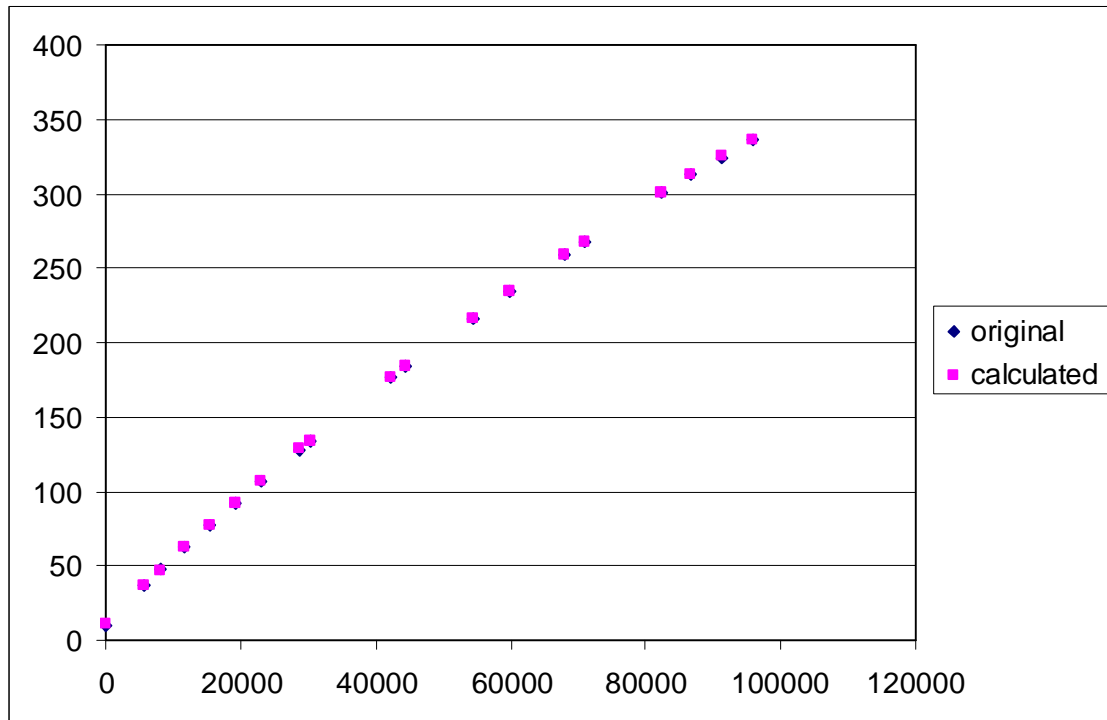


Figure 4.8 Regressed temperature (T) – enthalpy change (DH)

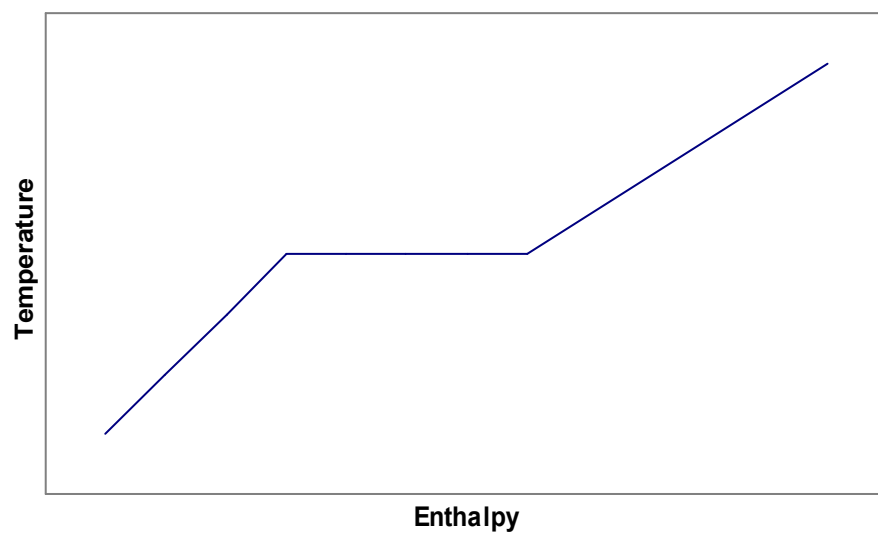


Figure 4.9 Temperature. enthalpy relation of streams that cannot be represented by the proposed polynomial correlation

Figure 4.8 compares the prediction of Equation 4.15 with the original data. It can be seen that the correlation fits very well with the original, as confirmed by the coefficient of determination R^2 which is equal to 1.000.

However, the proposed polynomial correlation is not suitable for representing process streams which have only one component and where there is phase change in the temperature range of interest. For instance, a steam that is heated up from ambient temperature to a superheated condition cannot be represented by the proposed polynomial correlation. The enthalpy . temperature curve of that type of stream is illustrated in Figure 4.9. For that type of stream, a separate stream is needed where there is a phase change, rather than making a segment.

4.4.1.5 Feasibility solver

In each step of Markov chain (see Appendix B.2 for simulated annealing parameters), the optimisation algorithm makes random move around the neighbourhood of the current solution. After each move, the minimum temperature approach and stream enthalpy balance constraints are checked: If any violation is observed, the feasibility solver is called to recover the network feasibility.

For the given heat exchanger unit illustrated in Figure 4.10, the minimum temperature approach constraint are formulated as follows:

$$\begin{aligned} TC_l^{out} - TH_l^{in} + \Delta T_{\min} &\leq 0 \\ TC_l^{in} - TH_l^{out} + \Delta T_{\min} &\leq 0 \end{aligned} \quad (4.16)$$

where TH_l^{in} and TC_l^{in} are the hot inlet temperature and cold inlet temperatures of heat exchanger l ; TH_l^{out} and TC_l^{out} are the outlet temperatures for the hot and cold streams, respectively.

The stream enthalpy constraints ensure the target temperatures of process streams are met. They are defined by Equation 4.17.

$$TT_{calc,j} - TT_j = 0 \quad (4.17)$$

where $TT_{calc,j}$ and TT_j are the temperatures calculated after transferring heat in the network and the target temperature, respectively.

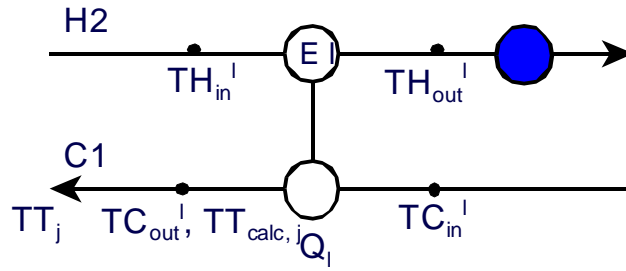


Figure 4.10 Generic grid diagram for minimum temperature approach constraint and stream enthalpy balance constraint

By combining Equations 4.15 and 4.11, the node temperature T_i can be determined by:

$$T_i = A_j \times \left(\sum_{l=1}^{N_{HX}} \frac{y_{il} Q_l}{ff_{lj}} \right)^4 + B_j \times \left(\sum_{l=1}^{N_{HX}} \frac{y_{il} Q_l}{ff_{lj}} \right)^3 + C_j \times \left(\sum_{l=1}^{N_{HX}} \frac{y_{il} Q_l}{ff_{lj}} \right)^2 + D_j \times \left(\sum_{l=1}^{N_{HX}} \frac{y_{il} Q_l}{ff_{lj}} \right) + E_j \quad (4.18)$$

When Equations 4.16 and 4.17 are combined, the infeasibility of the network becomes:

$$\text{infeasibility} = \sum_{l=1}^{N_{HX}} \min(TC_l^{\text{out}} - TH_l^{\text{in}} + \Delta T_{\min}, TC_l^{\text{in}} - TH_l^{\text{out}} + \Delta T_{\min}, 0)^2 + \sum_{j=1}^{N_{ST}} (TT_{\text{calc}, j} - TT_j)^2 = 0 \quad (4.19)$$

When each node temperature in Equation 4.18 is substituted into Equation 4.19, the problem of recovering the network feasibility becomes solving non-linear models:

$$f(Q_1, Q_2, \dots, Q_{N_{HX}}) = 0 \quad (4.20)$$

It can be seen from Equation 4.19 that the problem of recovering the network feasibility is a non-linear least square problem. The Levenberg-Marquardt algorithm (LMA: Gill *et al.*, 1978, shown in Figure 3.5) works very well in practice and become the standard of nonlinear least-squares (Press *et al.*, 2007; p.683). The LMA is employed in this work to recovery the network feasibility.

Although the feasibility recovering solver works well at most of the time, there are still failures because of the non-linear feature of the problem or the limitations of the network configuration proposed by the SA move. Note that the network configuration

and stream split fractions are not changed by the feasibility solver, and only heat loads of exchanger units are distributed around the network. The proposed structure and stream split fraction may never be feasible no matter how the heat loads are varied. In those failed cases, hot and cold utilities are used to compensate the unbalanced stream enthalpy. For the still violated minimum temperature approach constraints after implementing feasibility solver, an infinite penalty is imposed on the objective function of the optimisation so that the infeasible design is rejected.

4.4.1.6 Dealing with network topology constraints

In practical heat exchanger network design, there are several network topology constraints. These constraints may arise for economic reasons, or as a result of limitations on space and pumping capacity, control and safety considerations, or simply from preferences of the designer. In grassroots design, the maximum number of exchangers or stream splits is normally limited to generate cost-effective designs; while in retrofit design, the maximum number of modifications (repiping, resequencing) is constrained in order to retain features of the existing HEN. Another type of topology constraint is forbidden matches between pairs of streams.

To deal with these types of network topology constraints, annealing moves generating the new configuration are controlled so that the undesired features are not generated at all. For instance, if the maximum number of repiping is reached, the annealing move which repipes existing heat exchanger units is excluded from the list of moves by setting the particular repiping move probability to zero.

In next section, the application of the proposed simulated annealing optimisation-based design method with feasibility solver suitable for multi-segmented streams is demonstrated.

4.4.2 Illustrative example 4.2: Retrofit study of an existing crude oil preheat train using the SA algorithm

This example involves the same crude oil preheat train studied in illustrative example 4.1, with multi-segmented stream data. The stream data are listed in Table A.2

(Appendix A). The existing HEN structure is shown in Figure 4.5. The heat transfer areas for exchanger units calculated in illustrative example 4.1 are treated as the existing areas of the base case (Table 4.4). The cost of hot utility are calculated from the combustion heat, fuel oil price and furnace efficiency. The cost of cold utility is taken from Gadalla (2002). The costs of heat exchanger modifications are cited from Smith (2005). All these cost calculations are shown in Table 4.5.

Table 4.4 Existing heat exchangers (Illustrative example 4.2)

Hx no	Area (m ²)	Overall heat transfer coefficient (kW/°Cm ²)
1	292	0.5
2	280	0.5
3	20	0.5
4	2	0.5
5	156	0.5
6	161	0.5
7	285	0.5
8	278	0.5
9	16	0.5
10	37	0.5
11	19	0.5
12	14	0.5
13	273	0.5
14hu	135	0.667
15cu	24	0.714
16hu	16	0.667
17hu	11	0.667
18cu	20	0.714
23cu	55	0.714
24cu	1054	0.714
25cu	61	0.714
26cu	116	0.714
27cu	258	0.714
28cu	85	0.714
Total	3669	-

Table 4.5 Utility and exchanger modification costs

Parameter	Unit cost	
Flue gas (1500 . 800 °C)	306.8	\$/kW [®]
Cold water (10 . 40 °C)	5.25	\$/kW [®]
Exchanger additional area	$9665 \times (\text{additional area})^{0.68}$	\$
New exchanger unit	$94093 + 1127 \times (\text{exchanger area})^{0.9887}$	\$
Exchanger repiping	200,000	\$
Exchanger resequencing	150,000	\$

Then, the target of the retrofit study in the example is to design a cost-effective HEN which meets the following practical network topology constraints:

- Maximum number of repiping modification = 1
- Maximum number of new splitters = 1
- Maximum number of resequencing modification = 1
- Maximum number of new heat exchangers = 2
- Maximum number of new utility heat exchangers = 4
- Maximum number of stream splitters per stream = 2

The SA optimisation-based design approach developed in Section 4.4.1 is employed to solve the design problem in this example. The SA parameters and move probabilities used in the optimisation are presented in Tables 4.6 and 4.7, respectively. In order to demonstrate the benefits of feasibility solver, the problem is also optimised without the feasibility solver, with same SA parameters and move probabilities. The modifications (additional area added to existing units, number of resequencing and repiping modifications, costs of the modifications, *etc.*) to the existing HEN after both optimisations are shown in Table 4.8 and the energy and cost reductions with the modified HEN are summarised in Table 4.9. The structure of the modified HEN is presented in Figure 4.11.

Table 4.6 Simulated annealing parameters (illustrative example 4.2)

Initial annealing temperature	1.0×10^5
Final annealing temperature	1.0×10^{-8}
Markov chain length	30
Cooling parameter	0.005
Acceptance criteria	Metropolis (Metropolis <i>et al.</i> , 1953)

Table 4.7 Move probabilities (illustrative example 4.2)

Move decisions	Probabilities
Exchanger move, bypass move	0.8, 0.2
Exchanger move: add an exchanger, delete an exchanger, modify exchanger duty, exchanger relocation	0.2, 0.1, 0.45, 0.25
Bypass move: add a bypass, delete a bypass, modify the split fraction of a bypass	0.3, 0.3, 0.4
Exchanger relocation move: resequence modification, repipe modification	0.5, 0.5

Table 4.8 Modifications to the existing HEN (illustrative example 4.2)

	Without feasibility solver	With feasibility solver
Total new areas (m ²)	508	2866
Total cost of new areas (MM\$)	0.92	4.22
Number of resequence modifications	0	1
Number of repipe modifications	1	1
Total capital investment (MM\$)	1.12	4.77

Table 4.9 Energy and cost reduction of optimised design (illustrative example 4.2)

	Existing network	Without feasibility solver		With feasibility solver	
		Optimum	Saving	Optimum	Saving
Coil Inlet temperature (°C)	231	249	-	265	-
Hot utility (MW)	88.95	76.37	12.58 (14%)	64.39	24.56 (28%)
Cold utility (MW)	92.33	79.65	12.68 (14%)	67.45	24.88 (27%)
Operating cost (MM\$/y)	27.79	23.84	3.95 (14%)	20.12	7.67 (28%)
Total annualised cost (MM\$/y)	27.79	24.44	3.35 (12%)	22.69	5.10 (18%)

* Note: Operating time is 8600 hours in a year. The pay back criteria is assumed 2 years with 5% interest rate.

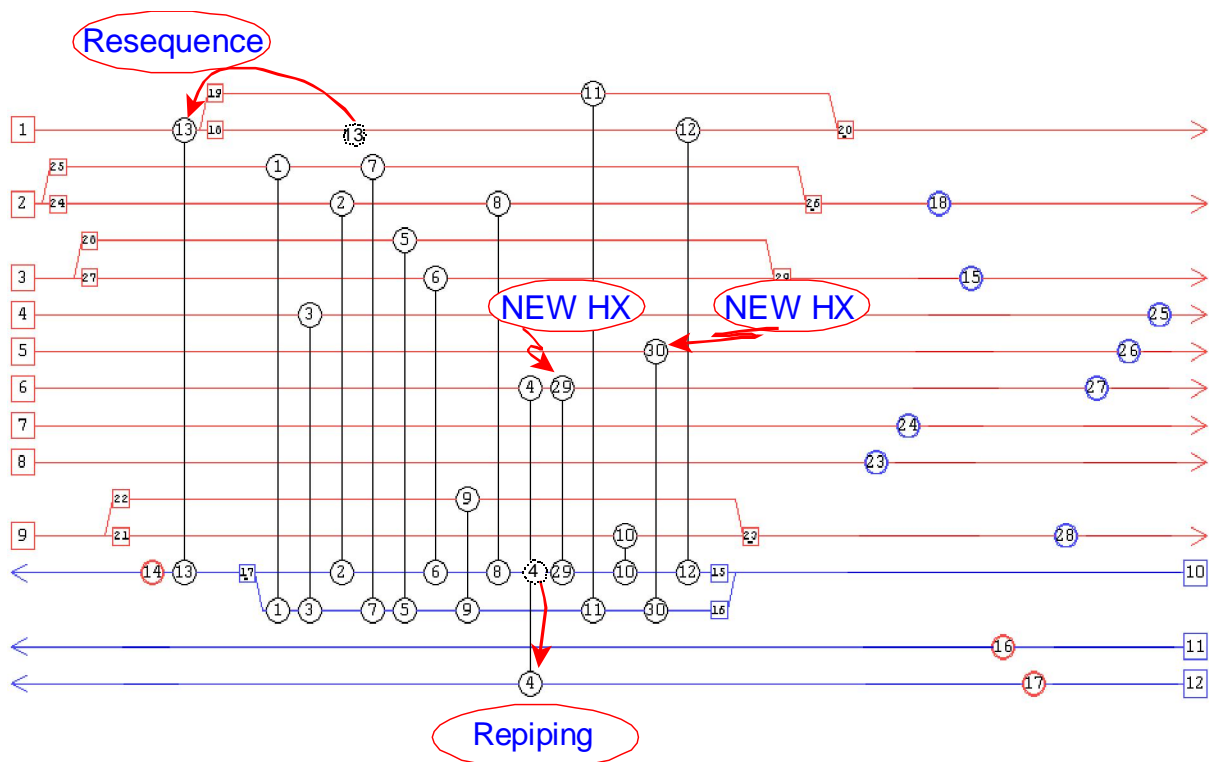


Figure 4.11 Modified HEN for illustrative example 4.2 (with feasibility solver)

It can be seen from Table 4.9 that the performance of the modified HEN is improved significantly by implementing the developed design methods: coil inlet temperature is increased from 231 °C to 265 °C, which consequently reduces the operating cost by 28% with only 4.77 MM\$ capital investment. The results with and without feasibility solver shown in Table 4.9 also present the advantages of the transformation of infeasible designs to feasible ones in the optimisation process: the total annualised cost is reduced by 18%, compared with the 12% reduction for the modified HEN optimised without the feasibility solver. The feasibility solver facilitates the HEN overcoming the infeasibility by itself. The capacity and potential of the network is explored before adding extra penalties. The generation of infeasible designs during the optimisation procedure can be minimised and the searching process is smoothed and discontinuities are avoided, which in turn avoid too early convergence. The SA optimisation-based method with feasibility facility for HEN design with multi-segmented streams will be combined with the design of crude oil distillation columns in Chapter 5 for the design of overall heat-integrated crude oil distillation system.

4.4.3 Methods for pinching existing networks with multi-segmented stream data and stream splitting

The network pinch method (Asante and Zhu, 1996) is a promising retrofit HEN design method which combines physical insights into retrofit problems and mathematical programming techniques. The bottleneck of the existing network configuration is first identified by redistributing heat loads of existing exchangers, which is referred to as pinching the existing network. Then each candidate structural modification that may overcome the bottleneck of the HEN configuration is optimised at a time for maximum heat recovery. As discussed in Section 4.2.2, the existing network pinch approach assumed constant thermal properties with temperature in the design of HENs and stream split fractions are not considered in pinching existing networks. In this section, the network pinch design method (Asante and Zhu, 1996) is modified to overcome the above limitations.

In the first step of the network pinch method, the network pinch is identified by redistributing heat transfer loads between the existing matches and in the meantime varying stream split fractions for maximum heat recovery (minimum utility demand).

Both heat loads and stream split fractions are adjusted to make sure that the network pinch is not caused by the heat transfer area limits but the topology of existing HEN. The redistribution of heat loads and variation of stream split fractions in the network for maximum heat recovery is of great importance due to its effect on determining the bottleneck of existing HEN topology and suggesting structural modifications that may overcome the bottleneck.

In the existing method (Asante and Zhu, 1996), the pinching problem was formulated as a linear problem because of the constant thermal property assumption and fixed stream split fraction assumption. The optimisation of linear problem is relatively easy, compared with non-linear problem. For process streams of which the dependence of thermal properties on temperature cannot be ignored, this pinching problem is no longer linear and becomes a much more complex minimisation problem for a constrained non-linear programming (NLP) system. As shown in Equation 4.21, given a network having N_{HX} heat exchangers and N_{BR} stream branches, the objective of the pinching problem is to minimise utility demand of the network (*Utility*), by varying heat loads of existing exchangers ($Q_1, Q_2, \dots, Q_{N_{HX}}$) and stream split fractions ($ff_1, ff_2, \dots, ff_{N_{BR}}$), subjected to minimum temperature approach constraints and stream enthalpy constraints, as shown in Equations 4.16 and 4.17.

$$\begin{aligned}
 \min \text{Utility} &= f(Q_1, Q_2, \dots, Q_{N_{HX}}, ff_1, ff_2, \dots, ff_{N_{BR}}) \\
 \text{st : } TC_l^{out} - TH_l^{in} + \Delta T_{\min} &\leq 0 \\
 TC_l^{in} - TH_l^{out} + \Delta T_{\min} &\leq 0 \\
 TT_{calc,j} - TT_j &= 0
 \end{aligned} \tag{4.21}$$

As presented in Section 4.3, the models are developed in this work for simulating a heat exchanger network where non-constant thermal properties are observed in the streams. Complex network structures can be represented and simulated. Moreover, no correlations between thermal property and temperature are required to simplify stream information input, and piece-wise segments are implemented to represent the non-constant thermal properties. Due to these features, Equation 4.21 is not easy to formulate exactly. The pinching problem is better to be treated as a black-box. A black-box is a system of which only the input and output are of interest, and the internal calculation procedure is not required.

The number of variables N_{VARY} in the pinching problem is the sum of the number of existing exchangers (N_{HX}) and the number of split branches (N_{BR}) in the network. Considering the large number of optimisation variables, and the non-linearity of the problem, the pinching problem is very complex. Normally N_{HX} is larger than N_{BR} , since N_{BR} is limited for the reason of controllability. The relative importance of the heat exchangers in the network suggests decomposing the pinching problem into two levels: in the outer loop the stream split fractions are optimised; in the inner loop the heat loads of existing exchangers in the network are redistributed. The minimum utility requirement attained in the inner loop serves as the objective function value for the outer loop optimisation. The decomposition of the pinching problem reduces the complexity of the problem since the number of optimisation variables in each level is smaller than the total number of optimisation.

The successive quadratic programming (SQP) method is a popular approach for process optimisation, and are most efficient if the number of active constraints is nearly as large as the number of variables, that is, if the number of free variables is relatively small (Nocedal and Wright, 2006; p.560). The SQP algorithm is selected as the optimisation solver for the outer loop where only the flow rates of stream branches are optimised. In particular, the optimisation subroutine E04UCF of the NAG FORTRAN library (NAG, 1990) is used to implement the Quasi-Newton method (Dennis and Schnabel, 1983) in the solution. The details of the SQP algorithm are explained in Biegler *et al.* (1997).

For the inner loop the flow ratios of each branch respect to the main streams are fixed, the optimisation problem is related purely to heat loads, and subject to minimum temperature approach constraints and stream enthalpy balance constraints, as shown in Equation 4.22. The inner loop optimisation is a highly constrained non-linear programming problem, involving a large number of optimisation variables. The commonly used SQP algorithm, which is normally suit optimisation problems with small number of variables, is not applied in the inner loop where with a large number of variables, N_{HX} , are involved.

$$\begin{aligned}
\min \text{Utility} &= f(Q_1, Q_2, \dots, Q_{N_{HX}}) \\
\text{st} : TC_l^{\text{out}} - TH_l^{\text{in}} + \Delta T_{\min} &\leq 0 \\
TC_l^{\text{in}} - TH_l^{\text{out}} + \Delta T_{\min} &\leq 0 \\
TT_{\text{calc},j} - TT_j &= 0
\end{aligned} \tag{4.22}$$

This work presents a novel approach for solving the inner loop optimisation problem. In Section 4.4.1, a feasibility solver is presented for converting the infeasible designs that violating minimum temperature approach constraints and stream enthalpy balance constraints, to feasible ones in the SA algorithm. A polynomial correlation is proposed to represent node temperatures in terms of enthalpy change (Equation 4.14). By employing the polynomial correlation, the infeasibility of network is formulated as a least-squares problem (Equation 4.19), which has an easier convergence and less calculation iterations compared with other types of NLP problems (Nocedal and Wright, 2006; p.246). The proposed polynomial correlation is also implemented to optimise the heat loads in the inner loop in order to avoid treating the inner loop optimisation as a black-box. If there are utility heat exchanger units located on stream j , the cumulative enthalpy change applied in Equation 4.18 excludes heat loads of those utility heat exchanger units. The calculated temperature of stream j is equivalent to the temperature after process-to-process heat recovery ($TT_{\text{ppcalc},j}$). It is clear that the smaller the difference between $TT_{\text{ppcalc},j}$ and the target temperature TT_j , the lower the utility demand. Therefore, the utility consumption in terms of heat loads of process exchangers can be formulated by:

$$\sum_{j=1}^{N_{SUT}} (TT_{\text{ppcalc},j} - TT_j)^2 \tag{4.23}$$

where

$$\begin{aligned}
TT_{\text{ppcalc},j} &= A_j \times \left(\sum_{l=1}^{N_{HX}-N_{UHX}} \frac{y_{il} Q_l}{ff_{lj}} \right)^4 + B_j \times \left(\sum_{l=1}^{N_{HX}-N_{UHX}} \frac{y_{il} Q_l}{ff_{lj}} \right)^3 + C_j \times \left(\sum_{l=1}^{N_{HX}-N_{UHX}} \frac{y_{il} Q_l}{ff_{lj}} \right)^2 + \\
&D_j \times \left(\sum_{l=1}^{N_{HX}-N_{UHX}} \frac{y_{il} Q_l}{ff_{lj}} \right) + E_j
\end{aligned}$$

And N_{UHX} is number of utility exchanger units in the network, N_{ST} is the total number of process streams, N_{SUT} is the number of process streams on which there is a utility heat exchanger.

Note: If there are not any utility heat exchangers on a particular stream, the difference between $TT_{ppcalc,j}$ and TT_j is treated as a stream enthalpy constraint. The number of such streams is noted as $N_{ST} - N_{SUT}$.

When Equation 4.23 is substituted into Equation 4.22 and a penalty function is used to convert the constrained optimisation problem to unconstrained one, the problem presented in Equation 4.22 can be written as:

Min

$$\sum_{j=1}^{N_{SUT}} (TT_{ppcalc,j} - TT_j)^2 + \gamma \times \left[\sum_{l=1}^{N_{HX}} \min(TC_l^{out} - TH_l^{in} + \Delta T_{min}, TC_l^{in} - TH_l^{out} + \Delta T_{min}, 0)^2 \right] + \sum_{j=1}^{N_{ST} - N_{SUT}} (TT_{calc,j} - TT_j)^2 \quad (4.24)$$

where

$$TT_{ppcalc,j} = A_j \times \left(\sum_{l=1}^{N_{HX} - N_{UHX}} \frac{y_{il} Q_l}{ff_{lj}} \right)^4 + B_j \times \left(\sum_{l=1}^{N_{HX} - N_{UHX}} \frac{y_{il} Q_l}{ff_{lj}} \right)^3 + C_j \times \left(\sum_{l=1}^{N_{HX} - N_{UHX}} \frac{y_{il} Q_l}{ff_{lj}} \right)^2 + D_j \times \left(\sum_{l=1}^{N_{HX} - N_{UHX}} \frac{y_{il} Q_l}{ff_{lj}} \right) + E_j$$

and

TC_l^{in} , TC_l^{out} , TH_l^{in} , TH_l^{out} and T_j are calculated by Equation 4.18

In Equation 4.24, a dynamic penalty factor γ is used to weight the constraints, according to the suggestion of Wang (2001). A small factor is employed at the initial stages of optimisation and it is increased later so that the search is biased toward feasible region space. Comparing Equation 4.24 with Equation 4.21, it can be seen that the two equations are similar, and both are least squares problems. Therefore, the same approach (Levenberg-Marquardt algorithm, Gill *et al.*, 1978) as employed in the feasibility solver in Section 4.4.1.5 is used to solve the inner loop optimisation where heat loads of existing matches are distributed for maximum heat recovery.

The two-level optimisation procedure is visualised in Figure 4.12. The outer loop is to optimise stream split fractions using the SQP algorithm, while the inner loop is to distribute the heat loads of existing matches for minimum energy consumption and that minimum energy consumption attained from the inner loop served as objective function of the outer loop. Note that, the optimum head loads distribution ratio found

in the inner loop are kept as fixed in the outer loop and the exact heat loads of exchangers are calculated from the available heat on a specific branch. By implementing the two-level pinching procedure, the size and complexity of the pinching problem are reduced. Consequently, there are more chances of finding out a better solution which ensures that the pinch is not caused by heat loads and stream split fractions but the configuration of existing HEN. The two-level pinching approach is examined in an existing preheat train in Section 4.4.4.

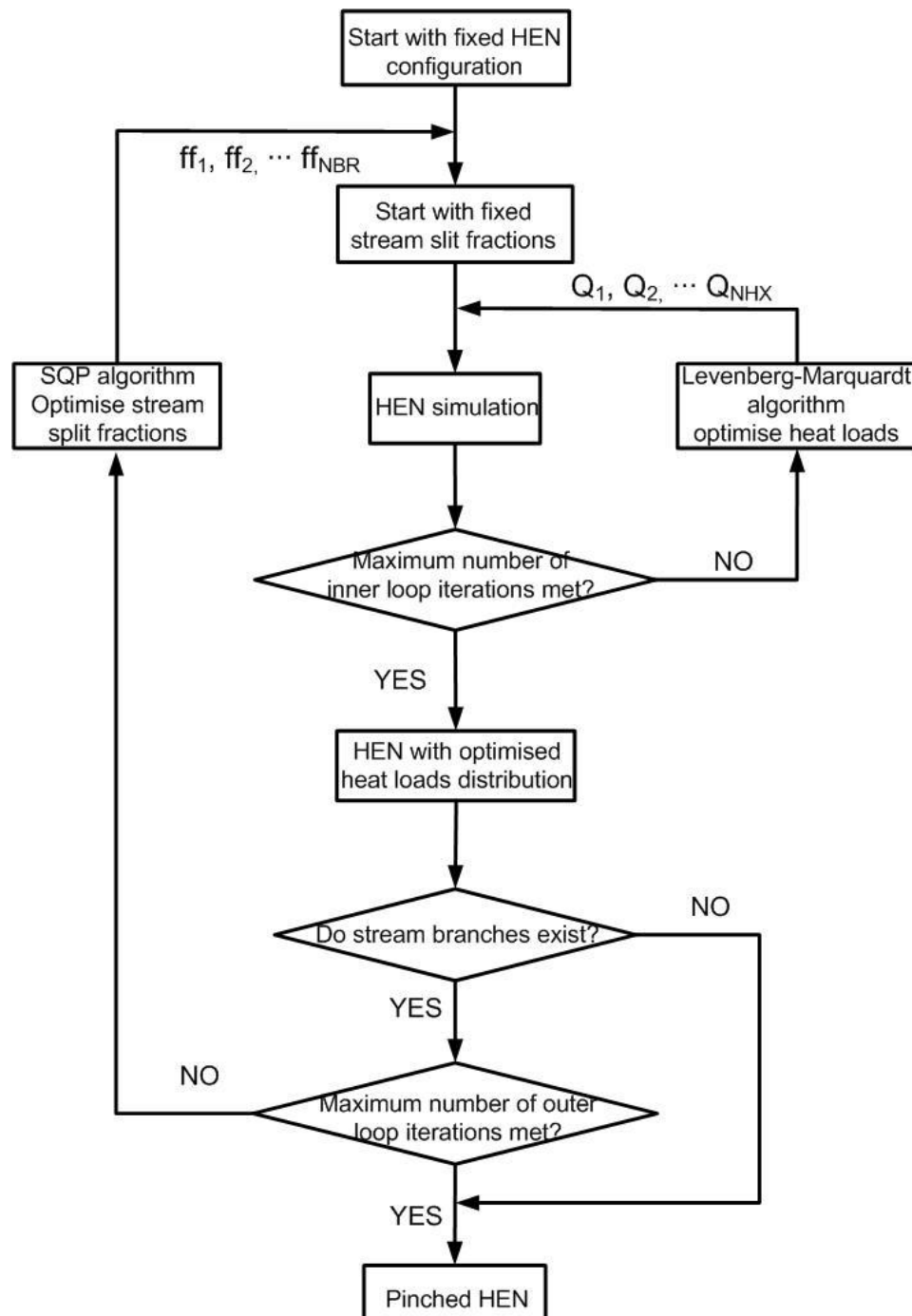


Figure 4.12 Optimisation approach for pinching a network

4.4.4 Illustrative example 4.3: Pinching an existing crude oil preheat train

This example applies the approach described above to pinch the crude oil preheat train studied in Sections 4.3.3 and 4.4.2. The stream data are listed in Table A.2 (Appendix A). The existing HEN structure is shown in Figure 4.5 while the existing heat transfer areas for exchanger units are presented in Table 4.4. The utilities are assumed the same as in the work of Gadalla (2002) and shown in Table 3.16 (Section 3.3.3).

The two-level approach developed in this work is implemented to study the structural bottleneck of the existing crude oil preheat train for a minimum temperature approach of 30 °C, which is a typical value for designing HEN in industry. In order to demonstrate the advantages of the new two-level approach, the existing crude oil preheat train is also pinched using the SQP algorithm of Dennis and Schnabel (1983) to optimise the heat loads and stream split fractions at the same time. In addition, the network is pinched by using the method of Asante and Zhu (1996), in which only heat loads are redistributed for maximum heat recovery while the effect of stream splitting is neglected, e.g. only the inner loop optimisation as shown in Figure 4.12 is implemented. The minimum utility demand attained using the three methods is compared in Table 4.10.

Table 4.10 Energy demand of pinched HEN

	Existing HEN	Pinched HEN		
		Approach 1	Approach 2	Approach 3
Coil Inlet Temperature (°C)	231	258	243	261
Hot Utility (MW)	88.95	74.17	82.42	73.02
Cold Utility (MW)	92.33	77.48	85.77	76.40
Total Utility (MW)	181.28	151.65	168.16	149.42

Approach 1: Network pinch: only heat loads varied; Approach 2: SQP algorithm: heat loads and split fractions varied in a single step; Approach 3: Two-level approach: network pinch varying both heat loads and split fractions

If only heat loads are varied, the minimum utility demand is 151.65 MW, 2.23 MW (1.5%) more than that given by the two-level approach. The additional energy recovered is by varying both heat loads and the stream split fractions. Stream splitting plays a significant role in determining the maximum heat recovery in a network with fixed configuration. Similarly, it can also be observed from Table 4.10 that 18.74 MW more energy is recovered using the proposed two-level approach

than that with the SQP algorithm to optimise both variables in one level. The proposed two-level approach is more capable of exploring the scope for heat recovering of the existing HEN configuration and determining the network topology bottleneck, and suggesting the modifications which could overcome the network pinch.

The change in flow fractions of braches, relative to the main stream, and redistribution of heat loads of existing matches for the pinched network are presented in Tables 4.11 and 4.12, respectively. Pinched heat exchanger units in the original network are shown in Figure 4.13.

Table 4.11 Split fraction of branches for pinched HEN by the new two-level approach
(with respect to main streams)

Branch No	15 (Str 10)	18 (Str 1)	21 (Str 9)	24 (Str 2)	27 (Str 3)
Split fraction	0.472	0.850	0.682	0.534	0.452

Table 4.12 Redistributed heat loads for pinched HEN by the new two-level approach

Hx no	Redistributed heat loads (MW)	Existing heat loads (MW)
1	11.87	13.25
2	14.12	13.19
3	0.93	0.86
4	10.10	0.11
5	16.29	7.47
6	1.63	7.33
7	13.74	11.42
8	10.76	11.52
9	1.70	0.89
10	2.91	2.05
11	1.32	2.37
12	3.87	1.74
13	7.64	8.76
14hu	57.61	73.54
15cu	0.00	3.08
16hu	8.78	8.78
17hu	6.63	6.63
18cu	0.00	1.09
23cu	1.32	1.32
24cu	47.86	47.87
25cu	4.26	4.33
26cu	11.18	11.18
27cu	10.20	20.19
28cu	1.58	32.44

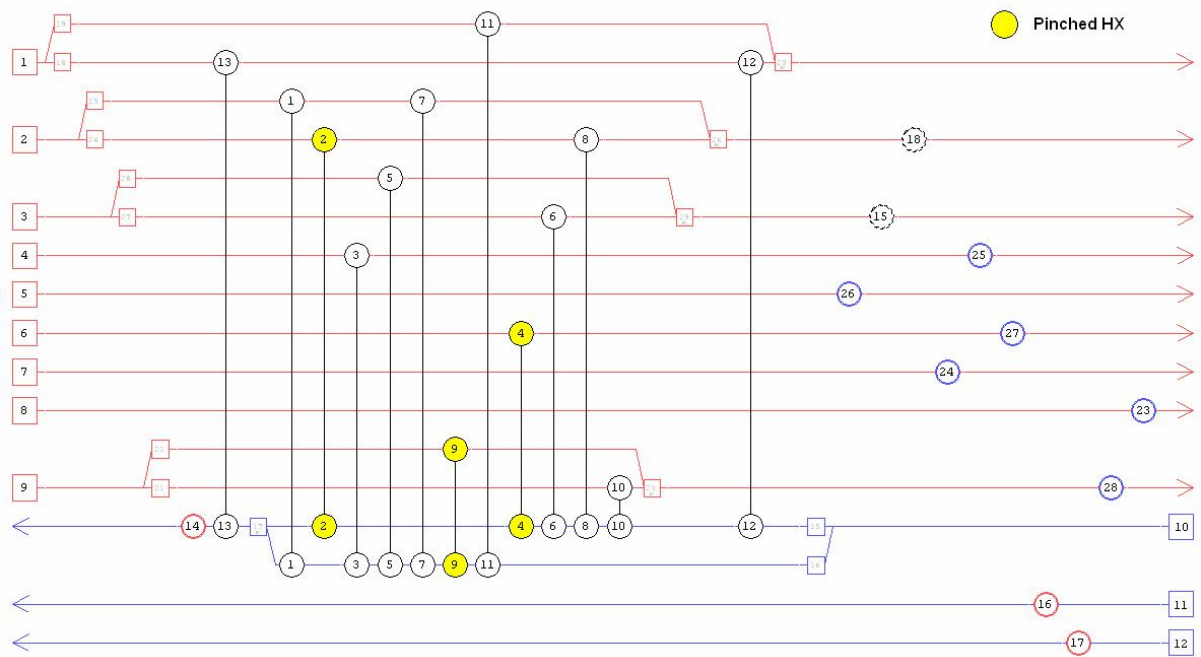


Figure 4.13 Pinch locations of the existing crude oil preheat train

4.4.5 Modified network pinch with combined structure searches and cost-optimisation

After the bottleneck of the HEN configuration is diagnosed by pinching the network, different types of modifications are suggested to overcome the pinch. The modifications fall into four groups: re-piping existing matches, re-sequencing existing matches, adding new matches and introducing stream splitting. In the work of Asante and Zhu (1996), each modification is modelled and optimised for maximum energy recovery and ranked according to the utility consumption. Up to this step, the diagnosis stage is accomplished, and followed by the optimisation stage which optimises the selected candidate modifications for minimum total annualised cost. However, in the diagnosis stage, capital cost is not considered, the heat loads may be redistributed such that additional area is needed in many existing heat exchanger units. In practice, adding additional heat transfer area to one heat exchanger unit is not only about installing new area. The associated pipe work also requires modifications, which is normally more expensive than the installed area (Smith, 2005). For example, adding 500 m² to 5 existing units is much more expensive and less favourable in industry than adding same amount of 500 m² to a single unit.

To take into consideration retrofit costs, in the current study, the network pinch approach of Asante and Zhu (1996) is modified as shown in Figure 4.14. In the new network pinch approach, the structure searches in the diagnosis stage and the cost-optimisation are combined into one stage. The design problem then becomes a search for the most cost-effective structural changes in only one step, rather than sequential steps of a search for structural changes followed by a capital-energy optimisation, as employed in the original network pinch approach of Asante and Zhu (1996). The one-step avoids missing potentially cost-effective designs in the diagnosis stage, by ranking the alternative designs based on costs, rather than heat recoveries.

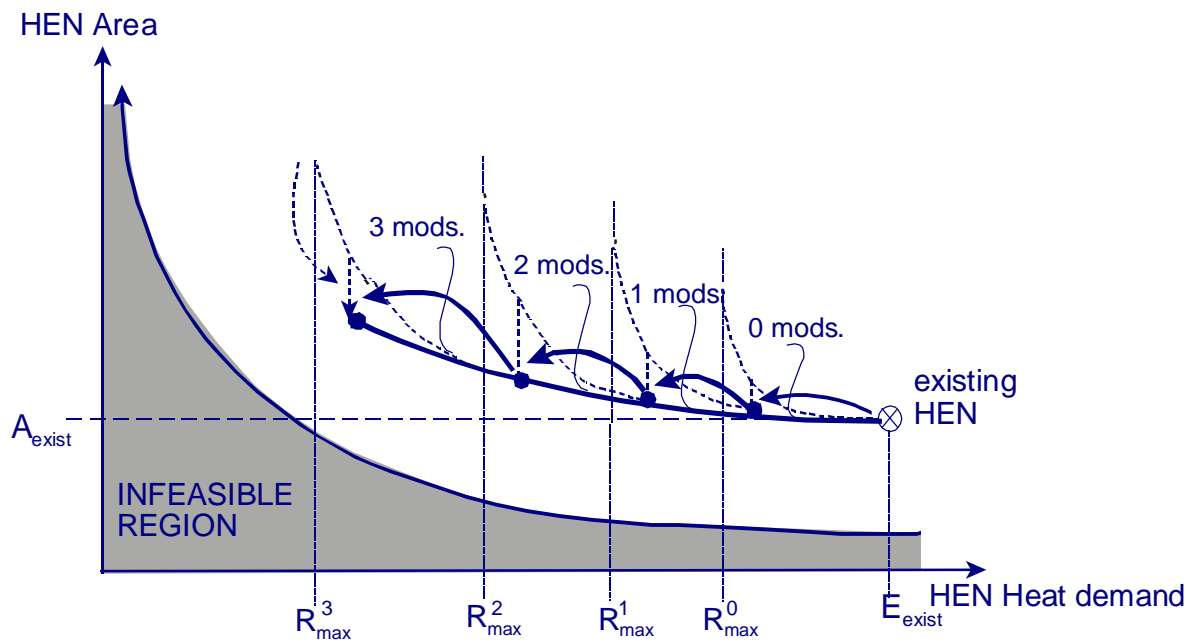


Figure 4.14 Modified network pinch approach design strategy

(mods: modifications; R_{\max}^i : maximum heat recovery with i modifications, kW; E_{exist} :

Energy demand of the existing network, kW; Solid black curve represents the current search procedure of structural modifications; Dotted curve stands for the search procedure of original network pinch approach of Asante and Zhu (1996))

In the proposed one-step approach, each candidate modification is optimised for minimum total cost directly. The minimum total cost found in the optimisation of each modification is used later as the criterion for ranking potential modifications. The design problem thus becomes a non-linear programming (NLP) problem. The

simulated annealing algorithm developed in Section 4.4.1 is employed to solve this NLP problem because of the following considerations:

- In the SA algorithm, the simulation and the optimisation algorithm are decoupled. No derivatives are required. The NLP optimisation problem is treated as a black-box; only objective function values of trial solutions are needed. That is, no simplifications to the simulation models are required for the sake of optimisation. The calculation of capital cost and operating cost can also be as complex as is required.
- As discussed in Section 4.4.1, compared with deterministic methods, stochastic methods have more chances of finding global optimum for non-linear problems due to their random characteristics. The non-linearity of the problem is increased greatly by the implementation of more accurate non-constant thermal properties for process streams.
- The network feasibility may be violated when simulating candidate solutions. It is not suitable to use deterministic methods, where a feasible initial design is normally required. The SA algorithm proposed in Section 4.4.1 is capable of dealing with an infeasible initial design facilitated by the feasibility solver.

There are many advantages to employ the SA algorithm as the optimisation method, such as solutions of better quality, more constraints that can be handled, and fewer simplifications to the models of HENs to ensure convergence. However, relative longer computation times are the cost of these benefits. Compared to the original sequential order of structure searches in the diagnosis stage and the cost optimisation stage where a deterministic method is employed to solve the optimisation problem, more time is needed (at least 10^2 more time is required, the length of calculation time depends on the setting of SA parameters, see Appendix B.2) using the SA algorithm in minimising the total annualised cost of modifications that may overcome the bottleneck of the exiting network.

In order to reduce the calculation time, the SA algorithm proposed in Section 4.4.1 is modified such that only one run is needed in searching one type of structural modification. In retrofit design of HEN, there are four types of structural modifications to overcome the network pinch by moving heat from below the pinch to above the pinch of the existing network. The four possible types of changes are: re-piping existing matches, re-sequencing existing matches, inserting a new match and

introducing additional stream splitting to the existing network. In the optimisation, both continuous variables and structural options of a particular type are optimised. If the SA algorithm makes a structural move, the structural modification is selected from those suggested after pinching the existing network. In the SA optimisation procedure, the best design of each potential modification is stored and reported at the end of the structure searching process. Note that the best design for each structural change from the modified SA algorithm is slightly worse than those gained from running the SA algorithm hundreds of times to optimise each potential modification and identify the most cost-effective design with the particular modification. However, given N candidates in a type of structural modifications, the calculation time is reduced to only $1/N$ of that required in running the SA algorithm each time in optimising each single candidate.

The modified network pinch approach takes into account different levels of complexity in the HEN retrofit. The complexities addressed include non-constant thermal properties, the effects of stream split fractions on determining the network pinch and the combination of the diagnosis stage and the cost optimisation stage to avoid missing cost-effective designs. In order to reduce the computational time, different methods are used to solve different types of design problems. For instance, if the constant heat capacity assumption stands, and initially there are no stream splits in the existing network, the pinching problem is solved by a linear solver (e.g. E04MBE of the NAG FORTRAN library) rather than the SQP method which is particularly suitable for non-linear system; Figure 4.15 shows the overall structure of the modified network pinch approach together with Figure 4.16 showing the sub-section of the overall network pinch approach.

The application of the modified network pinch approach with combined structure searches and cost optimisations is illustrated through adding a new exchanger unit in an existing preheat train.

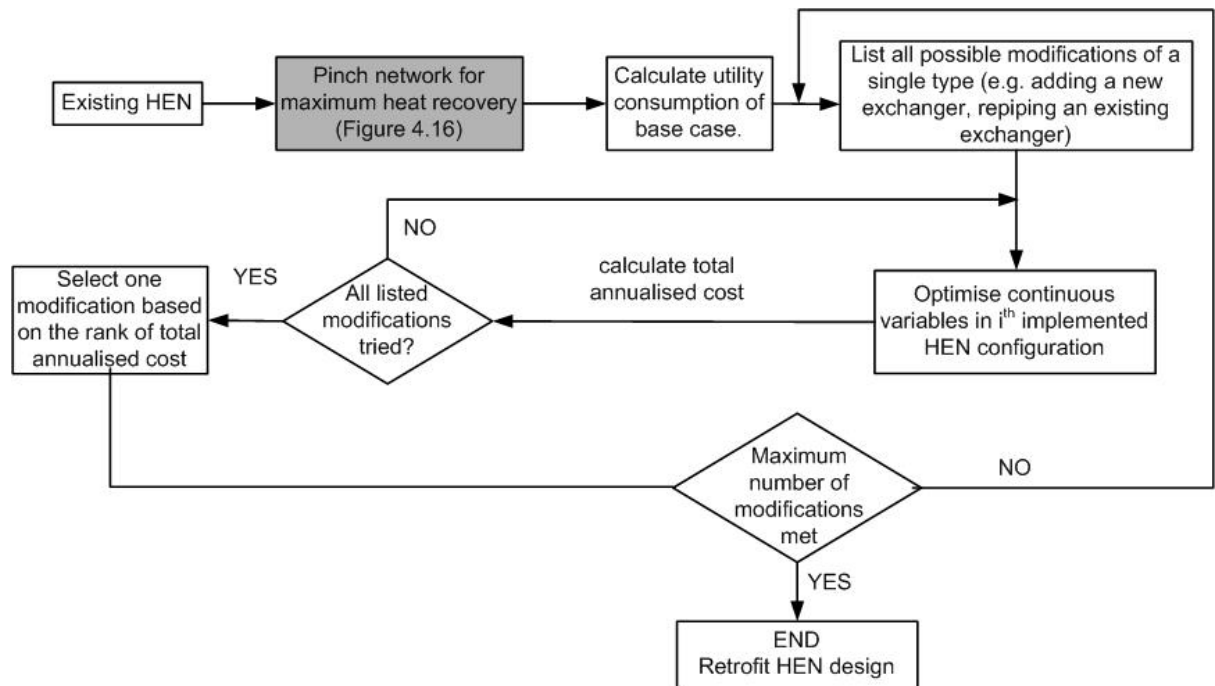


Figure 4.15 The modified network pinch procedure

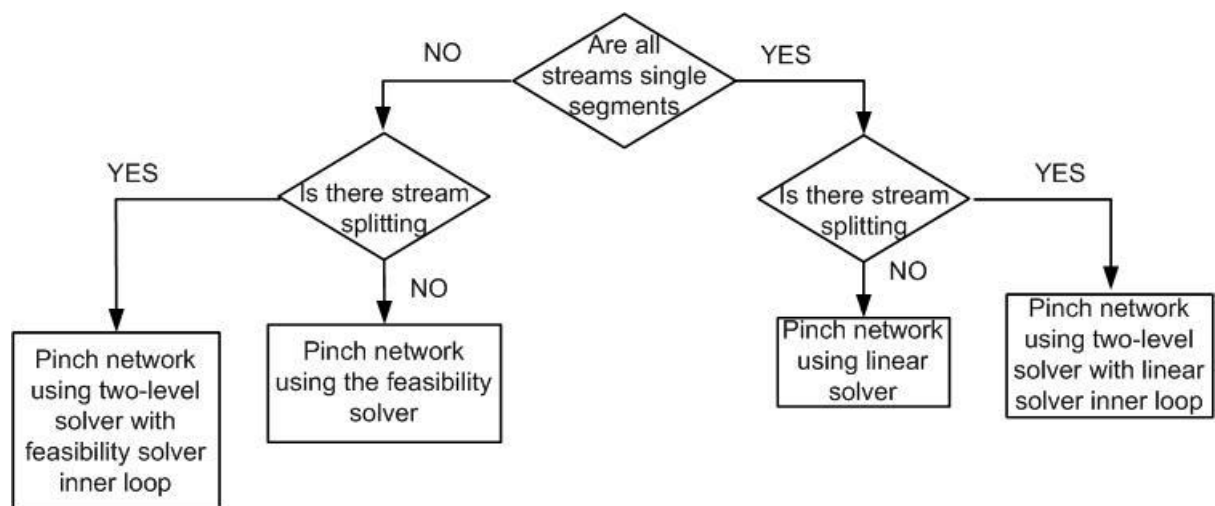


Figure 4.16 Pinch network for maximum heat recovery

4.4.6 Illustrative example 4.4: Adding a new exchanger to an existing preheat train

This example applies the approach described above to add a new match to the crude oil preheat train studied in Sections 4.3.3 and 4.4.2. The stream data are listed in Table A.2 (Appendix A). The existing HEN structure is shown in Figure 4.4, while the existing heat transfer area for exchanger units are presented in Table 4.4. The costs of utilities and exchanger modifications are set as those shown in Table 4.5. In

this example, the payback criterion is assumed to be 2 years with an interest rate of 5%.

The target of this example is to find out the most cost-effective retrofit HEN design allowing one new exchanger. The existing HEN is studied using the modified network pinch approach with combined structure search and cost optimisation. Table 4.13 shows the utility consumption, capital cost and total annualised cost of the optimised design with a new match found using the new approach. The performance of the best design without any topology modifications is also shown in Table 4.13, and compared with the results of adding a new exchanger.

It can be seen from Table 4.13 that by adding a new exchanger, the cost-effective retrofit design gained from the proposed new network pinch approach saves 20 MW hot utility and cold utility, or around 23% of the base case energy consumption. The capital investment required with this significant energy reduction is 3 MM\$, which is relatively small if compared with the operating cost reduction (6.37 MM\$/y). The payback time is around four month.

Table 4.13 Energy and cost reduction after adding a new match

	Existing network	No modification	Adding a new match
Hot Utility (MW)	88.95	72.97 (18%*)	68.59 (23%*)
Cold Utility (MW)	92.33	76.29 (17%*)	71.91 (22%*)
Operating cost (MM\$/y)	27.29	22.78 (18%*)	21.42 (23%*)
Additional area (m ²)	-	1334	1655
Capital investment (MM\$)	-	2.57	2.94
Payback (year)	-	0.33	0.32

*: percentage of saving with respect to base case

Table 4.13 also shows that a further 4 MW hot utility can be saved by adding a new exchanger, compared with no structural changes. These results indicate that in some cases, cost-effective retrofit does not always require topology modifications. The results also show that by using the new network pinch approach, the most cost-effective designs with a particular type of structural change could be indentified.

Figure 4.17 presents the most cost-effective design with a new exchanger.

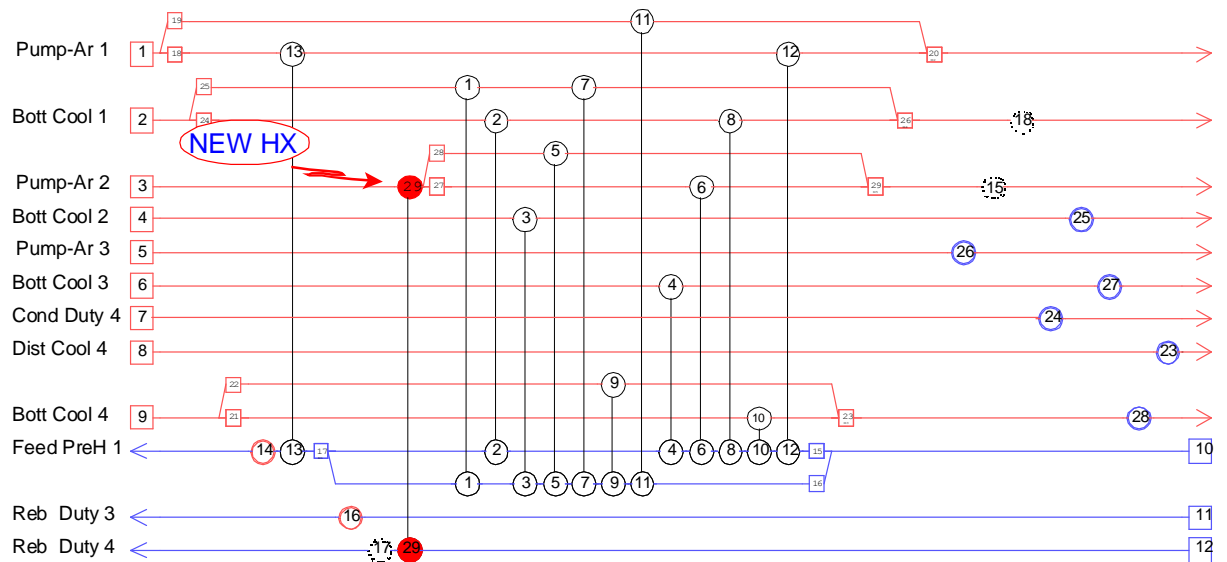


Figure 4.17 Suggested location of adding a match by the new approach

4.5 Summary of the chapter

Two design methods are proposed for HENs of process streams with temperature-dependent thermal property (e.g. heat capacity). The modelling of the HEN is discussed first, and then the simulated annealing optimisation-based design approach, facilitated by the proposed feasibility solver to transform infeasible HEN designs to feasible designs, is developed. The SA optimisation design method is suitable for both grassroots design and retrofit design, considering the existing network topology constraints and maximum number of modifications. The SA design method is applied in an existing crude oil preheat train, and it is proved to increase the performance of the existing HEN significantly.

The network pinch method for HEN retrofit (Asante and Zhu, 1996) is modified and extended as well for HENs of process streams with temperature-dependent thermal property. The two-level pinching approach is developed for the optimisation of continuous variables (heat loads and stream split fractions if there are existing stream splitters in the network) so that the heat recovery of the existing HEN is exploited to make sure that the bottleneck is the network topology rather than heat transfer areas. The advantages of the two-level strategy and the variation of stream split fractions are demonstrated through an illustrative example, and through comparisons of the results attained from the new pinching approach, the one-level SQP algorithm and the previous approach where stream split fractions of the existing

network are fixed. Moreover, the search for structural changes and capital-energy optimisation are combined into a single step for the first time, in order not to miss cost-effective designs in a HEN retrofit study. An illustrative example is shown to illustrate the application of the modified network pinch design approach.

The simulated annealing optimisation-based design method will be integrated with the design of crude oil distillation system in Chapter 5.

CHAPTER 5 DESIGN AND OPTIMISATION OF HEAT- INTEGRATED CRUDE OIL DISTILLATION SYSTEMS

5.1 Introduction

Crude oil distillation systems are very complex, normally including an atmospheric distillation unit, a vacuum distillation unit, a preflash drum or prefractionator column and a heat exchanger network (HEN) that recovers heat from pump-around streams and hot product streams to heat the cold crude. There are strong interactions between the distillation columns and the heat recovery system. For example, if the flow rate or temperature drop of one of the pump-arounds is increased, there will be more heat to recover in the preheat train, which in turn may decrease the furnace duty for preheating the crude oil. The change in the pump-around operation improves the potential of heat recovery with the atmospheric column, but at the same time reduces the internal reflux on the stages above the draw, so less separation takes place in the distillation column. If the flow of stripping steam to the bottom of the column is decreased, the temperature of the bottom product increases and the heat that can be recovered from this product increases.

Thus, the energy demand of the crude oil distillation system is determined not only by the design of the distillation columns but also by the design of the heat recovery system. For system design, there is a need to consider the interactions between the distillation columns and the HEN and to account for the interactions accurately. In this chapter, simulation of heat-integrated crude oil distillation systems is discussed first. In order to achieve sufficiently accurate modelling the heat-integrated system, the assumption that the thermal properties of process streams are constant with temperature (Rastogi, 2006) is overcome. Considering the complexity of the heat-integrated distillation system, an optimisation-based approach is proposed in this chapter to exploit the degrees of freedom in the design of fixed distillation configurations. This approach incorporates the simplified distillation models developed in Chapter 3 and the heat exchanger network models presented in

Chapter 4. The methodology is applicable to both grassroots and retrofit design of heat-integrated crude oil distillation systems, and to different design objectives, such as energy demand reduction, profit improvement, *etc.* Product specification constraints are taken into account in the methodology, together with other practical constraints, such as the capacity of the existing columns in retrofit designs, forbidden matches in the heat exchanger network topology, maximum number of topology modifications in retrofit designs, *etc.*, to make sure that the final design is practicable, industrially acceptable and applicable. The operating conditions and structures of both the distillation columns (e.g. pump-around location) and the heat exchanger network are varied in the optimisation. For optimising both continuous variables and integer variables, the design problem is formulated as a mixed integer non-linear programming (MINLP) problem. A suitable optimisation framework using a stochastic algorithm is developed to solve this highly non-linear and constrained problem.

Moreover, the need to study different distillation configurations is discussed. A novel configuration with a liquid side-draw prefractionator column upstream of the atmospheric unit is proposed. Modelling of the complex column with a liquid side-draw is presented; then the modelling of this type of column upstream of an atmospheric column is proposed.

5.2 Simulation of heat-integrated crude oil distillation systems

As discussed in the literature review (Section 2.3.1), there are two main approaches to represent the integration of crude oil distillation columns with the associated heat recovery system:

- Analysing the energy consumption target (minimum energy demand) and the required heat transfer area, through pinch analysis or heat demand. supply diagram for grassroots design, and area. energy curve for retrofit design (Suphanit, 1999; Gadalla *et al.*, 2003b; Bagajewicz, 2001a, b; Ji, 2002a, b, c). These approaches analyse stream data only . the details of the HEN configuration and design are not used.
- Calculating the energy consumption through HEN simulation (Rastogi, 2006). This approach incorporates stream data and details of the HEN structure and of heat exchange areas.

The first class of approaches (i.e. pinch analysis, heat demand. supply diagram and area. energy curve) can only predict the energy target and the corresponding total heat transfer area requirement. No HEN simulation is considered. These approaches are not able to account in detail for interactions between the heat recovery system and the distillation columns. The process for design of the heat-integrated crude oil distillation system is sequential, where the design of the HEN follows the design of the distillation columns. Because of its sequential nature, this design mode may miss some cost-effective design solutions. The advantage of these approaches is the simplicity and speed of analysing the heat recovery potential and the total heat transfer area requirement for a given energy demand of the distillation system. In sequencing study, the configuration of distillation system is a global issue that will have a radical impact on the energy demand, and therefore the HEN can be considered at an overview level. These approaches are suitable in optimising and selecting distillation configurations.

The second approach that is based on the simulation of HEN can account for interactions between the distillation system and the HEN in more detail. The approach is able to calculate the energy requirement of the distillation system after recovering heat from process streams in the heat exchanger network. The approach can integrate the design of HEN and distillation columns, which should lead to better designs of the whole system. Especially In the case of retrofit design, this second approach with HEN simulation is better, considering its ability of considering the existing heat transfer units in more detail. Section 5.2.1 presents the details of the heat integration approach based on HEN simulation.

As discussed in Section 4.1 and demonstrated in Section 4.3.3, assuming thermal properties constant with temperature, as in the work of Rastogi (2006), will introduce significant inaccuracies in the HEN design and analysis. This work implements multi-segment stream data to represent the process streams with temperature-dependent thermal properties. The models proposed in Section 4.3.2 are used for the simulation of a HEN with multi-segment stream data. Section 5.2.1 addresses the modelling of the interactions between the distillation system and the heat recovery system. After that in Section 5.2.2, the way of generating multi-segment stream data from column simulation results is presented.

5.2.1 Modelling the interactions within the crude oil distillation system

There are two modelling strategies for the simulation and design of chemical processes, sequential modular and equation-oriented strategies (Biegler *et al.*, 1997). In the sequential modular strategy, each unit is modelled and constructed as a sub-system. Then design models and thermodynamic models are solved sequentially from the upstream to downstream units of the process. The sequential modular modelling strategy is relatively more robust than the equation-oriented strategies in solving highly non-linear systems, as only one process unit is simulated at a time. The initialisation for only one unit is relatively easy to carry out. However, the disadvantages of the sequential modular strategy are that there are difficulties in treating complex computation sequences, as nested loops or simultaneous flowsheet and design specification loops (Dimian, 2003; p.46). Alternatively, in the equation-oriented strategy, all process unit models and thermodynamic models are combined into a single set of equations and the equations are solved simultaneously. With a sensible initialisation, the models are easier to solve and the calculation efficiency is higher, compared with the sequential modular strategy. However, it is difficult to construct and formulate a complex system using the equation-oriented strategy. The initialisation is another serious problem (Dimian, 2003; p.47).

The heat-integrated crude oil distillation system comprises distillation columns, the HEN and the process streams that interlink the distillation columns and the HEN, as shown in Figure 5.1. The simplified distillation models developed in Chapter 3 are semi-rigorous and highly non-linear. Considering temperature-dependent thermal properties, the HEN models presented in Chapter 4 are also non-linear. Moreover, non-linearity is observed in the thermodynamic property calculations (e.g. Peng Robinson equation of state). It can be seen from Figure 5.1 that many recycle streams exist in the crude oil distillation system, which makes the problem more complex and difficult to solve. If the crude oil distillation columns and the associated HEN are simulated simultaneously, the calculations of all recycle streams have to converge. Many simulations of the individual distillation column and HEN will be needed for one simulation of the overall system, which will be computationally intensive and the calculation may be trapped in an infeasible solution of either the

crude oil distillation columns or the HEN (Rastogi, 2006). The sequential modular strategy will be more appropriate, considering the high non-linearity of the overall system and the difficulties in converging the recycled pump-around and pump-back streams.

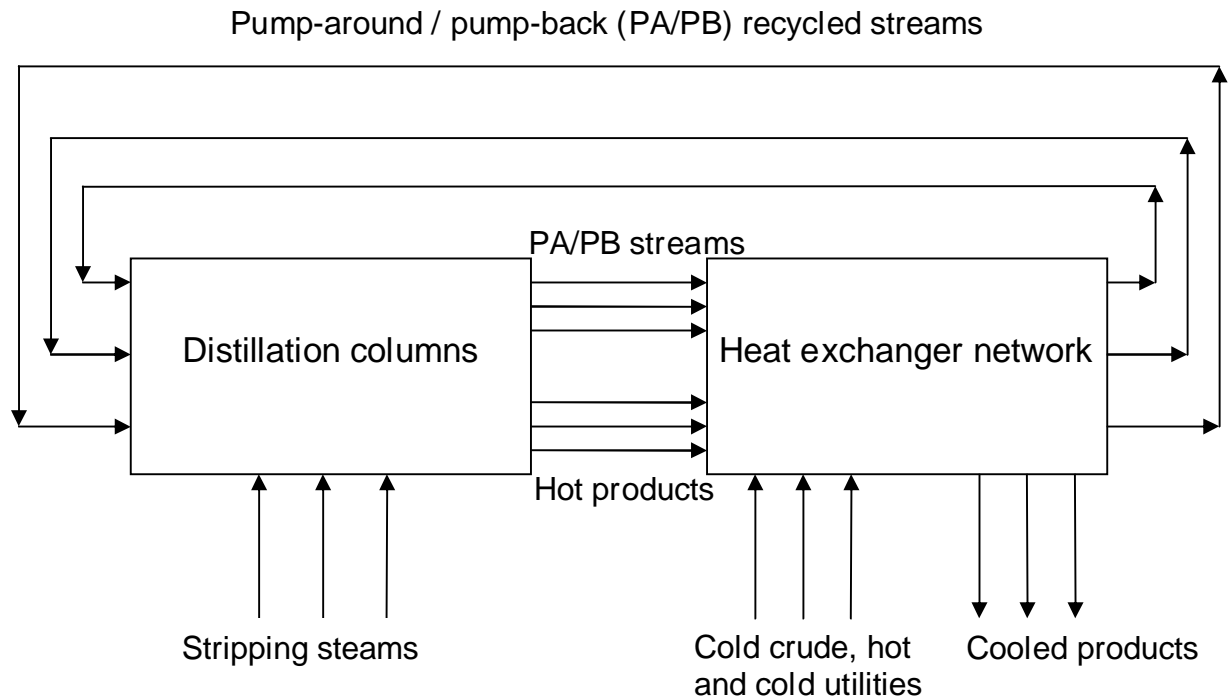


Figure 5.1 Interactions between crude oil distillation columns and heat exchanger network

Rastogi (2006) suggested a model for the interactions between the distillation columns and the HEN based on the sequential modular strategy. The model he developed solves the convergence problem caused by the recycle streams and be capable of considering the intense interactions between the crude oil distillation columns and the HEN. It starts with the simulation of distillation columns for specified operating conditions. Then the process stream data (i.e. supply temperature TS_j , target temperature TT_j , heat capacity flow rates CP_j , etc.) extracted from the column simulation results are used as the specification for the HEN simulation.

The HEN simulation is carried out, and stream temperatures are calculated after transferring heat in HEN ($TT_{calc,j}$). Comparing TT_j with $TT_{calc,j}$, a cost penalty function value is imposed on the objective function to compensate for the %unbalanced+ streams (streams where the target temperature is not achieved). The approach of

Rastogi (2006) is adopted in the present work with some modifications. Figure 5.2 shows the sequential modular strategy-based integration modelling of the present work. Different from that in the work of Rastogi (2006), instead of only checking stream balances, minimum temperature approaches are also checked since they may be violated as column operating conditions vary. Rather than imposing a cost penalty function to penalise such infeasible HEN designs (HEN designs that violate stream enthalpy balance constraints and minimum temperature approach constraints) directly, the feasibility solver developed in Section 4.4.1 is used to enforce the stream enthalpy balance constraints and minimum temperature approach constraints. Then if the HEN design is still infeasible, the cost penalty function will be used to penalise the design. The purpose of employing the feasibility solver is to overcome the infeasibilities of the proposed HEN design, and exploit the capacity and potential of the HEN to overcome the infeasibility by it self before imposing penalties. The interactions between the crude oil distillation columns and the associated heat recovery system are explored more fully if feasibility constraints are enforced, rather than applying penalties during the optimisation.

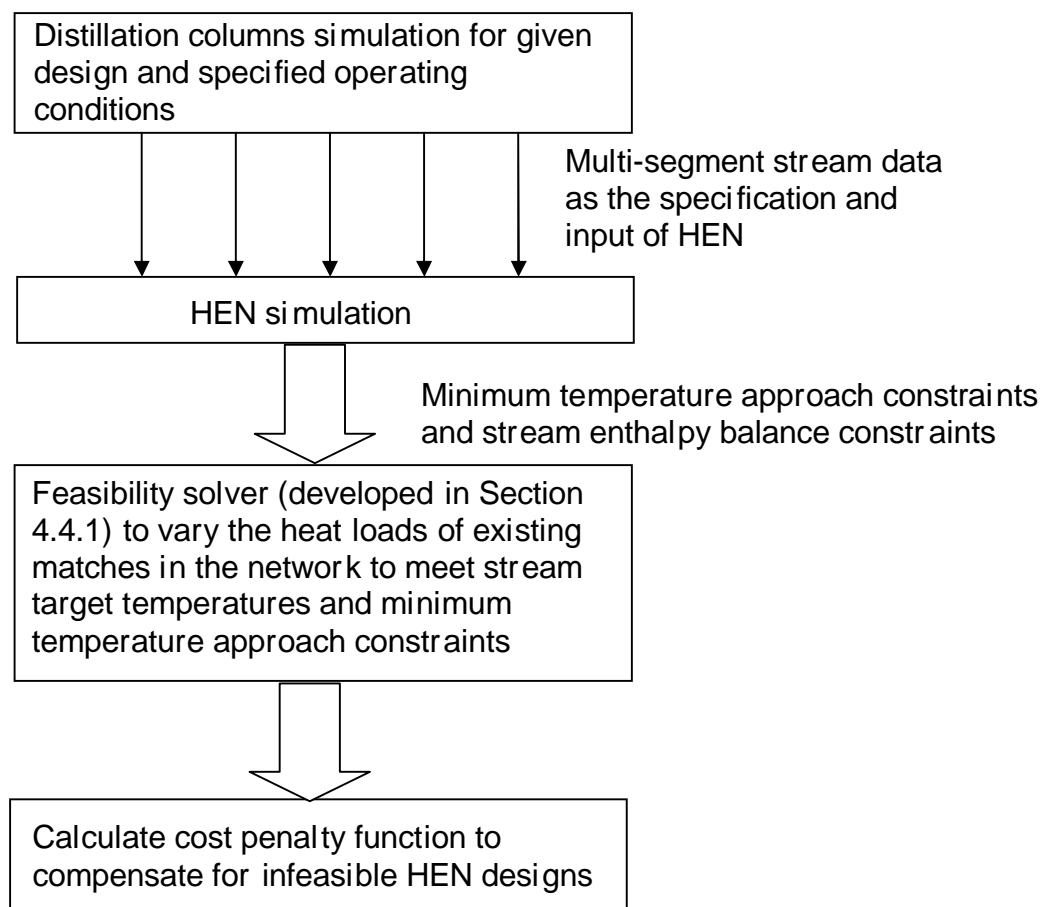


Figure 5.2 Sequential modular strategy in heat integration modelling

Section 5.2.2 presents the way of generating multi-segment stream data that are used as stream specifications in HEN designs.

5.2.2 Generation of multi-segment stream data

As explained in Section 4.3.1, stream data for HEN designs comprise supply temperature (TS_j), target temperature (TT_j), heat capacity flow rate (CP_j) or enthalpy change (DH_j) and film heat transfer coefficient (HTC_j). Note that only one parameter of CP_j and DH_j is independently specified.

As proposed in Section 5.2.1, the sequential modular strategy is used to model the interactions between the distillation columns and the associated HEN. The distillation columns are simulated first, then TS_j and TT_j are extracted from column simulation results for pump-around streams, products and the column feed, etc. The whole temperature range is broken into small temperature intervals and DH_j in the particular interval is calculated by thermodynamic models, e.g. Peng Robinson equation of state.

The multi-segment representation uses a piece-wise linear representation of the relationship between heat capacity and temperature. The multi-segment stream data generated must lie on temperature. enthalpy curve for the temperature range of interest. Considering this requirement, the segments are generated according to the following two rules:

- A new segment is generated for each temperature interval, for example 40 °C or 20 °C. The smaller the interval, the more accurate is the representation of the relationship between temperature and heat capacity. However, too many segments will cause intense calculation requirements in the simulation and design of the HEN. There is a trade-off between the accuracy of the calculation and the calculation speed in selecting the temperature interval. In the present work, the temperature interval is assumed as 40 °C in the case studies in Chapter 6.

- A new segment is generated where there is a phase change. There will be a large enthalpy change (latent heat) in a relatively small temperature range, when a phase change occurs. It is necessary to define temperature intervals appropriately in order not to miss this sharp change in enthalpy.

For stream heat transfer coefficients, two approaches are used to predict the values. The two approaches differentiate grassroots design and retrofit design. In the case of grassroots design, HTC_j is approximated based on the type of heat exchanger units that are going to be used in the HEN design (e.g. ref) and the fluid properties of the stream j . For retrofit design, where there is an existing network, HTC_j is regressed from existing heat transfer performance data.

For a heat exchanger l , given hot and cold side heat transfer coefficients $HTCH_l$ and $HTCC_l$, the overall heat transfer coefficient U_l is calculated by

$$\frac{1}{U_l} = \frac{1}{HTCH_l} + \frac{1}{HTCC_l} \quad (5.1)$$

5.3 Optimisation-based design approach

A heat-integrated crude oil distillation system is a complex system. It contains complex distillation column configurations, with side-strippers, pump-arounds or pump-backs and steam stripping, *etc.* The simplified models (Chapter 3) of such columns are highly non-linear. The physical property calculations are non-linear as well. Moreover, there are strong connections between the distillation columns and the associated HEN. The HEN models are non-linear since non-linear thermal properties are considered. There are many degrees of freedom in the design of the overall system, such as operating conditions of distillation columns and of the HEN, and structural options in the columns and the HEN. In order to consider all of these degrees of freedom, the design problem is formulated as a MINLP problem and a multiple-run simulated annealing algorithm is employed as the optimiser. This section discusses the proposed optimisation-based design approach.

5.3.1 Objective function

The purpose of optimisation in a process design is to identify an optimal solution, appropriately balancing between competing influences. Mathematically the procedure of identifying a best solution is to minimise or maximise a specified objective function. Which objective function is selected depends on the design objective. A widely-used objective function in process design is the total annualised cost (TAC), which is defined as the sum of the operating cost and annualised capital cost. The TAC can represent the trade-off between energy and capital investment. However, other industrially relevant issues, such as safety, reliability, *etc* are not captured using TAC. In the process conceptual design stage, energy and capital investment are more important than other factors (i.e. safety, reliability, maintainability, *etc.*) since economic benefits dominates in industry. The operating cost of a crude oil distillation process includes the cost for stripping steam, and the cost of hot and cold utilities cost. These utilities typically include fired heating (e.g. via gas and oil combustion), steam (e.g. medium pressure steam) and cooling water or air. In some cases, steam generated in heat recovery provides a value-added cold utility. For grassroots design, the capital cost includes the cost for all the distillation columns and heat exchanger units in the process. In the case of retrofit design, existing units are associated with zero costs, and only costs for modifications to the existing units are considered.

The calculation of each cost component is explained as following:

- The utility costs are calculated using unit cost data (cost per unit of energy) and the calculated demand for each utility. Unit cost data are provided as input to the optimisation. The unit cost data used in Chapter 6 are taken from Gadalla (2002).
- The cost for stripping steam is obtained from the unit cost and the flow rate.
- The hydraulic models of Fair, Kesler and Wankat (cited in Liu, 2000, p.28) are used to calculate the required diameters of the distillation columns. The cost models (Equations 3.11 . 3.14) of Guthrie (1969) are employed to calculate the capital cost of the simple distillation columns in the decomposed sequence, and M&S Index of 2006 (Chemical Engineering, 2006, see illustrative example 3.3) is used to update the capital cost. The costs for complex columns (e.g. atmospheric distillation unit) with side-strippers, pump-arounds, *etc.* are calculated by merging the decomposed sequence of simple columns. The cost calculation for distillation

column applies to all distillation units in grassroots design and new units installed in retrofit design.

- The capital cost calculation for exchanger units (Equation 3.10) is taken from Gadalla (2002). Different sets of parameters can be used for additional area installed in existing units and for new exchanger units.
- Cost for structural modifications to the existing HEN is defined as fixed cost per modification (Rodriguez, 2006), since structural modification cost is highly related to the existing piping work, and is case specific and very difficult to estimate.

Note that in addition to the costs considered above, other cost components can be included. For example, cost for pumps used in the distillation process. Furthermore, more complex formulations than those proposed in this work can be used as the simulation models and optimisation steps are decoupled, there is considerable freedom regarding the formulation of the objective functions (This aspect will be presented later in Section 5.3.4).

The net profit (NP) can be maximised allowing the product flow rates to vary. The value of products and cost of the crude oil feed are included in the objective function by:

$$NP = CC_{prod,j} \cdot PROD_j - CC_{crude} \cdot F - TAC \quad (5.2)$$

where CC_{crude} is the unit price of crude oil (\$/kmol); $CC_{prod,j}$ is the unit price of product j (\$/kmol); $PROD_j$ is the flow rate of product j (kmol/h) and F is the flow rate of crude oil feed (kmol/h). Note that other flow units can be used.

Some products of the crude oil distillation system are not end products, but are fed to downstream processes after the distillation process. For instance, light naphtha can be blended directly into the end product gasoline, and no downstream process is required. In the case of heavy naphtha, catalyst reforming is needed before it is blended into gasoline. For those products which do not need downstream processing, the price of the end product is used as the price of the distillation product directly as the cost associated to the blending process can be ignored. If there are downstream processes, the operating cost of treating a unit of product is subtracted from the original end product price to give the value of the distillation product. Table 5.1 lists

the prices of products and the crude oil feed used in this work. The prices are given per unit flow.

Table 5.1 Prices of distillation products and crude oil feed in crude oil distillation system

Item	End product	End product price ⁽¹⁾ (\$/barrel)	Downstream process	Operating cost of downstream treating ⁽²⁾ (\$/barrel)	Efficiency of end product production ⁽³⁾	Price for intermediate products (\$/barrel) (\$/kmol)	
Light Naphtha	Gasoline	91.7	N/A	N/A	N/A	91.7	73.4
Heavy Naphtha	Gasoline	91.7	Catalyst Reforming	2.96	0.8	71.0	92.7
Light Distillate	Jet fuel	83.7	Hydrotreating	0.36	0.95	79.1	128.1
Heavy Distillate	Diesel	84.6	N/A	N/A	N/A	84.6	215.7
Residue	Residue fuel oil	47.9	N/A	N/A	N/A	47.9	204.3
Crude oil	N/A	66.7	N/A	N/A	N/A	66.7	108.2

(1) http://tonto.eia.doe.gov/dnav/pet/pet_pri_spt_s1_d accessed on 15/05/07

(2) Robert (2000)

(3) Product yield, the values are taken from refining industry

The selection of objective function and the parameters in costing the overall system can be changed. The usage of other objective functions, cost components and prices of crude oil and products will not affect the fundamental basis of the proposed optimisation-based design approach.

5.3.2 Process constraints

Process constraints are considered in the optimisation in order to make sure that the solutions are industrially acceptable and practicable. The purpose of the distillation system is to separate crude oil into specified products. Hence, constraining product qualities is important in the optimisation; product quality is not considered in previous studies. Facilitated by the method proposed in Chapter 3 to estimate the true boiling curve from pseudo-component compositions, product constraints in terms of TBP points are included in this work. If the objective function is minimum total annualised cost, product flow rates are kept unchanged and added into the constraints. In the case of retrofit design, other constraints, such as hydraulic constraints of the existing distillation columns, are considered in the optimisation. There are several ways to

consider constraints, as discussed in Section 4.4.1. In the present work, a penalty function is used to convert the constrained problem to unconstrained problem. That is, if a constraint is violated, a penalty will be imposed: it will be added to or subtracted from the objective function, depending on whether the objective is to be minimised or maximised. The penalty is calculated as follows:

$$\begin{aligned}
 \text{Penalty} &= \gamma (x_i - x_{i, \text{spe}})^2 && \text{if } x_{i, \text{lower}} \leq x_i \leq x_{i, \text{upper}} \\
 \text{Penalty} &= \gamma (x_i - x_{i, \text{upper or lower}})^2 && \text{if } x_i > x_{i, \text{upper}} \text{ or } x_i < x_{i, \text{lower}} \\
 i &= 1, 2, 3 \dots n_{\text{vary}}
 \end{aligned} \tag{5.3}$$

where x_i is the simulating results of the dependent variable i ; $x_{i, \text{spe}}$ is the specified values of the dependent variable i ; $x_{i, \text{lower}}$ and $x_{i, \text{upper}}$ are the lower and upper bounds of the dependent variable i ; n_{vary} is the total number of constrained variables. The value of the penalty parameter γ depends on the stage of optimisation. At early stages of the optimisation, a small value of γ is used to avoid too early convergence. As the optimisation going on, γ is increased gradually to make sure that final solutions are feasible.

As discussed in Section 4.4.1, in the design and optimisation of the associated heat recovery system, there are other constraints that need to be considered: minimum temperature approach constraints and stream enthalpy balance constraints. Note that in retrofit design, minimum approach temperature can be as small as zero. Then, the minimum temperature approach constraints can be referred as temperature crossover constraints (the outlet temperatures of hot stream and cold stream cannot crossover). Moreover, network topology constraints may be imposed due to safety issues, economic considerations, etc. The approaches proposed in Section 4.4.1 are employed to deal with these constraints that are relevant to HEN design.

5.3.3 Optimisation variables

As the multiple-run simulated annealing algorithm is employed as the optimiser (see Section 5.3.4) in the design of heat-integrated crude oil distillation system, degrees of freedom considered in the optimisation are represented in the form of a move tree

(see Appendix B for the description of simulated annealing algorithm and parameters) as shown in Figure 5.3. Each node item in the move tree represents an optimisation variable; which move to make in the optimisation procedure depends on the assigned probability and the generated random number. The move probabilities provide flexibility in the optimisation procedure. If an optimisation variable has a significant influence on the performance of the system, a high probability can be assigned to it. The selection of move probabilities is problem-specific and experiments may be needed to set parameters that can lead to the optimum solution relatively efficiently.

The overall system comprises two sub-systems: distillation columns and the associated HEN. Thus, the moves are divided into two groups: distillation columns move and HEN move. There are probabilities (p for distillation columns and $1 - p$ for HEN) associated to each group, and the sum of them must be one. The probability of distillation column move p (or HEN move $1 - p$) is a very important degree of freedom (Rastogi, 2006). The optimisation variables considered in the HEN are the same as in the simulated annealing optimisation-based HEN design approach proposed in Chapter 4. Figure 5.3 presents the distillation column and HEN moves branches of the move tree.

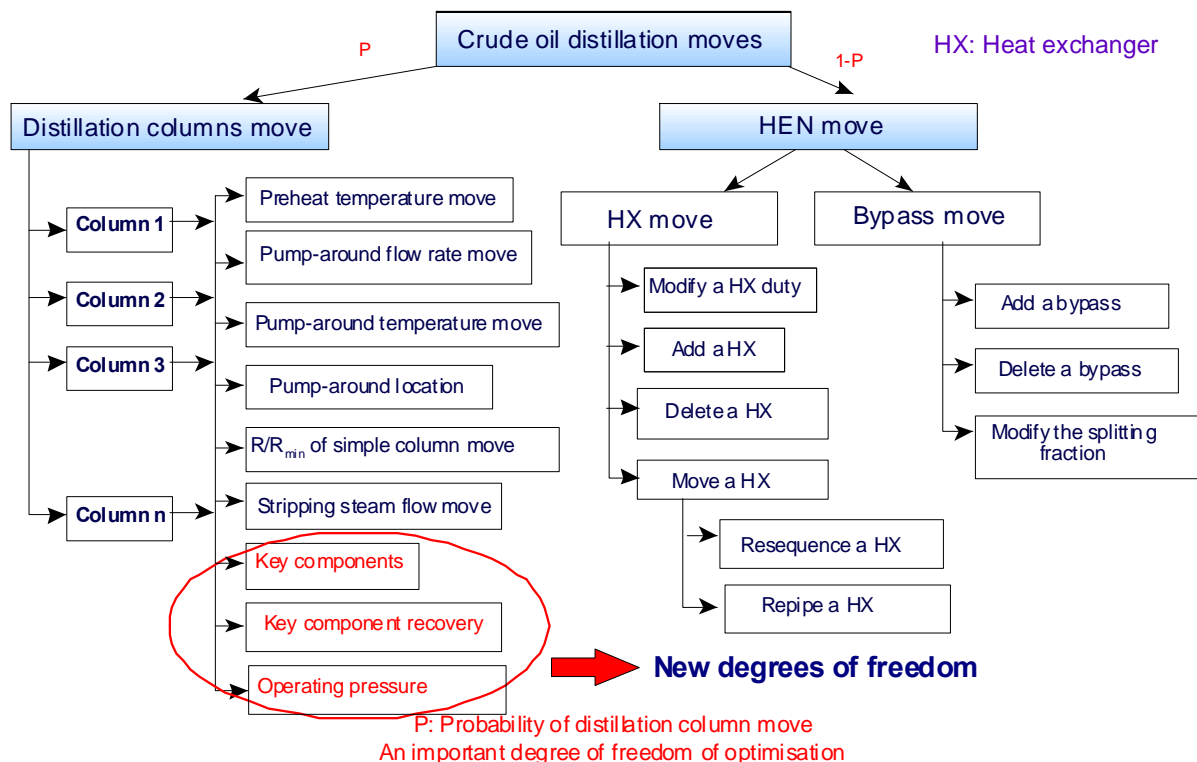


Figure 5.3 Optimisation variables in overall system design

If a distillation column move is proposed in the optimisation, one of the decomposed simple columns is selected to modify according to their move probabilities. Different probabilities can be assigned to individual simple columns to provide more flexibility in selecting columns in the optimisation, rather than assigning a same probability to all columns as implemented in previous work (Rastogi, 2006). Then one of the operating conditions or structural options in the selected simple column is modified. The varying operating conditions in minimising total annualised cost are: feed temperature, pump-around duties or flow rates, temperature drop through a pump-around, steam flow rate and ratio of finite reflux ratio to minimum reflux ratio (R/R_{\min}). The structural options in the distillation columns comprise location of pump-arounds.

In simplified distillation models, four variables, light key, heavy key and each of their recoveries, are used to specify the separation. If the design objective is net profit or in the case that one of the products is collected from more than one distillation column (sloppy splits), and product flow rates are not constant, these variables are included in the optimisation. These four variables have not been considered previously in optimising the profit of the distillation system. In the work of Gadalla (2002) and Rastogi (2006), the selection of key components is carried out manually when maximum net profit is the objective function, and without constraining the product properties. Key components and recoveries are important degrees of freedom due to their impact on the separation, and in turn, on the products obtained from the distillation. A systematic exploitation of these four variables is important in determining the profit of the overall system. Moreover, different configurations of crude oil distillation columns can be optimised and compared, facilitated by a systematic exploitation of product distributions.

The operating pressure in a distillation column is an important degree of freedom in the design. As the pressure is increased, heat recovery opportunities may be enhanced since higher a level of heat resource is generated. However, higher pressure is harmful to separation. Considering the trade-off between heat recovery and separation, operating pressures are included in optimisation variables for improving the performance of the overall system further, in terms of heat recovery and energy demand.

5.3.4 Optimisation framework and algorithm

In the design of heat-integrated crude oil distillation systems, both distillation columns and heat exchanger networks are optimised in a single framework. The simplified distillation models (Chapter 3) are highly non-linear. Moreover, the thermodynamic models (e.g. Peng-Robinson equation of state) in the physical property calculations are also highly non-linear. As stated in Section 5.3.3, the structural design decisions in distillation columns, such as pump-around locations, and the selection of key components for specifying separations in simplified distillation models, introduce discrete variables to the optimisation. When heat integration is accounted for through heat exchanger network simulation, HEN models (Chapter 4) are implemented in the optimisation. These models consider the dependence of heat capacity on temperature, which introduces non-linearities. In addition, many discrete and binary variables are introduced to represent the configuration of the HEN. Hence, the crude oil distillation system with integrated process models (distillation column models, HEN models and the model that simulates the interactions within the crude oil distillation system) is a MINLP problem. Even when pinch analysis is applied in modelling the heat integration of distillation sequencing problems, the design is still a MINLP problem. An optimisation framework that can address integer variables and non-linearities is required for developing crude oil distillation system designs.

As discussed in the literature review (Section 2.3), Rastogi (2006) considered distillation columns and details of the heat exchanger network together in the design methodology for crude oil distillation system. The design approach of Rastogi (2006) is superior to others (Liebmann, 1996; Suphanit, 1999; Bagajewicz, 2001a, b; Ji, 2002a, b, c; Gadalla, 2002) since both structural options and operating conditions of distillation columns and of the HEN are considered in a single framework. The optimisation framework in the present work extends that of Rastogi (2006).

Figure 5.4 presents the optimisation framework adopted in the present work for the overall system design. The optimiser starts with a given feasible structure and set of operating conditions of the crude oil distillation system. In grassroots design, a starting feasible design of the crude oil distillation system is required; in the case of retrofit design, the starting point can be the existing process. Structural options and

operating conditions (see Section 5.3.3 for optimisation variables) of the crude oil distillation system are changed by the optimiser and analysed, based on objective function. The objective function of the proposed design is calculated from the output of the distillation models and HEN models (see Section 5.3.1). In addition to the starting point, bounds on the optimisation variables are given as the input to the optimisation framework so that the optimiser changes the optimisation variables within the given range. These bounds represent constraints on the optimisation variables, many of which are related to the practicability of the solutions generated. The optimal solution therefore is forced to be feasible and implementable in practice. Other constraints are also considered as well in the optimisation framework. The constraints considered and how they are handled are presented in Section 5.3.2.

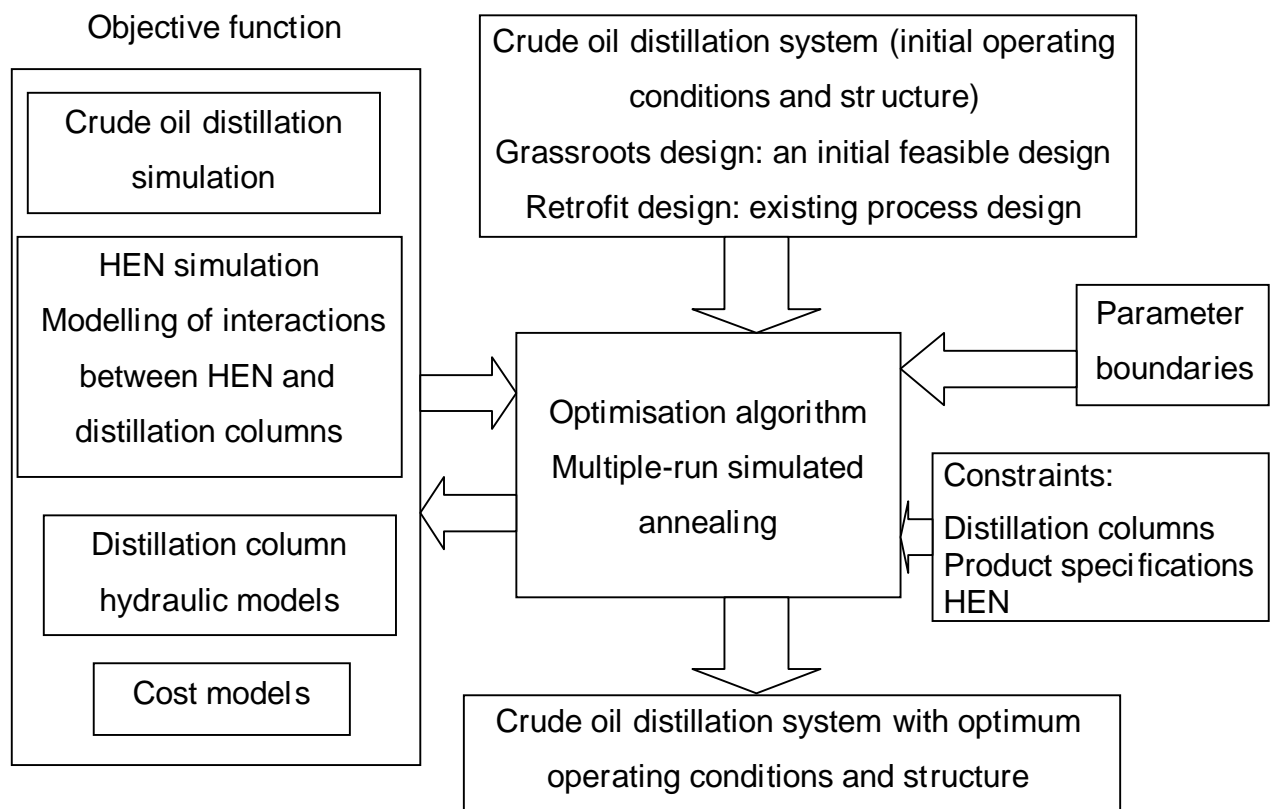


Figure 5.4 Optimisation framework

The optimiser in the optimisation framework has a very important role. It should be efficient and effective for generating different designs of the crude oil distillation system and analysing them. MINLP problems are among the most difficult problems to optimise (Biegler and Grossmann, 2004). The difficulties in optimising a MINLP problem arise mainly from the non-convex nature of the non-linearities and from the combinatorial nature introduced by discrete variables.

Conventional methods for solving MINLP problems are decomposing the problem into non-linear programming (NLP) and mixed integer linear programming (MILP) sub-problems, and then solving these sub-problems iteratively. Among the conventional methods, the most commonly used ones are Branch and Bound, Generalised Benders Decomposition, Outer Approximation and Extended Cutting Plane Method. A comprehensive review of these methods can be found in Grossmann and Kravanja (1995), Biegler *et al.* (1997) and Biegler and Grossmann (2004).

In these methods, the search algorithms used in the NLP sub-problems are generally deterministic, based on gradient information. It is very likely that the search algorithm converges to a local optimum instead of the global optimum (Arora, 2004; p.567). In addition, the use of gradient information limits the application of these methods to problems with continuous and differentiable functions. Moreover, conventional methods require significant amounts of time and memory to solve a MINLP problem as they are based on tree enumeration of the integer space.

Stochastic methods are alternatives to conventional methods for solving MINLP optimisation problems. Stochastic methods do not require detailed formulation of the problem or derivatives of the problem. The search for the optimum is based on the objective function values of different points in the search space. Stochastic methods can optimise discontinuous and non-differentiable problems (Arora, 2004; p. 565). In addition, most stochastic algorithms have more chances to escape from local optima than deterministic methods in solving non-convex problems (Arora, 2004; p.572).

Simulated annealing (SA) is a stochastic optimisation algorithm that has been widely applied for process design. It was first proposed to solve combinatorial problems by Kirkpatrick *et al.* (1983), who observed the analogies between the physical annealing process and an optimisation problem. Since then, it has been applied in a wide range of problems, including various problems related to synthesis and optimisation of process systems (Jung and Cho, 1993; Chou *et al.*, 1994; Floquet *et al.*, 1994; Linke, 2001; Choong, 2002; Jain, 2005). It has also been implemented for the design of crude oil distillation systems in the work of Rastogi (2006). Details of the annealing algorithm proposed by Kirkpatrick and his co-workers are presented in Appendix B.1.

Simulated annealing is selected to design heat exchanger networks with temperature-dependent thermal properties in Chapter 4 (Section 4.4.1). The advantages of this algorithm are discussed in Section 4.4.1, and the SA algorithm has shown its application in the design of a complex HEN (Illustrative example 4.2, Section 4.4.2). Based on the same reasons as presented in Section 4.4.1, simulated annealing is chosen to optimise the design of the overall system as well.

Due to the complexity of the optimisation problem of design of heat-integrated crude oil distillation systems, modifications have been made to the standard SA algorithm to solve the problem better. Although the SA algorithm has more chances of finding a global solution, compared with conventional methods, it is still possible for the SA algorithm to get trapped in a locally optimal solution for a highly non-linear and combinatorial problem that requires the optimisation of a large number of variables and with many constraints. In such a problem, a global solution cannot be guaranteed in finite computational time (see Section B.1 for more discussion). In order to gain confidence in the optimised solution, multiple runs of simulated annealing optimisation are implemented in this work. After one run is finished, the best solution found in the last run is used as the initial point to start the next run, with a different random number seed (The random number seed is used to generate random number, and different seed generates different sequence of random numbers in the optimisation.). By implementing this strategy, the SA algorithm is able to explore the solution of the previous run, starting at the initial cooling temperature. It helps to escape from the local optimum at which the standard algorithm converges in the last run. The SA algorithm accepts uphill moves; this is beneficial in finding a global solution. However, accepting uphill moves may cause the algorithm to converge to a solution with an objective function that is worse than a previously proposed design. This drawback is overcome by storing the best solution ever found during the optimisation procedure.

5.3.5 Implementation of the overall design approach

The models of crude oil distillation columns (Chapter 3), heat exchanger networks (Chapter 4) and the interactions within the crude oil distillation system (Section 5.2) are coded in FORTRAN programming language. The Peng-Robinson equation of

state (Suphanit, 1999) is incorporated for vapour-liquid equilibrium calculation. The overall optimisation framework presented in Section 5.3.4 is coded in FORTRAN programming language. The overall optimisation framework and the crude oil distillation models are embedded in COLOM (v2.1). The HEN modelling and design approaches (simulated annealing optimisation-based design approach and modified network pinch approach) developed in Chapter 4 are embedded in SPRINT (v2.2); access to SPRINT is available via COLOM. The input of the existing HEN structure in retrofit designs or the initialisation of the HEN in grassroots designs is through SPRINT. Then the SPRINT file is imported into COLOM for the design of the whole system. After the optimisation of the overall system, the optimised HEN design is exported to SPRINT. The procedure for applying the heat-integrated crude oil distillation system design approach is summarised as follows:

1. The crude oil assay is specified in HYSYS (v2004.2). The number of pseudo-components is selected. Using the built-in facility in HYSYS, the crude oil assay is cut into pseudo-components with calculated physical properties for each component. The physical properties include molecular weight, normal boiling temperature, critical temperature, critical pressure, critical volume, and Pitzer's acentric factor. The coefficients of vapour pressure calculation and the enthalpy correlation for each component are also calculated in HYSYS. In addition to pseudo-components, other chemical components, such as water (stripping steam) and light ends in the crude oil feed can also be specified.
2. The physical properties for all the components in the crude oil feed are then extracted from HYSYS to a CMP file (component file) through a macro interface written by Suphanit (1999). The CMP file is imported into COLOM (v2.1), where the physical properties are used in the thermodynamic models.
3. The structure and operating conditions of the crude oil distillation system are inputs for both grassroots design and retrofit design. The complex distillation columns (e.g. atmospheric distillation unit, vacuum distillation unit) are input in the form of decomposed indirect sequence of simple columns (Section 3.2.1). The cost of crude oil feed per unit flow rate and the unit value of end products coming from the distillation products of the columns need to be specified in the case that the objective is to maximise net profit. The temperature interval for

generating multi-segment stream data is specified. The product specifications are required in terms of product boiling points and flow rates.

For retrofit design, the optimisation procedure can start with existing structure (i.e. number of pump-arounds, number of actual stages and the diameter of each column section, number of side-strippers, *etc.*) and operating conditions (i.e. feed preheating temperature, steam flow rates, reflux ratio, pump-around flow rates, pump-around temperature drops, *etc.*) of the existing crude oil distillation columns. For grassroots design, an initial feasible design of crude oil distillation columns needs to be developed (e.g. following guidelines in Watkins, 1979).

4. In retrofit design, the existing heat exchanger network (i.e. number of process exchangers, utility exchangers and their connections in HEN, exchanger duties, and stream splitters flow fractions, *etc.*) is specified via SPRINT v2.2 and imported into COLOM v2.1. For grassroots design, an initial heat exchanger network is developed by fulfilling all the heating and cooling requirements of streams by utilities. The utility cost is specified, as well as the coefficients of the exchanger cost model (Equation 3.10). The minimum temperature approach for designing the HEN is set. The costs of structural modifications to existing HEN (i.e. re-piping, re-sequencing, *etc.*) are additional inputs in the case of retrofit design.
5. The optimisation variables are selected (see Section 5.3.3 for optimisation variables considered in the present work). The lower and upper bounds of the variables are then set.
6. The deviation tolerances of product boiling temperature points and flow rates are specified. Other practical constraints, such as hydraulic limitations of distillation columns, maximum number of re-piping and re-sequencing modifications, maximum number of new exchanger units, *etc.* are also specified.
7. The simulated annealing parameters are specified and the objective function is selected (see Section 5.3.1 for objective function considered in the present work). The number of SA runs to be carried out is specified and then the optimisation runs are performed.

8. The optimised design (structure and operating conditions) of the distillation columns and the associated HEN is obtained after the optimisation runs converge. The investment for the modifications in the new design is reported. The optimised HEN is then exported to SPRINT v2.2 for reporting optimised configuration and operating conditions, required additional area and capital investment, *etc.*

It is well known that, for MINLP problems, global solutions cannot be guaranteed, even when using stochastic methods. The quality of the optimised solution depends on the specified simulated annealing parameters. Hence, the optimisation procedure should be carried out several times with different sets of simulated annealing parameters and move probabilities to obtain confidence in the optimised solution.

5.4 Studies of different column configurations

Studies of distillation configurations are important, since the energy demand for separating a mixture is greatly affected by the distillation configuration. The exploration of distillation configurations can identify potential energy reduction opportunities and chances of using different levels of heating and cooling resources in the process. For example, in crude oil distillation processes, the progressive configuration which features as the succession of progressive separations may create more heat recovery opportunities. The research on synthesis of distillation sequences separating conventional chemical mixture is rich; however, only little work has studied different configurations of heat-integrated crude oil distillation systems.

Liebmann (1996) designed two configurations, the conventional atmospheric column and the atmospheric column with rectifiers. The design started from a direct sequence and an indirect sequence of simple columns. The simple columns were modified for better heat recovery potential, based on heuristic rules, and then merged into complex atmospheric columns. No optimisation has been carried out in the design procedure and the design requires iterations and trial and error. Suphanit (1999) carried out optimisations on different configurations and compared the best performance of each configuration. The configurations that have been studied in the work of Suphanit (1999) are: the conventional atmospheric column, the conventional

atmospheric column with a prefractionator column, the progressive distillation configuration, the direct sequence, the direct sequence with a side-rectifier in the last column, and the configuration of two columns with a side-stripper. These studies were of very limited scope. In particular, they were restricted by assumptions such as constant thermal properties with temperature for process streams, the location of pump-around must be on the same stage as side-stripper, no pump-around located above the top side-stripper in an atmospheric column, not considered pressure drop in distillation columns, not constrained product properties, *etc.* Moreover, the comparison was based on not fully optimised configurations since the problem is considered as a NLP problem and a deterministic method successive quadratic programming algorithm was used as the optimiser. This optimisation approach is easily trapped at local optima.

In this work, many more degrees of freedom are taken into account. These include the number of pump-arounds, location of pump-arounds, separations taking place in distillation columns, operating pressure of distillation columns, *etc.* The heat integration between distillation columns and the associated HEN is considered more accurately using multi-segment stream data, avoiding the assumption of constant heat capacities. Moreover, the multiple-run simulated annealing algorithm, which has more chances to find global optimum, is employed as the optimiser. Practical constraints, such as product specifications, the limits of existing equipment, *etc.* which could not be considered previously, are taken into account in the proposed design approach.

All of the above issues are beneficial for developing more accurate, industrially practical and applicable designs, which can better predict the best performance of the configurations that have been studied in previous work. There arises a need to re-optimize and compare various configurations to explore their potentials using the proposed design approach. Case study 6.4 in Chapter 6 will optimise three industrially established configurations of atmospheric crude oil distillation column and compare the optimised designs. The three configurations are: an atmospheric crude oil distillation unit without a prefractionator column, an atmospheric crude oil distillation unit with a prefractionator column, and the progressive distillation configuration. The study is limited to industrial concerns and queries and it is based on a study carried out for a global refiner.

In addition to these three industrially established configurations, another novel configuration is going to be optimised. The novel configuration proposed in this work is shown in Figure 5.5. The prefractionator column has a liquid side-draw and the liquid can be fed into the atmospheric distillation column at different locations. In Figure 5.5, the location of entering the prefractionator liquid to the atmospheric unit is defined as **XX**. Only four locations are considered, which will be explained further in Section 5.4.3. In this work, the location of entering the prefractionator liquid to the atmospheric unit is not systematically optimised. The location must be selected, and then the location of the liquid draw in the prefractionator column will be optimised. This novel configuration is inspired by an industrial case. Modifications are carried out to the industrial configuration to improve its energy efficiency. Compared with conventional prefractionator columns, the liquid side-draw reduces the flow rate of column bottom product. In turn, the heat load on the process furnace heating the main atmospheric distillation unit feed decreases. In case study 6.4, where the three industrially established configurations are optimised and compared, this novel configuration will also be optimised. In this section, the modelling of the proposed configuration is discussed.

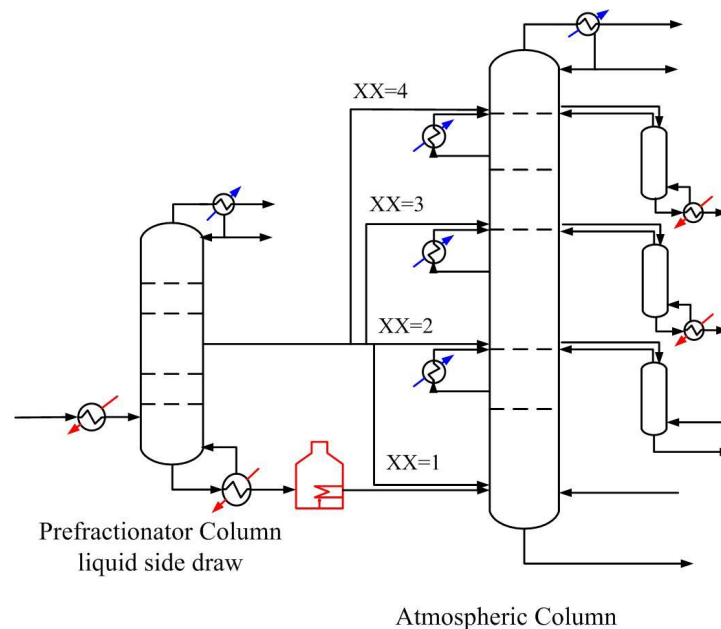


Figure 5.5 Novel configuration with a liquid side-draw prefractionator column

5.4.1 Modelling of liquid side-draw prefractionator columns

This section presents the modelling of prefractionator columns with a liquid side-draw. The model is applicable to both reboiled and steam-stripped columns. Columns with a side-draw are complex columns, which separate the feed into three products. The design issues that need to be addressed include feed preheating temperature, reflux ratio, side-draw location, flow rate of side-draw, type of vaporisation (i.e. reboiler and steam stripping), number of theoretical stages required in each section of the distillation column and the diameter of each section. Modelling of crude oil prefractionator columns with a liquid side-draw presents a significant challenge because of the complexity of the column and large number of components in crude oil feed and products. Some research has been carried out on the design of this type of columns (Gutierrez-Antonio and Jimenez-Gutierrez, 2007; Rooks *et al.*, 1996; Glinos and Malone, 1985). These existing design approaches are either based on short-cut or graphical method. The assumptions that are made restrict the applicability of the approaches to chemical mixtures with a few components. Moreover, the existing approaches are only applicable to reboiled columns, which is only part of the case under study.

Rastogi (2006) proposed simplified distillation models for vacuum towers, which comprise a main column and several pump-around sections with liquid side-draws, as shown in Figure 5.6. Rastogi (2006) suggested decomposing the complex vacuum tower into a thermally coupled sequence of a simple column and several supplementary rectifying sections with pump-arounds. The simple column and supplementary rectifying sections are then modelled by simplified methods with a proposed correlation to predict the number of stages at a finite reflux ratio condition rather than Molokanov correlation (Rastogi, 2006).

It can be seen that vacuum towers are similar to liquid side-draw prefractionator columns. Both columns have liquid side-draws. A key difference is that the liquid side-draw in prefractionator columns is not associated with a pump-around. Considering the similarity between vacuum towers and liquid side-draw prefractionator columns and the validity and calculation efficiency of the simplified vacuum tower models, the models developed in the work of Rastogi (2006) are modified and extended for the design and analysis of liquid side-draw prefractionator columns.

In order to model a side-draw prefractionator column, it is decomposed into thermodynamically equivalent sequence of a simple column and a supplementary rectifying section. Figure 5.7 shows the decomposition, in which the section between the bottom of the column and the liquid side-draw (sections 1 and 2 in Figure 5.7) is modelled as a simple column, while the column section between the liquid side-draw and the condenser (section 3 in Figure 5.7) is modelled as a supplementary rectifying section. The simple column and the supplementary rectifying section are connected by one vapour stream that feeds to the supplementary rectifying section and one liquid stream returned from the supplementary rectifying section.

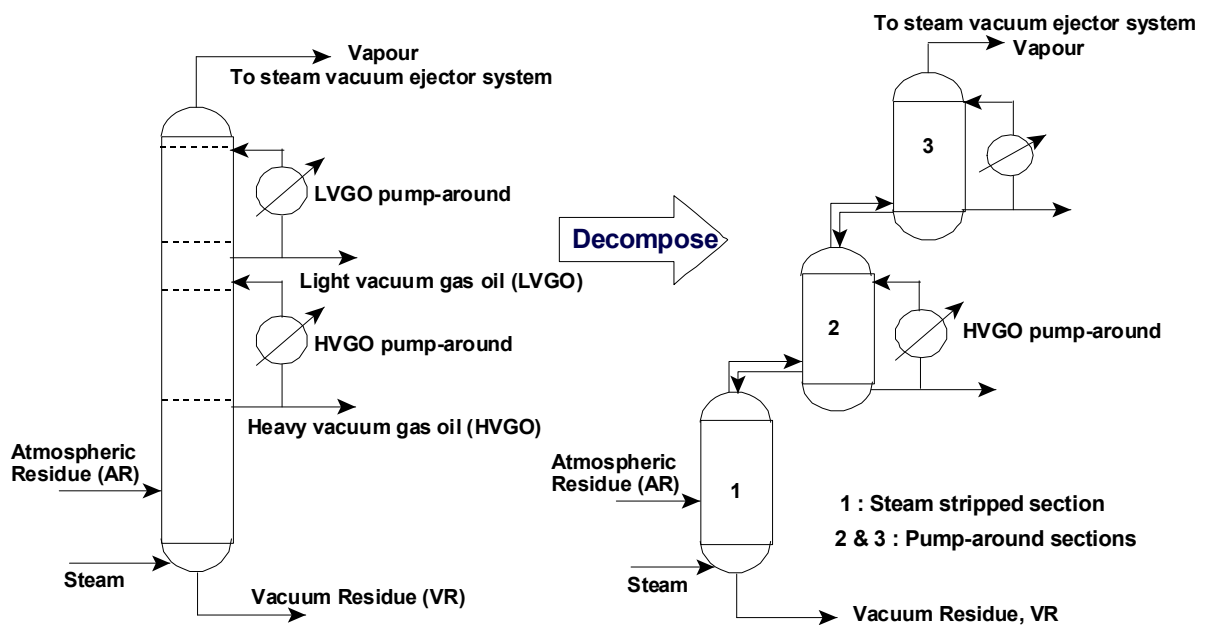


Figure 5.6 Decomposition of crude vacuum distillation column (Rastogi, 2006)

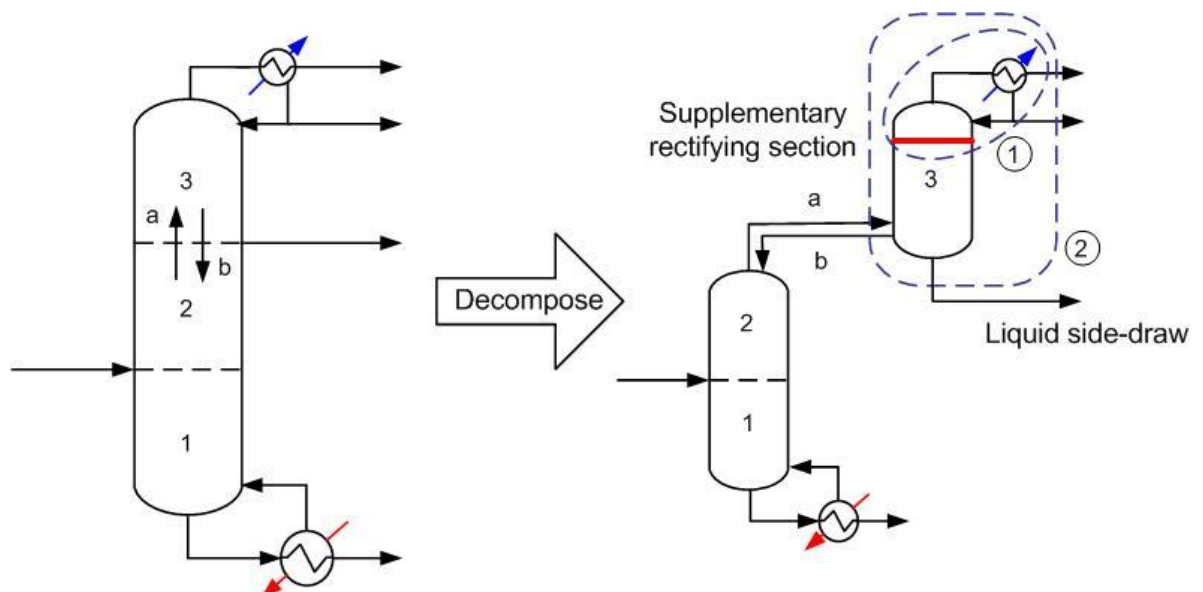


Figure 5.7 Decomposition of liquid side-draw prefractionator column

The upstream simple column in the decomposed sequence is modelled using the simplified methods developed in Chapter 3, assuming a hypothetical condenser. The upstream simple column can be either reboiled or steam-stripped. The temperature, pressure, flow rate and composition of the vapour stream (stream a in Figure 5.7) that feeds to the supplementary rectifying section and the liquid stream (stream b in Figure 5.7) returned from the supplementary rectifying section are then given by the calculation results of the upstream column.

For the supplementary rectifying section, new simplified methods are developed. The calculation procedure for grassroots design is listed as follows:

1. The Underwood Equations (Equations 2.1 and 2.2) are applied in this section for the minimum reflux calculation in the column. The minimum vapour flow rate of the top pinch is calculated.
2. A mass balance and enthalpy balance are performed around the top section (envelope 1 in Figure 5.7) to estimate the condenser duty and the vapour flow rate at the top of this section. The minimum reflux ratio is then calculated by the minimum vapour flow rate at the top of the column and the distillate (Equation 2.4).
3. An overall mass balance and energy balance are carried out in this section (envelope 2 in Figure 5.7) to determine the flow rate, composition, enthalpy, and temperature of the liquid side-draw.
4. The Fenske equation (Equation 2.5) is used for the total reflux calculation. Equation 2.6 is applied to calculate the distribution of non-key components between the top and bottom products at total reflux ratio condition.
5. At certain finite reflux ratio which is set to be a multiple of the minimum reflux ratio, the required number of stages at this section is calculated by the Molokanov correlation (Equation 2.7), given R , R_{\min} and N_{\min} .

The distribution of the non-key components between the top and bottom products of this section at finite reflux ratio is determined by interpolation between the distribution of non-key components at minimum reflux and total reflux (Seader and Henley, 1998; p.512).

6. Knowing the finite reflux ratio and distillate flow rate and composition, the condenser duty and bottom product are re-calculated by carrying out mass

balance and energy balance around the top section (envelope 1 in Figure 5.7) and around the whole section, respectively (Suphanit, 1999).

The retrofit calculations are carried out as iterative grassroots calculations. R/R_{\min} is varied if the recoveries are specified (or recoveries are varied if R/R_{\min} is specified) and the grassroots simplified model calculates the required number of theoretical stages in the column. The calculations terminate when the calculated and existing number of theoretical stages in the upstream simple column and the supplementary rectifying section are equal.

5.4.2 Illustrative example 5.1: A reboiled prefractionator column with a liquid side-draw

This example applies the proposed model to a reboiled prefractionator column with a liquid side-draw that is processing the crude feed presented in illustrative example 3.1. The assay data of the crude oil are shown in Table 3.1. Table 3.2 presents the feed molar compositions in terms of pseudo-components and also shows pseudo-component boiling temperatures. One reboiler is installed in the column. The feed conditions and column specifications, in terms of key components and recoveries for the decomposed sequence, are given in Table 5.2. Constant column pressure is assumed throughout the column. The physical properties are calculated by Peng-Robinson equation of state.

Table 5.2 Feed conditions and column specifications

Feed conditions		
Temperature (°C)	250.0	
Pressure (bar)	2.5	
Separation specifications		
	First column	Supplementary rectifying section
Light key	5 th	3 rd
Light key recovery	0.99	0.99
Heavy key	9 th	6 th
Heavy key recovery	0.99	0.99
R/R _{min}	2.20	1.65

This reboiled liquid-side-draw prefractionator column is simulated using the proposed simplified model. The simulation results are shown in Table 5.3. In order to validate

the proposed simplified model, the column is also simulated more rigorously in HYSYS (v2004.2). The stage distribution calculated by the simplified model is specified in the rigorous simulation. The reflux ratio and flow rate of the top product and side-draw are specified in the rigorous model. The simulation results of rigorous model are summarised in Table 5.3 for comparison.

Table 5.3 Simulation results of reboiled liquid side-draw prefractionator column

Parameter	Simplified model	Rigorous model
Product flow (kmol/h)		
Top product	610.8	610.8*
Liquid side-draw	457.4	457.4*
Bottom product	1542.5	1543.0
Product temperature (°C)		
Top product	75.2	76.1
Liquid side-draw	163.4	158.2
Bottom product	296.8	292.4
Reflux ratio	4.22	4.22*
Duty (MW)		
Condenser	26.30	26.38
Reboiler	26.51	24.37
Stage distribution		
Section 1 (Figure 5.7)	3.3	4*
Section 2 (Figure 5.7)	3.5	4*
Section 3 (Figure 5.7)	8.4	8*

*: specified

It is clear from Table 5.3 that the simulation results of simplified model show good agreement with those of rigorous model. The good match between the two sets of results validates the simplified model for liquid-side-draw prefractionator columns. The simplified model will then be used to simulate the proposed novel configuration for atmospheric crude oil distillation.

5.4.3 Installation of prefractionator column with liquid side-draw to atmospheric crude oil distillation unit

As shown in Figure 5.5, the liquid side-draw from the prefractionator column can be fed into the atmospheric column at different locations. Modelling of the distillation configuration is explained in this section. First of all, the atmospheric crude distillation unit (CDU) is decomposed into a sequence of thermally coupled simple

columns and each simple column is modelled by the simplified methods proposed in Chapter 3. The simplified methods are more robust in convergence and more computationally efficient than rigorous methods; however, the applicability will be compromised. Based on the simplified methods, four locations are considered are feeding the liquid side-draw from the prefractionator column, as is shown in Figure 5.8, in which stripping steams and reboilers are not shown.

If the location **XX** is equal to 1, the liquid side-draw is fed to the bottom of CDU. In this case, the liquid is mixed with the main CDU crude oil feed. For a location **XX** = 2, the liquid side-draw is mixed with the vapour stream from column 1, then the mixture of these two streams is fed into column 2. Similarly for the other two locations **XX** = 3 and **XX** = 4, in which the liquid side-draw mixes with the vapour stream from column 2 or 3 respectively, and then fed into column 3 or column 4 respectively. Note that only one location is considered; however, it is easy to model the liquid side-draw fed into the CDU at more than one location by splitting the liquid into several branches.

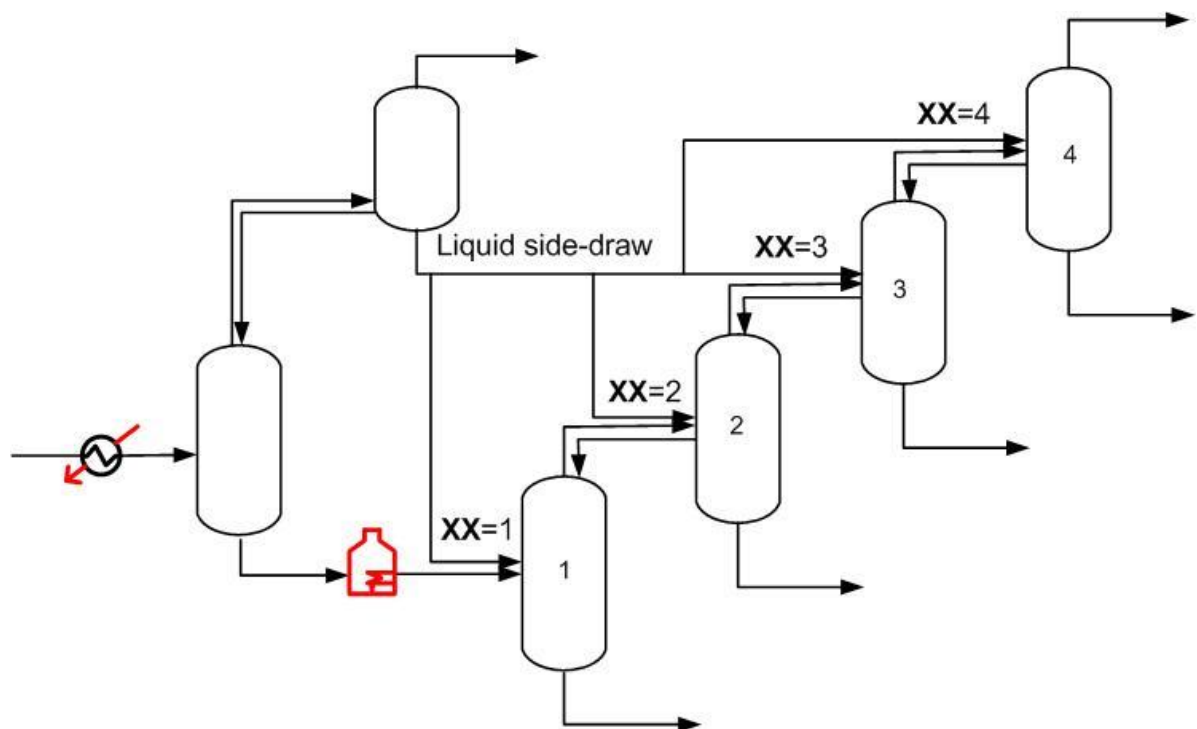


Figure 5.8 Liquid side-draw mixing scheme in decomposed sequence

After the liquid-side-draw prefractionator column is simulated using the model proposed in Section 5.4.1, the liquid conditions (e.g. flow rate, composition, temperature, pressure, and enthalpy) are known. Material and enthalpy balances are carried out to calculate the mixture (mixing the liquid side-draw and the vapour

stream coming from column n) conditions. Given the liquid side-draw has the following conditions: flow rate L , composition $x_{L,i}$, molar enthalpy H_L and pressure P_L . The corresponding conditions for the vapour stream coming from column n are V_n , $x_{n,i}$, H_n and P_n . The mixture conditions are calculated by:

$$F_{mix} = L + V_n \quad (5.4)$$

$$x_{mix,i} = \frac{L \cdot x_{L,i} + V_n \cdot x_{n,i}}{L + V_n} \quad (5.5)$$

$$H_{mix} = \frac{V_n \cdot H_n + L \cdot H_L}{L + V_n} \quad (5.6)$$

$$P_{mix} = \min(P_L, P_n) \quad (5.7)$$

An isothermal flash calculation is then performed to determine the temperature of the mixture under the condition of the given flow rate, composition, enthalpy and pressure. Thus, the new feed stream to column $n+1$ is attained and the remaining calculations for simple columns are carried out using the simplified distillation models developed in Chapter 3.

Studies of distillation configurations are important, since the energy demand for separating a mixture is greatly affected by the distillation configuration. A systematic exploration of distillation configurations can identify potential energy reduction opportunities and chances of using different levels of heating and cooling resources in the process. This section proposes a novel crude oil distillation configuration. New simplified models are developed for the design and analysis of this novel configuration. The proposed simplified models for the novel configuration are consistent with the simplified distillation models proposed in Chapter 3. The consistency between the models facilitates a systematic exploration of the configuration using the proposed crude oil distillation system design approach.

5.5 Conclusions

This chapter presents an optimisation-based design approach for heat-integrated crude oil distillation systems. The modelling of interactions between distillation

columns and the associated HEN through simulation of HEN configurations is presented. Multi-segment stream data are implemented in the design. The interactions between the distillation columns and the associated HEN are accounted for more accurately than in previous work. The design of distillation columns and the HEN are carried out within a single framework.

The optimisation-based design approach is applicable to different objective functions, such as minimum total annualised cost in grassroots design (or energy reduction in retrofit design) and maximum net profit. Product specifications are added in the process constraints, which is necessary in controlling product qualities and make sure that the separation is not compromised to achieve energy savings. Other process constraints, such as hydraulic constraints, maximum number of modifications to the existing design, and minimum temperature approach, are also considered. Key components and recoveries are considered as degrees of freedom for allowing a systematic exploitation of product distributions and product slate when the design objective is maximum net profit. Moreover, distillation operating pressures are considered as optimisation variables in the proposed new design approach, which creates opportunities to enhance heat recovery. An optimisation framework is proposed which incorporates the simplified distillation models, HEN models, and the modelling of interactions between distillation columns and the associated HEN. The SA algorithm, which is capable of solving this complex MINLP problem, is proposed as the optimiser in the optimisation framework. The implementation of the proposed optimisation-based design approach is then presented.

This chapter also motivates the study of different distillation configurations. A novel configuration is proposed and the modelling of this configuration is presented.

The applications of the proposed optimisation-based design approach will be illustrated by four case studies in Chapter 6.

CHAPTER 6 CASE STUDIES

In Chapter 5, the multiple-run simulated annealing algorithm based optimisation framework has been proposed for the design of heat-integrated crude oil distillation systems. The simplified distillation models developed in Chapter 3, together with HEN models developed in Chapter 4, are implemented in the new optimisation framework. The application of the proposed design approach will be illustrated in this chapter by four case studies, including retrofit design, grassroots design and comparisons between different distillation configurations.

Case Study 6.1 applies the proposed design methodology to reduce energy demand in an existing heat-integrated atmospheric distillation column. The previous approach of Rastogi (2006), which assumed constant stream thermal properties and unconstrained product properties during the optimisation, is also applied in this case study. The results from both approaches are compared to demonstrate the advantages of the new approach.

In Case Study 6.2, the same existing heat-integrated atmospheric distillation column is studied, aiming at maximum net profit. In this case study, product flow rates are optimised systematically according to their price, while product properties are constrained. In previous approaches, the variation of product flow rate was carried out by changing one of the key components arbitrarily and without checking product properties.

Case Study 6.3 presents the application of the new approach in an existing heat-integrated crude oil distillation system, which includes an atmospheric column, a vacuum column, and an existing preheat train. Pressure drops are considered and pump-around locations are optimised.

Case Study 6.4 shows the application of the proposed approach in a grassroots design of heat-integrated crude oil distillation columns. In this case study, several configurations are optimised and compared. The configurations are: the conventional atmospheric column without a prefractionator column, the configuration with a prefractionator column, the progressive configuration and the novel configuration

with a liquid side-draw prefractionator column proposed in Chapter 5. The products generated by these configurations are constrained to have similar boiling properties, within tolerance.

6.1 Case study 6.1: Energy demand reduction in an existing heat-integrated atmospheric distillation column

This case study applies the proposed design methodology to an existing heat-integrated atmospheric distillation column, taken from Gadalla (2002). The atmospheric distillation unit was originally introduced by Suphanit (1999), who set up the distillation unit by following one example and the design guidelines shown in a text book of Watkins (1979). This case was then used in Gadalla (2002) as a retrofit example and in Rastogi (2006) to demonstrate the proposed simultaneous design methodology of distillation columns and the preheat train. The existing preheat train associated with the distillation column, which was used in Gadalla (2002) and Rastogi (2006), will not be employed here since the existing HEN is such a poor design that it has no value as a benchmark. In order to set up a more credible study basis to highlight the advantages of optimising distillation columns and the associated HEN in a single framework, the existing HEN is taken to be the optimised HEN for the existing column operating conditions. The optimum HEN design is obtained by applying the simulated annealing optimisation-based design approach presented in Chapter 4.

The objective of this case study is to reduce energy demand by optimising the distillation column and the preheat train at the same time. The design approach proposed in Chapter 5 is applied to this case study. The main feature of the new approach is that non-constant stream thermal properties are implemented to account more accurately for the integration of the distillation columns and preheat train. In the new approach, product properties are checked and constrained to make sure that the separation will not be compromised in order to reduce energy demand.

The design approach, which assumes constant thermal properties in heat integration and unconstrained product properties, is also applied to the same atmospheric

distillation column. The results from the two approaches are compared and the advantages of the new approach are presented.

As the main purpose of this case study is to emphasize the differences between the previous approach and current approach, pressure drop in the columns is not considered and pump-around locations are fixed. These issues will be taken into account in Case Study 6.3.

6.1.1 Base case problem data

The atmospheric distillation unit processes 100,000 bbl/day (2610.7 kmol/h) of crude to produce five products: atmospheric residue (RES), heavy distillate (HD), light distillate (LD), heavy naphtha (HN) and light naphtha (LN). The configuration of the atmospheric distillation unit is shown in Figure 6.1, in which the equivalent decomposed sequence of simple columns is also shown. Three side-strippers and three pump-arounds are installed in the column. Steam at 4.5 bar and 260 °C is injected at the bottom of the main column and the bottom side-stripper (HD side-stripper), while reboilers are installed in the top and middle side-strippers (HN and LD side-strippers).

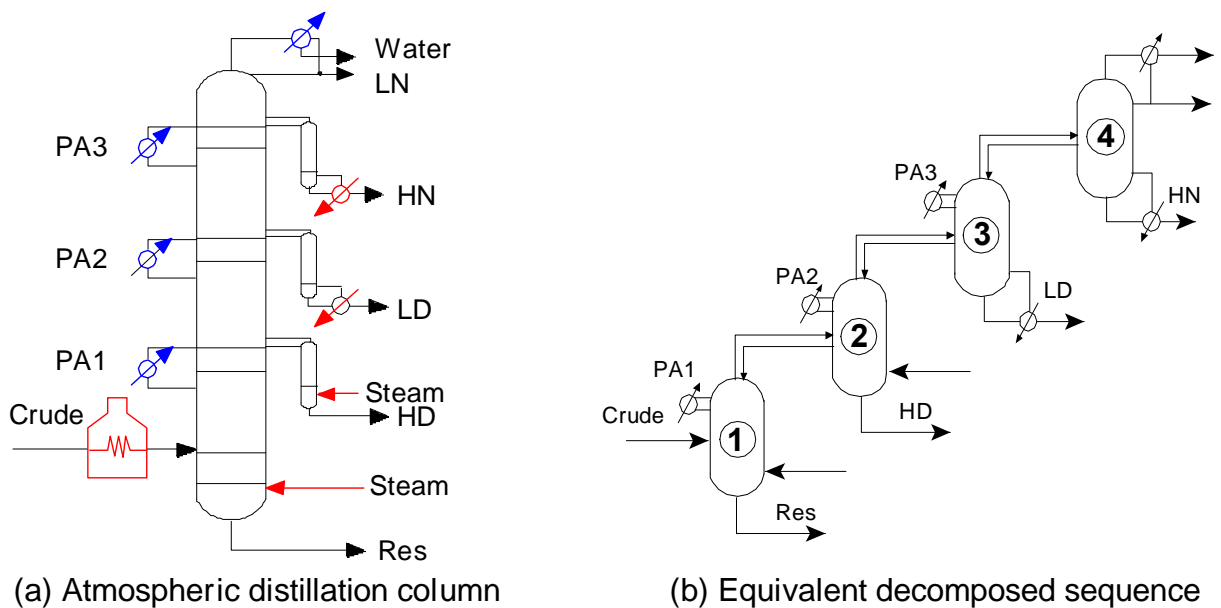


Figure 6.1 Case Study 6.1: Atmospheric distillation column and thermodynamic equivalent decomposed sequence of simple columns

The crude oil mixture is Tia Juana Light crude (Venezuela) (Watkins, 1979), the true boiling data of which are given in Table 6.1. This assay is cut into 25 pseudo-components using the oil characterisation technique embedded in HYSYS process simulator (v2004.2). The physical and thermodynamic properties (i.e. molecular weight, vapour pressure, boiling temperature, critical properties, *etc.*) of each pseudo-component are also provided by the simulator. The normal boiling temperature of these components and the molar composition of the crude oil are presented in Table C.1.1 (Appendix C).

Table 6.1 Case Study 6.1: Crude oil assay data

% Distilled (by volume)	TBP (°C)
0	-3.0
5	63.5
10	101.7
30	221.8
50	336.9
70	462.9
90	680.4
95	787.2
100	894.0

Density: 865.4 kg/m³

The crude oil is heated up from 25 °C to 266 °C in the preheat train, and is then heated in the furnace to reach 365 °C before entering the distillation unit. Table 6.2 lists the key components for the separations carried out in the sequence of columns that is thermodynamically equivalent to the atmospheric unit. The existing number of theoretical stages in each column section and the operating conditions, such as the steam flow rates and the pump-around duties and temperature drops, are as those presented in Table 6.3. The data are given in terms of the sequence of simple columns. Products generated by the existing distillation unit are listed in Table 6.4, including flow rates and true boiling temperature points, which are used as the indication of product qualities in the present work.

Table 6.2 Case Study 6.1: Key components and recoveries in each simple column

Parameter	Columns*			
	1	2	3	4
Light key component	13	11	7	4
Heavy key component	16	14	9	6

*: See Figure 6.1b decomposed sequence of simple columns

The existing heat exchanger network is taken from the optimised grassroots HEN design of the fixed distillation column for a minimum temperature approach of 30 °C. In this case study, temperature-dependent heat capacities of process streams are implemented. A new segment is generated each 40 °C and when a phase change takes place. Details of the multi-segment process stream data are summarised in Table C.1.2 (Appendix C), including supply temperature, target temperature and enthalpy change of each segment. The schematic of the existing HEN is shown in Figure 6.2. The existing network contains 23 exchanger units, including the process furnace, with a total area of 5332 m². The breakdown of area for each exchanger unit is listed in Table C.1.3 (Appendix C), together with heat loads, heat transfer coefficient (UA) values and temperature approaches.

Table 6.3 Case Study 6.1: Existing atmospheric crude oil distillation column (Gadalla, 2002)

Parameter	Column 1	Column 2	Column 3	Column 4
Feed preheat temp (°C)	365	-	-	-
Operating pressure (bar)	2.5	2.5	2.5	2.5
Vaporisation mechanism	Steam	Steam	Reboiler	Reboiler
Reflux ratio	-	-	-	4.17
Steam flow (kmol/h)	1200	250	-	-
Pump-around duty (MW)	12.84	17.89	11.20	-
Pump-around T (°C)	30	50	20	-
Condenser duty (MW)	-	-	-	47.87
Reboiler duty (MW)	-	-	8.78	6.63
No. of theoretical stages in rectifying section (N _R)	9	10	8	9
No. of theoretical stages in stripping section (N _S)	5	5	7	6
Diameter in rectifying section (m)	8.0	8.0	7.5	7.0
Diameter in stripping section (m)	5.5	3.0	3.5	3.0

The current hot and cold utility requirements of the crude oil distillation system are 63.8 MW and 67.3 MW respectively, costing a total operating cost of 11.67 MM\$/y, including stripping steam cost. Note that in crude oil distillation processes, hot utility is fired heater, and is expensive per unit of heating; cold utility is cooling water, and is relatively cheaper than hot utility. The detailed energy requirement and operating cost of the existing process are summarised in Table C.1.4 (Appendix C). The unit cost of utilities, stripping steam and the capital cost of heat exchanger modifications proposed in this case study are listed in Table C.1.5 (Appendix C). The same data

set for utility costs, stripping steam cost and capital cost of heat exchanger modifications will be used in the other retrofit case studies in this chapter.

Table 6.4 Case Study 6.1: Product information of existing atmospheric crude oil distillation column

Parameter	Products				
	RES	HD	LD	HN	LN
T5 (°C, TBP, in mole)	353	285	190	117	3
T50 (°C, TBP, in mole)	462	339	248	156	71
T95 (°C, TBP, in mole)	798	372	317	196	118
Flow rate (kmol/h)	635	149	653	496	678

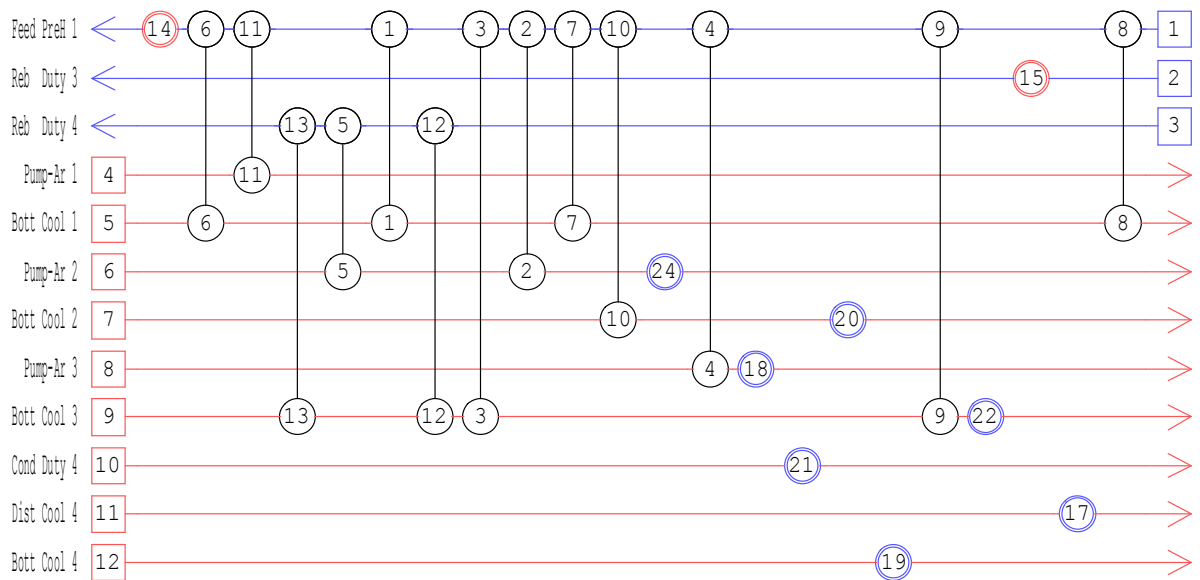


Figure 6.2 Case Study 6.1: Structure of existing heat exchanger network (optimised preheat train design for fixed distillation column operating conditions)

Stream data are given in Table C.1.2, Appendix C; Exchangers 14 and 15 are heaters; all other exchangers are coolers.

6.1.2 Optimisation approach and results

The purpose of this case study is to reduce energy demand of the existing system. Therefore, the objective function is minimum total annualised cost (see Section 5.3.1 for definition and calculation of the total annualised cost). The structure of the existing atmospheric distillation column (e.g. stage distribution and existing diameter)

is fixed and only column operating conditions are optimised. The column operating conditions which are going to be varied are shown in Table 6.5. These variables are optimised at the same time as the operating conditions and structure of the associated HEN. The optimisation variables of the HEN are listed in Table 6.6.

Table 6.5 Case Study 6.1: Optimisation variables of atmospheric distillation column

Column	Optimisation variables
1	1. Feed preheating temperature 2. Pump-around duty 3. Temperature-drop through pump-around 4. Flow rate of stripping steam 5. Flow rate of liquid between columns 1 and 2
2	6. Pump-around duty 7. Temperature-drop through pump-around 8. Flow rate of stripping steam 9. Flow rate of liquid between columns 2 and 3
3	10. Pump-around duty 11. Temperature-drop through pump-around 12. Flow rate of liquid between columns 3 and 4
4	13. Reflux ratio

Table 6.6 Case Study 6.1: Optimisation variables of preheat train

Continuous variables
1. Duties of heat exchanger s 2. Flow fractions of stream splitters
Structural modifications
3. Adding/Deleting heat exchanger 4. Moving heat exchanger (re-sequence, re-pipe) 5. Adding/Deleting stream splitter

The lower and upper bounds of the preheat feed temperature are set as 330 and 370 °C respectively. For the temperature drops through pump-arounds, these limits are 10 and 80 °C. In the optimisation, the flow rate of stripping steam is varied. In terms of hydrocarbon partial pressure at the feed stage, the range is 1% to 99% of the column operating pressure (Suphanit, 1999). Similarly, pump-around duties except the pump-around above the top side-stripper, is a function of degree of thermal coupling in the simplified distillation model (Suphanit, 1999). Thus, degrees of thermal coupling are optimised instead of pump-around duties. In the simplified distillation model, the liquid flow rate between two simple columns in the decomposed sequence is related to the reflux ratio of the upstream column. Reflux ratio of each simple column is an important degree of freedom. The reflux ratio is taken to be 1.05 to 2.0 times of the minimum reflux ratio.

The lower and upper limits of split fraction are 0 and 1 respectively. The lower bound of a heat exchanger duty is 0, and the upper bound is the lower value of the total enthalpy change of the hot and cold streams in that particular match.

Hydraulic constraints are imposed to make sure that the production capacity of the existing distillation column is not exceeded. The existing diameters of each column section, given in Table 6.3, are checked during the optimisation. In order to make sure the final design generates desired products, product specification constraints are implemented. The product flow rate deviation is set to be within 1% of the base case and the maximum product TBP point deviation is 8 °C. Tighter tolerance can be specified if needed. Note that, tighter the product specification tolerances are, lower energy saving might be achieved, if compared with looser tolerance. Therefore, the product specification tolerance should be selected properly according to the requirement. In order to illustrate the effect of different tolerances, tighter tolerance (1% in flow rate, and 5% in TBP) is specified in Case Study 6.3.

The existing HEN was designed for a minimum temperature approach of 30 °C. In the retrofit procedure, the minimum temperature approach is 25 °C. The maximum number of new exchangers and of new splitters is two, while one re-piping modification and one re-sequencing modification of existing exchangers are allowed.

The existing distillation column is simulated first with the base case data given in Section 6.1.1 as a sequence of simple columns. The existing preheat train is then simulated as shown in Figure 6.2 with the multi-segment stream data generated from the distillation column. The simulated annealing optimisation starts with the simulation of the base case and makes randomised moves to generate different design alternatives according to the assigned probabilities, as listed in Table 6.8.

Table 6.7 Case Study 6.1: Simulated annealing parameters

Initial annealing temperature	1.0×10^5
Final annealing temperature	1.0×10^{-4}
Markov chain length	30
Cooling temperature	0.05
Acceptance criteria	Metropolis (Metropolis <i>et al.</i> , 1953)

Table 6.8 Case Study 6.1: Move probabilities

Move decisions	Probability
Distillation column move, heat exchanger network move	0.5, 0.5
Simple column 1, 2, 3, 4	0.25, 0.25, 0.25, 0.25
Simple column 1: preheat temperature move, pump-around duty move [#] , temperature drop through pump-around, pump-around location move, R/R _{min} move, stripping steam flow rate move ⁺ , key component move, key component recovery move, pressure move	0.5, 0.1, 0.1, 0, 0.15, 0.15, 0, 0, 0
Simple column 2: preheat temperature move, pump-around duty move [#] , temperature drop through pump-around, pump-around location move, R/R _{min} move, stripping steam flow rate move ⁺ , key component move, key component recovery move, pressure move	0, 0.3, 0.3, 0, 0.2, 0.2, 0, 0, 0
Simple column 3: preheat temperature move, pump-around duty move [#] , temperature drop through pump-around, pump-around location move, R/R _{min} move, stripping steam flow rate move ⁺ , key component move, key component recovery move, pressure move	0, 0.4, 0.4, 0, 0.2, 0, 0, 0, 0
Simple column 4: preheat temperature move, pump-around duty move [#] , temperature drop through pump-around, pump-around location move, R/R _{min} move, stripping steam flow rate move ⁺ , key component move, key component recovery move, pressure move	0, 0, 0, 0, 1, 0, 0, 0, 0
Exchanger move, bypass move (stream splitting move)	0.8, 0.2
Exchanger move: add a exchanger move, delete a exchanger move, modify exchanger duty move, exchanger relocation move	0.2, 0.1, 0.45, 0.25
Bypass move: add a bypa ss, delete a bypass, modify the splitting fraction of a bypass	0.3, 0.3, 0.4
Exchanger relocation move: resequence move, re pipe move	0.5, 0.5

#: Pump-around duty is optimised in terms of degree of thermal coupling;

+: Stripping steam flow rate is optimised in terms of partial pressure of hydrocarbon at the feed stage

As discussed in Section 5.3.4, in the new approach, multiple runs of simulated annealing optimisation are implemented to gain confidence in the final optimum solution. After one run is finished, the best solution found in the last run is used as the initial point to start the next run, with a different random number seed. Five runs are carried out in this case study. The parameters relating to the simulated annealing algorithm are summarised in Table 6.7. As discussed in Appendix B.2, these parameters indicate the trade-off between the quality of the final solution and the required computational time. For example, the longer the Markov chain length is, the

longer the time needed, and the better the solution the algorithm may find in terms of the value of the objective function. However, according to experience, after these parameters reach particular values, the performance of the final solution increases only slightly. That is, the computational time consumed does not vary linearly with solution performance (e.g. objective). The specification of simulated annealing parameters should consider the trade-off between the quality of solution and the required time. In this case study, these parameters are set based on experience and trial and error. For a Markov chain length of 30, the overall time required for the multiple run (5 runs) is around 32 hr. This time is quite considerable, but justified by the quality of the solution. If a quicker result is required, a shorter Markov chain length should be used. In this case, the global optimum may not be approached, solutions obtained may still be valuable.

Table 6.9 presents the performance of the final design solution, including utility demand, stripping steam cost, cost of heat exchanger network modifications and total annualised cost. Compared with the base case, it can be seen that the performance of the system is improved significantly by implementing the proposed design approach: hot and cold utility demand are reduced by 11.50 MW and 14.81 MW respectively, which consequently reduces the operating cost by 18% with only 0.50 MM\$ capital investment in the heat exchanger network.

Table 6.9 Case Study 6.1: Energy consumption and operating cost of optimum system

		Base case / Existing system	Optimum system	Reduction Actual(relative)
Hot utility demand	MW	63.80	52.30	11.50 (18%)
Cold utility demand	MW	67.26	52.45	14.81 (22%)
Utility operating cost	MM\$/y	9.92	8.10	1.82 (18%)
Stripping steam operating cost	MM\$/y	1.75	1.43	0.32 (18%)
Additional exchanger area	m ²	-	1914	-
HEN capital investment	MM\$	-	0.50	-
Total operating cost	MM\$/y	11.67	9.53	2.14 (18%)
Total annualised cost*	MM\$/y	11.67	9.82	1.85 (16%)
T _{min}	°C	30	25	-
Payback	y	-	0.27	-

Utility and steam unit costs are given in Table C.1.5 (Appendix C)

Details of additional area cost is given in Table C.2.4 (Appendix C)

*: 2 year payback, with 5% interest

The optimised operating conditions of the atmospheric distillation column are listed in Table 6.10, and are compared with those of the base case. It can be observed from Table 6.10 that the feed preheat temperature is decreased by 11 °C, and the pump-around duty and temperature drop through the pump-arounds are selected to the optimum values, which are beneficial to both internal reflux in each section and heat recovery in the preheat train. Flow rates between each adjacent column section are optimised as well, together with the total reflux ratio. The total reflux ratio is decreased and in turn decreases the reboiler duties of simple column section 3 and 4 from 8.78 MW and 6.63 MW to 4.49 MW and 2.35 MW, respectively. Note that because of the stochastic characteristic of SA optimisation, SA carries out random variations of design variables to generate a design solution and accepts the solution when the acceptance criterion is met. Some changes in degrees of freedom after optimisation may not always be necessary. For example, in this case study, the temperature drop of pump-around in column section 3 is increased in the optimum design, which actually cannot generate any benefits but the change was accepted by SA. Thus, sensitivity analysis may be needed to check if the changes in optimisation variables do contribute to improve the system performance.

Table 6.10 Case Study 6.1: Optimum operating conditions of atmospheric column

Column	Optimisation variable		Base case value	Optimum value
1	Feed preheating temperature	°C	365	354
	Pump-around duty	MW	12.84	6.98
	Temperature drop across pump-around	°C	30	44
	Flow rate of stripping steam	kmol/h	1200	1034
	Flow rate of liquid between columns 1 and 2	kmol/h	393	370
2	Pump-around duty	MW	17.89	15.33
	Temperature drop across pump-around	°C	50	42
	Flow rate of stripping steam	kmol/h	250	153
	Flow rate of liquid between columns 2 and 3	kmol/h	130	172
3	Pump-around duty	MW	11.20	10.68
	Temperature drop across pump-around	°C	20	48
	Flow rate of liquid between columns 3 and 4	kmol/h	883	285
4	Reflux ratio	-	4.17	3.08

The products generated from the optimum atmospheric distillation column are shown in Table 6.11, including flow rates and qualities, indicated by three key true boiling points (T5, T50 and T95). The product information of the optimum atmospheric

column is compared with that of the base case. It can be seen from Table 6.11 that product qualities and quantities lie within the specified range, and the separation in the optimum unit is not compromised while reducing energy consumption.

The optimised HEN associated with the optimised atmospheric column is shown in Figure 6.3. The multi-segment stream data from the optimum distillation unit are summarised in Table C.2.1 (Appendix C). Two new exchangers (exchangers 27 and 28 in Figure 6.3) are added to the existing network, and exchangers 3 and 5 are re-sequenced and re-piped, respectively. The total additional area needed for the optimised exchanger network is 1914 m², a breakdown of which is listed in Table C.2.2 (Appendix C).

Table 6.11 Case Study 6.1: Product information of optimum atmospheric column

Parameter	Products				
	RES	HD	LD	HN	LN
Flow rate . optimum case (kmol/h)	641	144	649	492	685
. base case (kmol/h)	635	149	653	496	678
. deviation (kmol/h)	+6	-5	-4	-4	+7
T5 . optimum case (°C)	346	279	182	109	3
. base case (°C)	353	285	190	117	3
. deviation (°C)	-7	-6	-8	-8	0
T50 . optimum case (°C)	460	340	248	158	71
. base case (°C)	462	339	248	156	71
. deviation (°C)	-2	+1	0	+2	0
T95 . optimum case (°C)	797	376	319	201	121
. base case (°C)	798	372	317	196	118
. deviation (°C)	-1	+4	+2	+5	+3

Table 6.12 presents the product information of the optimum system obtained from the approach without specification of products and single segment stream data (constant thermal properties), and from the new approach. It can be seen from the table that the product flow rates and TBP points of the optimum design obtained by the approach without product specifications differ considerably from those of the base case. That is, the products generated by the optimum design do not meet quality requirements. This limitation is overcome in the new approach.

Comparisons of energy savings obtained by the two approaches are provided in Table 6.13, including hot and cold utility demand, total operating cost, *etc.* It can be observed from Table 6.13 that much more energy saving is claimed in the previous approach, which is caused by assuming constant heat capacity, and not constraining the product properties. The constant heat capacity assumption overestimates the potential to reduce the energy demand of the existing distillation unit. The lack of constraints on product properties may cause the separation to be compromised by energy reduction.

Table 6.12 Case Study 6.1: Comparisons of products generated from optimum distillation unit gained by two approaches

Parameter	Products				
	RES	HD	LD	HN	LN
Flow rate . optimum case (kmol/h)	693	135	613	492	678
. <i>optimum case (kmol/h)</i>	<i>641</i>	<i>144</i>	<i>649</i>	<i>492</i>	<i>685</i>
. base case (kmol/h)	635	149	653	496	678
T5 . optimum case (°C)	329	262	188	119	3
. <i>optimum case (°C)</i>	<i>346</i>	<i>279</i>	<i>182</i>	<i>109</i>	<i>3</i>
. base case (°C)	353	285	190	117	3
T50 . optimum case (°C)	448	333	244	156	71
. <i>optimum case (°C)</i>	<i>460</i>	<i>340</i>	<i>248</i>	<i>158</i>	<i>71</i>
. base case (°C)	462	339	248	156	71
T95 . optimum case (°C)	799	371	314	196	118
. <i>optimum case (°C)</i>	<i>797</i>	<i>376</i>	<i>319</i>	<i>201</i>	<i>121</i>
. base case (°C)	798	372	317	196	118

First value . the approach without product specifications and single segment stream data

Second value – new approach

Table 6.13 Case Study 6.1: Compar isons of energy saving of optimum system attained by the two approaches

		Base case / Existing system	Optimum system	<i>Optimum system</i>
Hot utility demand	MW	63.80	44.75	52.30
Cold utility demand	MW	67.26	37.52	52.45
Utility operating cost	MM\$/y	9.92	6.91	8.10
Stripping steam operating cost	MM\$/y	1.75	0.71	1.43
Additional exchanger area	m ²	-	3463	1918
HEN capital investment	MM\$	-	0.58	0.50
Total operating cost	MM\$/y	11.67	7.62	9.53
Total annualised cost	MM\$/y	11.67	7.93	9.82
Specified T_{min}	°C	30	25	25
Payback	y	-	0.14	0.27

First value . the approach without product specifications and single segment stream data

Second value – the new approach

The operating conditions of the optimised unit obtained by the two approaches are presented in Table C.3.1 (Appendix C). The previous approach requires relatively more additional area in the existing heat exchanger network, which is caused by a poor temperature prediction from the constant heat capacity assumption (see discussion in Section 4.1)

In conclusion, the new approach controls product qualities during the optimisation. Desired products are generated from the optimum distillation unit and the separation will not be compromised to reduce energy consumption. The interactions between the heat exchanger network and the distillation column are considered more accurately. More reliable predictions of potential for energy saving are provided and more reliable modifications to the existing HEN are suggested.

6.2 Case study 6.2: Profit improvement by optimising product distributions in an existing heat-integrated atmospheric distillation column

This case study presents the application of the proposed design approach to the same existing heat-integrated atmospheric distillation column as presented in Case Study 6.1 (Section 6.1). The objective in this case study is to improve net profit by varying product flow rates responding to the market price. As presented in Section

5.3.1, the net profit is defined as the total product value minus total costs (Equation 5.2), which include operating cost and cost for crude oil feed. Note that a systematic exploitation of product flow rates cannot be considered in previous approaches. In previous approaches, one key component of a particular simple column in the decomposed sequence is changed manually to generate more valuable products, but product qualities are not checked or constrained during the optimisation.

6.2.1 Base case problem data

The details of the existing atmospheric column are presented in Section 6.1.1: the schematic of the distillation column is shown in Figure 6.1; the existing operating conditions are listed in Table 6.2; the column product information is summarised in Table 6.4; the energy demand and operating cost of the existing column are presented in Table C.1.4.

The same heat exchanger network presented in Case Study 6.1 is implemented as the existing preheat train. The grid diagram of the existing heat exchanger network is shown in Figure 6.2 and details of all exchangers are presented in Table C.1.3, including existing areas, heat loads, UA values and approach temperatures. The multi-segment process stream data and utility data are provided in Table C.1.2.

The current hot and cold utility requirements of the crude oil distillation system are 63.8 MW and 67.3 MW respectively, incurring a total operating cost of 11.67 MM\$/y, including the stripping steam cost. As discussed in Section 5.3.1, some products of the atmospheric distillation column are not end products and will experience downstream processing. These products are referred to as distillation products. The distillation product prices are determined by deducting the downstream processing cost from the end product prices. The product prices and crude oil price used in this case study are presented in Table 6.14. Based on these values, the net profit of the existing distillation system is 494.3 MM\$/y.

Table 6.14 Case Study 6.2: Prices of distillation products and crude oil feed

Item	End product	End product price ⁽¹⁾ (\$/barrel)	Downstream process	Operating cost of downstream treating ⁽²⁾ (\$/barrel)	Efficiency of end product production ⁽³⁾	Price for intermediate products (\$/barrel) (\$/kmol)	
Light Naphtha	Gasoline	91.7	N/A	N/A	N/A	91.7	73.4
Heavy Naphtha	Gasoline	91.7	Catalyst Reforming	2.96	0.8	71.0	92.7
Light Distillate	Jet fuel	83.7	Hydrotreating	0.36	0.95	79.1	128.1
Heavy Distillate	Diesel	84.6	N/A	N/A	N/A	84.6	215.7
Residue	Residue fuel oil	47.9	N/A	N/A	N/A	47.9	204.3
Crude oil	N/A	66.7	N/A	N/A	N/A	66.7	108.2

(1) http://tonto.eia.doe.gov/dnav/pet/pet_pri_spt_s1_d accessed on 15/05/07

(2) Robert (2000)

(3) Product yield, the values are taken from refining industry

6.2.2 Optimisation approach and results

The objective of this case study is maximum net profit. In addition to the distillation optimisation variables as shown in Table 6.5 and the optimisation variables in the preheat train as listed in Table 6.6, the separation taking place in the distillation column will be optimised to generate more valuable products while maintaining the product qualities. In the simplified distillation model, the separation in the column is specified by light and heavy key components and their associated recoveries. Thus, key components and associated recoveries are included as optimisation variables in Case Study 6.2. The ratio of finite reflux ratio to the minimum reflux ratio in each column section is not optimised because key component recoveries are considered as optimisation variables. In this case study, no structural modifications to the existing distillation column are considered. Hence, the pump-around locations in the atmospheric column are not optimised. The lower and upper bounds of the continuous variables are the same as those presented in Section 6.1.2.

The hydraulic limits of the distillation column are applied in Case Study 6.2. As the product flow rates are allowed to change in this case study, the product flow rate constraints are not implemented. Product property constraints in terms of TBP points are still applied. In this case study, deviation of product TBP points should not exceed 8 °C to make sure desired products are generated. The minimum

temperature approach in the existing heat exchanger network is 30 °C and the retrofit HEN design is for a minimum temperature approach of 25 °C, which is the same as in Case Study 6.1.

The multiple-run simulated annealing optimisation-based design framework is applied to optimise this case study for maximum net profit, starting with the existing distillation column and the existing heat exchanger network. The simulated annealing parameters and move probabilities implemented in the optimisation are presented in Table 6.7 and Table 6.15.

Table 6.15 Case Study 6.2: Move probabilities

Move decisions	Probability
Distillation column move, heat exchanger network move	0.5, 0.5
Simple column 1, 2, 3, 4	0.25, 0.25, 0.25, 0.25
Simple column 1: preheat temperature move, pump-around duty move [#] , temperature drop through pump-around, pump-around location move, R/R _{min} move, stripping steam flow rate move ⁺ , key component move, key component recovery move, pressure move	0.4, 0.15, 0.15, 0, 0, 0.1, 0.1, 0.1, 0
Simple column 2: preheat temperature move, pump-around duty move [#] , temperature drop through pump-around, pump-around location move, R/R _{min} move, stripping steam flow rate move ⁺ , key component move, key component recovery move, pressure move	0, 0.25, 0.25, 0, 0, 0.2, 0.15, 0.15, 0
Simple column 3: preheat temperature move, pump-around duty move [#] , temperature drop through pump-around, pump-around location move, R/R _{min} move, stripping steam flow rate move ⁺ , key component move, key component recovery move, pressure move	0, 0.35, 0.35, 0, 0, 0, 0.15, 0.15, 0
Simple column 4: preheat temperature move, pump-around duty move [#] , temperature drop through pump-around, pump-around location move, R/R _{min} move, stripping steam flow rate move ⁺ , key component move, key component recovery move, pressure move	0, 0, 0, 0, 0, 0, 0.5, 0.5, 0
Exchanger move, bypass move	0.8, 0.2
Exchanger move: add a exchanger move, delete a exchanger move, modify exchanger duty move, exchanger relocation move	0.2, 0.1, 0.45, 0.25
Bypass move: add a bypass, delete a bypass, modify the splitting fraction of a bypass	0.3, 0.3, 0.4
Exchanger relocation move: resequence move, repipe move	0.5, 0.5

#: Pump-around duty is optimised in terms of degree of thermal coupling;

+: Stripping steam flow rate is optimised in terms of partial pressure of hydrocarbon at the feed stage

Table 6.16 presents the results of the best design solution found during the optimisation, including the net profit, corresponding cost of utilities, stripping steam and capital investment for exchanger modifications. These results are compared with those of the base case in Table 6.16. The optimum product slate is listed in Table 6.17, in terms of flow rates and TBP points. Table 6.17 also presents a comparison of product information for the optimum design and the base case. Table 6.18 shows the optimum operating conditions of the atmospheric distillation column, in terms of each simple column in the decomposed sequence. Table 6.18 also compares the optimum operating conditions with those of the base case. New key components and recoveries of each column in the decomposed sequence are presented in Table D.1 (Appendix D).

Table 6.16 Case Study 6.2: Summary of capital investment and profit improvement

		Base case / Existing system	Optimum system	Change Actual(Relative)
Hot utility demand	MW	63.80	61.22	-2.58 (-4%)
Cold utility demand	MW	67.26	58.77	-8.49 (-13%)
Utility operating cost	MM\$/y	9.92	9.48	-0.44 (4%)
Stripping steam operating cost	MM\$/y	1.75	1.16	-0.59 (-34%)
Additional exchanger area	m ²	-	2394	-
HEN capital investment	MM\$	-	0.54	-
Total operating cost	MM\$/y	11.67	10.64	-1.03 (9%)
Increase in product value	MM\$/y	-	34.09	-
Net profit	MM\$/y	494.3	529.1	+34.8 (7%)

Table 6.17 Case Study 6.2: Product information of optimum atmospheric column

Parameter	Products				
	RES	HD	LD	HN	LN
Flow rate . optimum case (kmol/h)	637	176	651	492	654
. base case (kmol/h)	635	149	653	496	678
. deviation (kmol/h)	+2	+28	-2	-4	-24
T5 . optimum case (°C)	345	277	182	109	2
. base case (°C)	353	285	190	117	3
. deviation (°C)	-8	-8	-8	-8	-1
T50 . optimum case (°C)	461	337	243	153	68
. base case (°C)	462	339	248	156	71
. deviation (°C)	-1	-2	-5	-3	-3
T95 . optimum case (°C)	798	380	315	195	117
. base case (°C)	798	372	317	196	118
. deviation (°C)	0	+8	-2	+1	-1

Table 6.18 Case Study 6.2: Optimum operating conditions of atmospheric column

Column	Optimisation variable		Base case value	Optimum value
1	Feed preheating temperature	°C	365	357
	Pump-around duty	MW	12.84	13.66
	Temperature drop across pump-around	°C	30	48
	Flow rate of stripping steam	kmol/h	1200	779
2	Pump-around duty	MW	17.89	14.85
	Temperature drop across pump-around	°C	50	42
	Flow rate of stripping steam	kmol/h	250	183
3	Pump-around duty	MW	11.20	24.22
	Temperature drop across pump-around	°C	20	24
4	Reflux ratio	-	4.17	3.09

It can be seen from Table 6.16 that the net profit of the atmospheric distillation system is greatly increased by 34.8 MM\$/y (7%), from 494.3 MM\$/y in the base case. The hot and cold utility requirements are reduced by 2.58 MW (4%) and 8.49 MW (13%) respectively. The stripping steam consumption is 34% less than that of the base case. The decreases in the utility and stripping steam consumption contribute to 1.03 MM\$/y (9%) reduction in the operating cost. The value of all products is increased by 34.09 MM\$/y, compared with that of the base case. The production of the most valuable product per unit mole, heavy distillate, is increased by 28 kmol/h, and that of the least valuable product, light naphtha, is reduced by 24 kmol/h. It can be observed from Table 6.17 that although product flow rates vary responding to the market price, product properties are constrained within the allowed ranges.

It can be observed from the results that the reduction in operating cost achieved in this case study (9%) is relatively low, compared with that of the design with fixed product generation (18% in Case Study 6.1). The results indicate that more energy is required when producing more valuable products.

The capital investment in the optimised design is 0.54 MM\$, required by the additional area and structural modifications (re-piping, re-sequencing) to the existing heat exchanger network. The capital investment is relatively low, compared with the savings in operating cost (1.03 MM\$/y). The structural modifications to the existing heat exchanger network are visualised in Figure 6.4. The overall required additional area is 2394 m², the breakdown of which is shown in Table D.2 (Appendix D).

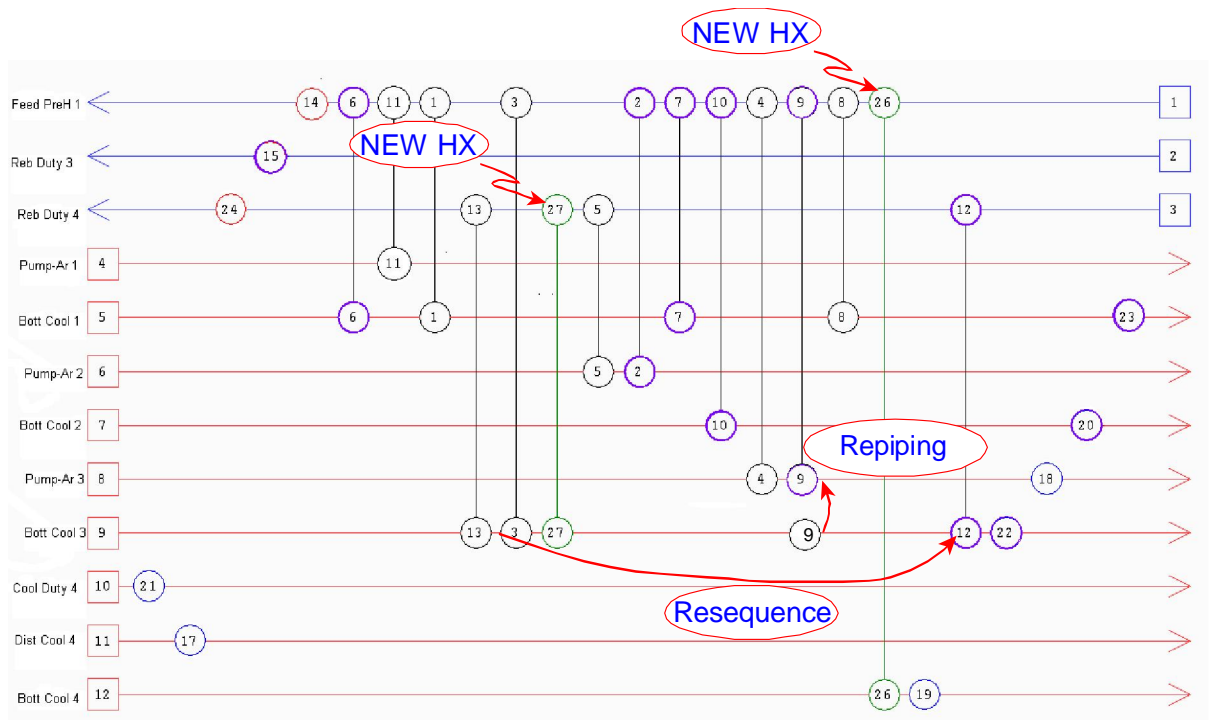


Figure 6.4 Case Study 6.2: Modified heat exchanger network

6.3 Case study 6.3: Energy demand reduction in existing heat-integrated crude oil distillation system

This case study presents the application of the proposed design approach in an existing crude oil distillation system, including an atmospheric column, a vacuum column and a shared preheat train, which recovers heat from pump-around streams and product streams to heat up the cold crude feed.

The objective of this case study is to reduce energy consumption of the existing system. The existing distillation columns are taken from Rastogi (2006), in which the atmospheric distillation column is exactly the same as the base case of Case Study 6.1 (Section 6.1), except for the pressure drop consideration. The simplified models developed by Rastogi (2006) for the vacuum column and for considering pressure drop will be implemented in this case study. The pump-around locations of the atmospheric column are included as the optimisation variables in this case study. Thus, the extended model developed in Section 3.3, which accounts for the effect of pump-around location on the separation performance, will be implemented in Case Study 6.3. In this case study, the trade-off between the heat recovery and the

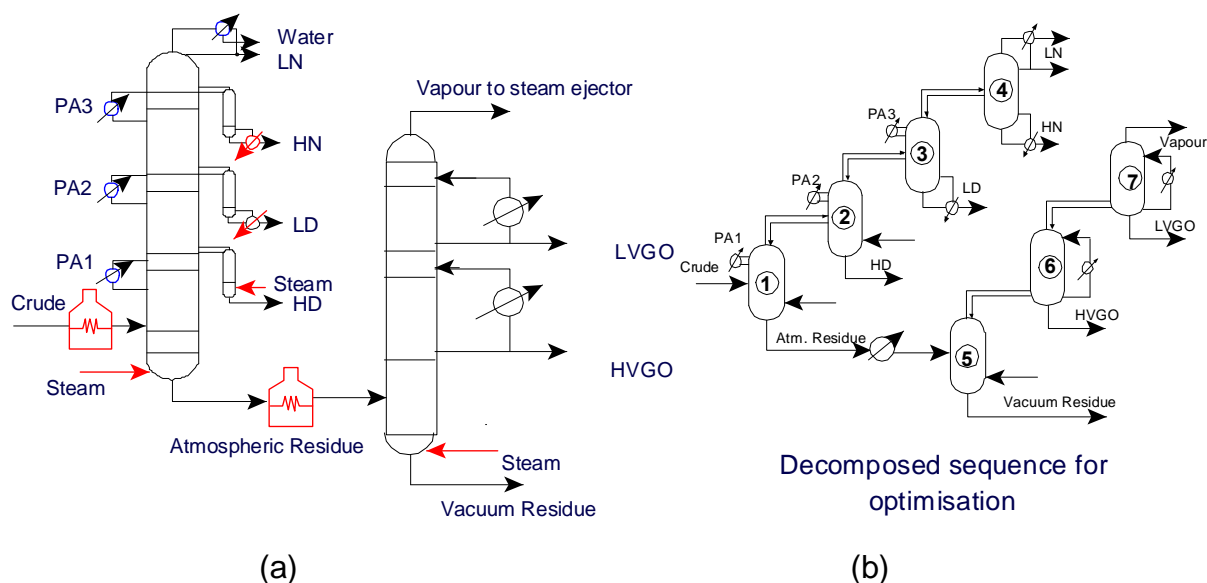
separation performance is exploited to improve the performance of the overall system.

The existing preheat train associated with the distillation column, which was used in Rastogi (2006), will not be employed in this case study. The reason for not using the preheat train in Rastogi (2006) is the same as discussed in Section 6.1. The simulated annealing optimisation-based design approach presented in Chapter 4 is applied to the multi-segment process stream data extracted from the existing operating conditions of the distillation columns. An optimum HEN design is thus generated for the distillation columns of fixed design and operation. This optimum preheat train is then used as the existing HEN associated with the existing distillation columns.

6.3.1 Base case problem data

The existing crude oil distillation system is shown in Figure 6.5. 100,000 barrels/day (2610.7 kmol/h) of Tia Juana Light Venezuela crude oil (crude assay listed in Table 6.1) is fractionated into various products in the atmospheric column and vacuum column. Light naphtha (LN), heavy naphtha (HN), light distillate (LD) and heavy distillate (HD) are produced in the atmospheric column. The atmospheric residue is fed into the vacuum column to be further separated into vacuum residue (VR), heavy vacuum gas oil (HVGO), light vacuum gas oil (LVGO) and vapour (VAP). These products, except for the vapour, are further processed in downstream units (FCC, coker, etc.) to produce final products. The vapour is sent to the fuel gas recovery system of the refinery. There are three pump-arounds (PA1, PA2 and PA3) in the atmospheric column and two vacuum pump-arounds (HVGO pump-around and LVGO pump-around) in the vacuum column to recover energy.

Figure 6.5 also shows the decomposed sequence of thermally coupled simple columns, which are used to simulate the atmospheric and vacuum columns. The simple columns are numbered from one to seven in Figure 6.5. The first four columns stand for the atmospheric column and the next three represent the vacuum column. The existing conditions of the distillation columns in this case study will be presented in terms of the decomposed simple columns.



LN: Light naphtha
 HN: Heavy Naphtha
 LD: Light distillate
 HD: Heavy distillate
 AR: Atmospheric residue

Vap: Vapour
 LVGO: Light vacuum gas oil
 HVGO: Heavy vacuum gas oil
 VR: Vacuum residue

Figure 6.5 Case Study 6.3: Atmospheric and vacuum distillation columns, showing the equivalent decomposed sequence of simple columns (Rastogi, 2006)

(a) Atmospheric and vacuum distillation columns

(b) Equivalent decomposed sequence

The existing atmospheric column is the same as that presented in Case Study 6.1, apart from the assumed pressure drops shown in Table 6.19. The vacuum column, with associated pressure drops, is taken from Rastogi (2006), and presented in Table 6.19.

Table 6.19 Case Study 6.3: Pressure specifications for atmospheric and vacuum columns

Column No	Atmospheric column				Vacuum column		
Parameter	1	2	3	4	5	6	7
Condenser pressure (bar)	2.010 [#]	1.640 [#]	1.340 [#]	1.014 ⁺	0.110 [#]	0.105 [#]	0.100 ⁺
Condenser pressure drop (bar)				0.050 ⁺			
Reboiler/bottom pressure (bar)	2.500 ⁺	2.200 ⁺	2.000 ⁺	1.600 ⁺	0.120 ⁺		
Reboiler pressure drop (bar)			0.010 ⁺	0.010 ⁺			

⁺: Specified, [#]: Calculated by assuming linear pressure profile

Table 6.20 shows the light key and heavy key components in each simple column. The existing number of theoretical stages in each column section and the operating conditions, such as the steam flow rates, the pump-around duties, temperature drops

and locations, *etc.*, of the atmospheric column and vacuum column are presented in Table 6.21. Flow rates and true boiling temperature points of the products separated by the existing distillation units are listed in Table 6.4.

Table 6.20 Case Study 6.3: Key components in each simple column

Column No Key components	Atmospheric column				Vacuum column		
	1	2	3	4	5	6	7
Light key component	13	11	7	4	19	16	15
Heavy key component	16	14	9	6	20	18	16

Table 6.21 Case Study 6.3: Existing atmospheric and vacuum crude oil distillation columns (decomposition of Figure 6.5b)

	Atmospheric column				Vacuum column		
Column specifications	1	2	3	4	5	6	7
Feed preheat temp (°C)	365	-	-	-	400	-	-
Reflux ratio	-	-	-	4.49	-	-	-
Steam flow (kmol/h)	1200	250	-	-	700	-	-
Pump-around duty (MW)	13.14	18.69	9.642	-	-	16.01	11.31
Pump-around T (°C)	30	50	20	-	-	150	100
Pump-around location ⁺	1	1	1	-	-	-	-
Condenser duty (MW)	-	-	-	52.40	-	-	-
Reboiler duty (MW)	-	-	9.128	6.519	-	-	-
No. of theoretical stages in rectifying section (N _R)	9	10	8	9	2	2	2
No. of theoretical stages in stripping section (N _S)	5	5	7	6	3	-	-
Diameter in rectifying section (m)	8.0	8.0	7.5	7.0	12.0	12.0	9.0
Diameter in stripping section (m)	5.5	3.0	3.5	3.0	10.0	-	-

+: Stage number from top of simple column at which the pump-around exists

The existing heat exchanger network is designed for a minimum temperature approach of 25 °C. Figure 6.6 shows the grid diagram of the existing HEN and Table E.1 (Appendix E) presents the details of the HEN, including area required for each exchanger, approach temperature differences and *UA* values. The details of multi-segment stream data can be found in Table E.2 (Appendix E). The existing HEN contains 30 exchanger units, with 7073 m² total area, including utility exchangers and two furnaces. The current hot and cold utility requirements of the crude oil distillation system are 86.68 MW and 88.93 MW respectively, incurring to a total operating cost of 16.06 MM\$/y, including the stripping steam cost of 2.59 MM\$/y.

The detailed energy requirement and operating cost of the existing process are summarised in Table E.3 (Appendix E).

Table 6.22 Case Study 6.3: Product information of existing atmospheric and vacuum crude oil distillation column

Parameter	Products						
	HD	LD	HN	LN	VR	HVGO	LVGO
T5 (°C, TBP, in mole)	287	191	117	3	523	381	352
T50 (°C, TBP, in mole)	340	248	156	71	623	443	388
T95 (°C, TBP, in mole)	372	317	196	118	857	513	430
Flow rate (kmol/h)	153	651	492	683	234	245	102

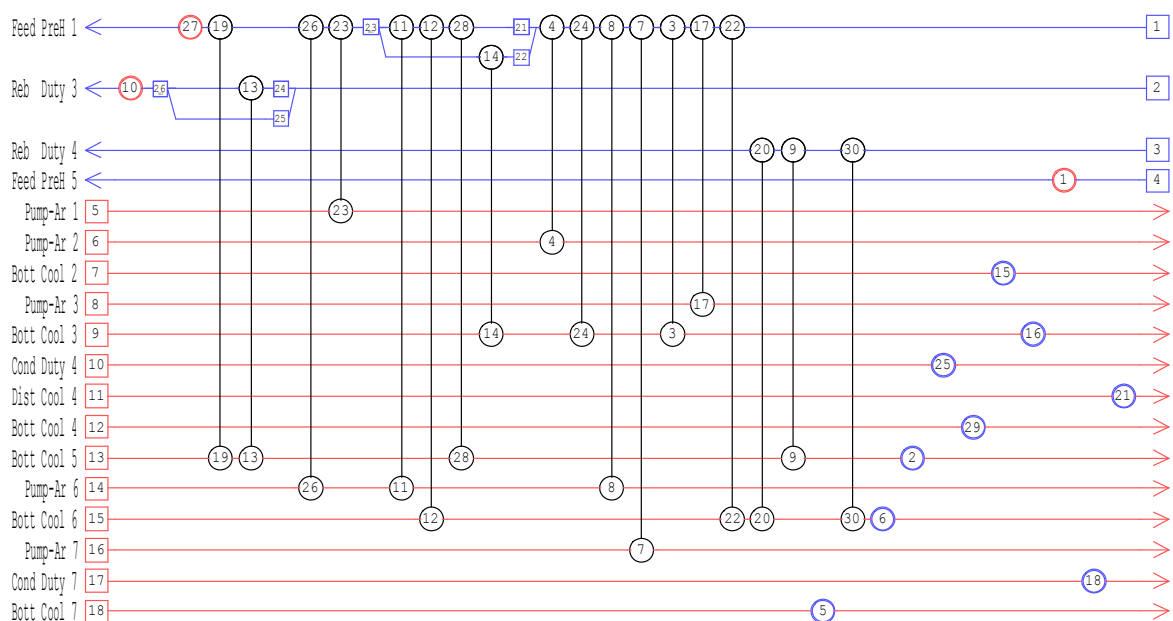


Figure 6.6 Case Study 6.3: Structure of existing heat exchanger network (stream data are given in Table D.2, Appendix D)

6.3.2 Optimisation approach and results

This case study aims at reducing energy demand of the existing crude oil distillation system. The objective function used in the optimisation is minimum total annualised cost, comprising utility cost, steam stripping cost and annualised capital cost for modifications to the existing HEN. The operating conditions of the atmospheric column presented in Table 6.5, the locations of pump-arounds in the atmospheric distillation column, the operating conditions of the vacuum column presented in

Table 6.23, and the operating conditions and structure of the HEN presented in Table 6.6, are optimised together to achieve the design objective. The structures of the existing atmospheric and vacuum distillation columns are not changed in the optimisation, i.e. the configuration of distillation columns, existing stage distribution and existing diameters. Only pump-around locations are varied in the optimisation.

Table 6.23 Case Study 6.3 Optimisation variables for vacuum distillation column

Simple column	Optimisation variables
5	1. Atmospheric residue preheating temperature 2. Flow rate of stripping steam
6	3. HVGO pump-around duty 4. Temperature drop across HVGO pump-around
7	5. LVGO pump-around duty 6. Temperature drop across LVGO pump-around

The lower and upper bounds of the continuous variables in the atmospheric column and the associated HEN are the same as those presented in Section 6.1.2. In the existing design, the pump-arounds are located at the stage just below the side-straw stage. In the optimisation, the pump-around locations are expressed as the stage number (where the pump-around exists) in the simple column. Thus, the lower limit of the pump-around location is one, and the upper limit is equal to the number of existing theoretical stages in the rectifying section of the associated simple column.

The lower and upper bounds of the preheat temperature for the vacuum column are 350 and 410 °C. The lower and upper limits of the LVGO pump-around and the HVGO pump-around are 50 and 200 °C, respectively. Similar to the atmospheric column, pump-around duties in the vacuum column are optimised in terms of degrees of thermal coupling between simple columns, and a steam flow rate is expressed through the partial hydrocarbon pressure on the feed stage. Thus, these variables are changed between 0 to 1, and 1% to 99% of the feed stage pressure, respectively.

The hydraulic limits of the distillation column are applied in this case study. The product flow rate deviations and TBP deviations are constrained within 1% of the base case and 5 °C. The retrofit HEN design is for a minimum temperature approach of 20 °C.

Table 6.24 Case Study 6.3: Move probabilities

Move decisions	Probability
Distillation column move, heat exchanger network move	0.5, 0.5
Simple column 1, 2, 3, 4, 5, 6, 7	0.33, 0.11, 0.11, 0.11, 0.11, 0.11, 0.11
Simple column 1: preheat temperature move, pump-around duty move [#] , temperature drop through pump-around, pump-around location move, R/R _{min} move, stripping steam flow rate move ⁺ , key component move, key component recovery move, pressure move	0.3, 0.2, 0.2, 0.1, 0.1, 0.1, 0, 0, 0
Simple column 2: preheat temperature move, pump-around duty move [#] , temperature drop through pump-around, pump-around location move, R/R _{min} move, stripping steam flow rate move ⁺ , key component move, key component recovery move, pressure move	0, 0.2, 0.2, 0.2, 0.2, 0.2, 0, 0, 0
Simple column 3: preheat temperature move, pump-around duty move [#] , temperature drop through pump-around, pump-around location move, R/R _{min} move, stripping steam flow rate move ⁺ , key component move, key component recovery move, pressure move	0, 0.25, 0.25, 0.25, 0.25, 0, 0, 0, 0
Simple column 4: preheat temperature move, pump-around duty move [#] , temperature drop through pump-around, pump-around location move, R/R _{min} move, stripping steam flow rate move ⁺ , key component move, key component recovery move, pressure move	0, 0, 0, 0, 1, 0, 0, 0, 0
Simple column 5: preheat temperature move, pump-around duty move [#] , temperature drop through pump-around, pump-around location move, R/R _{min} move, stripping steam flow rate move ⁺ , key component move, key component recovery move, pressure move	0.6, 0, 0, 0, 0.2, 0.2, 0, 0, 0
Simple column 6: preheat temperature move, pump-around duty move [#] , temperature drop through pump-around, pump-around location move, R/R _{min} move, stripping steam flow rate move ⁺ , key component move, key component recovery move, pressure move	0, 0.4, 0.3, 0, 0.3, 0, 0, 0, 0
Simple column 7: preheat temperature move, pump-around duty move [#] , temperature drop through pump-around, pump-around location move, R/R _{min} move, stripping steam flow rate move ⁺ , key component move, key component recovery move, pressure move	0, 0.4, 0.3, 0, 0.3, 0, 0, 0, 0
Exchanger move, bypass move	0.8, 0.2
Exchanger move: add a exchanger move, delete a exchanger move, modify exchanger duty move, exchanger relocation move	0.2, 0.1, 0.45, 0.25
Bypass move: add a bypass, delete a bypass, modify the splitting fraction of a bypass	0, 0, 1
Exchanger relocation move: resequence move, re pipe move	0.5, 0.5

[#]: Pump-around duty is optimised in terms of degree of thermal coupling;

⁺: Stripping steam flow rate is optimised in terms of partial pressure of hydrocarbon at the feed stage

The multiple-run simulation annealing based design framework is applied to optimise this case study for minimum total annualised cost, starting with the existing distillation columns and the existing HEN. The simulated annealing parameters and move probabilities implemented in the optimisation are presented in Table 6.7 and Table 6.24.

Table 6.25 presents the summary of the best solution found during the optimisation and compares the best solution with the base case. Table 6.25 presents the annualised cost, utility cost, stripping steam and capital investment for exchanger modifications. Tables 6.26 and 6.27 show the column operating conditions of the optimised design and the products generated in the optimised design. Comparisons between the optimised case and the base case are also presented in Tables 6.26 and 6.27.

Table 6.25 Case Study 6.3: Energy consumption and operating costs of optimum system

		Base case / Existing system	Optimum system	Saving
Hot utility demand	MW	86.68	73.80	12.88 (15%)
Cold utility demand	MW	88.93	84.95	3.98 (4%)
Crude oil temperature before entering atmospheric furnace	°C	254	284	-
Utility operating cost	MM\$/y	13.47	11.52	1.95 (15%)
Stripping steam operating cost	MM\$/y	2.59	2.76	-0.17 (7%)
Additional exchanger area	m ²	-	1587	-
HEN capital investment	MM\$	-	0.40	-
Total operating cost	MM\$/y	16.06	14.28	1.78 (11%)
Total annualised cost	MM\$/y	16.06	14.49	1.57 (10%)
T _{min}	°C	25	20	-
Payback	y	-	0.3	-

Utility and steam unit costs are given in Table C.1.5 (Appendix C)

Details of additional area cost is given in Table C.2.4 (Appendix C)

The hot and cold utility requirements are reduced by 12.88 MW (15%) and 3.98 MW (4%) respectively. Pump-around locations are moved down to achieve more heat recovery. However, as a result, column sections below pump-arounds are lacked of reflux, additional stripping steam ensures that the separation is not compromised. Although the stripping steam cost increases slightly (0.17 MM\$/y), the total operating cost decreases by 1.78 MM\$/y (11%) mainly, due to a large reduction (12.9 MW) in

the furnace duty. It can be observed from Table 6.27 that the products are constrained within allowed ranges.

Table 6.26 Case Study 6.3: Optimum operating conditions of atmospheric column and vacuum column

Column	Optimisation variable		Base case	Optimum
1	Feed preheating temperature	°C	365	365
	Pump-around duty	MW	13.14	13.16
	Temperature drop across pump-around	°C	30	27
	Pump-around location	-	1	5
	Flow rate of stripping steam	kmol/h	1200	1214
	Flow rate of liquid between columns 1 and 2	kmol/h	417	417
2	Pump-around duty	MW	18.69	19.03
	Temperature drop across pump-around	°C	50	51
	Pump-around location	-	1	2
	Flow rate of stripping steam	kmol/h	250	449
	Flow rate of liquid between columns 2 and 3	kmol/h	177	179
3	Pump-around duty	MW	9.642	9.947
	Temperature drop across pump-around	°C	20	31
	Pump-around location	-	1	4
	Flow rate of liquid between columns 3 and 4	kmol/h	1086	1045
4	Reflux ratio	-	4.49	4.40
5	Feed preheating temperature	°C	400	400
	Flow rate of stripping steam	kmol/h	700	625
6	HVGO pump-around duty	MW	16.01	15.80
	Temperature drop across HVGO pump-around	°C	150	51
7	LVGO pump-around duty	MW	11.31	17.41
	Temperature drop across LVGO pump-around	°C	100	120

Table 6.27 Case Study 6.3: Product information of optimum columns

Parameter	Products						
	HD	LD	HN	LN	VR	HVGO	LVGO
Flow rate . optimum case (kmol/h)	152	652	493	683	234	245	101
. base case (kmol/h)	153	651	492	683	234	245	102
. deviation (kmol/h)	-1	+1	+1	0	0	0	-1
T5 . optimum case (°C)	288	192	121	3	523	381	352
. base case (°C)	287	191	117	3	523	381	352
. deviation (°C)	+1	+1	+4	0	0	0	0
T50 . optimum case (°C)	340	248	160	71	623	443	388
. base case (°C)	340	248	156	71	623	443	388
. deviation (°C)	0	0	+4	0	0	0	0
T95 . optimum case (°C)	372	317	196	118	857	513	430
. base case (°C)	372	317	196	118	857	513	430
. deviation (°C)	0	0	0	0	0	0	0

The modified HEN is shown in Figure 6.7. The total additional area required is 1587 m² (Details are presented in Table E.4, Appendix E). No re-piping and re-sequencing modifications are needed in the modified HEN. However, 11 exchangers need additional heat transfer area and two new exchangers are added. The capital investment needed for the modifications is comparatively low, 0.40 MM\$/y, compared with the potential saving in the operating cost.

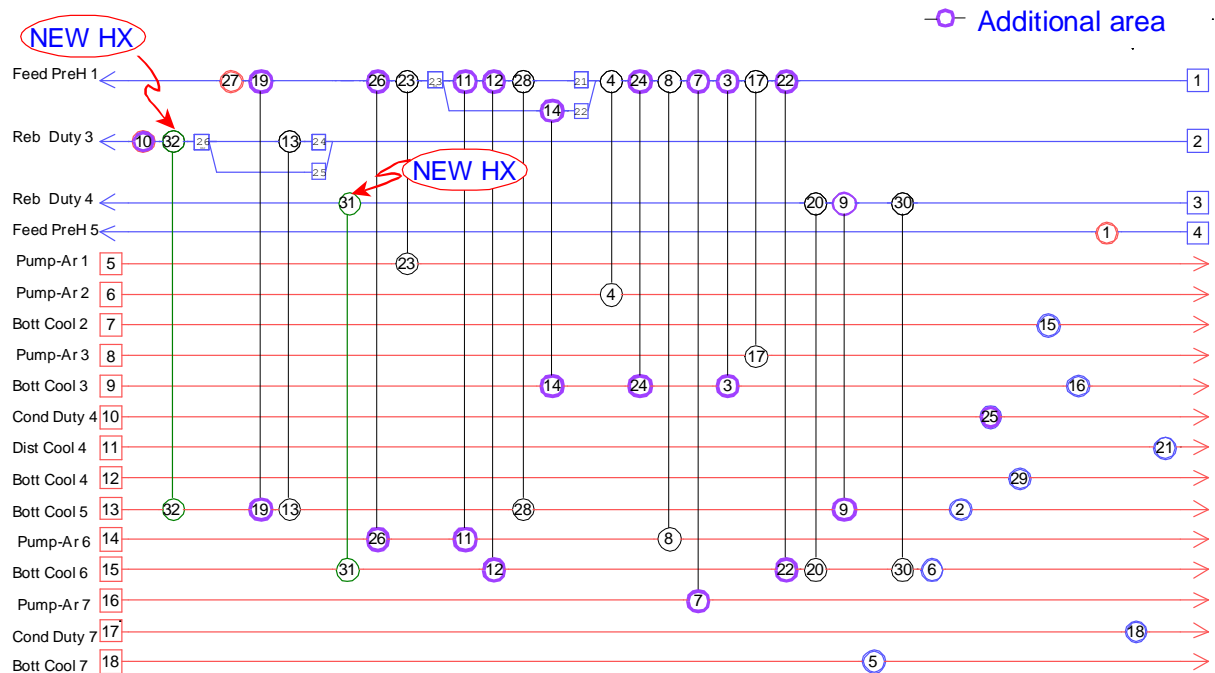


Figure 6.7 Case Study 6.3: Modified heat exchanger network

There is a significant reduction in the furnace duty in the optimised design of the overall system. The energy saving is obtained by changing operation in distillation columns and installing new heat transfer units and adding additional area to existing exchanger units. Note that 11 exchangers require additional area in the new design, which may impose problems in carrying out these modifications in a single shut-down, when the time is limited.

6.4 Case study 6.4: Grassroots design for heat-integrated atmospheric crude oil distillation

This case study applies the proposed design approach to various crude oil distillation configurations which performs same separation as from the existing atmospheric distillation column presented in Case Study 6.1. The purpose of this case study is to

demonstrate the potential of the new optimisation-based design approach and identify the potential of various crude oil distillation configurations, in terms of heat recovery, operating cost and total annualised cost. In order to highlight the energy efficiency of these configurations, the capital cost of distillation columns only includes the cost for distillation trays and shells and other cost items such as installation cost, basement cost, *etc.*, are not considered. Thus, if compared with industrial crude oil distillation units cost, the cost used in this work is underestimated.

The configurations under study are:

- Conventional atmospheric distillation column, without a prefractionator column (Case Study 6.1), which is used as a reference case and benchmark.
- Atmospheric distillation column with a prefractionator column, which is widely established in industry and may spread separation load using distributed separation sequence.
- Progressive configuration (US4664785), which is a relatively novel configuration and well known as a configuration with high energy efficiency
- Novel configuration . atmospheric column, with a liquid side-draw prefractionator column (see Section 5.4.1), which is observed in an industry case study to have good performance with respect to energy demand.

Products specifications are taken from the existing atmospheric distillation column presented in Case Study 6.1. Then other three configurations are designed for the same product specifications by applying the methods proposed in Section 3.2. Note that products from different configurations are not specified to be exactly the same but within some tolerance since the configurations generating these products are different. The descriptions of these configurations are presented in Section 6.4.1.

As the purpose of this case study is to demonstrate the relative merit of the various configurations, grassroots design is implemented, rather than retrofit design. In order to focus on the distillation configurations, the interactions between the distillation columns and the preheat train are simplified using pinch analysis to determine utility demand, rather than details of the heat exchanger network design. Multi-segment stream data are implemented to increase the accuracy of the heat recovery potential estimation. The heat recovery potential may not be achievable in practice because of

economic reasons. Distillation configurations which provide better potential for heat recovery can be identified through this case study.

Liebmann (1996) designed two atmospheric configurations based on heuristic rules. No optimisation has been carried out in the design procedure. In the work of Suphanit (1999), several configurations were optimised and compared; however, the studies that have been carried out were of very limited scope. The optimisations and comparisons were based on NLP optimisation method, which is easily trapped in locally optimal solutions. Moreover, Suphanit (1999) did not include pump-around locations as degrees of freedom in his study since the models he developed were not able to consider the pump-around locations. Constant heat capacities were assumed in previous work (Suphanit, 1999), which introduced considerable inaccuracy in estimating the heat recovery potential. Due to above limitations in previous studies, there is a need to re-optimize and compare various crude oil distillation configurations using the design approach proposed in the present work. The new design approach has many advantages, such as the enhanced scope and range in the degrees of freedom, the improved consideration of product quality and the increased robustness and comprehensiveness of the optimisation algorithm.

6.4.1 Problem data

The separation target is to fraction 100,000 barrels/day (2610.7 kmol/h) of Tia Juana Light Venezuela crude oil (crude assay listed in Table 6.1) into five products: atmospheric residue (RES), heavy distillate (HD), light distillate (LD), heavy naphtha (HN) and light naphtha (LN). The products generated from the existing atmospheric crude oil distillation column presented in Case Study 6.1 are used as the specifications of this case study. Table 6.4 listed the information of products required to be produced in each configuration. In this section, the four configurations that will be optimised are presented.

Conventional atmospheric distillation column, without a prefractionator column

The first configuration is simply a conventional atmospheric distillation column, without a prefractionator column. As shown in Figure 6.8, three side-strippers are

used to strip lighter components from products and four pump-arounds are used to recover heat in the column. Steam at 4.5 bar and 260 °C is injected at the bottom of the main column and the bottom side-stripper (HD side-stripper), while reboilers are installed in the top and middle side-strippers (HN and LD side-strippers). This configuration is slightly different from that presented in Case Study 6.1. One more pump-around is installed at the top of the column, above the top side-stripper. As discussed in Section 3.3.5, pump-arounds benefit heat recovery. Figure 6.8 also shows the equivalent decomposed sequence of simple columns.

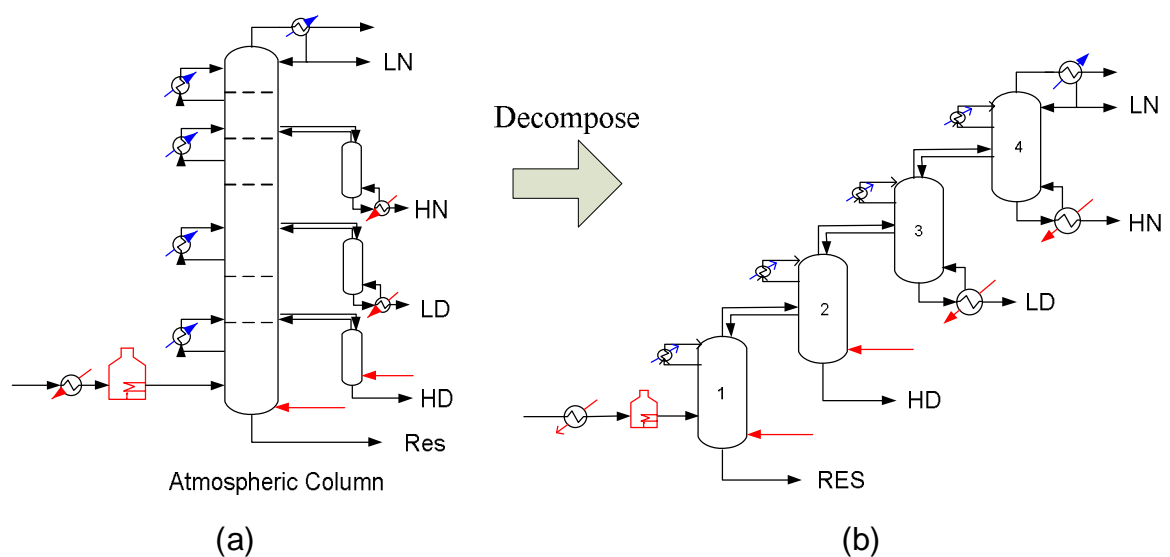


Figure 6.8 Case Study 6.4: Conventional atmospheric distillation column without a prefractionator column, showing the equivalent decomposed sequence of simple columns (a) Atmospheric column (b) Equivalent decomposed sequence

Atmospheric distillation column with a prefractionator column

Figure 6.9 presents the configuration with an atmospheric distillation column and a prefractionator column, and the decomposed sequence. The lightest product LN is produced from the prefractionator column, and the remaining four products HN, LD, HD and residue are separated in the atmospheric column. Compared with the configuration with only an atmospheric column, in this configuration, HN is produced from the top of the atmospheric column rather than the HN side-stripper and only two side-strippers are attached to the main atmospheric column rather than three side-strippers in the previous configuration (Configuration without a prefractionator column). The prefractionator column and LD side-stripper are reboiled, corresponding to the reboiled HN and LD side-strippers in the configuration without a prefractionator. Steam at 4.5 bar and 260 °C is injected at the bottom of the main

column and the bottom side-stripper of the atmospheric column. There are four pump-arounds in this configuration to recover heat: one pump-around on the prefractionator column, two below the draw stages of LD and HD side-strippers and one located above the top side-stripper of the atmospheric column.

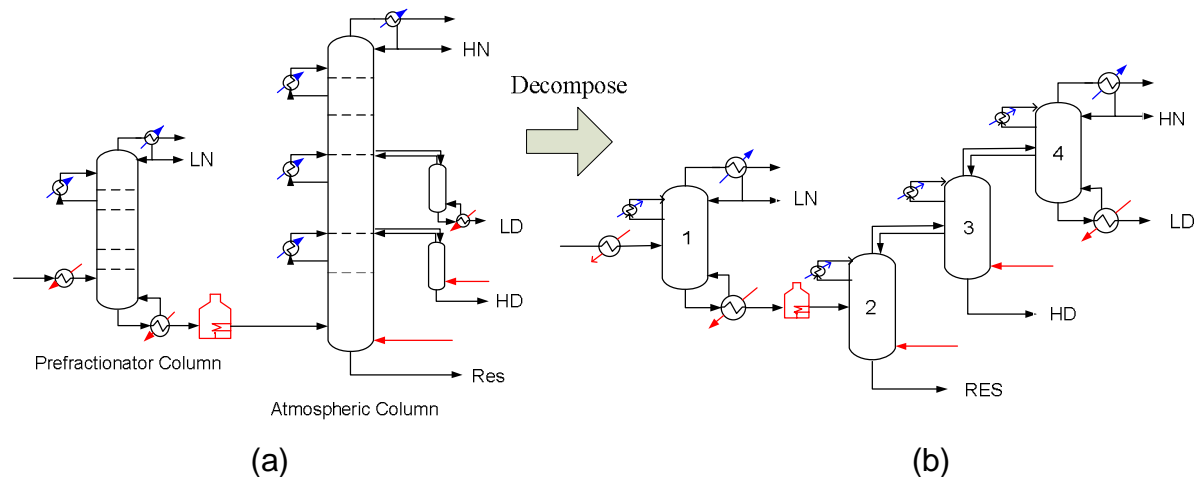


Figure 6.9 Case Study 6.4: Atmospheric distillation column with a prefractionator column, showing the equivalent decomposed sequence of simple columns
(a) Original configuration (b) Equivalent decomposed sequence

Progressive configuration

This configuration is designed based on patent US4664785 and Rhodes (1997). This configuration has been first-ever applied at Mider Refinery and referred to be a promising configuration with high energy efficiency (Rhodes, 1997). The main features of the progressive configuration are that successive separation of increasingly heavy products and distributed separations take place in a relatively large number of columns. More heat recovery opportunities may be created in the succession of progressive separations. The patented configuration is modified as its product slate is different from the product slate required in this case study; however, the main features are retained. Figure 6.10 shows the modified progressive configuration used in this case study, comprising eight columns in total. As seen in the figure, LN is collected from Column 1. Columns 2 and 3 are the first series of columns which feed the second series of Columns 4 and 5. Column 4 separates LN from HN, and Column 5 separates HN from LD. The bottom product of Column 3 is processed in atmospheric Column 6, and HD is collected from the side-stripper attached to the main column of the atmospheric unit. The overhead of Column 6 is

Figure 6.11 shows the schematic of this configuration, in which there is a prefractionator column with a liquid side-draw and an atmospheric column. The side-draw liquid is fed into the atmospheric column at the same stage as the HN side-stripper (location **XX** = 4 in Figure 5.5, Section 5.4). Product LN is collected from both the overhead of the prefractionator column and the atmospheric column. Steam at 4.5 bar and 260 °C is injected at the bottom of the main atmospheric column and the HD side-stripper, and reboilers are installed in the HN and LD side-strippers and the prefractionator column. There are four pump-arounds in the configuration: one located below the liquid side-draw in the prefractionator column and three installed on the atmospheric column. Compared with conventional simple prefractionator columns, the liquid side-draw reduces the flow rate of bottom product of the column. Hence, the heat load on the process furnace heating the main atmospheric distillation unit feed decreases. The simplified model proposed in Section 5.4 is implemented to simulate this configuration.

As discussed in the opening of this section, the purpose of this case study is to generate energy efficient designs for each configuration and to demonstrate the relative merit of the various configurations. Pinch analysis is implemented in this case study to predict the energy demand of each configuration, rather than considering the detailed design of the heat exchanger networks. The minimum temperature approach in each configuration is assumed to be the same to assure a fair comparison. Hence, a temperature approach of 30 °C is used for all four configurations in the following optimisations.

Except for the progressive configuration, the other three configurations are only slightly different from each other. The differences come from the prefractionator column: whether there is a prefractionator column installed and whether there is a liquid side-draw from the column. Considering the similarity between these three configurations, the number of pump-arounds in these configurations is selected to be the same to make sure comparisons are fair, since pump-around streams are key heat sources in the heat recovery system. Moreover, the maximum number of total theoretical stages in each configuration is constrained and the limit is set to be the same for each configuration so that comparisons between these configurations are not prejudiced by unlimited equipment allowances. The capital cost calculations are carried out by applying Equations 3.10 . 3.12. For all configurations, plant life is

assumed to be 10 years with an interest rate of 10% for calculating annualised capital cost.

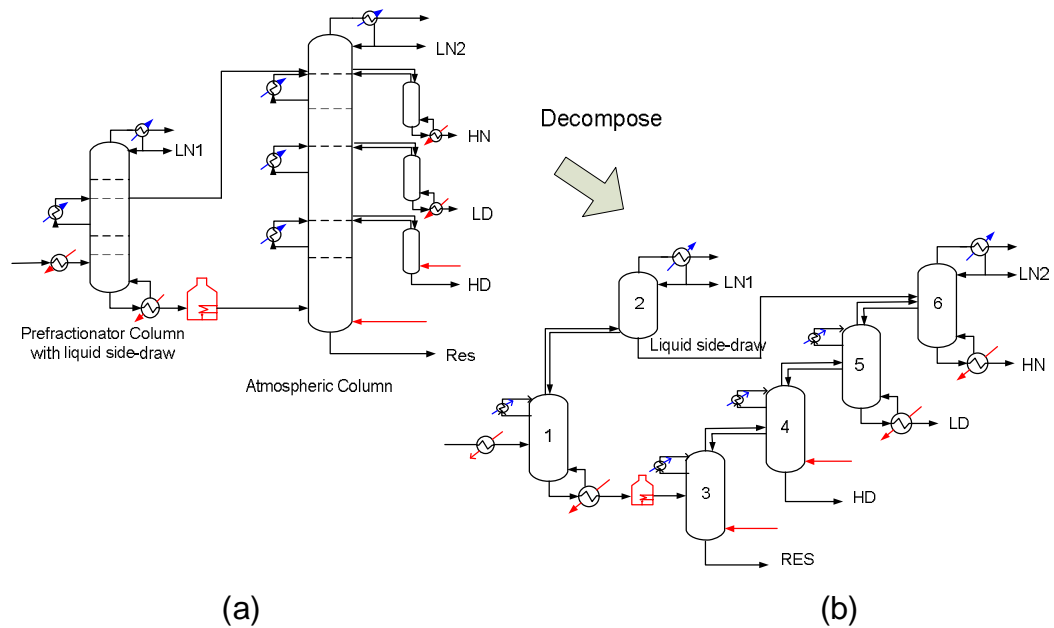


Figure 6.11 Case Study 6.4: Novel configuration with an atmospheric column and a liquid-side-draw prefractionator column

(a) Original configuration (b) Equivalent decomposed sequence

6.4.2 Optimisation approach and results for the configuration without a prefractionator column

The purpose of this case study is to compare performance of different crude oil distillation configurations, in terms of energy efficiency. Hence, the objective function of the optimisation is minimum total annualised cost (see Section 5.3.1 for definition and calculation). The column operating conditions varied in the optimisation are the same as those of Case Study 6.1, and are shown in Table 6.5. The pump-around locations are included in the degrees of freedom.

The lower and upper bounds of the preheat feed temperature are set as 350 and 375 °C respectively, while for the temperature drop through pump-arounds, the limits are 20 and 150 °C. The boundaries of other variables are the same as those presented in Section 6.1.2. The operating pressure in the atmospheric column is 2.5 bar.

The multiple-run simulated annealing optimisation-based design framework is applied to obtain the optimum design of the configuration without a prefractionator column, using the base case of Case Study 6.1 as the starting point (operating conditions are presented in Table 6.3). The simulated annealing parameters and move probabilities implemented in the optimisation are presented in Table 6.7 and Table 6.28. The product flow rate deviations are set to be within 1% of the product specifications (see Table 6.4 for products information) and the allowed maximum product TBP point difference with the base case is 5 °C. The total number of theoretical stages is constrained to be less than 74.

Table 6.28 Case Study 6.4: Move probabilities (Configuration without a prefractionator column)

Move decisions	Probability
Distillation column move, heat exchanger network move	1, 0
Simple column 1, 2, 3, 4	0.3, 0.2, 0.2, 0.3
Simple column 1: preheat temperature move, pump-around duty move [#] , temperature drop through pump-around, pump-around location move, R/R _{min} move, stripping steam flow rate move ⁺ , key component move, key component recovery move, pressure move	0.3, 0.15, 0.2, 0.15, 0.1, 0.1, 0, 0, 0
Simple column 2: preheat temperature move, pump-around duty move [#] , temperature drop through pump-around, pump-around location move, R/R _{min} move, stripping steam flow rate move ⁺ , key component move, key component recovery move, pressure move	0, 0.25, 0.25, 0.2, 0.15, 0.15, 0, 0, 0
Simple column 3: preheat temperature move, pump-around duty move [#] , temperature drop through pump-around, pump-around location move, R/R _{min} move, stripping steam flow rate move ⁺ , key component move, key component recovery move, pressure move	0, 0.25, 0.25, 0.25, 0.25, 0, 0, 0, 0
Simple column 4: preheat temperature move, pump-around duty move [#] , temperature drop through pump-around, pump-around location move, R/R _{min} move, stripping steam flow rate move ⁺ , key component move, key component recovery move, pressure move	0, 0.25, 0.25, 0.25, 0.25, 0, 0, 0, 0

#: Pump-around duty is optimised in terms of degree of thermal coupling;

+: Stripping steam flow rate is optimised in terms of partial pressure of hydrocarbon at the feed stage

The performance summary of the best design of this configuration is presented in Table 6.29, including utility demand, stripping steam flow rate, annualised capital cost for distillation columns and HEN, and total annualised cost. The corresponding distillation columns required are shown in Table 6.30, in terms of the number of

theoretical stages in each column section and the total number of stages. The operating conditions of the optimised design of the configuration without a prefractionator column are provided in Table F.1 (Appendix F). Table 6.31 presents the product slate of the best design found in the optimisation.

The hot and cold utility demands for the configuration without a prefractionator column are 42.66 MW and 41.49 MW respectively. The total annualised cost is 8.45 MM\$/y. The amount of stripping steam required in the best design is 1073 kmol/h. It can be seen from Table 6.31 that the product slate of the best design is within the allowed range. In total, 63 theoretical stages are required to achieve the desired separation. These results will be discussed again in the summary of this case study (Section 6.4.6) and compared with the best designs of other configurations.

Table 6.29 Case Study 6.4: Performance summary of optimum design (Configuration without a prefractionator column)

	Value
Hot utility (MW)	42.66
Cold utility (MW)	41.49
Stripping steam (kmol/h)	1073
Heat exchanger area cost (MM\$/y)	0.22
Column capital cost (MM\$/y)	0.32
Total annualised cost (MM\$/y)	8.45

Table 6.30 Case Study 6.4: Theoretical stage distribution of optimum design*
(Configuration without a prefractionator column)

	Column 1	Column 2	Column 3	Column 4
Rectifying section	10	11	9	7
Stripping section	3	6	8	9
Total number of stages	63			

*: in terms of simple columns in decomposed sequence, and rounded up to integers; Figure 6.9 shows the decomposed sequence of simple columns.

Table 6.31 Case Study 6.4: Product slate of optimum design (Configuration without a prefractionator column)

Products	Flow rate kmol/h	TBP (°C, mole%)		
		5%	50%	95%
Light Naphtha (LN)	677	3	70	118
Heavy Naphtha (HN)	496	117	156	196
Light Distillate (LD)	652	190	248	317
Heavy Distillate (HD)	151	285	339	372
Residue (RES)	634	353	462	798

6.4.3 Optimisation approach and results for the configuration with a prefractionator column

This section presents the design of the configuration with a prefractionator column by the new optimisation-based approach. The objective during the optimisation is minimum total annualised cost, which is implemented in the optimisation of all configurations. The degrees of freedom considered in the atmospheric column are the same as those in the configuration without a prefractionator column, except that there is no HD side-stripper. In addition, the degrees of freedom in the prefractionator column (Column 1 in the decomposed sequence) considered are: feed preheating temperature, pump-around duty, temperature drop through pump-around, pump-around location and R/R_{\min} . The variable boundaries in the atmospheric column are the same as presented in Section 6.4.2. For the prefractionator column, the lower and upper limits of the feed preheating temperature are 180 and 300 °C; limits of pump-around variables are the same as in the atmospheric column, which are implemented throughout this case study wherever there is a pump-around installed. The same strategy is applied to the limits of R/R_{\min} and stripping steam if they are considered as optimisation variables.

The model proposed in Chapter 3 (Section 3.2.5) is applied to set up an initial design of the configuration with a prefractionator column, and this design is used as the starting point of the simulated annealing optimisation algorithm. The key components and recoveries are selected in each simple column so that the product profiles are the same as presented in Table 6.4, within tolerance. The maximum TBP deviation is from heavy naphtha, which is the last product in the configuration and not constrained when setting up the initial design. Considering the difference between each configuration, this TBP deviation is acceptable. The operating conditions of the initial design and the product slate are presented in Tables F.2 and F.3 (Appendix F), respectively. The optimisation starts with the initial design and makes randomised moves to generate different design alternatives according to the assigned probabilities, as listed in Table 6.32. The simulated annealing parameters are the same as those used in the optimisation of the configuration without a prefractionator column (see Table 6.7 for the simulated annealing parameters). In the optimisation,

product specifications are the same as in the initial design ($\pm 1\%$ of flow rate and ± 5 °C of TBP). The total number of theoretical stages is constrained to be less than 74, the same as implemented in the configuration without a prefractionator column.

Table 6.32 Case Study 6.4: Move probabilities (Configuration with a prefractionator column)

Move decisions	Probability
Distillation column move, heat exchanger network move	1, 0
Simple column 1, 2, 3, 4	0.3, 0.3, 0.2, 0.2
Simple column 1: preheat temperature move, pump-around duty move [#] , temperature drop through pump-around, pump-around location move, R/R_{min} move, stripping steam flow rate move ⁺ , key component move, key component recovery move, pressure move	0.3, 0.2, 0.1, 0.2, 0.2, 0, 0, 0, 0
Simple column 2: preheat temperature move, pump-around duty move [#] , temperature drop through pump-around, pump-around location move, R/R_{min} move, stripping steam flow rate move ⁺ , key component move, key component recovery move, pressure move	0.3, 0.15, 0.2, 0.15, 0.1, 0.1, 0, 0, 0
Simple column 3: preheat temperature move, pump-around duty move [#] , temperature drop through pump-around, pump-around location move, R/R_{min} move, stripping steam flow rate move ⁺ , key component move, key component recovery move, pressure move	0, 0.25, 0.25, 0.2, 0.15, 0.15, 0, 0, 0
Simple column 4: preheat temperature move, pump-around duty move [#] , temperature drop through pump-around, pump-around location move, R/R_{min} move, stripping steam flow rate move ⁺ , key component move, key component recovery move, pressure move	0, 0.25, 0.25, 0.25, 0.25, 0, 0, 0, 0

#: Pump-around duty is optimised in terms of degree of thermal coupling;

+: Stripping steam flow rate is optimised in terms of partial pressure of hydrocarbon at the feed stage

Table 6.33 presents the results summary of the optimum design found during the optimisation. The distillation columns required with this design are shown in Table 6.34, in terms of total number of theoretical stages and stage distribution. The corresponding operating conditions are listed in Table F.4 (Appendix F) and the products generated from this optimum design are presented in Table 6.35.

Table 6.33 Case Study 6.4: Performance summary of optimum design (Configuration with a prefractionator column)

	Value
Hot utility (MW)	52.40
Cold utility (MW)	51.11
Stripping steam (kmol/h)	1119
Heat exchanger area cost (MM\$/y)	0.22
Column capital cost (MM\$/y)	0.28
Total annualised cost (MM\$/y)	9.97

Table 6.34 Case Study 6.4: Theoretical stage distribution of optimum design* (Configuration with a prefractionator column)

	Column 1	Column 2	Column 3	Column 4
Rectifying section	3	10	11	8
Stripping section	10	2	2	8
Total number of stages	54			

*: in terms of simple columns in decomposed sequence, and rounded up to integers

Table 6.35 Case Study 6.4: Product slate of optimum design (Configuration with a prefractionator column)

Products	Flow rate kmol/h	TBP (°C, mole%)		
		5%	50%	95%
Light Naphtha (LN)	657	2	69	118
Heavy Naphtha (HN)	515	108	155	196
Light Distillate (LD)	658	190	248	317
Heavy Distillate (HD)	141	285	339	372
Residue (RES)	639	352	461	797

Table 6.33 indicates that the hot and cold utility demands of the best of the configuration with a prefractionator column are both 10 MW higher than those of the configuration without a prefractionator column. Note that this observation is in the opposite trend as the general opinion about the installation of a prefractionator column. This energy intensity is caused by the requirement of separating all the light naphtha in the prefractionator column, which is not how prefractionator is applied in the refining industry. In industry, most prefractionator columns are used to separate lighter components from the crude oil, and the overhead flow rate is usually small. The prefractionator column as employed in this case study requires large amount of energy input, and is not beneficial in increasing energy efficiency. Although the installation of prefractionator column in this case study does not increase the energy efficiency, the prefractionator is capable of reducing the size of distillation columns, indicated by lower capital investment of the configuration with a prefractionator

column (saving 0.24 MM\$, 13% off). Table 6.35 shows that the properties of the products generated by both configurations are similar.

6.4.4 Optimisation approach and results for the progressive configuration

This section presents the design of progressive configuration. As shown in Figure 6.10 (Section 6.4.1), distributed separations occur to produce products LN, HN and LD. How to distribute these products is an important degree of freedom. Two steps are performed in the design and optimisation of this configuration. Firstly, the product distributions are fixed as the set of arbitrary values as listed in Table 6.36 and the optimisation of other variables such as feed temperatures, R/R_{\min} , steam flow rates if steam stripped, pump-around duties, temperature drops and locations, are carried out for minimising the total annualised cost of the configuration. In the second step, product distributions of light naphtha (LN), heavy naphtha (HN) and light distillate (LD) are considered as degrees of freedom. Moreover, as increasingly heavy products are separated successively in the progressive distillation, distillation columns that produce LN, HN and LD can be operated at higher pressure than ambient pressure without causing coking problems. Higher operating pressure may be beneficial to heat recovery but harmful to separation. Considering the trade-off between heat recovery and separation, column operating pressures except that of atmospheric column 6, are included as optimisation variables in the second step.

First step: fixing product distributions and operating pressures

In this step, product distributions are fixed as the values listed in Table 6.36 and operating pressures of each column fixed as 2.5 bar. An initial design of the progressive configuration that fulfils the desired product distributions and product specifications (see Table 6.4), is obtained by applying the method proposed in Section 3.2.5 to select appropriate key components and recoveries. The operating conditions of each column as discussed below are selected arbitrarily and will be optimised later. Tables F.5 and F.6 present the initial design, including operating conditions of each column and properties of products generated by the design.

The optimisation variables considered in the optimisation are: feed temperatures of Column 1 . 6 and Column 8 (indicated by cooler or heater in Figure 6.10), R/R_{\min} , steam flow rates if the column is steam stripped, and variables associated with pump-around (duty, temperature drop and location). The limits of R/R_{\min} , steam flow rates and pump-around associated variables are the same as presented in Section 6.4.2 and Section 6.4.3. Table 6.37 shows the lower and upper bounds of the feed preheating temperature of each column in the configuration. These bounds are estimated based on the bubble and dew points of the feeds. Table 6.38 presents the move probabilities of these variables used in the simulated annealing optimisation algorithm.

Table 6.36 Case Study 6.4: Fixed product distributions (First step of the progressive configuration)

Products	Fraction
LN1 from Column 1/ total LN	0.68
HN1 from Column 4/ total HN	0.34
HN2 from Column 5/ total HN	0.54
LD1 from Column 8/ total LD	0.35

Table 6.37 Case Study 6.4: Limits of feed temperatures in optimisation (First step of the progressive configuration)

Limits (°C)	Column 1	Column 2	Column 3	Column 5	Column 6	Column 8
Lower bound	130	220	290	180	330	150
Upper bound	190	280	350	250	375	220

The optimisation algorithm starts with simulation of the initial design. During the optimisation, product flow rates and TBP points are constrained to be the same as in the initial design (flow rate deviations: less than 1%; TBP deviations: less than 5°C). Tables 6.39 to 6.41 present the best design found during the optimisation, including the performance summary, distillation columns required and products generated by the design. The optimum operating conditions are provided in Table F.7 (Appendix F).

Table 6.38 Case Study 6.4: Move probabilities (First step of the progressive configuration)

Move decisions	Probability
Distillation column move, heat exchanger network move	1, 0
Simple column 1, 2, 3, 4, 5, 6, 7, 8	0.125, 0.125, 0.125, 0.125, 0.125, 0.125, 0.125, 0.125,
Simple column 1: preheat temperature move, pump-around duty move [#] , temperature drop through pump-around, pump-around location move, R/R _{min} move, stripping steam flow rate move ⁺ , key component move, key component recovery move, pressure move	0.5, 0, 0, 0, 0.5, 0, 0, 0, 0
Simple column 2: preheat temperature move, pump-around duty move [#] , temperature drop through pump-around, pump-around location move, R/R _{min} move, stripping steam flow rate move ⁺ , key component move, key component recovery move, pressure move	0.5, 0, 0, 0, 0.5, 0, 0, 0, 0
Simple column 3: preheat temperature move, pump-around duty move [#] , temperature drop through pump-around, pump-around location move, R/R _{min} move, stripping steam flow rate move ⁺ , key component move, key component recovery move, pressure move	0.33, 0, 0, 0, 0.33, 0.34, 0, 0, 0
Simple column 4: preheat temperature move, pump-around duty move [#] , temperature drop through pump-around, pump-around location move, R/R _{min} move, stripping steam flow rate move ⁺ , key component move, key component recovery move, pressure move	0, 0, 0, 0, 1, 0, 0, 0, 0
Simple column 5: preheat temperature move, pump-around duty move [#] , temperature drop through pump-around, pump-around location move, R/R _{min} move, stripping steam flow rate move ⁺ , key component move, key component recovery move, pressure move	0.5, 0, 0, 0, 0.5, 0, 0, 0, 0
Simple column 6: preheat temperature move, pump-around duty move [#] , temperature drop through pump-around, pump-around location move, R/R _{min} move, stripping steam flow rate move ⁺ , key component move, key component recovery move, pressure move	0.16, 0.16, 0.16, 0.16, 0.16, 0.17, 0, 0, 0
Simple column 7: preheat temperature move, pump-around duty move [#] , temperature drop through pump-around, pump-around location move, R/R _{min} move, stripping steam flow rate move ⁺ , key component move, key component recovery move, pressure move	0.35, 0, 0, 0, 0.3, 0.35, 0, 0, 0
Simple column 8: preheat temperature move, pump-around duty move [#] , temperature drop through pump-around, pump-around location move, R/R _{min} move, stripping steam flow rate move ⁺ , key component move, key component recovery move, pressure move	0.5, 0, 0, 0, 0.5, 0, 0, 0, 0

#: Pump-around duty is optimised in terms of degree of thermal coupling;

+: Stripping steam flow rate is optimised in terms of partial pressure of hydrocarbon at the feed stage

The results in Table 6.39 indicate that the progressive configuration has slightly lower energy efficiency than the configuration with a prefractionator column, Although more columns are used in the progressive configuration than the other two configurations already optimised, the column capital cost of the best design in this configuration is less than that of the other two (28% less than the configuration without a prefractionator column and 18% less than the configuration with a prefractionator column). The lower column capital cost comes from the smaller columns in the progressive configuration due to smaller feed flow rates in successive separation. Comparing the products generated by this configuration with those from the configuration without a prefractionator column, flow rate difference is less than 1% and TBP differences are generally less than 8 °C, except for the HN product with 13 °C variations. Considering the difference between these configurations and there will be downstream processing of the products, this deviation is likely to tolerable.

Table 6.39 Case Study 6.4: Performance summary of optimum design (First step of the progressive configuration)

Parameter	Value
Hot utility (MW)	55.04
Cold utility (MW)	32.36
Stripping steam (kmol/h)	1824
Heat exchanger area cost (MM\$/y)	0.27
Column capital cost (MM\$/y)	0.23
Total annualised cost (MM\$/y)	11.13

Table 6.40 Case Study 6.4: Theoretical stage distribution of optimum design* (First step of the progressive configuration)

Parameter	Column 1	Column 2	Column 3	Column 4
Rectifying section	6	7	4	3
Stripping section	1	3	3	5
Parameter	Column 5	Column 6	Column 7	Column 8
Rectifying section	5	2	8	7
Stripping section	6	2	5	7
Total number of stages	74			

*: in terms of simple columns in decomposed sequence, and rounded up to integers

Table 6.41 Case Study 6.4: Product slate of optimum design (First step of the progressive configuration)

Products	Flow rate kmol/h	TBP (°C, mole%)		
		5%	50%	95%
Light Naphtha (LN)	681	3	71	128
Heavy Naphtha (HN)	489	104	156	209
Light Distillate (LD)	655	182	247	318
Heavy Distillate (HD)	148	288	339	376
Residue (RES)	637	350	461	798

Second step: optimising product distributions and operating pressures

In this step, the progressive configuration is optimised again. In addition to the variables considered in the first step, product distributions of light naphtha, heavy naphtha and light distillate and column operating pressures are varied in the optimisation. In the simplified distillation model, separation in a column is specified by key components and recoveries. Thus, key components and recoveries in Columns 1 . 5 and Column 8 are varied so that flow rates of the products collected from these columns are optimised. In this optimisation, the product coming out from each simple column is not constrained; instead, the total flow rates and the TBP of blended products LN, HN and LD are checked and constrained. The operating pressures of the columns where LN, HN and LD are produced are varied between 1.0 . 6.0 bar, to increase heat recovery opportunities. The bottom temperature of Columns 1 . 5 and column 8 are constrained not to exceed 380 °C to avoid coking.

Table 6.42 presents the optimised product distributions and Table 6.43 shows the optimised operating pressures. These values are compared with those from the initial values, fixed in the previous step of optimisation. It can be seen from Table 6.42 that more LN is produced in Column 1, less HN is produced in Column 4, more HN is processed in Column 5 and less LD is fractionated in Column 8. Table 6.43 shows that the operating pressures of Column 4 and Column 5 are increased to around 5 bar and that of Column 1 is reduced by 0.6 bar. With the optimised product distributions and operating pressure, together with the optimised operating conditions (provided in Table F.8, Appendix F), this best design requires less energy input than the design of fixed pressures and product distributions. The summary of the best design is listed in Table 6.44, and the comparisons with those of the design with fixed pressures and distributions are also shown in Table 6.44. It can be seen from Table 6.44 that the hot utility requirement and the total annualised cost are

reduced by 12% and 9% when optimising product distributions and operating pressures in the progressive configuration. The costs of the other items are similar in both steps of optimisation. The new distillation columns and stage distributions are presented in Table 6.44. Table 6.45 shows the properties and flow rates of the products generated by the optimised design.

Table 6.42 Case Study 6.4: Optimum product distributions (Second step of the progressive configuration)

Products	Original Fraction	Fraction
LN1 from Column 1/ total LN	0.68	0.78
HN1 from Column 4/ total HN	0.34	0.25
HN2 from Column 5/ total HN	0.54	0.62
LD1 from Column 8/ total LD	0.35	0.27

The hot utility demand in this design step of the progressive configuration is less than that of the configuration with a prefractionator column. However, more stripping steam in this design, as a result, the total annualised is cost higher than that for the configuration with a prefractionator column.

Table 6.43 Case Study 6.4: Optimised operating pressures (Second step of the progressive configuration)

Pressure (bar)	Column 1	Column 2	Column 3	Column 4	Column 5	Column 8
Original value	2.50	2.50	2.50	2.50	2.50	2.50
Optimised value	1.89	2.29	2.48	5.06	5.48	2.13

Table 6.44 Case Study 6.4: Performance summary of optimum design (Second step of the progressive configuration)

	Value with fixed pressure and product distribution	Value
Hot utility (MW)	55.04	48.31
Cold utility (MW)	32.36	28.74
Stripping steam (kmol/h)	1824	1859
Heat exchanger area cost (MM\$/y)	0.27	0.29
Column capital cost (MM\$/y)	0.23	0.22
Total annualised cost (MM\$/y)	11.13	10.14

Table 6.45 Case Study 6.4: Theoretical stage distribution of optimum design*
(Second step of the progressive configuration)

Parameter	Column 1	Column 2	Column 3	Column 4
Rectifying section	2	7	5	3
Stripping section	1	3	2	3
Parameter	Column 5	Column 6	Column 7	Column 8
Rectifying section	6	2	8	7
Stripping section	6	4	5	3
Total number of stages	67			

*: in terms of simple columns in decomposed sequence, and rounded up to integers

Table 6.46 Case Study 6.4: Product slate of optimum design (Second step of the progressive configuration)

Products	Flow rate	TBP (°C, mole%)		
	kmol/h	5%	50%	95%
Light Naphtha (LN)	691	3	72	123
Heavy Naphtha (HN)	490	100	159	214
Light Distillate (LD)	643	176	248	318
Heavy Distillate (HD)	150	288	339	376
Residue (RES)	635	351	462	798

6.4.5 Optimisation approach and results for the novel configuration with a liquid-side-draw prefractionator column

The novel configuration with a liquid-side-draw prefractionator column proposed in Section 5.4 is optimised in this section. As indicated in Figure 6.11, light naphtha is collected from the overhead of both the prefractionator and atmospheric columns. The distribution of the light naphtha between these two columns is fixed in this study: the ratio of light naphtha collected from the prefractionator column to the total amount of naphtha produced in the configuration is 0.91. Based on the fixed light naphtha distribution and the information of the desired products (see Table 6.4), an initial design is obtained by applying the method proposed in Section 3.2. Tables F.9 and F.10 provide the operating conditions of the initial design and the information of products generated by the initial design. The degrees of freedom considered in the optimisation are the same as in other configurations (except for the second step of the progressive configuration where product distributions and operating pressures are optimised). The bounds of the optimisation variables are as presented in Section

6.4.2. The move probabilities of these variables used in simulated annealing optimisation are presented in Table 6.47.

Table 6.47 Case Study 6.4: Move probabilities (Novel configuration with a liquid side-draw prefractionator column)

Move decisions	Probability
Distillation column move, heat exchanger network move	1, 0
Simple column 1, 2, 3, 4, 5, 6	0.2, 0.1, 0.2, 0.2, 0.2, 0.1
Simple column 1: preheat temperature move, pump-around duty move [#] , temperature drop through pump-around, pump-around location move, R/R_{min} move, stripping steam flow rate move ⁺ , key component move, key component recovery move, pressure move	0.3, 0.2, 0.2, 0.1, 0.2, 0, 0, 0, 0
Simple column 2: preheat temperature move, pump-around duty move [#] , temperature drop through pump-around, pump-around location move, R/R_{min} move, stripping steam flow rate move ⁺ , key component move, key component recovery move, pressure move	0, 0, 0, 0, 1, 0, 0, 0, 0
Simple column 3: preheat temperature move, pump-around duty move [#] , temperature drop through pump-around, pump-around location move, R/R_{min} move, stripping steam flow rate move ⁺ , key component move, key component recovery move, pressure move	0.3, 0.15, 0.2, 0.15, 0.1, 0.1, 0, 0, 0
Simple column 4: preheat temperature move, pump-around duty move [#] , temperature drop through pump-around, pump-around location move, R/R_{min} move, stripping steam flow rate move ⁺ , key component move, key component recovery move, pressure move	0, 0.25, 0.25, 0.2, 0.15, 0.15, 0, 0, 0
Simple column 5: preheat temperature move, pump-around duty move [#] , temperature drop through pump-around, pump-around location move, R/R_{min} move, stripping steam flow rate move ⁺ , key component move, key component recovery move, pressure move	0, 0.25, 0.25, 0.25, 0.25, 0, 0, 0, 0
Simple column 6: preheat temperature move, pump-around duty move [#] , temperature drop through pump-around, pump-around location move, R/R_{min} move, stripping steam flow rate move ⁺ , key component move, key component recovery move, pressure move	0, 0, 0, 0, 1, 0, 0, 0, 0

#: Pump-around duty is optimised in terms of degree of thermal coupling;

+: Stripping steam flow rate is optimised in terms of partial pressure of hydrocarbon at the feed stage

The multiple-run simulation annealing optimisation-based design framework is applied to optimise this configuration for minimum total annualised cost, starting with the initial design. The simulated annealing parameters implemented in the optimisation are presented in Table 6.7. During the optimisation, product flow rates

of each simple column in the decomposed sequence are constrained not to deviate more than 1% of the initial design and TBP not to deviate more than 5 °C.

Table 6.48 presents the summary of the best design obtained during the optimisation. The results indicate that this novel configuration is superior to other three configurations, in terms of the utility demand and total annualised cost. The hot utility consumption of this novel configuration is 8.54 MW (20%) less than that of the configuration without a prefractionator column, 18.28 MW (35%) less than that of the configuration with a prefractionator column and 14.19 (29%) less than the progressive configuration with optimised product distributions and operating pressures. As costs of other items (column capital cost, stripping steam cost and heat exchanger area cost) are compatible to the other three configurations, the reduction in hot utility demand of this novel configuration contributes to the lowest total annualised cost of all configurations, which is 7.24 MM\$/y, compared with 8.45 MM\$/y, 9.97 MM\$/y and 10.14 MM\$/y of the configuration without a prefractionator column, with a prefractionator column and the progressive configuration (with optimised product distributions and operating pressures), respectively.

Table 6.49 shows the required number of theoretical stages in each section of the prefractionator and atmospheric columns. 74 stages in total are needed in the optimised design. Table 6.50 lists products information of the optimised design, showing that the generated products are similar to those of the other three configurations. The maximum difference between this configuration and the original specifications are for the LN flow rate (16 kmol/h) and the maximum TBP difference (-12 °C of T95) for the HN product.

Table 6.48 Case Study 6.4: Performance summary of optimum design (Novel configuration with a liquid side-draw prefractionator column)

Parameter	Value
Hot utility (MW)	34.12
Cold utility (MW)	42.22
Stripping steam (kmol/h)	1151
Heat exchanger area cost (MM\$/y)	0.23
Column capital cost (MM\$/y)	0.29
Total annualised cost (MM\$/y)	7.24

Table 6.49 Case Study 6.4: Theoretical stage distribution of optimum design* (Novel configuration with a liquid side-draw prefractionator column)

Parameter	Column 1	Column 2	Column 3	Column 4	Column 5	Column 6
Rectifying section	8	16	5	7	5	2
Stripping section	8	-	3	6	4	10
Total number of stages	74					

*: in terms of simple columns in decomposed sequence, and rounded up to integers

Table 6.50 Case Study 6.4: Product slate of optimum design (Novel configuration with a liquid side-draw prefractionator column)

Products	Flow rate kmol/h	TBP (°C, mole%)		
		5%	50%	95%
Light Naphtha (LN)	694	3	72	118
Heavy Naphtha (HN)	497	121	163	208
Light Distillate (LD)	646	187	250	321
Heavy Distillate (HD)	144	286	340	376
Residue (RES)	630	352	463	799

6.4.6 Summary of case study

Four configurations, performing similar separations, are considered and optimised for minimum total annualised cost in this case study. The configurations studied are: the configuration without a prefractionator column, the configuration with a prefractionator column, the progressive configuration (including the case where pressure selection and product distribution are accounted for) and the novel configuration with a liquid side-draw prefractionator column. This section presents the summary and comparisons of the optimised design of these configurations.

Figures 6.12 and 6.13 present comparisons of utility demand and total annualised cost of the four configurations. It can be seen that the novel configuration with a liquid side-draw prefractionator column shows the best performance in terms of energy efficiency. The conventional configuration without a prefractionator column ranks second with respect to utility demand and total annualised cost. This configuration has been employed almost exclusively in refining industry for years. The results obtained in this case study indicate that there is significant potential to improve the widely established conventional atmospheric configuration in refining industry. Another observation from the comparisons is that the progressive

configuration does not show significant advantages in this case study. Moreover, it can be concluded that the optimisation of pressure and product distributions in the progressive configuration considerably improves energy efficiency of the configuration. Note that, as capital cost of distillation columns is somehow underestimated in this case study, the total annualised cost trend found in this case study may not always apply if higher capital cost is assumed.

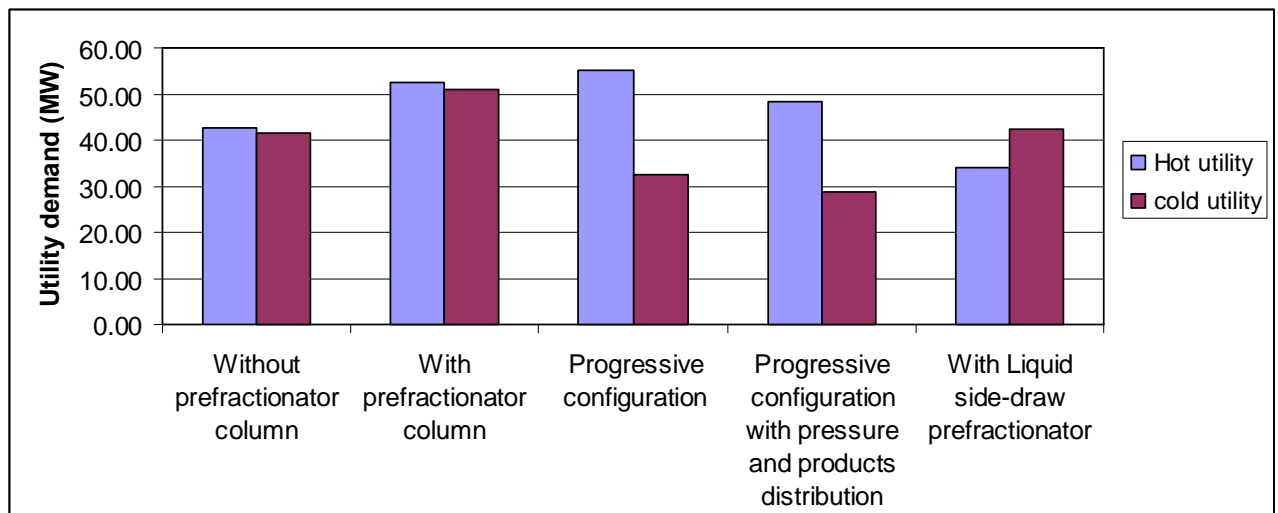


Figure 6.12 Case Study 6.4: Comparisons of the utility demand of various configurations

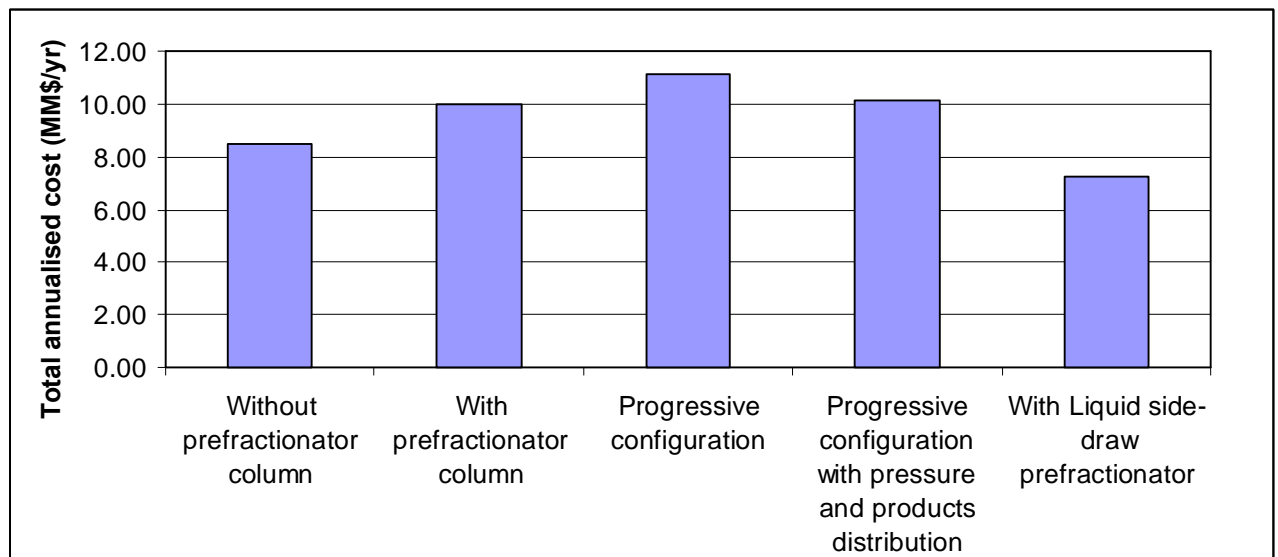


Figure 6.13 Case Study 6.4: Comparisons of the total annualised cost of various configurations

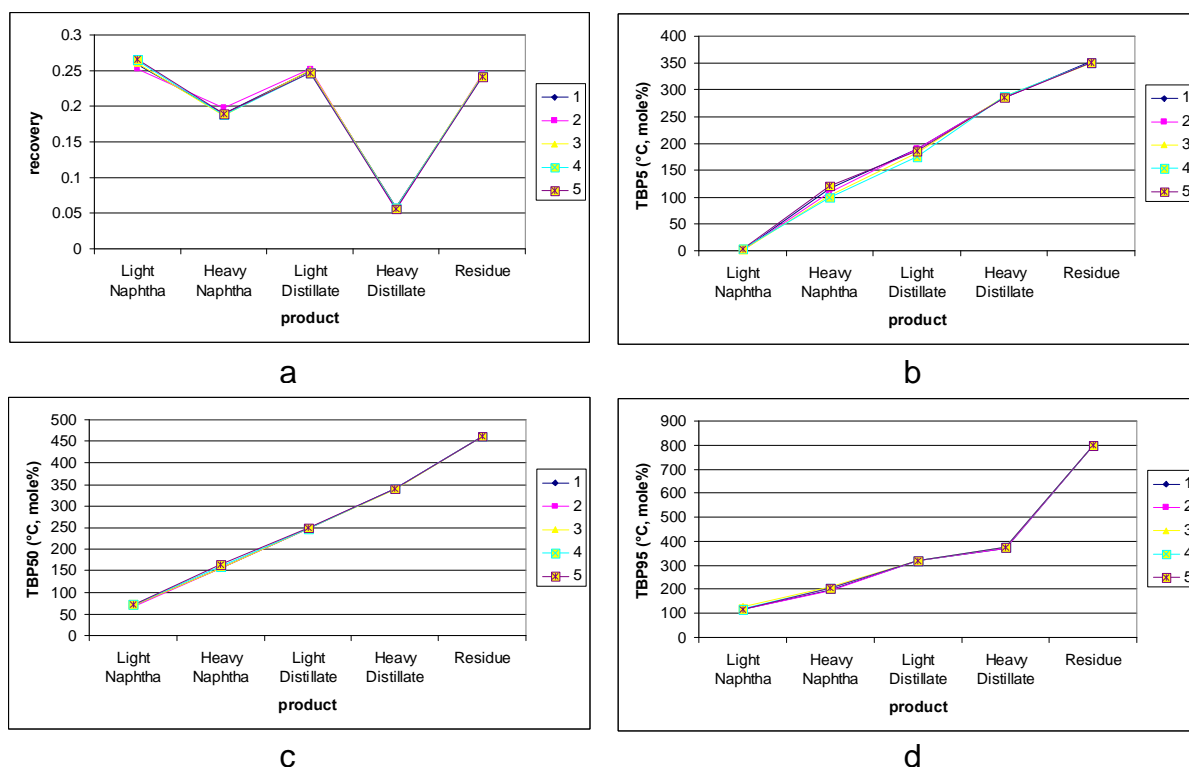


Figure 6.14 Case Study 6.4: Comparisons of products generated by various configurations

(a) Product recoveries with respect to crude feed; (b) T5 of products; (c) T50 of products; (d) T95 of products; 1: The configuration without a prefractionator column, 2: The configuration with a prefractionator column, 3: The progressive configuration with fixed product distributions and operating pressures, 4: The progressive configuration with optimum product distributions and operating pressures, 5: The novel configuration with a liquid side-draw prefractionator column

Figure 6.14 presents the comparisons of products generated by each configuration, including product recoveries with respect to the crude feed and T5, T50 and T95 of each product as an indication of product quality. Shown by Figure 6.14a, all configurations produce similar amounts of products. Moreover, proven by the closeness of the points in Figure 6.14 b . d, product qualities stay the same in each configuration. In conclusion, the comparisons above have been carried out above on an equitable basis.

The results of this case study show different trend from what has been published or observed in industry. For example, the configuration with a prefractionator column consumes more energy than that without a prefractionator column and the progressive configuration does not show significant advantages, if compared with

other configurations. The differences in the trend come from several reasons: the prefractionator column is operated differently in this case study, compared with industry usage (see Section 6.4.3 for more detailed discussion); the original progressive configuration in the patent is designed for different crude oil feed and product specifications, and may not suit the crude oil feed and product specifications required in this case. Note that if the crude oil feed or the product specifications are changed, different results may come and different trend may be observed. However, the results presented have demonstrated the relative merit of the various configurations and provide different ideas from what normally observed in the industry or from other sources, when carrying out configuration selections. Moreover, the outstanding performance of the novel configuration motivates further research of this configuration and sequencing study of crude oil distillation systems.

6.5 Summary

This chapter presents several case studies to illustrate the application of the proposed design methodology for grassroots and retrofit design. Reliable models are used for distillation and the heat recovery system. Product properties are checked and constrained during the optimisation procedure. Moreover, more degrees of freedom are considered in optimising the overall system, compared to previous work. The range of design issues addressed, the constraints imposed and the approach to product specification all allow this approach to be readily applied to industrial cases for the first time.

Case Study 6.1 shows that the previous assumption of constant heat capacities in modelling and analysis of heat integration could exaggerate the energy savings in a retrofit. It can also be concluded from this case that the optimisation with unconstrained products compromises the separation performance when energy saving is the goal. These deficiencies may lead to a less reliable final design. Using more reliable models and including product constraints, an 18% reduction in energy demand is achieved, compared with the inflated 31% saving predicted by the approach with single segment stream data and unconstrained products.

Maximisation of the net profit is covered in Case Study 6.2, in which the same existing atmospheric column and preheat train as in Case Study 6.1 is studied again. With a systematic exploitation of product flow rates by varying key components and recoveries in simplified distillation models, the value of products can be dramatically increased. The operating conditions and associated HEN are optimised as well. During the optimisation, product property constraints and practical constraints such as hydraulic limits and maximum number of modifications to the existing preheat train, *etc.*, are applied to make sure that the desired separation is achieved. The net profit of the existing unit is increased by 34.8 MM\$/y (7%) with a relatively low capital investment.

In Case Study 6.3, the proposed approach is applied to a more complex retrofit case, including atmospheric and vacuum columns and a shared heat exchanger network. The trade-off between heat recovery and separation is explored, facilitated by the simplified distillation model proposed in Chapter 3, which is able to account for the effect of pump-around location on the separation performance. The energy reduction achieved is 15% of the base case demand.

In addition to the retrofit applications, grassroots applications are also shown in this chapter. Case Study 6.4 presents grassroots design of heat-integrated crude oil distillation columns, which achieve similar separations. Four configurations are optimised and compared. The results of the optimised design of each configuration are presented, including energy demand, distillation columns required, optimum operating conditions and the information of products generated. Various calculations may be drawn from the comparison of the different configurations: the proposed novel configuration with a liquid-side-draw prefractionator column is a promising configuration; the industrially established configuration without a prefractionator column has considerable energy saving potential; product distributions and operating pressures are important degrees of freedom and the optimisation of these variables could significantly improve the energy efficiency of the system.

This chapter has conclusively shown that the proposed approach is applicable to both grassroots and retrofit design of heat-integrated crude oil distillation systems. It is capable of designing reliable and industrially applicable crude oil distillation systems for particular objectives.

Although the proposed approach is developed mainly for crude oil distillation systems, the approach is valid for general heat-integrated distillation systems. It can be modified and extended to other distillation processes, such as naphtha fractionation, separation of catalytic cracking and hydrocracking reactor products, coker fractionators, *etc.* This approach may also be modified for sequencing studies of crude oil distillation systems.

CHAPTER 7 CONCLUSIONS AND FUTURE WORK

7.1 Conclusions

In this thesis, an industrially applicable design methodology for heat-integrated crude oil distillation systems (i.e. crude oil distillation columns and the associated preheat train), has been presented. In this design approach, relevant design issues are considered more realistically than have previously been possible, more accurate models of the system components are leading to more reliable and industrially applicable design solutions.

Refining product specifications and the effect of pump-around location on the separation performance are included in the simplified distillation column models for the first time. Two heat exchanger network design methodologies have been extended to account for temperature-dependent thermal properties of the process streams in preheat trains. The proposed design methodology of the overall heat-integrated crude oil distillation system is optimisation-based. The product properties are constrained during the optimisation. Moreover, product slate and product distributions can be explored systematically for a certain design objective (maximum overall profit or minimum total annualised cost). Operating pressures of distillation columns can be considered as degrees of freedom, to improve the energy efficiency of the overall system.

The main contributions of the work presented in this thesis are summarised below:

7.1.1 Simplified modelling of crude oil distillation columns

Simplified models, based on the Fenske-Underwood-Gilliland method and the decomposition approach proposed by Liebmann (1996), were developed in the work of Suphanit (1999), Gadalla *et al.* (2003a) and Rastogi (2006) for grassroots and retrofit design of atmospheric and vacuum columns. Compared with relatively more accurate rigorous models, simplified models have the advantages in calculation

speed and robustness in terms of convergence. These features are particularly valuable in a systematic design approach, in which many degrees of freedom are manipulated and exploited.

However, existing simplified models does not include refining product specifications in terms of flow rates and boiling temperature points in a systematic way. In this thesis, a new approach is proposed to allow refining product specifications to be met in simplified models. Instead of setting up a rigorous simulation and selecting key components by trial and error, as in the previous approach (Gadalla *et al.*, 2002a), the proposed model identifies the appropriate key components and associated recoveries systematically for generating the desired products that are specified in terms of flow rate and three true boiling temperature points. The developed method is applicable to a simple column and a sequence of simple columns that is decomposed from complex crude oil distillation columns. Two illustrative examples have been provided, showing that the developed simplified distillation models are capable of identifying key components and recoveries efficiently. Comparisons between the results of the simplified simulation and of a rigorous simulation validate the simplified models. Facilitated by the new approach, the simplified distillation models can now be applied to refining industry for the design and analysis of the crude oil distillation columns with certain separation requirements. The applicability of simplified distillation columns is significantly enhanced. The extended models also facilitate the study of different configurations of crude oil distillation columns achieving similar separations.

Pump-around locations have a significant impact on the performance of atmospheric distillation columns. If a pump-around of fixed duty is moved down the column, the draw temperature of the pump-around stream increases, which in turn increases the heat recovery potential; however, the internal reflux is reduced on the stage above the draw, so less separation takes place in the column. This trade-off implies that pump-around locations should be considered in the modelling and optimisation of atmospheric distillation systems. The existing simplified models of the atmospheric column (Rastogi, 2006) are extended and modified to account for the effect of pump-around location on separation performance. The new models are examined in an illustrative example, which shows that the location of pump-around is an important degree of freedom.

No simplified models have been published for the industrially-relevant atmospheric column configuration where the pump-around is located above the top side-stripper. In this work, the simplified models are extended to allow modelling of this configuration. The new models thus allow the number of pump-arounds installed on the atmospheric column and their location to be comprehensively considered with respect to potential for heat recovery potential and separation performance.

7.1.2 Heat exchanger network design for process streams with temperature-dependent thermal properties

The thermal properties (e.g. heat capacity) of a crude oil and other process streams in a preheat train may vary considerably, due to the large temperature range during the heating and cooling and the large number of components involved in the crude oil and fractions. Assuming constant thermal properties with temperature may introduce significant inaccuracies in the design and analysis of the preheat train. No researchers have considered this issue and no methods are available in open literature for designing heat exchanger networks (HENs) for process streams with varying thermal properties. In this work, two heat exchanger network (HEN) design methods are developed for process streams with temperature-dependent heat capacities.

The modelling of HENs for systems of streams with non-constant heat capacities is discussed first. A multi-segment formulation represents the streams. The advantage of this formulation is that the correlation between thermal property and temperature is not needed. The non-linear behaviour of the thermal property is modelled as a set of piecewise linear segments, each representing the stream over a range of temperatures. The multi-segment representation of the varying thermal property is simple and easy to implement. Models for each unit within the HEN (i.e. heat exchangers, utility heat exchangers, stream splitters and mixers) and the interconnections between the units are developed. A node-based representation, capable of representing complex HEN structure (including stream splitting and mixing, utility exchangers located anywhere in the HEN, any number of exchangers

on a given stream or branch, *etc.*), is used to model the interconnections between the units.

An optimisation-based design approach applying simulated annealing algorithm is developed for HEN design of process streams with varying thermal properties. This method modifies and extends the work of Rodriguez (2005). A novel feasibility solver is developed to transform infeasible designs that violate minimum temperature approach constraints and stream enthalpy balance constraints, to feasible designs during the optimisation. The proposed HEN design methodology is applicable to both grassroots design and retrofit design. Practical constraints, such as network topology constraints and a maximum number of modifications to the existing configuration in retrofit design, are considered to ensure practically applicable design solutions. The proposed design methodology is demonstrated by application to an existing preheat train. The results show that the heat recovery of the existing HEN is increased significantly (28% reduction in hot utility requirement) with limited capital investment. Comparisons of the solution attained from the approaches with and without a feasibility recovering (the infeasible designs are transformed into feasible design in recovering the feasibility) facility indicate that recovering feasibility can smooth the optimisation process and lead to better solutions.

Another approach for HEN design, the network pinch approach (Asante and Zhu, 1996), which is a promising retrofit design methodology of great industrial applicability, is modified and extended to design HENs for process streams with temperature-dependent thermal properties. In the process of pinching the existing HEN (pinching the existing network is identifying the bottleneck of existing network topology), heat loads of exchangers are varied, together with stream split fractions, which are not considered in the previous approach. Moreover, in the diagnosis stage, cost optimisations are carried out directly, rather than sequentially maximising heat recovery and then optimising the cost. This merging of two stages is helpful to avoid missing designs with high energy savings and low capital investment. An example illustrates the application of the new network pinch approach.

7.1.3 Design methodology of heat-integrated crude oil distillation system and the applications

Crude oil distillation columns interact strongly with the associated heat recovery system. Capturing the interactions is of great importance in the design and analysis of the overall system. In this work, multi-segment stream data are implemented in the modelling of the heat recovery system to improve accuracy. A sequential modular strategy, which is modified and extended from the work of Rastogi (2006), is applied in the modelling of the heat exchanger network. Compared to equation oriented strategies, convergence problems and large numbers of iterations can be avoided. In the work of Rastogi (2006), penalties are simply applied to streams not achieving energy balance. In this work, a new feasibility solver is implemented to overcome the infeasibility of a proposed HEN design. The feasibility solver helps the optimiser to explore the potential of the proposed HEN design before adding penalties. The interactions between the crude oil distillation columns and the associated heat recovery system can be explored more fully if feasibility constraints are enforced, rather than applying penalties during the optimisation.

Facilitated by the new simplified models of crude oil distillation columns, design of HENs for streams with temperature-dependent thermal properties, and the modelling of the interactions between distillation columns and HENs, an optimisation-based methodology is proposed in this thesis for the design of heat-integrated crude oil distillation systems. The design approach, which extends the work of Rastogi (2006), is based on optimisation using the multiple run simulated annealing algorithm and is capable of optimising both structural options and operating conditions in the system. Compared with previous studies (Liebmann, 1996; Suphanit, 1999; Gadalla *et al.*, 2003b; Rastogi, 2006), the advantages of the new design approach are: product properties are checked and constrained during the optimisation so that the separation is not compromised to achieve energy savings; product slate and product distributions in the distillation columns can be exploited systematically; operating pressures of distillation columns can be optimised. The consideration of product property constraints and exploration of product slate facilitate the maximisation of net profit while maintaining product qualities. Varying operating pressures in the optimisation can further increase heat recovery opportunities since temperature is a function of operating pressure. In addition, different configurations of crude oil

distillation columns can be studied and compared as a result of considering product property specifications and systematic exploitation of product distributions where distributed separations take place in the new design approach.

A novel configuration with an atmospheric distillation column and a liquid side-draw prefractionator column for crude oil fractions is proposed. The performance of the novel configuration is shown to be promising by comparison with other industrially established configurations of crude oil fractions in a case study.

Case studies illustrate the application of this new design methodology. For an existing atmospheric column, 18% energy saving is suggested by the new approach, rather than the overestimated 31% energy saving predicted when product properties are not constrained and thermal properties are assumed constant with temperature in the HEN design. By applying the new approach, the net profit can be increased by 34.7 MM\$/y (7%) due to a systematic exploitation of product slate (e.g. flow rate of products). For a specified separation of a crude oil, different distillation configurations are optimised and compared. The results indicate various important conclusions, which could be used to demonstrate the relative merit of the various configurations. The proposed novel configuration, with an atmospheric distillation column and a liquid side-draw prefractionator column, shows a promising performance, which motivates further research.

The developed approach for the design of heat-integrated crude oil distillation systems makes a step change in the capability of systematic design approaches. Compared with previous research, more industrially relevant issues are considered which leads to the applicability to a wider range of industrial problems. This approach has been applied in refining industry, and great improvement of the system performance has shown in the design solutions.

7.2 Future work

The following issues merit further research:

1. As discussed in Section 3.2, the method of systematically selecting key components and recoveries in simplified models with product specifications requires a sensible initial guess of key components and recoveries. Due to the non-linearity of the problem, solutions cannot be guaranteed if the initial guess is not provided properly. A development of a sensible initialisation strategy is likely to be helpful in increasing the robustness of the proposed method in singular situations.
2. The simplified model with product specifications developed in Section 3.2 only addresses specifications of true boiling point temperatures. The proposed model can be extended and applied to allow product specifications of bulk physical properties, such as Specific Gravity, Reid Vapour Pressure, Viscosity, Sulphur Content, *etc.*
3. As simulated annealing is employed as the optimisation algorithm of the proposed design methodology, the calculation time is considerably long. Most of the time is consumed on the simulation of distillation columns. There is a trade-off between the accuracy of the model and the time required. More work may reduce the calculation time of the simplified models, or reduce the number of unnecessary trials carried out during optimisation procedure. Moreover, because of the stochastic characteristic of simulated annealing optimisation, sensitivity analysis is needed after the optimisation to check if the variations of design variables contribute to improve the system performance.
4. The optimisation framework and models presented in this work can be extended and modified to a systematic study of various sequences of crude oil distillation columns (Case Study 6.4 optimised three industrially established configurations and a novel configuration proposed in this work and compared the best design from each of the configuration) for a specified product slate.
5. Crude oil distillation systems usually process different types of crude oils or blends of crude oils, depending on availability and market price. It is very important that a given crude oil distillation system can process different types of crude oils, and can do so with low operating costs. The approach presented in this work can be extended to address the flexibility of the design of crude oil distillation systems with respect to crude oil stock.

6. The optimisation framework and models presented in this work can be modified and extended to apply to other heat-integrated refinery distillation systems, such as separation systems downstream of the fluidised catalytic cracking (FCC) and delayed coker.

REFERENCES

Al-Muslim, H. and I. Dincer, Thermodynamic analysis of crude oil distillation systems, *Int. J. Energy Res.*, 29, 637-655 (2005)

Ahmad, S., B. Linnhoff and R. Smith, Cost optimum heat exchanger networks. 2: Targets and design for detailed capital cost models, *Comp. Chem. Eng.*, 14 (7), 751-767 (1990)

Arora, J. S., *Introduction to Optimum Design*, Academic Press, 2nd edition (2004)

Asante, N. D. K. and X. X. Zhu, An automated approach for heat exchanger network retrofit featuring minimal topology modifications, *Comp. Chem. Eng.*, 20, S7-S12 (1996)

Athier, G., P. Floquet, L. Pibouleau, and S. Domenech, Synthesis of heat-exchanger network by simulated annealing and NLP procedures, *AIChE J.*, 43(11), 3007-3020 (1997)

Bagajewicz, M., and Ji, S., Rigorous procedure for the design of conventional atmospheric crude fractionation units. Part I: Targeting, *Ind. Eng. Chem. Res.*, 40(2), 617-626 (2001a)

Bagajewicz, M., and Soto, J., Rigorous procedure for the design of conventional atmospheric crude fractionation units. Part II: Heat exchanger network, *Ind. Eng. Chem. Res.*, 40(2), 627-634 (2001b)

Biegler, L. T., I. E. Grossmann, and A. W. Westerberg, *Systematic methods of Chemical Process Design*, Prentice Hall Inc., USA (1997)

Biegler, L. T. and I. E. Grossmann, Retrospective on optimization, *Comp. Chem. Eng.*, 28(9), 1169-1192 (2004)

Björk, K. M., and R. Nordman, Solving large-scale retrofit heat exchanger network synthesis problems with mathematical optimization methods, *Chemical Engineering and Processing*, 44, 869-876 (2005)

Björk, K. M., and T. Westerlund, Global optimisation of heat exchanger network synthesis problems with and without the isothermal mixing assumption, *Comp. Chem. Eng.*, 26(11), 1581-1593 (2002)

Carlberg, N. A., and A. W. Westerberg, Temperature-heat diagram for complex columns. 3. Underwood's method for the Petlyuk configuration, *Ind. Eng. Chem. Res.*, 28, 1386 (1989)

Cerda, J., and A. W. Westerberg, Shortcut methods for complex distillation columns. 1. Minimum reflux, *Ind. Eng. Chem. Proc. Des. Dev.*, 20, 546 (1981)

Cerda, J., A. W. Westerberg, D. Mason, and B. Linnhoff, Minimum utility usage in heat exchanger network synthesis - a transportation problem, *Chem. Eng. Sci.*, 38(3), 373-387 (1983)

Cerda, J., and A. W. Westerberg, Synthesizing heat exchanger networks having restricted stream/stream matches using transportation problem formulations, *Chem. Eng. Sci.*, 38(10), 1723-1740 (1983)

Choong, K.L., Optimisation of batch and semi-batch crystallisation processes, PhD Thesis, UMIST, Manchester, UK(2002)

Chou, C. J., C. C. Liu, and Y. T. Hsiao, A multiobjective optimisation approach to loading balance and grounding planning in three-phase four-wire distribution systems, *Electric Power Systems Research*, 31, 163-174 (1994)

COLOM software, Version 2.1, Centre for Process Integration, The University of Manchester, UK

Dennis, J. E., and R. B. Schnabel, *Numerical Methods for Unconstrained Optimization and Nonlinear Equations*, Prentice-Hall Inc., New Jersey, USA (1983)

Devos, A., Bezons et al, Process for distillation of petroleum by progressive separation, United States Patent, 4,664,785 (1987, May 12)

Demian, A. C., Integrated Design and Simulation of Chemical Processes, Elsevier: Amsterdam (2003)

Dolan, W. B., P. T. Cummings, and M. D. Le Van, Process optimization via simulated annealing: application to network design, *AIChE J.*, 35, 725-736 (1989)

Dolan, W. B., P. T. Cummings, and M. D. Le Van, Algorithmic efficiency of simulated annealing for heat exchanger network design, *Comp. Chem. Eng.*, 14(10), 1039-1050 (1990)

Dong, H. G., C. Y. Lin, and C. T. Chang, Simultaneous optimisation strategy for synthesizing heat exchanger network with multi-stream mixers, *Chem. Eng. Res. Des.*, 86, 299-309 (2008)

Eduljee, H. E., *Hydrocarbon Processing*, 54(10), 120 (1975)

Erbar, J. H., and R. N. Maddox, *Petrol Refiner*, 40(5), 183 (1961)

Fenske, M. R., *Ind. Eng. Chem.*, 24, 482-485 (1932)

Floquet, P., L. Pibouleau, and S. Domenech, Separation sequence synthesis: how to use simulated annealing procedure? *Comp. Chem. Eng.*, 18(11/12), 1141-1148 (1994)

Floudas, C. A., A. R. Ciric, and I. E. Grossmann, Automatic synthesis of optimum heat exchanger network configurations, *AIChE J.*, 32(2), 276-290 (1986)

Fraga, E. S., and T. R. S. Matias, Synthesis and optimization of a nonideal distillation system using a parallel genetic algorithm, *Comp. Chem. Eng.*, 20, S79-S84 (1996)

Furman, K. C., and N. V. Sahinidis, A critical review and annotated bibliography for heat exchanger network synthesis in the 20th century, ., *Ind. Eng. Chem. Res.*, 41, 2335-2370 (2002)

Gadalla, M. A., Retrofit of heat-integrated crude oil distillation systems, PhD Thesis, UMIST, Manchester, UK (2002)

Gadalla, M., M. Jobson, and R. Smith, Shortcut models for retrofit design of distillation columns, *Trans IChemE*, September 81(A), 971-986 (2003a)

Gadalla, M., M. Jobson, and R. Smith, Optimization of existing heat-integrated refinery distillation systems, *Trans IChemE*, January, 81(A), 147-152 (2003b)

Gadalla, M., M. Jobson, and R. Smith, Increase capacity and decrease energy for existing refinery distillation columns, *Chemical Engineering Progress*, April, 44-50 (2003c)

Gadalla, M., M. Jobson, R. Smith, and P. Boucot, Design of refinery distillation processes using key component recoveries rather than conventional specification methods, submitted once to *Chem. Eng. Res. Des.* in November (2002a), under revision

Gill, P. E., W. Murray, and J. SIAM, *Numer. Anal.*, 15(5) 977-992 (1978)

Gilliland, E. R., Multi-component rectification. Estimation of the number of theoretical plates as a function of the reflux ratio, *Ind. Eng. Chem.*, 32, 1220 (1940)

Glinos, K. N., and M. F. Malone, Design of sidestream columns, *Ind. Eng. Chem. Process Des. Dev.*, 24, 822-828 (1985)

Grossmann, I. E., and Z. Kravanja, Mixed-integer nonlinear programming techniques for process systems engineering, *Comp. Chem. Eng.*, 19(Suppl.), S189-S204 (1995)

Gutierrez-Antonio, C., and A. Jimenez-Gutierrez, Design of side-stream azeotropic distillation columns, *Chem. Eng. Res. Des.*, 85(10), 1384-1389 (2007)

Guthrie, K. M., W. R. Grace & Co., Data and techniques for preliminary capital cost estimating, *Chem. Eng.*, 114-142 (1969)

HYSYS Process Simulation, Version 2004.2, Aspen Technology Inc. USA

Isafiade, A. J., and D. M. Fraser, Interval-based MINLP superstructure synthesis of heat exchange networks, *Chem. Eng. Res. Des.*, 86, 245-257 (2008)

Jain, S., Synthesis of batch distillation processes, PhD Thesis, UMIST, Manchester, UK (2005)

Ji, S., and Bagajewicz, M., Design of crude fractionation with preflashing or prefractionation: energy targeting, *Ind. Eng. Chem. Res.*, 41(2), 3003-3011(2002a)

Ji, S., and Bagajewicz, M., Design of crude distillation plants with vacuum units. I. Targeting, *Ind. Eng. Chem. Res.*, 41(24), 6094-6099 (2002b)

Ji, S., and Bagajewicz, M., Design of crude distillation plants with vacuum Units. II. Heat exchanger network design, *Ind. Eng. Chem. Res.*, 41(24), 6100-6106 (2002c)

Jones, D. S. J., *Elements of Petroleum Processing*, John Wiley & Sons Inc, West Sussex, England, 1st Edition (1995)

Jung, W. S., and N. Z. Cho, Determination of design alternatives and performance criteria for safety systems in a nuclear power plant via simulated annealing, *Reliability Engineering and System Safety*, 41, 71-94 (1993)

Kirkbride, C. G., *Petroleum Refiner*, 23(9), 87-102 (1944)

King, C. J., *Separation Processes*, McGraw-Hill Inc., New York, 2nd edition, Chapter 9 (1980)

Kumar, V., A. Sharma, I. R. Chowdhury, S. Ganguly, D. N. Saraf, A crude distillation unit model suitable for online applications, *Fuel Processing Technology*, 73, 1-21 (2001)

Inamdar, S.V., S .K. Gupta, and D. N. Saraf, Multi-objective optimisation of an industrial crude unit using the elitist non-dominated sorting Genetic Algorithm, *Trans IChemE*, 82(A5), 611-623 (2004)

Lang, P., G. Szalmas, G. Chikany, and S. Kemeny, Modelling of a crude distillation column, *Comp. Chem. Eng.*, 15(2), 133-139 (1991)

Lewin. D. R., H. Wang and O. Shalev, A generalized method for HEN synthesis using stochastic optimization --- I. General framework and MER optimal synthesis, *Comp. Chem. Eng.*, 22(10), 1503-1513 (1998a)

Lewin. D. R., H. Wang and O. Shalev, A generalized method for HEN synthesis using stochastic optimization --- II. The synthesis of cost-optimal networks, *Comp. Chem. Eng.*, 22(10), 1387-1405 (1998b)

Liebmann, K., Integrated crude oil distillation design, PhD Thesis, UMIST, Manchester, UK (1996)

Liebmann, K., V. R. Dhole, and M. Jobson, Integrated design of a conventional crude oil distillation tower using pinch analysis, *Trans IChemE*, March, 76(A), 335-347 (1998)

Lin, B., and D.C. Miller, Solving heat exchanger network synthesis problems with Tabu Search, *Comp. Chem. Eng.*, 28 (8), 1451-1464 (2004)

Linke, P., Reaction and separation process integration, PhD Thesis, UMIST, Manchester, UK (2001)

Linnhoff, B., and E. Hindmarsh, The pinch design method for heat exchanger network, *Chem. Eng. Sci.*, 38(5), 745-764 (1983)

- Liu, Z. Y., Retrofit design for debottlenecking distillation processes, PhD Thesis, UMIST, Manchester, UK (2000)
- Makwana, Y., and U. V. Shenoy, A new algorithm for continuous energy targeting and topology trap determination of heat exchanger networks, *Technical Report*, Indian Institute of Technology, Bombay, India (1993)
- Marquardt, D., An algorithm for least-squares estimation of nonlinear parameters, *SIAM Journal on Applied Mathematics*, 11, 431-331 (1963)
- Metropolis, N., A. W. Rosenbluth, M. N. Rosenbluth, A. H. Teller, and E. Teller, Equation of state calculations by fast computing machines, *Journal of Chemical Physics*, 21(6), 1087-1091 (1953)
- Michalewicz, Z., *Genetic algorithm + data structure = evolution program*, 2nd ed., Berlin: Springer-Verlag. p. 340 (1994)
- Molokanov, Y. K., T. P. Korablina, N. I. Mazurina, and G. A. Nikiforov, *Int. Chem. Eng.*, 12(2), 209 (1972)
- Morton, W., Optimization of a heat exchanger network superstructure using nonlinear programming, *Proc. Instn. Mech. Engrs.*, 216, 89-104 (2002)
- Nelson, W. L., *Petroleum Refinery Engineering*, McGraw-Hill Book Company, 4th Edition, New York, USA (1958)
- Nielsen, J. S., V. Briones, and A. C. Kokossis, An integrated framework for the optimal design of heat recovery systems, Paper presented in *AIChE Annual Meeting*, San Francisco, November (1994)
- Nocedal, J., and S. J. Wright, *Numerical Optimisization*, 2nd edition, Springer, New York (2006)
- Numeric Algorithm Group, *NAG FORTRAN library, Routine E04UCF*, Oxford, UK (1990)
- Papoulias, S. A., and I.E. Grossmann, A structural optimisation approaches in process synthesis . I. *Comp. Chem. Eng.*, 7(6), 695-734 (1983)
- Petlyuk, F. B., V. M. Platonov, and D. M. Slavinskii, Thermodynamically optimal method for separating multi-component mixtures, *Int. Chem. Eng.*, 5(3), 555 (1965)
- Press, W. H., B. P. Flannery, S. A. Teukolsky and W. T. Vetterling, *Numerical Recipes in C: The Art of Scientific Computing*, 3rd edition, Cambridge University Press, Cambridge (2007)
- Ravagnani, M. A. S. S., A. P. Silva, A. L. Andrade, Detailed equipment design in heat exchanger networks synthesis and optimisation, *Applied Thermal Engineering*, 23, 141-151 (2003)

- Ravagnani, M. A. S. S., A. P. Silva, P. A. Arroyo and A. A. Constantino, Heat exchanger network synthesis and optimisation using genetic algorithm, *Applied Thermal Engineering*, 25, 1003-1017 (2005)
- Rastogi, V., Heat integration crude oil distillation system design, PhD Thesis, The University of Manchester, Manchester, UK (2006)
- Rhodes, A. K., Environmentally advanced refinery nears start-up in Germany, *Oil & Gas Journal*, 95(11), 1997
- Robert, E. *Petroleum Refining Process Economics*, Maples, 2nd edition, Pennwell Corp., (2000)
- Rooks, R. E., M. F. Malone and M. F. Doherty, A geometric design method for side-stream distillation columns, *Ind. Eng. Chem. Res.*, 35, 3653-3664 (1997)
- Rodriguez, C. A., Fouling mitigation strategies for heat exchanger networks, PhD Thesis, The University of Manchester, UK (2005)
- Rusche, F. A., Gilliland plot revisited, *Hydrocarbon Processing*, February, 79-80 (1999)
- Seader, J. D., and E. J. Henley, *Separation Process Principles*, John Wiley & Sons, Inc., New York (1998)
- Sharma, R., A. Jindal, D. Mandawala, and S. K. Jana, Design/retrofit targets of pump-around refluxes for better energy integration of a crude distillation column, *Ind. Eng. Chem. Res.*, 38, 2411-2417 (1999)
- Shell, *The Petroleum Handbook*, 6th edition, Elsevier: Amsterdam (1983)
- Shenoy, U. V., *Heat Exchanger Network Synthesis*, Gulf Publishing Company, Houston, Texas (1995)
- Smith, R., *Chemical process design and integration*, John Wiley & Sons Ltd., 2nd Edition, West Sussex, England (2005)
- Sobocan, G., and P. Glavic, A simple method for systematic synthesis of thermally integrated distillation sequences, *Chemical Engineering Journal*, 89, 155-172 (2002)
- Strangio, V. A., and R. E. Treybal, Reflux-stages relations for distillation, *Ind. Eng. Chem., Process Des. Develop.*, 13, 279-285 (1974)
- Stupin, W. J., and F. J. Lockhart, Thermally coupled distillation - a case history, *Chemical Engineering Progress*, 68(10), 71-72 (1972)
- Suphanit, B., Design of complex distillation system, PhD Thesis, UMIST, Manchester, UK (1999)
- Triantafyllou, C., and R. Smith, The design and optimisation of fully thermally coupled distillation columns, *Trans IChemE*, 70 (A2), 118-132 (1992)

- Trosset, M.W., *What is Simulated Annealing?* Optimization and Engineering, 2, 201-213 (2001)
- Underwood, V., Fractional distillation of multi-component mixtures, *Chemical Engineering Progress*, 44, 603 (1948)
- Van Laarhoven, P.J.M. and Aarts, E.H.L., *Simulated Annealing, Theory and Applications*, D. Reidel Publishing Co. (1987)
- Wang K., Qian, Y., Yan, Y. and Yao, P., Synthesis and optimization of heat integrated distillation systems using an improved genetic algorithm, *Comp. Chem. Eng.*, 23, 125-136 (1998)
- Wang, T., *Global optimisation for constrained nonlinear programming, in computer science*, University of Illinois, Urbana, Illinois. p.220 (2001)
- Watkins, R. N., *Petroleum Refinery Distillation*, Gulf Publishing Company, 2nd Edition, Texas, USA (1979)
- Wolberg, J., *Data Analysis Using the Method of Least Squares: Extracting the Most Information from Experiments*, Springer (2005)
- Yee, T. F., I. E. Grossmann, and Z. Kravanja, Simultaneous optimisation models for heat integration . I. Area and energy targeting and modeling of multi-stream exchangers, *Comp. Chem. Eng.*, 14(10), 1151-1164 (1990)
- Yee, T. F., and I. E. Grossmann, A screening and optimisation approach for the retrofit of heat-exchanger networks, *Ind. Eng. Res.*, 30, 146-162 (1991)
- Zhu X. X., Automated synthesis of HENs using block decomposition and heuristic rules, *Comp. Chem. Eng.*, 19(Suppl.), S155-S160 (1995)
- Zhu X. X., B.K. O'Neil, J.R. Roach, and R.M. Wood, A new method for heat exchanger synthesis using area targeting procedures, *Comp. Chem. Eng.*, 19(2), 197-222 (1995a)
- Zhu X. X., B.K. O'Neil, J.R. Roach, and R.M. Wood, Area targeting methods for the direct synthesis of heat exchanger networks with unequal film coefficients. *Comp. Chem. Eng.*, 19(2), 223-239 (1995b)
- Zhu, X.X., B. K. O'Neill, J. R. Roach, and R. M. Wood, A method for automated heat exchanger network synthesis using block decomposition and non-linear optimization, *Trans IChemE*, November, 73(A), 919-930 (1995c)

APPENDIX A: DATA FOR ILLUSTRATIVE EXAMPLE 4.1

Table A.1 Constant stream data of illustrative example 4.1

Stream	Name	Supply temperature	Target temperature	Enthalpy change
		°C	°C	MW
1	Pump-Ar 1	298	268	12.828
2	Bott Cool 1	339	100	50.460
3	Pump-Ar 2	250	200	17.882
4	Bott Cool 2	257	50	5.195
5	Pump-Ar 3	170	150	11.175
6	Bott Cool 3	282	40	20.299
7	Cond Duty 4	100	77	47.865
8	Dist Cool 4	77	40	1.321
9	Bott Cool 4	189	40	6.187
10	Flue gas	1500	800	68.593
11	Feed PreH 1	25	365	154.494
12	Reb Duty 3	271	282	8.783
13	Reb Duty 4	182	189	6.625
14	CW	10	40	71.908

Table A.2 Segmented stream data of illustrative example 4.1

Stream	Name	Supply temperature	Target temperature	Enthalpy change
		°C	°C	MW
1	Pump-Ar 1	298	268	12.828
2	Bott Cool 1	339	299	9.604
		299	259	9.164
		259	219	8.705
		219	179	8.228
		179	139	7.735
		139	100	7.024
3	Pump-Ar 2	250	210	14.416
		210	200	3.467
4	Bott Cool 2	257	217	1.142
		217	177	1.077
		177	137	1.011
		137	97	0.943
		97	57	0.874
		57	50	0.148
5	Pump-Ar 3	170	150	11.175
6	Bott Cool 3	282	242	3.949
		242	202	3.705
		202	162	3.471
		162	122	3.238
		122	82	3.004
		82	42	2.768
		42	40	0.164
7	Cond Duty 4	100	77	47.865
8	Dist Cool 4	77	40	1.321
9	Bott Cool 4	189	149	1.852
		149	109	1.707
		109	69	1.568
		69	40	1.059
10	Flue gas	1500	800	68.593
11	Feed PreH 1	25	65	12.465
		65	105	13.572
		105	145	14.660
		145	166	8.044
		166	185	9.197
		185	225	20.107
		225	265	21.076
		265	305	21.782
		305	345	22.310
		345	365	11.282
12	Reb Duty 3	271	282	8.783
13	Reb Duty 4	182	189	6.625
14	CW	10	40	71.908

Table A.3 Heat exchanger loads data of illustrative example 4.1

Hx no	Heat duty (MW)
1	13.25
2	13.19
3	0.86
4	0.11
5	7.47
6	7.33
7	11.42
8	11.52
9	0.89
10	2.05
11	2.37
12	1.74
13	8.76
14hu	73.54
15cu	3.08
16hu	8.78
17hu	6.63
18cu	1.09
23cu	1.32
24cu	47.87
25cu	4.33
26cu	11.18
27cu	20.19
28cu	32.44

*: hu, cu: hot utility, cold utility exchangers, respectively

APPENDIX B: SIMULATED ANNEALING

B.1 Simulated annealing

Simulated Annealing (SA) algorithm is a generic probabilistic meta-algorithm for the global optimisation problem, namely locating a good approximation to the global optimum of a given function in a large search space. The SA algorithm is typically applied to problems in which gradient-based methods are not effective, such as non-convex, non-differentiable or discontinuous problems.

The SA algorithm was inspired by the annealing in metallurgy. In the annealing process, a metal is melted at high temperature and then left to cool very slowly. In the melted state, the system is characterised by a highly disordered configuration, with the metal atoms distributed randomly. As cooling proceeds, the internal energy of the system decreases and the system becomes more ordered. If the cooling process is carried out slowly enough, so that the system at any time is approximately in thermodynamic equilibrium, the metal freezes into a stable crystalline structure with minimum internal energy. On the other hand, if either cooling is insufficiently slow or the initial temperature of the system is not high enough, the metal forms a glassy meta-stable structure with higher energy than the desirable crystalline state.

The connection between the annealing process and mathematical optimisation was first observed by Kirkpatrick *et al.* (1983), who proposed the application of the SA algorithm in solving a combinatorial problem. They successfully applied the algorithm in optimising the famous travelling sales man problem. Several analogies between the physical annealing process and an optimisation problem were observed. The current state of the thermodynamic system is analogous to the current point in the search space, the internal energy of the system is analogous to the objective function, the undesirable meta-stable glassy states correspond to local optimum and the minimum internal energy crystalline structure is analogous to the global optimum.

The SA algorithm proposed by Kirkpatrick and his co-workers to optimise combinatorial problems is visualised in Figure B.1. The algorithm uses a global

parameter to control the optimisation procedure, which is analogous to the annealing temperature (T_a) in the original annealing process. At the beginning of the optimisation, the annealing temperature is initialised to a proper high value. The process starts with an initial solution, which may be either randomly generated or calculated with some approximate methods or heuristics. A random nearby solution, called move, is generated around the current solution. The objective function of this new solution is calculated and compared with the objective function of the current trial solution. If the new value is lower than the previous one (assuming a minimisation problem), the new trial solution is accepted immediately. Otherwise, it is accepted with a probability given by the Boltzmann factor or by any other suitable acceptance criteria. At each annealing temperature, this process is repeated a number of times, before the annealing temperature is reduced, and the whole cycle is repeated. The algorithm stops when a pre-established termination criterion is met.

The main advantages of the SA algorithm is its ability to avoid being trapped at local optimum by not only accepting moves that improve the objective function (downhill moves) but also by accepting moves that deteriorate the objective function (uphill moves). The probability of accepting an uphill move depends on the difference between the corresponding objective function values and on the annealing temperature. Uphill moves that produce small differences in the objective function are more likely to be accepted than those that produce large differences. Uphill moves have also a higher probability of being accepted at the start of the optimisation, when the annealing temperature is high. At the initial stage, almost every move is accepted and the search behaves as a pure random search. As the optimisation progresses and the annealing temperature reduces, the probability of accepting uphill moves decreases. At the final stage of the optimisation, when the annealing temperature is close to its final value, almost only downhill moves are accepted and the algorithm becomes equivalent to a descent method.

A drawback of the acceptance of uphill moves in the SA algorithm is that the algorithm may actually converge to a worse solution than a previously tried solution. This shortcoming is overcome by modifying the algorithm so that it stores the best solution ever found during the optimisation procedure. This is implemented by tracking the best solution found so far. At the end of the procedure, the stored best solution is reported.

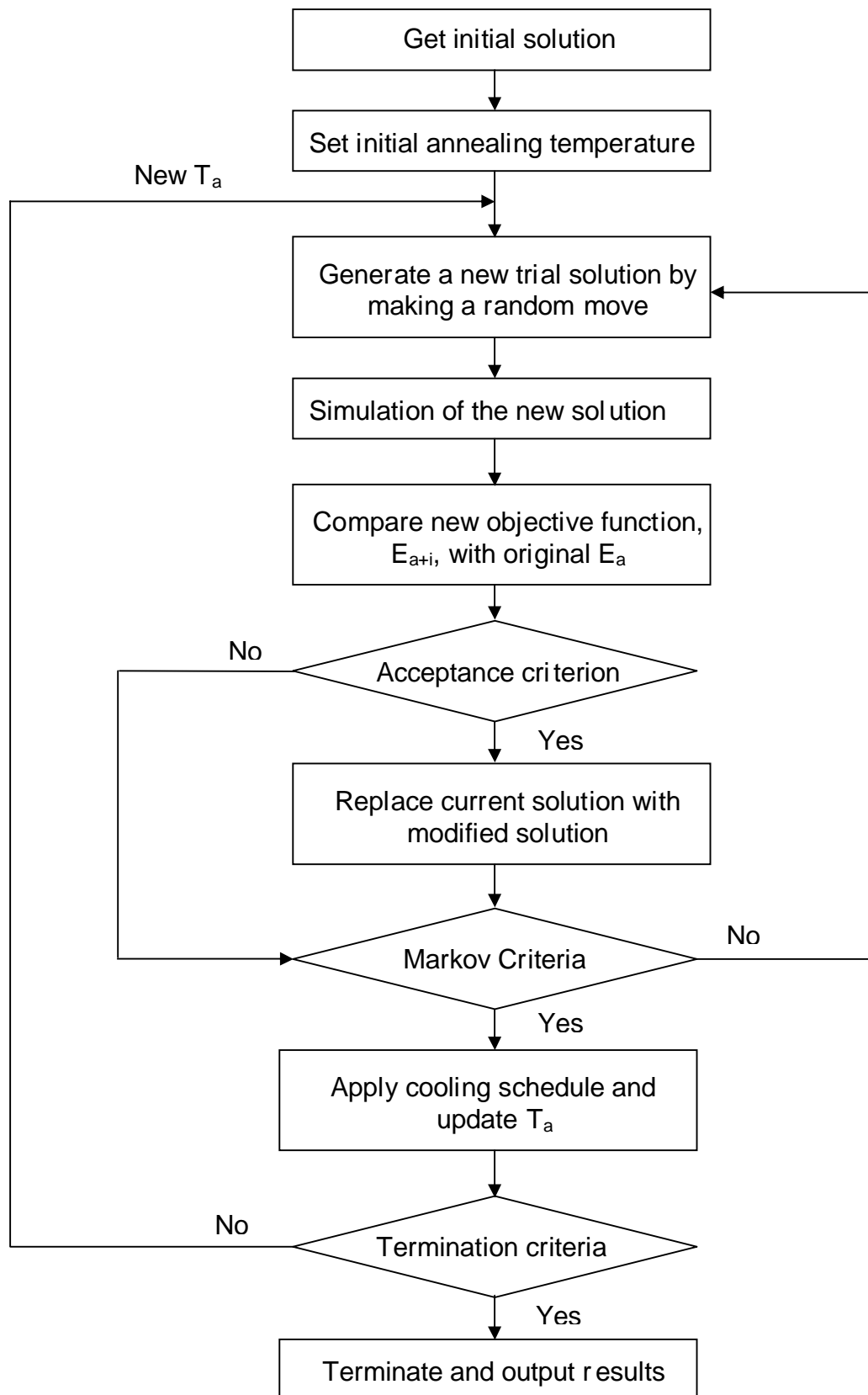


Figure B.1 Flowchart for the simulated annealing algorithm

B.2 Simulated annealing parameters

This section discusses some important parameters of the simulated annealing algorithm except those discussed in Section 4.4.1 and Section 5.3.

Acceptance criterion

The acceptance criterion is used to decide whether a trial solution is accepted or rejected. As already discussed, the most important feature of the SA algorithm is the ability to accept uphill moves, which avoids the method from being stuck in local optimum. A suitable acceptance criterion must be able to accept uphill moves with a large probability at the early stage of optimisation, and progressively decrease this probability as the search progresses.

The Metropolis acceptance criterion (Metropolis *et al.*, 1953) was the one employed by Kirkpatrick *et al.* (1953) when the use of SA as an optimisation strategy was devised. The same criterion is used in the present work. The Metropolis criterion accepts all the moves that improve the objective function. Moves that deteriorate the objective function are accepted with a probability, p , which is a function of the difference between the two corresponding objective functions, f , and the annealing temperature, T_a . The acceptance probability is calculated as:

$$p = \begin{cases} 1 & \text{if } \Delta f \leq 0 \\ \exp\left(-\frac{\Delta f}{T_a}\right) & \text{if } \Delta f > 0 \end{cases} \quad (\text{B.1})$$

where $\Delta f = E_{a+1} - E_a$

Initial annealing temperature

The performance of the SA algorithm is greatly affected by the initial annealing temperature. A too high temperature will unnecessarily increase the time required for the algorithm to converge. On the other hand, a too low temperature will limit the number and magnitude of the uphill moves accepted, thus losing the ability of the algorithm to escape from local optima.

The setting of initial annealing temperature depends on the nature of the problem and the scaling of the objective function. Several approaches have been proposed to

estimate a proper value for this parameter. Van Laarhoven and Aarts (1987) suggested that the initial annealing temperature should be selected so that a certain initial probability of accepting uphill moves is obtained.

Cooling schedule

The cooling schedule is another important factor in the SA algorithm. The reduction of the annealing temperature must be slow enough to avoid being trapped in a local optimum. However, a too slow cooling will unnecessarily increase the computational time.

The cooling schedule employed in the present work is given by Equation B.2 (Van Laarhoven and Aarts, 1987). The speed of cooling is controlled by the cooling parameter θ . The bigger the value is, the faster the cooling process. This parameter takes values between 0 and 1, with a typical value around 0.05. σ_a^k represents the standard deviation of the objective functions of all the trial solutions generated at the same temperature T_a^k . Including this factor in the cooling schedule has the effect of accelerating the cooling when the standard deviation of the objective function is small.

$$T_a^{k+1} = T_a^k \left(1 + \frac{T_a^k \ln(1+\theta)}{3\sigma_a^k} \right) \quad (\text{B.2})$$

Markov chain length

There are two loops in the SA algorithm (Figure B.1): the Markov loop and the annealing temperature loop. The Markov loop is the inner loop and the annealing temperature loop is the outer loop. A sequence of moves are carried out at each annealing temperature, which corresponds to a Markov chain and the number of the moves is known as the Markov chain length.

The SA algorithm only guarantees to converge into a global optimum when an infinite Markov chain is used (Trosset, 2001). Obviously, this is not a practically realisable, and a finite value for this parameter has to be employed. The value of the Markov chain length should be set based on a balance between the quality of the solution and computational time. Too short Markov chain length will lead to an optimisation procedure converging to a local optimum; too long Markov chain length

will increase the probability of find the global optimum however at the expense of the infinite computational time. The optimal Markov chain length depends on the type and dimensionality (number of optimisation variables) of the problem being solved.

The Markov criteria is defined as either

1. The number of moves accepted is equal to half of the Markov chain length ($M_{CL}/2$),
or
2. The number of moves evaluated is equal to the Markov chain length (M_{CL}).

Using these Markov criteria, the actual Markov chain length is dynamic, varying with the annealing temperature, T_a . At a high annealing temperature, the effective Markov chain length is $M_{CL}/2$ since almost every trial move is accepted. As the annealing temperature is progressively reduced and the number of accepted moves decreases, the Markov chain length increases up to a maximum of M_{CL} . In this way, the algorithm spends more time searching for the solution at low temperatures, when the probability of being close to the global optimum is higher, than high temperatures, when the solution space is randomly searched.

Termination criteria

Several criteria for deciding when to stop the search procedure are shown as follows. If any of these conditions is met, the algorithm stops.

1. The annealing temperature reaches the lower boundary, T_{af} .
2. No moves are accepted consecutively for a given number of annealing temperature loops (typically ten).
3. After a certain number of overall annealing temperature loops have been completed. In the present work, the maximum number of annealing temperature loops is taken as 25000.

It is observed in the present work that the first criterion is usually reached and the third criterion is hardly reached in SA runs.

APPENDIX C: DATA FOR CASE STUDY 6.1

C.1 Problem data

Table C.1.1 Case Study 6.1: Feed composition of crude oil mixture (derived from assay data, Suphanit, 1999)

Component Number	NBP (°C)	Flow rate (kmol/h)
1	9	110.9
2	36	106.9
3	61	139.3
4	87	175.8
5	111	175.8
6	136	169.7
7	162	169.4
8	187	166.2
9	212	156.6
10	237	140.1
11	263	127.9
12	288	115.6
13	313	106.2
14	339	101.3
15	364	94.5
16	389	84.6
17	414	73.9
18	447	95.2
19	493	61.8
20	538	49.2
21	584	54.5
22	625	39.3
23	684	40.2
24	772	28.2
25	855	26.6
Total flow rate (kmol/h)		2610.7

Table C.1.2 Case Study 6.1: Process and utility stream data of existing unit

Stream	Name	Supply temperature	Target temperature	Enthalpy change
		°C	°C	MW
1	Feed PreH 1	25	65	12.465
		65	105	13.572
		105	145	14.660
		145	166	8.044
		166	185	9.197
		185	225	20.107
		225	265	21.076
		265	305	21.782
		305	345	22.310
		345	365	11.282
2	Reb Duty 3	271	282	8.783
3	Reb Duty 4	182	189	6.625
4	Pump-Ar 1	298	268	12.828
5	Bott Cool 1	339	299	9.604
		299	259	9.164
		259	219	8.705
		219	179	8.228
		179	139	7.735
		139	100	7.024
6	Pump-Ar 2	250	210	14.416
		210	200	3.467
7	Bott Cool 2	257	217	1.142
		217	177	1.077
		177	137	1.011
		137	97	0.943
		97	57	0.874
		57	50	0.148
8	Pump-Ar 3	170	150	11.175
9	Bott Cool 3	282	242	3.949
		242	202	3.705
		202	162	3.471
		162	122	3.238
		122	82	3.004
		82	42	2.768
		42	40	0.164
10	Cond Duty 4	100	77	47.865
11	Dist Cool 4	77	40	1.321
12	Bott Cool 4	189	149	1.852
		149	109	1.707
		109	69	1.568
		69	40	1.059
13	CW	10	40	67.261
14	Flue Gas	1500	800	63.805

Table C.1.3 Case Study 6.1: Heat exchanger data

Exchanger No.	Area (m ²)	Heat duty (MW)	UA (kW/°C)	T approach (°C)
1	883	24.48	441.2	30.0
2	486	12.84	243.1	50.5
3	102	3.33	50.8	52.5
4	169	5.27	84.5	59.7
5	177	5.02	88.6	52.5
6	103	3.54	51.3	65.2
7	438	11.60	218.8	40.7
8	253	10.92	126.3	74.6
9	315	11.73	157.3	31.8
10	70	2.86	34.9	41.5
11	707	12.90	353.4	33.7
12	25	1.12	12.6	84.0
13	11	0.49	5.3	88.9
14hu	104	55.02	64.1	630.7
15hu	16	8.78	15.4	528.7
17cu	55	1.32	28.9	30.0
18hu	64	5.90	50.7	112.5
19cu	111	6.19	74.2	27.8
20cu	46	2.33	30.8	35.0
21cu	1054	47.87	772.9	60.9
22cu	126	3.64	71.6	29.4
23cu	10	0	-	-
24cu	10	0.02	0.1	159.8

$T_{\min} = 30.0$ °C; hu: hot utility exchanger; cu: cold utility exchanger

Table C.1.4 Case Study 6.1: Energy consumption and operating costs of existing unit

		Existing unit
Heat energy consumption	MW	63.80
Cold energy consumption	MW	67.26
Utility operating cost	MM\$/y	9.92
Stripping steam operating cost	MM\$/y	1.75
Heat exchanger network total area	m ²	5312
Total operating cost	MM\$/y	11.67
T_{\min}	°C	30.0

Table C.1.5 Case Study 6.1: Utility, stripping steam and exchanger modification costs

	Unit cost	
Flue gas (1500 . 800 °C)	150.0	\$/kW [®]
Cold water (10 . 40 °C)	5.25	\$/kW [®]
Stripping steam	0.14	\$/kmol
Exchanger additional area	$1530 \times (\text{additional area})^{0.63}$	\$
New exchanger unit	$13000 + 1530 \times (\text{exchanger area})^{0.63}$	\$
Exchanger repiping	60,000	\$
Exchanger resequencing	35,000	\$

*: 260 °C and 4.5 bar

C.2 Results for optimum crude oil distillation system

Table C.2.1 Case Study 6.1: Process and utility stream data of optimised unit

Stream	Name	Supply temperature °C	Target temperature °C	Enthalpy change MW
1	Feed PreH 1	25	65	12.465
		65	105	13.572
		105	145	14.660
		145	166	8.044
		166	185	9.197
		185	225	20.107
		225	265	21.076
		265	305	21.782
		305	345	22.310
		345	354	4.969
2	Reb Duty 3	271	280	4.493
3	Reb Duty 4	183	188	2.352
4	Pump-Ar 1	303	263	6.326
		263	259	0.645
5	Bott Cool 1	335	295	9.571
		295	255	9.151
		255	215	8.688
		215	175	8.209
		175	135	7.712
		135	100	6.281
6	Pump-Ar 2	257	217	14.587
		217	215	0.734
7	Bott Cool 2	297	257	1.170
		257	217	1.109
		217	177	1.046

		177	137	0.981
		137	97	0.916
		97	57	0.849
		57	50	0.146
8	Pump-Ar 3	175	135	8.917
		135	127	1.740
9	Bott Cool 3	280	240	3.908
		240	200	3.667
		200	160	3.434
		160	120	3.203
		120	80	2.971
		80	40	2.735
		40	40	0.011
10	Cond Duty 4	103	77	38.966
11	Dist Cool 4	77	40	1.357
12	Bott Cool 4	188	148	1.842
		148	108	1.698
		108	68	1.560
		68	40	1.023
13	CW	10	40	52.453
14	Flue Gas	1500	800	52.298

Table C.2.2 Case Study 6.1: Additional area and cost of optimised heat exchanger network

Exchanger No.	Existing area (m ²)	Additional area (m ²)	Capital cost (\$)
2	486	407	67166
3	102	200	43109
4	169	249	49531
6	103	481	74868
7	438	334	59512
8	253	77	23522
10	70	4	3600
13	11	33	13868
22cu	126	10	6588
26new	-	25	24510
27new	-	97	40255
Total		1914	406531

C.3 Comparison of new optimisation approach with the approach without product specifications and constant thermal property stream data

Table C.3.1 Case Study 6.1: Comparison of optimised operating conditions between two approaches

Column#	Optimisation variable		Base case value	Previous approach ⁺	New approach [*]
1	Feed preheating temperature	°C	365	359	354
	Pump-around duty	MW	12.84	10.22	6.98
	Temperature drop across pump-around	°C	30	23	44
	Flow rate of stripping steam	kmol/h	1200	561	1034
	Flow rate of liquid between columns 1 and 2	kmol/h	393	320	370
2	Pump-around duty	MW	17.89	15.11	15.33
	Temperature drop across pump-around	°C	50	50	42
	Flow rate of stripping steam	kmol/h	250	29	153
	Flow rate of liquid between columns 2 and 3	kmol/h	130	70	172
3	Pump-around duty	MW	11.20	9.42	10.68
	Temperature drop across pump-around	°C	20	28	48
	Flow rate of liquid between columns 3 and 4	kmol/h	883	729	285
4	Reflux ratio	-	4.17	3.12	3.08

#: number of simple column; ⁺: approach without product specifications and constant thermal property stream data; ^{*}: new approach with product specifications and multi-segmented stream data

APPENDIX D DATA FOR CASE STUDY 6.2

Table D.1 Case Study 6.2: Key components and recoveries for separation of products of optimum solution

Parameters	Columns*			
	1	2	3	4
Light key component	13	11	7	4
Heavy key component	16	14	9	6
Light key recovery	0.930	0.943	0.925	0.995
Heavy key recovery	0.879	0.934	0.963	0.996

*: See Figure 7.1b decomposed sequence of simple columns

Table D.2 Case Study 6.2: Additional area and cost of optimised heat exchanger network

Exchanger No.	Existing area (m ²)	Additional area (m ²)	Capital cost (\$)
2	486	86	25318
6	103	667	92022
7	438	259	50707
9	315	938	114072
10	70	21	10416
12	25	44	16598
15hu	16	7	5213
20cu	46	11	6931
22cu	126	84	24945
23cu	10	37	14882
26new	-	66	34429
27new	-	174	52467
Total		2396	448000

APPENDIX E DATA FOR CASE STUDY 6.3

Table E.1 Case Study 6.3: Heat exchanger data

Exchanger No.	Area (m ²)	Heat duty (MW)	UA (kW/°C)	T approach (°C)
1hu	64	21.91	42.4	460.4
2cu	135	9.64	90.2	66.7
3	170	8.14	85.0	63.4
4	1250	18.69	625.1	25.2
5cu	33	2.49	22.2	60.8
6cu	99	7.80	66.2	63.5
7	203	11.31	101.3	80.5
8	366	14.27	182.8	37.9
9	176	3.60	87.7	28.4
10hu	5	3.37	2.8	1206.1
11	44	1.59	21.8	67.8
12	41	1.50	20.4	65.0
13	302	5.76	151.1	25.4
14	85	1.83	42.6	36.1
15cu	69	5.25	45.7	37.9
16cu	141	5.84	93.9	29.9
17	195	9.62	97.3	93.5
18cu	5	0.52	0.2	183.9
19	47	2.02	23.5	80.4
20	10	0.28	2.8	100.0
21cu	10	0.22	6.6	30.0
22	5	0.55	2.2	248.7
23	659	13.12	329.7	37.3
24	86	3.30	43.1	63.8
25cu	2274	52.40	1516.0	30.7
26	10	0.15	2.8	51.9
27hu	102	61.39	68.1	723.4
28	319	7.02	159.4	25.8
29cu	105	5.25	70.0	26.2
30	64	2.69	32.1	66.8

T_{min} = 25.0 °C; hu: hot utility exchanger; cu: cold utility exchanger

Table E.2 Case Study 6.3: Process and utility stream data of existing unit

Stream	Name	Supply temperature	Target temperature	Enthalpy change
		°C	°C	MW
1	Feed PreH 1	25	65	12.465
		65	105	13.572
		105	145	14.660
		145	166	8.044
		166	185	9.197

		185	225	20.107
		225	265	21.076
		265	305	21.782
		305	345	22.310
		345	365	11.282
2	Reb Duty 3	260	271	9.128
3	Reb Duty 4	163	170	6.518
4	Feed PreH 5	340	380	15.120
4		380	400	6.792
5	Pump-Ar 1	292	262	13.117
6	Pump-Ar 2	237	197	15.058
		197	187	3.620
7	Bott Cool 2	253	213	1.171
		213	173	1.106
		173	133	1.038
		133	93	0.968
		93	53	0.896
		53	50	0.071
8	Pump-Ar 3	151	131	9.611
9	Bott Cool 3	271	231	3.872
		231	191	3.633
		191	151	3.400
		151	111	3.167
		111	71	2.933
		71	40	2.104
10	Cond Duty 4	72	46	52.403
11	Dist Cool 4	46	40	0.217
12	Bott Cool 4	170	130	1.772
		130	90	1.631
		90	50	1.495
		50	40	0.350
13	Bott Cool 5	346	306	5.221
		306	266	4.966
		266	226	4.722
		226	186	4.468
		186	146	4.204
		146	106	3.931
		106	100	0.525
14	Pump-Ar 6	303	263	4.588
		263	223	4.359
		223	183	4.123
		183	153	2.933
15	Bott Cool 6	303	263	2.827
		263	223	2.685
		223	183	2.539
		183	143	2.390
		143	103	2.235
		103	100	0.144
16	Pump-Ar 7	263	223	4.718
		223	183	4.459

		183	163	2.130
17	Cond Duty 7	263	194	0.052
18	Bott Cool 7	221	181	0.877
		181	141	0.822
		141	101	0.768
		101	100	0.017
19	Flus Gas	1500	800	86.676
20	CW	10	40	88.928

Table E.3 Case Study 6.3: Energy consumption and operating costs of existing unit

		Existing unit
Heat energy consumption	MW	86.68
Cold energy consumption	MW	88.93
Crude oil temperature before entering atmospheric furnace	°C	254
Utility operating cost	MM\$/y	13.47
Stripping steam operating cost	MM\$/y	2.59
Heat exchanger network total area	m ²	7073
Total operating cost	MM\$/y	16.06
T _{min}	°C	25

Table E.4 Case Study 6.3: Additional area and cost of optimised heat exchanger network

Exchanger No.	Existing area (m ²)	Additional area (m ²)	Capital cost (\$)
3	170	126	32163
7	203	223	46205
9	176	69	22134
10hu	5	4	3507
11	44	173	39278
12	41	32	13474
14	85	105	28775
19	47	290	54410
22	5	49	17719
24	86	209	44251
25cu	2274	135	33578
26	10	129	32703
28	319	10	6295
31new	-	10	7974
32new	-	23	12337
Total		1587	394803

APPENDIX F DATA FOR CASE STUDY 6.4

Table F.1 Case Study 6.4: Operating conditions of optimum design* (Configuration without a prefractionator column)

Column specifications	Column 1	Column 2	Column 3	Column 4
Feed preheat temp (°C)	375	-	-	-
Operating pressure (bar)	2.5	2.5	2.5	2.5
Vaporisation mechanism	Steam	Steam	Reboiler	Reboiler
R /R _{min}	1.43	1.15	1.05	1.05
Steam flow (kmol/h)	910	200	-	-
Pump-around duty (MW)	12.38	18.70	13.36	7.57
Pump-around T (°C)	49	45	92	63
Pump-around location	6	2	1	6

*: in terms of decomposed sequence of simple columns, see Figure 6.8

Table F.2 Case Study 6.4: Operating conditions of the initial design* (Configuration with a prefractionator column)

Column specifications	Column 1	Column 2	Column 3	Column 4
Feed preheat temp (°C)	240	365	-	-
Operating pressure (bar)	2.5	2.5	2.5	2.5
Vaporisation mechanism	Reboiler	Steam	Steam	Reboiler
R /R _{min}	1.22	1.62	8.69	1.20
Steam flow (kmol/h)	-	1200	250	-
Pump-around duty (MW)	10.00	9.52	13.36	11.20
Pump-around T (°C)	50	50	30	50
Pump-around location	1	1	1	1

*: in terms of decomposed sequence of simple columns, see Figure 6.9

Table F.3 Case Study 6.4: Product slate of the initial design (Configuration with a prefractionator column)

Products	Flow rate kmol/h	TBP (°C, mole%)		
		5%	50%	95%
Light Naphtha (LN)	661	2	69	119
Heavy Naphtha (HN)	518	109	155	196
Light Distillate (LD)	645	192	248	317
Heavy Distillate (HD)	146	284	338	372
Residue (RES)	642	352	460	797

Table F.4 Case Study 6.4: Operating conditions of optimum design* (Configuration with a prefractionator column)

Column specifications	Column 1	Column 2	Column 3	Column 4
Feed preheat temp (°C)	240	374	-	-
Operating pressure (bar)	2.5	2.5	2.5	2.5
Vaporisation mechanism	Reboiler	Steam	Steam	Reboiler
R /R _{min}	1.05	1.30	1.16	1.27
Steam flow (kmol/h)	-	1045	74	-
Pump-around duty (MW)	8.51	0.00	21.59	16.01
Pump-around T (°C)	78	-	22	62
Pump-around location	2	-	2	6

*: in terms of decomposed sequence of simple columns, see Figure 6.9

Table F.5 Case Study 6.4: Operating conditions of the initial design* (Progressive configuration)

	Column							
Column specifications	1	2	3	4	5	6	7	8
Feed preheat temp (°C)	157	250	320	-	212	365	-	188
Operating pressure (bar)	2.5	2.5	2.5	2.5	2.5	2.5	2.5	2.5
R /R _{min}	1.20	1.05	1.75	1.30	1.40	1.50	1.17	1.65
Steam flow (kmol/h)	-	-	12	-	-	1600	-	-
Pump-around duty (MW)	-	-	-	-	-	5.11	-	-
Pump-around T (°C)	-	-	-	-	-	30	-	-
Pump-around location	-	-	-	-	-	1	-	-

*: in terms of decomposed sequence of simple columns, see Figure 6.10

Table F.6 Case Study 6.4: Product slate of the initial design (Progressive configuration)

Products	Flow rate kmol/h	TBP (°C, mole%)		
		5%	50%	95%
Light Naphtha (LN)	678	3	71	128
Heavy Naphtha (HN)	491	104	156	209
Light Distillate (LD)	659	182	247	318
Heavy Distillate (HD)	149	289	340	376
Residue (RES)	634	351	462	798

Table F.7 Case Study 6.4: Operating conditions of optimum design* (First step of the progressive configuration)

	Column							
Column specifications	1	2	3	4	5	6	7	8
Feed preheat temp (°C)	190	250	320	-	211	364	-	184
Operating pressure (bar)	2.5	2.5	2.5	2.5	2.5	2.5	2.5	2.5
R /R _{min}	1.47	1.05	1.56	1.06	1.45	1.17	1.11	1.26
Steam flow (kmol/h)	-	-	10	-	-	1595	-	-
Pump-around duty (MW)	-	-	-	-	-	3.90	-	-
Pump-around T (°C)	-	-	-	-	-	35	-	-
Pump-around location	-	-	-	-	-	2	-	-

*: in terms of decomposed sequence of simple columns, see Figure 6.10

Table F.8 Case Study 6.4: Operating conditions of optimum design* (Second step of the progressive configuration)

	Column							
Column specifications	1	2	3	4	5	6	7	8
Feed preheat temp (°C)	189	232	306	-	242	362	-	202
Operating pressure (bar)	1.89	2.29	2.48	5.06	5.48	2.13	1.89	2.29
R /R _{min}	1.24	1.14	1.35	1.13	1.15	1.48	1.12	1.40
Steam flow (kmol/h)	-	-	10	-	-	1595	-	-
Pump-around duty (MW)	-	-	-	-	-	5.30	-	-
Pump-around T (°C)	-	-	-	-	-	23	-	-
Pump-around location	-	-	-	-	-	2	-	-

*: in terms of decomposed sequence of simple columns, see Figure 6.10

Table F.9 Case Study 6.4: Operating conditions of the initial design* (Configuration with a liquid side-draw prefractionator column)

Column specifications	Column 1	Column 2	Column 3	Column 4	Column 5	Column 6
Feed preheat temp (°C)	250	-	365	-	-	-
Operating pressure (bar)	2.5	2.5	2.5	2.5	2.5	2.5
Vaporisation mechanism	Reboiler	-	Steam	Steam	Reboiler	Reboiler
R /R _{min}	1.10	1.30	1.65	1.32	1.10	1.60
Steam flow (kmol/h)	-	-	1200	500	-	-
Pump-around duty (MW)	3.82	-	7.09	8.19	9.61	-
Pump-around T (°C)	50	-	50	50	50	-
Pump-around location	1	-	1	1	1	-

*: in terms of decomposed sequence of simple columns, see Figure 6.11

Table F.10 Case Study 6.4: Product slate of the initial design (Configuration with a liquid side-draw prefractionator column)

Products	Flow rate kmol/h	TBP (°C, mole%)		
		5%	50%	95%
Light Naphtha (LN)	698	3	72	119
Heavy Naphtha (HN)	490	120	162	206
Light Distillate (LD)	652	186	250	321
Heavy Distillate (HD)	140	287	341	376
Residue (RES)	630	352	463	799

Table F.11 Case Study 6.4: Operating conditions of optimum design* (Configuration with a liquid side-draw prefractionator column)

Column specifications	Column 1	Column 2	Column 3	Column 4	Column 5	Column 6
Feed preheat temp (°C)	266	-	375	-	-	-
Operating pressure (bar)	2.5	2.5	2.5	2.5	2.5	2.5
Vaporisation mechanism	Reboiler	-	Steam	Steam	Reboiler	Reboiler
R /R _{min}	1.06	1.32	1.35	1.16	1.05	1.66
Steam flow (kmol/h)	-	-	991	160	-	-
Pump-around duty (MW)	9.26E-4	-	6.69	9.24	13.14	-
Pump-around T (°C)	148	-	20	35	22	-
Pump-around location	1	-	5	2	5	-

*: in terms of decomposed sequence of simple columns, see Figure 6.11